Development and Applications of Tailored Polymer Sorbents for Selective Extraction of Fluoride, Boron and Mercuric Ions from Natural Waters

By

Neha Thakur
(CHEM 01201104017)

Bhabha Atomic Research Centre, Mumbai

A thesis submitted to the

Board of Studies in Chemical Science Discipline

In partial fulfillment of requirements

for the Degree of

DOCTOR OF PHILOSOPHY

of

HOMI BHABHA NATIONAL INSTITUTE

May, 2015

HOMI BHABHA NATIONAL INSTITUTE

Recommendations of the Viva Voce Board

As members of the Viva Voce Board, we certify that we have read the dissertation prepared by **Neha Thakur** entitled "**Development and Applications of Tailored Polymer Sorbents for Selective Extraction of Fluoride, Boron and Mercuric ions from Natural Waters**" and recommend that it may be accepted as fulfilling the dissertation requirement for the Degree of Doctor of Philosophy.

f Lalit Varshney

Chairman – Dr. A. Goswami Date: 01.05.15

Guide - Dr. Sangita D.Kumar Date: 01.05.15

Pandey

Co- guide - Dr. A.K. Pandey Date: 01/5/2015

External Examiner- Dr. R. K. Dutta Date: 01/05/2015

Lalit Varshney

Member - Dr. Lalit Varshney Date: 01/05/2015

Member - Dr. N.L. Misra Date: 01/05/2015

Final approval and acceptance of this dissertation is contingent upon the candidate's submission of the final copies of the dissertation to HBNI.

I hereby certify that I have read this dissertation prepared under my direction and recommend that it may be accepted as fulfilling the dissertation requirement.

Date: 01.05.15

Place: Bhabha Atomic Research Centre, Mumbai.

Pandey

Co-Guide

Guide

STATEMENT BY AUTHOR

This dissertation has been submitted in partial fulfillment of requirements for an advanced degree at Homi Bhabha National Institute (HBNI) and is deposited in the Library to be made available to borrowers under rules of the HBNI.

Brief quotations from this dissertation are allowable without special permission, provided that accurate acknowledgement of source is made. Requests for permission for extended quotation from or reproduction of this manuscript in whole or in part may be granted by the Competent Authority of HBNI when in his or her judgment the proposed use of the material is in the interests of scholarship. In all other instances, however, permission must be obtained from the author.

Neha Thakur

DECLARATION

I, hereby declare that the investigation presented in the thesis has been carried out by me. The work is original and has not been submitted earlier as a whole or in part for a degree / diploma at this or any other Institution / University.

Neha Thakur

List of publications arising from the thesis

Journal

1. Matrix supported tailored polymer for solid phase extraction of fluoride from variety of aqueous streams, ***N. Thakur,*** S.A. Kumar, D.N. Wagh, S. Das, A.K. Pandey, S.D. Kumar, A.V.R. Reddy, *Journal of Hazardous Materials,* **2012,** *201-202,* 193-201.

2. Extractive fixed-site polymer sorbent for selective boron removal from natural waters, ***N. Thakur,*** S.A. Kumar, R. Shinde, A.K. Pandey, S.D. Kumar, A.V.R. Reddy, *Journal of Hazardous Materials*, **2013,** *260***,** 1023-1031.

3. A fluoride ion selective Zr(IV)-polyacrylamide magnetic composite, ***N. Thakur,*** S.A. Kumar, H. Parab, A.K. Pandey, P. Bhatt, S.D. Kumar, A.V.R. Reddy, *RSC Adv,* **2014,** *4***,** 10350-10357.

4. Functionalized polymer sheet sorbent for selective preconcentration and determination of mercury in natural waters, ***N. Thakur,*** S.A. Kumar, A.K. Pandey, S.D. Kumar, A.V.R. Reddy, *Analytical methods***, 2014,** *6*, 7823-7830.

5. Development of a visual optode sensor for on-site determination of Hg (II), ***N. Thakur,*** S.A. Kumar, A. Kumar. K.S. , A.K. Pandey, S.D. Kumar, A.V.R. Reddy, *Sensors and Actuators B: Chemical***, 2015,** *211***,** 346-353.

6. Fixed-site membranes: fabrication, characterization and applications, ***N. Thakur***, S. A. Kumar, A. K. Pandey, S. D. Kumar and A.V.R. Reddy, *Procedia Engineering*, **2012,** *44*, 1581-1582.

Symposia

1. Fixed-site membranes: fabrication, characterization and applications, ***N. Thakur***, S. A. Kumar, A. K. Pandey, S. D. Kumar and A.V.R. Reddy, **Euromembrane** symposium held at London during 23rd-27th September 2012.

2. Polyacrylamide supported SPADNS -Zirconium resin for fluoride removal, ***N. Thakur,*** S.A. Kumar, D.N. Wagh, , A.K. Pandey, S.D. Kumar, A.V.R. Reddy,; DAE-BRNS Symposium on "Emerging Trends in Separation Science and Technology (**SESTEC 2012**) held at Mithibai college, Vile parle, Mumbai, during 27th Feb-1st March 2012.

3. Tailored polymer membrane for solid phase extraction of boron from aqueous solutions, ***N. Thakur,*** S.A. Kumar, A.K. Pandey, S.D. Kumar, A.V.R. Reddy, International Symposium on Sediment Management (**I2SM 2012**) held at Alibaug, Maharashtra during 20th- 22nd March, 2012. (**Best Poster Award**)

4. Target specific tailored sheet sorbents for selective removal of toxic ions from aqueous streams: An overview, ***N. Thakur,*** S.A. Kumar, R. Shinde, A.K. Pandey, S.D. Kumar, A.V.R. Reddy, National Conference on Frontiers in Physical, Chemical and Biological Sciences (**FPCBS-2013**) at University of Pune, Pune during 4-6th Oct. 2013.

5. Synthesis and characterization of different sheet sorbents for preconcentration and determination of mercury from aqueous solution, ***N. Thakur,*** S.A. Kumar, A.K. Pandey, S.D. Kumar, A.V.R. Reddy; Theme meeting on Membrane Separation for Fuel Cycle Applications (**MEMSEP-2013**) held at BARC, Mumbai during 16-18th Sep 2013.

Other Publications

1. Synthesis and application of a unified sorbent for simultaneous preconcentration and determination of trace metal pollutants in natural waters, S.A. Kumar, S. Pandey, ***N. Thakur***, H. Parab, R. Shinde, A.K. Pandey, D.N. Wagh, S.D. Kumar, A.V. R Reddy, *Journal of Hazardous Materials,* **2013,** *262*,265-273.
2. A visual strip sensor for determination of iron, S.A. Kumar**,** ***N. Thakur***, H. Parab, S. Pandey, R. Shinde R, A.K. Pandey, S.D. Kumar, A.V. R Reddy, *Analytica Chimica Acta***, 2014,** *851*, 87-94.

(Neha Thakur)

Dedicated To……

My Family

ACKNOWLEDGEMENTS

Every project has a number of people involved in it directly and indirectly. As the project has reached its final stage, it is time to express my heartfelt gratitude towards all those who are a part of this project. This thesis work would not have been possible without their support and inspiration. Herewith I would like to take this opportunity to express my gratitude to them for their help and support.

First and Foremost, I would like to express my sincere gratitude to my research guide ***Dr. Sangita D. Kumar*** *for the continuous support of my Ph.D. study and research, for her patience, motivation, enthusiasm, and immense knowledge. Her guidance from the initial to the final level enabled me to develop an understanding of the subject. She devoted her valuable time and effort to help me execute the work in good time.*

I am highly indebted to my Co-guide ***Dr. Ashok K. Pandey*** *for his invaluable help and assistance for the present work. I would not have made it through this process without his guidance. His ideas, enthusiasm and support towards project greatly helped to shape up this research work.*

In equal measure, I extend my gratitude to ***Dr. A.V.R. Reddy****, Head Analytical Chemistry, for his wholehearted encouragement and support, without whom it would have been impossible to carry out the work. I express my gratitude towards* ***Dr. B.N. Jagatap****, Director, Chemistry Group and* ***Dr. Tulsi Mukherjee,*** *Ex. Director, Chemistry Group, for their support.*

I am immensely thankful to ***Dr. A. Goswami****, Head, RCD and Chairman of my Ph.D. doctoral committee, for his support throughout the work. I would also like to thank the* *members of my Ph.D. committee:* ***Dr. Lalit Varshney*** *and* ***Dr. N.L. Misra*** *for their valuable suggestions, timely cooperation and guidance.*

Words will not be enough to express my gratitude to ***Dr. (Smt) Sanjukta A. Kumar*** *and* ***Dr. (Smt) Harshala Parab*** *for their assistance in the experimental work and support at each step of my thesis work. Working with them is always a pleasure and a lesson to me.*

I would also like to thank ***Dr. R. Verma , Dr. D N Wagh, Dr. Ajish Kumar*** *and* ***Dr. A.K. Tyagi*** *for their kind support during my entire research work.*

I am indebted to many of my fellow lab mates, particularly ***Mrs. N.S. Shenoy, Mrs. Aayushi Dhudwarkar, Mrs. Shailaja Pandey, Dr. Sadananda Das, Dr. Rakesh Shinde, Apurva Naik,*** *and* ***Vivek Chavan*** *for all the precious help and cooperation that they lent to me during my research work. My sincerest thanks are due to* ***Mrs. Juby K Ajish****, for providing me the moral support and a soothing hand whenever needed. I, also extend my sincere thanks to all my friends and colleagues of Analytical Chemistry Division for their love and support.*

My deepest gratitude goes to my **family** *for their unflagging love, support and encouragement throughout my life. My* **parents** *deserve special mention for their support in all my pursuits and their persistent confidence in me. I owe my every achievement to them. I also thank my* **siblings** *for their love and support at all the times.*

Words fail to express my appreciation to my husband **Tanmay** *for his unconditional love, relentless support and endless patience, especially during the final stages of this Ph.D. I am privileged to have him around me.*

Last but not least, I would like to thank everyone, whose contributions were important for the successful realization of this thesis, but I could not mention them personally.

Neha Thakur

Table of Contents

CONTENTS **x**

SYNOPSIS **xvii**

LIST OF FIGURES **xxviii**

LIST OF TABLES **xxxiv**

Chapter 1: Introduction

1.1 **Statement of Current Problem** **3**

1.2 **Different Methods of Separation and Preconcentration** **9**

1.2.1 **Precipitation and Co-precipitation** **11**

1.2.1.1 ***Applications of Precipitation and Co-precipitation Methods for Removal of Fluoride, Boron and Mercury*** **12**

1.2.2 **Liquid/Liquid Extraction (Solvent Extraction)** **13**

1.2.2.1 ***Applications of Solvent Extraction Methods Used for Removal of Fluoride, Boron and Mercury*** **16**

1.2.3 **Solid Phase Extraction** **18**

1.2.3.1 ***Sorption*** **19**

1.2.3.2 ***Ion Exchange*** **20**

1.2.3.3 ***Applications of Solid Phase Extraction Methods Used for Removal of Fluoride, Boron and Mercury*** **22**

1.2.4 **Membrane Based Methods** 30

1.2.4.1 ***Membrane Filtration*** 32

1.2.4.2 ***Applications of Membrane based Methods Used for Removal of Fluoride, Boron and Mercury*** 35

1.2.4.3 ***Membranes as Sorbents*** 36

1.3 **Types of Polymeric Membranes** 37

1.3.1 ***Plasticized membrane*** 38

1.3.2 ***Grafted membrane*** 40

1.4 **Methods of modification of polymer membranes** 42

1.4.1 ***High Energy Radiation Method*** 43

1.4.2 ***Photo irradiation Method*** 46

1.5 **Scope of the Thesis** 48

Chapter 2: Experimental

2.1 **Introduction** 55

2.2 **Materials** 55

2.3 **Apparatus** 56

2.3.1 ***UV Multi-Lamp Photoreactor*** 56

2.3.2 ***Micrometer Screw Gauge*** 57

2.3.3 ***pH Meter*** 57

2.4 **Synthetic Strategies for Different Polymer Sorbents** 58

2.4.1 ***Synthesis of Polypropylene Sheet Sorbents*** 58

2.4.1.1 ***In-situ UV Irradiation Method*** 58

2.4.1.2 ***Room Temperature Crosslinking Method*** 62

2.4.2 *In-House Membrane Preparation by Solution Casting Method* 64

2.4.3 *Synthesis of Magnetic Resin Sorbent* 65

2.5 Characterization Techniques 66

2.5.1 *Degree of Grafting* 66

2.5.2 *Water Uptake Capacity* 67

2.5.3 *Scanning Electron Microscopy (SEM)* 68

2.5.4 *Infra-Red Spectroscopy (IR)* 71

2.5.5 *Energy Dispersive X-Ray Fluorescence Spectrometer (EDXRF)* 73

2.5.6 *UV-Visible Absorption Spectroscopy (UV-Vis)* 75

2.5.7 *X Ray Diffraction (XRD)* 77

2.5.8 *Vibrating Sample Magnetometer (VSM)* 79

2.6 Analytical Instrumentation 81

2.6.1 *Ion Chromatography (IC)* 82

2.6.2 *Inductively Coupled Plasma Mass Spectrometer (ICP-MS)* 84

2.6.3 *Cold Vapor Atomic Absorption Spectroscopy (CV-AAS)* 88

2.7 Calibration of Instrumental Methods 91

2.7.1 *Standard Calibration Method* 91

2.7.2 *Standard Addition Method* 92

2.7.3 *Internal Standard Method* 92

2.8 Batch Sorption Studies 93

2.9 Sorption Isotherms 95

2.9.1 *Langmuir Isotherm* 95

2.9.2 *Freundlich Isotherm* 97

2.10 **Sorption Kinetics** **99**

2.10.1 ***Pseudo First-Order Kinetic Model*** **101**

2.10.2 ***Pseudo Second-Order Kinetic Model*** **102**

Chapter 3: Development of Polymeric Sorbents for Solid Phase Extraction of Fluoride

Section 3 A: Polymeric Sheet Sorbent for Fluoride

3A.1 **Introduction** **105**

3A.2 **Experimental** **112**

3A.2.1 ***Synthesis of Sheet Sorbents*** **113**

3A.2.2 ***Stability of thorium in Polymeric Matrix*** **114**

3A.2.3 ***Sorption Studies*** **114**

3A.3 **Result and Discussion** **115**

3A.3.1 ***Characterization of the Sorbents*** **115**

3A.3.2 ***Sorption and Desorption Studies*** **119**

3A.3.3 ***Kinetic Models*** **126**

3A.4 **Mechanism of Fluoride Sorption** **130**

3A.5 **Comparison of the Sheet Sorbents with Existing Sorbents** **132**

3A.6 **Application to Real Samples** **133**

3A.7 **Conclusions** **135**

Section 3 B: Magnetic Polymeric Composite for Fluoride

3B.1 **Introduction** **138**

3B.2 **Experimental** 141

3B.2.1 ***Synthesis of magnetic Composite*** 141

3B.2.2 ***Stability of Zirconium in Polymeric Matrix*** 142

3B.2.3 ***Sorption Studies*** 143

3B.3 **Results and Discussion** 144

3B.3.1 ***Characterization of Magnetic Sorbent*** 144

3B.3.2 ***Sorption and Desorption Studies*** 149

3B.3.3 ***Sorption Isotherms*** 155

3B.3.4 ***Kinetic Models*** 158

3B.4 **Mechanism of Fluoride Sorption** 161

3B.5 **Comparison Studies of Magnetic Sorbent With Existing Sorbents** 161

3B.6 **Application to Real Samples** 163

3B.7 **Conclusions** 163

Chapter4: Development of Polymeric Sheet Sorbent for Solid Phase Extraction of Boron

4.1 **Introduction** 166

4.2 **Experimental** 174

4.2.1 ***Synthesis of Boron Selective Polymer Sheet Sorbent*** 174

4.2.2 ***Sorption Studies*** 175

4.3 **Results and Discussion** 176

4.3.1 ***Characterization Studies*** 176

4.3.2 ***Sorption and Desorption Studies*** 179

4.3.3 *Sorption Isotherms* 183

4.3.4 Kinetic Models 187

4.4 Mechanism of Boron Sorption 190

4.5 Comparison of Extractive Sorbent With Existing Sorbents 191

4.6 Real Sample Analysis 192

4.7 Conclusions 194

Chapter 5: Development of Polymer Sheet Sorbents for Mercury (II) Detection and Quantification

Section 5 A: Polymeric Sheet Sorbent For Detection and Quantification of Mercury (II)

5A.1 Introduction 198

5A.2 Experimental 206

5A.2.1 *Synthesis of Polymer Sheets* 206

5A.2.2 *Sorption Studies* 207

5A.3 Results and Discussion 208

5A.3.1 *Comparison of Sheet Sorbents* 208

5A.3.2 *Characterization of Sheet Sorbent* 211

5A.3.3 *Tolerance Studies* 214

5A.4 Mechanism of Mercury Sorption 215

5A.5 Real Sample Analysis 217

5A.6 Analytical Application of Developed Sheet Sorbent 218

5A.7 Conclusions 221

Section 5 B: Development of Visual Optode Sensor for Mercury (II)

5B.1 Introduction 224

5B.2 Experimental 229

5B.2.1 *Synthesis of Sensor Molecule* 229

5B.2.2 *Fabrication of Optode* 230

5B.2.3 *Optimization of Experimental Parameters* 231

5B.3 Results and Discussion 233

5B.3.1 *Optimised Composition of Optode* 233

5B.3.2 *Analytical Parameters of Optode* 241

5B.4 Sensing Mechanism of Optode 242

5B.5 Application to Real Samples 243

5B.6 Conclusions 244

Chapter 6: Summary and Future Scope 247

References 256

List of Publications Included in the Present Thesis 291

SYNOPSIS

Development and Applications of Tailored Polymer Sorbents for Selective Extraction of Fluoride, Boron and Mercuric ions from Natural Waters

Water pollution is a serious problem because of contamination of large percentage of water resources by various pollutants [1,2]. Due to the advancement in the industrialization sector, wastewaters from industries such as metallurgical, tannery, chemical manufacturing, mining, battery manufacturing industries etc. usually contain one or more toxic ions responsible for water contamination. More than seven hundred organic and inorganic pollutants have been reported in water along with microbial populations [3]. Among these, certain organic and inorganic pollutants are highly dangerous because of their toxic and carcinogenic nature. Moreover, some of these contaminants are non- biodegradable and hence persist in the environment for a long time. Therefore, it is necessary to remove such contaminants from the aqueous streams before releasing them into the environment, because there is possibility of their entry into the food chain through waste discharges into water bodies. Although the list of such contaminants prevailing in water bodies is exhaustive, the present thesis work was focused on developing sorbents for extracting fluoride, boron and mercuric ions from contaminated streams.

Ion-exchange, solvent extraction, chemical precipitation, reverse osmosis and solid-phase extraction are some of the commonly used methods for the treatment of contaminated waters [4-10]. At an industrial level, pollutants such as toxic ions are removed from water by using columns and contactors filled with suitable sorbents but continuous increase in their variety and amount in the effluents to be treated makes some of the existing methods inefficient and sometimes even ineffective [11]. Consequently, the development of new and more effective methodologies for their removal has become essential.

Over the last few decades, solid phase extraction (SPE) using variety of sorbents has been one of the most promising methods because of its ease of operation and the possibility to scale up. Tailoring of natural/synthetic polymers with functional groups or inorganic moiety is regarded as one of the most effective techniques for toxic ion removal because targeted ions can be chemically bonded by the organic-inorganic polymer hybrids. These kinds of materials often present the best properties of each of its components in a synergic way and have high performances of physical, chemical and mechanical properties [12]. Therefore, efforts were focused to develop newer sorbents with improved sorption capacities. The possible mechanism of solid phase extraction of the selected ions has been evaluated.

Along with the development of newer sorbents, the detection and monitoring of toxic elements at ultratrace concentrations in natural and waste waters is important. As such, the tolerance limits set by the different agencies for some toxic ions such as mercury and arsenic are in ng mL^{-1} range. Detection of analytes at such low concentration requires an effective preconcentration step to bring their concentration in the analytical range of the chosen measurement methods. In this regard, the selectivity of the developed sorbent for a particular species to be extracted plays an important role. Therefore, efforts were made for the development of highly selective sorbents, where high preconcentration factor was achieved.

The major objectives of the present thesis work are to develop the functionalized polymer sorbents based methods for the extraction of fluoride, boron and mercuric ions from various aqueous streams. Special emphasis was given on synthesizing the sorbents in the form of polymer sheets that can be used with ease in the analytical applications. The selection of fluoride and boron as the target species have been based on the fact that these elements can be toxic or micronutrients depending upon their concentrations.

Mercuric ion has been selected as a target species for the simple reason that among the various heavy metal ions, it is one of the most significant pollutants due to its high toxicity and widespread industrial applications. Fluoride and mercury related health hazards occurring from the consumption of contaminated water are well known especially the dental fluorosis and the Minamata disease respectively.

Introduction to the subject with the scope and the work carried out are discussed in this thesis. The work done on the above mentioned theme has been organized into six chapters which have been discussed briefly in what follows.

CHAPTER I: Introduction

This chapter provides a background to the studies carried out in the present thesis. As the theme of the thesis is to develop polymer sorbents for selective extraction of fluoride, boron and mercuric ions, this chapter begins with the existing scenario of water bodies followed by a brief overview on the presence of fluoride, boron and mercury ions in the environment, their chemistry and their toxicity levels. The necessity for the removal and monitoring of these ions from various aqueous samples has been discussed in this chapter. A detailed literature survey of various chemical separation methods currently being employed for the extraction of fluoride, boron and mercuric ions is included e.g solvent extraction, precipitation, solid-phase extraction and membrane filtration. Based on the existing literature on the chosen subject and the availability of the state of the art instruments, the chapter ends with a brief description of the objectives and the scope of the work.

CHAPTER II: Experimental

This chapter deals with the experimental work carried out. Sample and standard preparation along with different calibration methods are discussed in this chapter. The general methods used for the synthesis of different polymer sorbents in the form of sheets and resin are elaborated in the chapter. For functionalizing the existing polypropylene sheets in-situ UV irradiation method and room temperature crosslinking were used and are discussed in this chapter. Heat induced chemical methods of polymerization used for the synthesis of magnetic sorbent has been elaborated. A brief overview of different physical and chemical characterization techniques used for characterizing the developed sorbents such as Fourier Transform Infrared Spectroscopy (FTIR), X-ray powder diffraction (XRD), optical spectroscopy (UV–Vis), scanning electron microscopy (SEM) and energy dispersive X-ray fluorescence (EDXRF) is given in this chapter. The principle along with the optimization of instrumental parameters of analytical techniques used for the quantification of selected ions such as Ion chromatography (IC), Inductively coupled mass spectrometry (ICPMS) and Cold vapor atomic absorption spectrometry (CV-AAS) is briefly explained in this chapter.

CHAPTER III: Development of polymer sorbents for solid phase extraction of fluoride

This chapter deals with the synthesis of two types of the polymer sorbents for the solid phase extraction of fluoride from various natural waters. The chapter is divided into two sections, first section describes the synthesis of an inorganic – organic polymer sheet sorbent and in the second section, synthesis of a magnetic polymer composite for the selective removal of fluoride from aqueous solution is described. The characterization and applications of the sorbents are discussed in detail.

The sorbents were developed by photo-initiator induced graft-polymerization of a precursor monomer bis[2-methacryloyloxy)-ethyl] phosphate (MEP) on polypropylenechains using dimethyl phenoxy acetphenone (DMPA) as a UV-initiator. The selection of precursor monomer was based on its ability to form highly stable complex with Th(IV) ions. Thorium has high chemical affinity towards fluoride and un-neutralized positive charge on Th(IV) in the sorbent provides fixed positive charges for fluoride sorption. The synthesized sorbents were characterized for their different surface morphology by scanning electron microscope and the loading of thorium in the grafted sorbents was confirmed by EDXRF. The developed sorbents were characterized in terms of parameters that influence the defluoridation of aqueous streams like pH, loading capacity, contact time, effect of competing ions, reusability and chemical stability of Th complex in the host matrix. Finally, both the sorbents were examined for their efficacy for fluoride removal from real water samples collected from Channu region of Punjab.

The polyacrylamide (PAM) magnetic composite (PAM/Fe_3O_4) was synthesized by bulk polymerization of the acrylamide monomer in the presence of Fe_3O_4 nanoparticles. The as-synthesized magnetic composite was equilibrated with 5 wt% zirconium oxychloride solution. Physical and chemical characterization of the composite was carried out using SEM, FTIR and EDXRF. The magnetic hysteresis was obtained using a vibrating sample magnetometer (VSM). The experimental conditions such as contact time, initial fluoride concentrations, pH, reusability and the presence of competing anions affecting the performance of the Zr(IV)-polyacrylamide magnetic sorbent in the defluoridation was examined. Adsorption kinetics and isotherms were studied to evaluate the fluoride sorption mechanism in the Zr(IV)-polyacrylamide magnetic sorbent. Experimentally obtained fluoride sorption capacity was 124.5 mg g^{-1} which was quite high when compared to the existing super-paramagnetic fluoride sorbents. The chemical stability of the Zr complex in the host matrix was evaluated. The developed sorbent was applied for the removal of fluoride from real ground water samples in the presence of high concentrations of interfering ions. The magnetic property of the sorbent was utilized for its separation from aqueous media by applying an external magnetic field.

CHAPTER IV: Development of polymeric sheet sorbent for solid phase extraction of boron

This chapter deals with the synthesis, characterization and application of an extractive fixed-site polymer sorbent for selective removal of boron in its neutral form from natural waters. The fixed-site polymer sorbent was prepared by crosslinking poly(vinylbenzyl chloride) in the pores of polypropylene sheet with a cyclic diamine piperazine as a crosslinker. The precursor sheet thus formed was chemically modified with 1% solution of N-methyl D-glucamine (NMDG) which is selective for boron. The extent of the functionalization of preformed polymer PVBCl crosslinked with piperazine in the pores of the host microporous polypropylene substrates was found to be 86±10 wt.%. FTIR spectra of the PVBCl crosslinked precursor and NMDG functionalized sheet sorbent were used to identify the functional groups present in them.

Parameters that influence the boron uptake from aqueous streams like pH, uptake capacity, contact time, effect of competing ions and reusability were evaluated. The kinetic studies confirmed that the sorption of boron occurred through chemical bonding between sorbate and sheet surface. The vicinal diols of the NMDG fixed on the sorbent led to the formation of a stable complex with boric acid and thus helped in its efficient removal. Because of this, most of the common interfering anions had no effect on the boron sorption in the NMDG-sheet sorbent. Due to the matrix elimination in the sorption process, the sorbent based preconcentration method was extended for its applicability in the determination of boron. The desorption of boron followed by quantification using UV visible techniques was carried out. Finally the sorbent was examined for its boron removal efficacy from real water samples and it was found that the percentage recovery was greater than 95%.

CHAPTER V: Development of polymeric sorbents for detection and quantification of mercury (II)

The chapter is divided into two sections which deal with the synthesis and applications of polymer based sheet sorbents which can selectively preconcentrate mercury as well as detect it at lower concentrations.

The main objective was to develop a sheet sorbent having mercury(II) specific functional groups as well as metal nanoparticles. Different functionalized polypropylene sheet sorbents consisting of silver nanoparticle embedded in polyacrylamide(Ag-PAM-PP) matrix and gold coated 1,8-octanedithiol modified (HS-Octyl-S-Au-PP) sheet were synthesized and tested for their efficacy for mercury ion sorption. Among the two, Ag-PAM-PP has showed 96% uptake compared to 64% by HS-Octyl-S-Au-PP sorbent. Therefore Ag-PAM-PP substrate was used as a template to preconcentrate and measure mercury in aqueous solution. The galvanic reaction of Ag Nps with the sorbed mercury ions leading to silver amalgam formation is the driving force for its retention on the membrane. Characterization of silver incorporated polyacrylamidesheet was carried out using UV-Vis spectrometry, field emission scanning electron microscope (FESEM) and X-ray Diffraction (XRD). Further it was possible to quantify the sorbed mercury on the sorbent sheet in the range 20 ng mL^{-1} to 10 μg mL^{-1} using EDXRF and CV-AAS techniques. The direct determination of the preconcentrated mercury in the sheet sorbent by EDXRF enhanced the analytical detection limits of EDXRF by 10 fold. In addition, the incorporation of Ag NPs in the sorbent facilitates its color change upon mercury sorption, which can be used for qualitative screening of mercury at the site before its quantitative determination using EDXRF/ CV-AAS in the laboratory later.

The second section deals with the development of an optical sensor film for highly selective and sensitive determination of Hg(II) ions in aqueous solution. Rhodamine derivatives have excellent photophysical properties, such as its absorption and emission wavelengths are longer and it has large absorption coefficient. Therefore, it can be utilized to develop chemosensors for metal ions. One such rhodamine 6G derivative, a phenylthiosemicarbazide derivative was reported as a highly selective and sensitive chemodosimeter for Hg(II) ions in aqueous solutions [13]. In this thesis, this derivative was incorporated in a polymer sheet support to form a Hg(II) selective sensing film.

Phenylthiosemicarbazide Rhodamine 6G derivative was synthesized by literature reported procedure and the synthesized derivative was encapsulated in a polymeric support consisting of cellulose triacetate and tri-(2-ethylhexyl) phosphate as a plasticiser. The resultant transparent colourless film was further optimised for getting maximum sensitivity towards Hg(II) ions. To obtain the best measurement conditions for detecting Hg(II) the effect of pH, time taken to obtain maximum absorbance and tolerance towards others cations were evaluated. Under the optimized conditions, this sensor showed a wide linear dynamic range of 10 to 5000 ng mL^{-1} Hg(II) with a lowest detection limit of 1.3 ng mL^{-1}. In addition to its stability and reproducibility, this optode showed a high selectivity towards Hg(II) ions as compared to other co-existing ions in real water samples. The developed optode was found suitable for detection of Hg(II) ions in a variety of real ground water samples.

CHAPTER VI: Summary and Future Scope

In this chapter a brief summary of the achievements of the present investigations as well as future perspectives that can be explored on different aspects of selective extraction of ions utilizing various fundamental chemical concepts is given.

- The host polypropylene base substrates provided mechanical integrity for using these as the flat sheet sorbents or membranes.
- Th-bis[2-methacryloyloxy)-ethyl]phosphate grafted fibrous and microporous sheet substrates were developed for selective fluoride extraction.
- N- methyl- D-Glucamine was anchored in pores of polypropylene membranes and was found to extract boron from natural waters quantitatively.
- Flat sheet silver nanoparticles embedded sorbent for preconcentration and determination of mercuric ions has been developed.
- Direct analysis of the preconcentrated mercury on the flat sheet sorbents using EDXRF and CV-AAS was achieved.
- This helped in enhancing the detection limits of EDXRF and also eliminated the interferences caused by undesirable components in the matrix.
- The functionalized sheet sorbents developed can be utilized for modifying the transport properties of the membranes and as a base material for developing the membrane based chemical sensors.
- This study would also be useful for designing nanocomposite membranes for a desired application.

References

1. Murty M.N. and Kumar S. India Infrastructure Report (2011), 285.
2. Droste, R.L. Theory and practice of water and wastewater treatment; John Wiley &Sons, New York (1997).
3. John, D.Z. Handbook of drinking water quality: Standards and controls; Van Nostrand Reinhold, New York (1990).
4. Esalah, O.J.; Weber, M.E and Vera, J.H. *Can. J. Chem. Eng.* 2000, ***78***,948.
5. Lertlapwasin, R.; Bhawawet, N.; Imyim, A and Fuangswasdi, *S. Sep. Purif. Technol.* 2010, ***72***, 70.
6. Emamjomeh, M.M and Sivakumar, M. *J. Environ. Manag.* 2009, ***90***, 1663.
7. Mahmoud, A and Hoadley, A.F. *Water Res.* 2012, ***46***, 3364.
8. Yurloval, L.; Kryvoruchko, A and Kornilovich, B. *Desalination* 2002, ***144***, 255.
9. Greenlee, L.F.; Lawler, D.F.; Freeman, B.D.; Marrot, B and Moulin, P. *Water Res.* 2009, ***43***, 2317.
10. Benit, Y and Ruiz, M.L. *Desalination* 2002,***142***, 229.
11. Khotimchenko, M., Kovalev V. and Khotimchenko Y. J. *Hazard. Mater.*, 2007, **149**,693.
12. Samiey, B., Cheng, C-H., Wu, J., *Materials* 2014, ***7***, 673.
13. Yang, Y. K., Yook, K. J. and Tae , J., *J. Am. Chem. Soc.*, 2005, **127**,16760.

List of Figures

Fig. No		**Page No.**
1.1	Classification of various separation methods	**10**
1.2	Schematic diagram of a magnetic solid phase extraction process	**24**
1.3	Functionalization of magnetic nano-particles	**27**
1.4	Typical diagram of Reverse Osmosis process	**34**
1.5	Schematic diagram showing steps involved in the preparation of plasticized membrane	**39**
1.6	Pictorial representation of grafted polymer	**41**
1.7	Pictorial representation of crosslinked polymer	**42**
1.8	Scheme showing preirradiation method of grafting	**44**
1.9	Scheme showing peroxidation method of grafting	**45**
1.10	Scheme showing simultaneous method of grafting	**46**
1.11	Scheme showing direct method of photoirradiation	**47**
1.12	Scheme showing in-direct method of photoirradiation	**48**
2.1	Schematic diagram of multi-lamp photo-reactor	**57**
2.2	Steps involved in the synthesis of tailored sorbents for fluoride	**60**
2.3	Synthesis of polyacrylamide in polypropylene substrate by in-situ grafting	**61**
2.4	Reaction scheme involved in the synthesis of NMDG functionalized PVBCl sorbent	**63**
2.5	Pictorial representation of synthesis of magnetic composite for fluoride	**66**
2.6	Depiction of different phenomena occurring on interaction of electron beam with specimen	**69**
2.7	Various components of a typical Scanning Electron Micrograph	**70**
2.8	Schematic diagram of Infrared Spectroscopy System	**72**
2.9	Consequence of interaction of incoming X-ray radiation	**73**

2.10	Components of a typical XRF	**74**
2.11	A working schematic of the UV-visible spectrophotometer	**76**
2.12	A simplified diagram of the X-Ray diffractometer	**79**
2.13	Schematic representation of Vibrating sample magnetometer	**81**
2.14	Schematic representation of an Ion chromatography system	**83**
2.15	Schematic of an ICP-MS system	**85**
2.16	Diagram of a quadrouple mass filter	**86**
2.17	The atomic absorption process	**89**
2.18	Schematic Diagram of a typical CV-AAS	**90**
2.19	General form of Langmuir isotherm	**97**
2.20	Schematic of mass transport steps involved in sorption process	**100**
3.1	Schematic representation of PP membrane grafting followed by chemical treatment to prepare fluoride selective sorbent	**113**
3.2	Scanning electron micrographs of sorbents (a) and (b) sheet sorbent before and after grafting and (c)and (d) fibrous sorbent before and after grafting	**117**
3.3	EDRXF Spectrum of thorium-loaded MEP sorbent	**119**
3.4	Uptake of fluoride ions in fixed size (1x1 cm^2) Th-MEP sheet sorbent	**120**
3.5	Uptake of fluoride in Th-MEP sheet sorbent as a function of pH	**121**
3.6	Desorption of fluoride from the sorbent in aqueous solution having basic range of pH	**123**
3.7	Effect of different competing anions on fluoride uptake in Th-poly(MEP) sheet sorbent at fixed fluoride concentration (5 mg L^{-1})	**124**
3.8 (a)	Fluoride uptake as a function of time in sheet Th-MEP sorbent at fixed fluoride concentration (5 mg L^{-1})	**125**
3.8 (b)	Fluoride uptake as a function of time in fibrous Th-MEP sorbent at fixed fluoride concentration (5 mg L^{-1})	**126**
3.9 (a)	Comparison of fluoride sorption kinetics data fitted with pseudo first order rate equation	**127**
3.9 (b)	Comparison of fluoride sorption kinetics data fitted with pseudo second order	**128**

rate equation
3.10 Chemical structures of MEP grafted (a) and different possible complexes of Th(IV)-phosphate sites(b)Mechanism of fluoride interaction with sorbent (c) in the poly(propylene) sorbents **131**
3.11 Defluoridation scheme using synthesized sorbent **144**
3.12 SEM images of the magnetic sorbent before (a) after (b) fluoride sorption **145**
3.13 EDXRF spectrum of Zr(IV)-loaded polyacrylamide/Fe_3O_4 composite **146**
3.14 FTIR spectra of the composite sorbent before (a) after (b) fluoride sorption **147**
3.15 VSM magnetization curves of the Zr-PAM/Fe_3O_4 samples with varying mass ratio of Fe_3O_4 to Zr-PAM **148**
3.16 ICPMS spectra of leached sorbent showing absence of zirconium (b and c are the sorbent treated aqueous samples at pH 2 and pH 4) and a - 2 μgL^{-1} Zr standard **149**
3.17 Uptake of fluoride by the sorbent as a function of pH of equilibrating solution **150**
3.18 Effect of dosage of the sorbent on the uptake of fluoride (Fluoride concentration: 5 mg L^{-1}; volume of solution : 25 mL) **151**
3.19 Effect of different co-existing anions on fluoride uptake (Fluoride concentration :10 mg L^{-1}, concentration of co-existing ions: 200 mg L^{-1}) **152**
3.20 Desorption profile of fluoride sorbed Zr-PAM magnetic composite under different pH values **153**
3.21 Uptake of fluoride by the magnetic sorbent as a function of concentration of equilibrating solution **155**
3.22(a) Freundlich isotherms for the uptake of fluoride by magnetic sorbent **156**
3.22(b) Langmuir isotherms for the uptake of fluoride by magnetic sorbent **157**
3.23 Fluoride uptake in the Zr-PAM/Fe3O4 as a function of time **158**
3.24(a) Fluoride sorption kinetics data fitted with pseudo first order rate equation **159**
3.24(b) Fluoride sorption kinetics data fitted with pseudo second order rate equation **160**
4.1 White Mulberry tree exhibiting signs of boron toxicity **168**
4.2 Distribution of $B(OH)_3/[B(OH)_4]^-$ as a function of pH **170**

4.3 Chemical structures of piperazine (a) DABCO (b) used as crosslinkers **174**

4.4 Steps involved in quantification of boron preconcentrated in sheet sorbent by curcumin method **176**

4.5 SEM images of host poly(propylene) microporous substrates (a) blank membrane and (b) after anchoring PVBCl **177**

4.6 EDX images of NMDG functionalized sorbents (a) before boron sorption and (b) after boron sorption **178**

4.7 FTIR spectra of the polymer membrane (a) PVBCl crosslinked membrane (b) and its modified form with NMDG **179**

4.8 Uptake of boron in NMDG microporous sheet sorbent as a function of pH of equilibrating solution (boron concentration : 5 mg L^{-1}) **181**

4.9 Desorption of boron from NMDG sheet sorbent as a function of pH **182**

4.10 Uptake of boron in NMDG microporous sheet sorbent as a function of concentration of equilibrating solution **184**

4.11 (a) Langmuir and (b) Freundlich isotherms for the uptake of boron by NMDG functionalized sheet sorbent **186**

4.12 Boron uptake as a function of time (Concentrations of boron in well stirred 25 mL solutions was kept as 5 mg L^{-1}) **188**

4.13 Comparison of boron sorption kinetics data fitted with (a) pseudo first order (b) pseudo second order rate equations **189**

4.14 Interaction mechanism of boron with the NMDG functionalized sorbent **191**

5.1 Aquatic mercury cycle showing interconversion of different forms of mercury **200**

5.2 Chemical structures of components (a) 1,8-octanedithiol, (b) acrylamide (AM), (c) N-N'-methylene-bis-acrylamide (MBA), (d) α,α'-dimethoxy-α'-phenyl acetophenone (DMPA) used in the synthesis of the sorbents **206**

5.3 Sorption of Hg (II) in HS-octyl-S-Au-PP and Ag-PAM-PP sorbents as a function of pH of equilibrating solution (1×1 cm^2 size of sorbents were equilibrated with 25 mL Hg(II) standard solution **210**

5.4 Sorption of Hg(II) in the sorbent sheets as a function of equilibration time (1×1 **211**

cm^2 sheet sorbents were equilibrated with 25 mL Hg(II) standard solution)

5.5 (a) UV - Vis absorption spectrum showing characteristic SPR of AgNps **212**

5.5 (b) X-ray Diffraction pattern spectrum of Ag-PAM-PP sorbent **213**

5.6 SEM image (a) and BSE image (b) of Ag Nps in Ag-PAM-PP sheet **213**

5.7 Change in SPB of Ag Nps embedded in PAM substrate as a function of Hg(II) concentration **216**

5.8 Variation of color in Hg(II) equilibrated Ag-PAM-PP sorbent (a) Blank , (b) 0.5 mg L^{-1}, (c) 1 mg L^{-1}, (d) 2 mgL^{-1}, (e) 5 mg L^{-1} Hg(I) **217**

5.9 EDXRF spectrum of Hg(II) sorbed Ag-PAM-PP sorbent **219**

5.10 EDXRF Calibration plotof Hg(II),1×1 cm^2 Ag-PAM-PP was equilibrated with 25 mL Hg (II) standard solutions and measured by EDXRF **219**

5.11 Calibration curve obtained by CV-AAS of desorbed Hg from the Ag-PAM-PP sorbent (Size of Ag-PAM-PP = 1×1 cm^2 , Volume of desorbed solution = 15mL) **220**

5.12 Spirolactam ring-opening process of rhodamine derivative **227**

5.13 Two step reaction involved in synthesis of Rh6G-P derivative from Rh6G **230**

5.14 Chemical structures of components (a) Cellulose Triacetate (CTA), (b) Tri-(2-Ethylhexyl) Phosphate (TEHP), (c) Rhodamine 6G derivative (Rh6G-P) used in the synthesis of optode **231**

5.15 Absorbance as a function of the amount of Rh6G-P in the optode membrane (CTA (100 mg) and TEHP (50 mg) were kept constant) **234**

5.16 Atomic force microscopic image of an optode sample **235**

5.17 Absorbance of the optode (2x1 cm^2) equilibrated with the solution having 2000 ng mL^{-1} Hg(II) and varying pH **236**

5.18 Absorbance as a function of equilibration time (optode membrane equilibrated with 10 mL of 2mgL^{-1} Hg(II) solution for different time intervals) **237**

5.19 Absorbance spectra of the optode for different concentrations of Hg(II) (a) (10 ng mL^{-1} to 5000 ng mL^{-1} under the optimized conditions) (b) Optode absorbance Vs concentration of Hg(II) plot ((10 ng mL^{-1} to 5000 ng mL^{-1}) **238**

5.20 Change in the color of the optode with different concentration of Hg(II) (a) Blank , (b) 10 ng mL^{-1}, (c) 100 ng mL^{-1},(d) 1000 ng mL^{-1} and (e) 5000 ng m L^{-1} **239**

5.21 Comparison of change in the fluorescence spectrum of the optode sample equilibrated with solution having 10 ng mL^{-1} Hg(II) concentration (solid line) with respect to spectrum of a blank optode (broken line) **239**

5.22 Individual UV-Vis spectra of the sensor optode in presence of different metal ions (500 mg L^{-1} of each Na^{+}, Ca^{2+}, K^{+}, $Mg^{2+,}$1mg L-1 of each Cd^{2+}, Cr^{2+}, $Fe2^{+}$, Pb^{2+} , Ni^{2+}) and Hg(II) (5 mg L^{-1}) **240**

5.23 (a) Hg^{2+} recognition mechanism by the incorporated Rh6G-P derivative in the optode (b) Blank synthesized film and (c) Optode membrane equilibrated with Hg(II) solution **243**

List of tables

Table. No		**Page No.**
1.1	Commonly use ion –exchangers with their exchange capacities	**21**
2.1	Typical operating conditions of ICP-MS	**87**
3.1	Concentration of fluoride and its biological effects	**107**
3.2	Composition of six different set of membranes (size = 5x5 cm^2)	**116**
3.3	Grafting yield obtained from six different set of membranes	**116**
3.4	Rate constants obtained from the graphs for Th-poly(MEP) sheet and fibrous sorbents	**129**
3.5	Comparison of fluoride loading capacities in different sorbents	**132**
3.6	Composition of ground water sample collected from Channu, Punjab, India	**134**
3.7	Removal of fluoride from ground water samples collected from Channu, Punjab, India using Th-poly(MEP) fibrous sorbent	**134**
3.8	Values of the constants derived from Freundlich and Langmuir isotherms	**157**
3.9	Rate constants obtained from the graphs for the sorbent (Fluoride concentration: 5 mg L^{-1}; volume of solution : 25 mL)	**161**
3.10	Comparison of Fluoride loading capacity of various adsorbents	**162**
3.11	Removal of fluoride from ground water samples collected from Channu, Punjab, India using Zr- PAM/Fe_3O_4 sorbent	**163**
4.1	Effect of the choice of crosslinker on boron uptake (Volume of solution = 25 mL)	**180**
4.2	Effect of different competing anions on boron uptake in NMDG membrane (boron concentration (5 mg L^{-1}) in solution)	**183**
4.3	Values of the constants derived from Freundlich and Langmuir isotherms	**187**
4.4	Rate constants obtained using pseudo first order and pseudo second order	**190**

rate equations
4.5 Comparison of boron sorption capacities in different sorbents **192**
4.6 Removal of Boron from seawater and ground-water samples collected from Thirumangalam area, Tamilnadu and Bangalore, India using fixed-site sorbent **193**
4.7 Comparison of spectrophotometric and ICP-MS analysis of boron **194**
5.1 General techniques for sample pre-treatment, pre-concentration, separation and quantification of total mercury and its species in waters **203**
5.2 Sorption efficiency of functionalized polypropylene (PP) sheet sorbents for Hg^{2+} in solution having pH 6 **209**
5.3 Tolerance of co-existing ions in Ag-PAM-PP sorbent at fixed mercury concentration (5 mg L^{-1}) in solution **214**
5.4 Uptake of Hg(II) by sheet substrates from the ground-water and seawater samples **217**
5.5 Comparison of the lowest detection limits for the quantification of Hg^{2+} **221**
5.6 Comparison of the detection limits obtained in different molecular probes **242**
5.7 Analysis of Hg(II) in groundwater samples collected from Madurai, Tamilnadu **244**

Chapter -1

INTRODUCTION

1.1 Statement of Current Problem
1.2 Different Methods of Separation and Preconcentration
  1.2.1 Precipitation and Co-precipitation
    1.2.1.1 Applications of Precipitation and Co-precipitation Methods for Removal of Fluoride, Boron and Mercury
  1.2.2 Liquid/Liquid Extraction (Solvent Extraction)
    1.2.2.1 Applications of Solvent Extraction Methods Used for Removal of fluoride, Boron and Mercury
  1.2.3 Solid Phase Extraction
    1.2.3.1 Sorption
    1.2.3.2 Ion Exchange
    1.2.3.3 Applications of Solid Phase Extraction Methods Used for Removal of fluoride, Boron and Mercury
  1.2.4 Membrane based Methods
    1.2.4.1 Membrane Filtration
    1.2.4.2 Applications of Membrane based methods for Removal of Fluoride, Boron and Mercury

1.2.4.3 Membranes as Sorbents

1.3 Types of Polymeric Membranes

1.3.1 Plasticized membrane

1.3.2 Grafted membrane

1.4 Methods of modification of polymer membranes

1.4.1 High Energy Radiation Method

1.4.2 Photo-irradiation Method

1.5 Scope of the Thesis

1.1. Statement of current problem

Atharav Veda says, “Water is the elixir of life”. Water has most appropriately been compared to 'ambrosia' because it purifies the body from all kinds of toxins and gives new life. It also frees the body from different 'doshas' (ailments) and is hence known as Bheshagya- which purifies the body from all kinds of impurities. For any civilization to sustain, access to clean water is one of the basic necessities. Clean and plentiful water provides the foundation for prosperous communities. We rely on clean water to survive, yet right now we are heading towards a serious scarcity of clean water. The United Nations reports that though access to improved drinking water has expanded, nearly one billion people do not have safe drinking water [1].

As the world population increases, water consumption also increases. Some observers have estimated that by 2025, more than half of the world population will be facing water-based vulnerability or a water crisis [2,3]. Advancements in science and technology have improved the quality of life but at the same time it has led to an adverse impact on environment, especially on water resources. A wide variety of toxic inorganic and organic chemicals are discharged into the environment as industrial wastes, causing serious water, air, and soil pollution. The extensive growth of industrial activities during this century has generated serious water pollution problems especially in developing countries like India for both the surface water and groundwater resources.

Water pollution caused by toxic heavy metal ions has become a serious environmental problem. Heavy metals (such as Pt, Pd, Ag, Cu, Cd, Pb, Hg, Ni, Co, Zn, *etc*.) are natural constituents of the earth crust and present in the environment as a result of weathering and erosion of parent rocks [4]. In addition to natural sources, they are introduced in ecosystems through wastewaters originating from anthropogenic sources such as chemical manufacturing, metal finishing, welding, alloys manufacturing, painting, mining, extractive metallurgy, plating, tannery and battery industry and using metal-containing fertilizers and pesticides [5]. The presence of low concentration of a these toxic ions cause a major difficulty in the use and reuse of water streams. Water containing significant concentrations of these pollutants is harmful to human beings, animals and aquatic organisms. Some of these toxic ions get easily accumulated in the human body through the food chain, causing a variety of diseases and disorders [6]. It is estimated that, worldwide, approximately 250 million new cases of waterborne diseases occur each year with over 10 million resulting in death.

There are now regulations governing the disposal of industrial waste water in terms of toxic chemicals content. People around the globe are also being urged to use water responsibly for present and future generations, and there is a lot of technological advancement dealing with the recycling of industrial water and its treatment before it is discharged into the environment. In this regard, it has become necessary to remove various toxic ions from industrial effluents for their subsequent safe disposal. The other alternative is to rely on nontraditional sources of water to supplement the ever increasing demands of growing population. In the last few decades, ground water has become one of the important sources of water for meeting the requirements of various sectors in developing countries. Though groundwater contributes only 0.6% of the total water resources on earth, it is the major and the preferred source of drinking water in rural as well as urban areas because treatment of the same, including disinfection is often not required. The groundwater present caters to 80% of the total drinking water requirement and 50% of the agricultural requirement in countries like parts of rural India. But the increasing industrial advancement and urbanization leads to the pollution of available groundwater resources [7,8]. During to its complex flow history, groundwater passes through various geological formations leading to consequent contamination in shallow aquifers. In India itself, as many as 19 states, including Delhi are affected by groundwater contamination problem. Geogenic contaminants, including salinity, iron, fluoride, and arsenic have affected groundwater in over 200 districts spread across 19 states [7]. Elevated levels of different ions found in water resources have restricted their use for human activities. It has been estimated that fluorosis, a disease associated with consumption of fluoride contaminated water is prevalent in 17 states of India as many ground water sources have fluoride concentration as high as 30 mg L^{-1}. Hence, removal of such toxic ions from contaminated natural waters and wastewaters has been a subject of extensive industrial research. Although the list of such toxic ions prevailing in water bodies is exhaustive the present thesis work has been focused on developing polymer sorbents for extracting fluoride, boron and mercuric ions from contaminated aqueous streams.

Fluoride (F^-), Boron (B) and mercury (Hg) are some of the most toxic inorganic contaminants found in the environment [9]. Apart from their natural sources, they are released into the aquatic systems from a number of industries such as metal plating, smelting, mining, paint industries, leather tanning, pigments, textiles and alloy industries as well as from sewage [10-11].

Exposure of fluoride has been associated with dental fluorosis which slowly progresses to skeletal fluorosis at later stages. Water contamination by boron is another widespread environmental problem due to the wide application of boron compounds in industries such as food preservation, agriculture, electronics, glass and ceramics, health care products, and nuclear power production. The signs of acute toxicity in humans include nausea, vomiting, diarrhoea, dermatitis and lethargy, irritation of the eye, the upper respiratory tract and the nesopharynx. Hence removal of boron from natural waters is gaining lot of attention these days. Due to several industrial applications of mercury, it has become a widespread pollutant in ground waters. Mercury is of high concern because of its potential long-term accumulation in the ecosystem. It has a tendency to accumulate in the biological system via bioaccumulation. Bioaccumulation is defined as the process where at each level in a food chain, from bacteria to plankton to small fish, larger fish, and fish-eaters, organisms take in more element than they excrete thereby accumulating the excess in their organs. For instance, when a fish feeds on a marine or aquatic organism that had consumed methyl mercury contaminated plankton, the methyl mercury is not excreted but instead, it is retained in its tissues. When this fish is preyed upon by another fish or another marine predator, the accumulated methyl mercury in the fish is passed on to the predator and in a similar fashion the methyl mercury is passed on up the food chain until eventually the concentration of the methyl mercury becomes far higher than its initial concentration. For this reason therefore, any organism at the top of the food chain i.e. humans, polar bears, etc. faces a serious risk of mercury poisoning upon eating such a fish. The in famous Minamata is caused by mercury poisoning as a result of eating mercury contaminated fish. Mercury has very high tendency to bind to protein and it mainly affects the renal and nervous system. Looking at the disastrous consequences of these toxic ions, there is an ever growing need to remove or reduce them from contaminated water streams by different methods and methodologies.

A number of methods are available for the removal of these inorganic pollutants from water streams. Their removal from (drinking) water can be achieved through precipitation, flocculation, solvent extraction, ion exchange, reverse osmosis, etc. [12]. However, most of these methods are unacceptable, owing to the disposal of sludge, their high cost, low efficiency and inapplicability to a wide range of pollutants.

Among various methods, the process of adsorption has now become one of the preferred methods for the removal of toxic contaminants from water as it has been found to be effective, versatile and relatively simple [13]. Adsorption has the additional advantages of its applicability at very low concentrations, suitability for using batch and continuous processes, ease of operation, little sludge generation, possibility of regeneration and reuse of adsorbents and low capital cost. The adsorption process has now acquired global importance for reducing the problem of contamination of water as well as air. The process has also become a significant addition to Green Chemistry endeavors.

All the adsorption based separation procedures commonly used involve the application of different sorbents that can bind selectively with the element of interest to be removed from water sources. However, the major problem in this field is to select novel types of adsorbents. The major disadvantages of the existing adsorbents such as activated carbon, zeolites, clays and agricultural residues are their low adsorption capacities and their relatively weak interactions with the targeted ions. Sometimes the targeted element is present in ultra-trace quantities in natural waters which make its separation even more challenging. Therefore, the use of highly selective sorbents for the removal or preconcentration of toxic ions remains in demand, especially in developing countries where ground water is commonly used for consumption. However, specific requirements of modifying the existing sorbents depending upon prevailing chemical conditions have to be optimized in view of the above considerations.

More recently, promising organic-inorganic hybrid polymers have been used for the removal of toxic ions from wastewater [14-22]. In these compounds, the functional variation of organic materials is combined with advantages of a thermally stable and robust inorganic substrate, resulting in strong binding affinities towards targeted ions and relatively high adsorption capacities. Functionalized hybrid polymeric materials as adsorbent are regarded as one of the most effective techniques because metal ions can be chemically bonded to them by the organic-inorganic polymer hybrids. These kinds of materials often present the best properties of each of its components in a synergic way and have high performances of physical, chemical and mechanical properties [23].

Currently organic-inorganic hybrid polymeric materials are intensively studied for their efficient applications. The intrinsic multifunctional character of these materials makes them potentially useful in multiple fields such as in electroanalytical applications [24], their extensive use in the field of membranes such as ultra-and nanofiltration [25,26], superhydrophobic surfaces [27,28], highly transparent films [29,30], pH sensitive composites [31], solar cells [32,33], electrolyte [34], molecular shuttles [35], semiconductors [36], gas separation [37,38], catalysts [39], biosensors [40], drug delivery systems [41], coatings for corrosion protection [42], adsorbents of toxic compounds [14-22] *etc*. Looking at the widespread use of these polymers, in this work, as a first step, efforts were focused to develop newer inorganic-organic polymeric sorbents with improved sorption capacities which could be used as cheaper adsorbents. Particular attention is focused on application of these sorbents for the sorption of selected ions from environmental samples as well as in understanding the mechanism behind that.

However, prior to developing methods of separation and preconcentration, the chemistry of the targeted element and its composition needs to be understood. Therefore the occurrence, uses, chemistry and the need of these elements for sustaining human life is described in the introduction part of their respective chapters.

In this chapter an overview on the fundamentals of separation, different available methods of separation, the chemistry involved behind their separation and the need to develop various simple, cost effective and environmental friendly separation and preconcentration methods for fluoride, boron and mercuric ions has been emphasized. Based on the existing literature on the chosen subject, the chapter ends with a brief description of the objectives and the scope of the thesis. An overview of different available methods used for the separation of targeted elements from aqueous streams has been discussed briefly in what follows.

1.2. Different Methods of Separation and preconcentration

The growing demand for safe potable water, the increasing amount of industrial wastes containing varying concentrations of toxic ions and the need for highly efficient and clean technologies for water decontamination, has led to an emphasis on selective removal and preconcentration of ions from variety of matrices. The aim of the research study undertaken was to meet the above demands by developing different functionalized polymer sorbents for the selective extraction of fluoride, boron and mercuric ions from various aqueous streams. In other words developed sorbents should be able to achieve separation of targeted ion in its native form from contaminated water sources in the presence of different interfering ions.

The literature survey showed that adsorption, ion-exchange, precipitation-coagulation, and solid-phase extraction methods are the most frequently used methods for the uptake of these ions from aqueous medium (Fig 1.1) [43]. Membrane based methods like reverse osmosis, nanofiltration, and electrodialysis [44-46] find limited application for the removal of these ions. Basic theory and principle involved in each of the above separation method is described individually in the following sections.

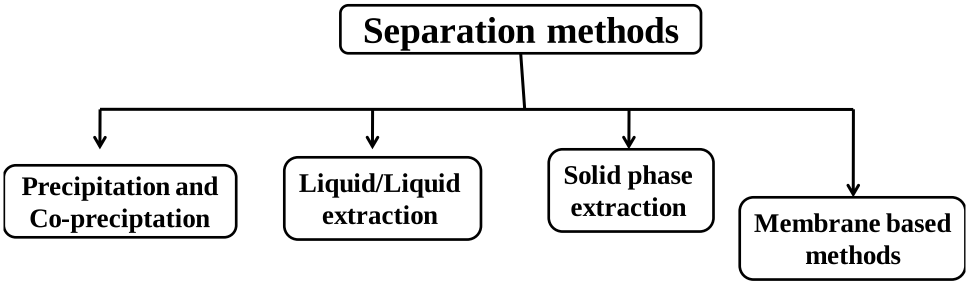

Fig. 1.1 *Classification of various separation methods*

1.2.1. Precipitation and Co-precipitation

The process of precipitation transforms dissolved contaminants into insoluble solids, assisting in the contaminant's subsequent removal from the liquid phase through sedimentation or filtration. A precipitate is formed when the ionic product exceeds the solubility product of a particular compound. Precipitation can be carried out in two ways, i.e. (i) matrix precipitation (ii) precipitation of trace components. Matrix precipitation is associated with large consumption of reagents, prolonged duration of the process and co-precipitation. The precipitation method has limited applications because the precipitate formation process depends on various factors, such as composition of the aqueous phase, pH, temperature, nature of the counter ions forming the precipitate and sequence in which solutions are mixed. A slight alternation in any of these factors leads to poor precipitation yield.

Co-precipitation, which was earlier regarded as an unpleasant companion of a desired precipitate, is now considered as an effective method of preconcentration. Co-precipitation is the transfer of a substance into a precipitate of some compound if the substance does not form its own solid phase under the given conditions. Depending on the physical and chemical properties of the components and the experimental conditions, co-precipitation is due to the adsorption of the trace component on the surface of the collector. It also occurs because of the formation of isomorphic mixed crystals, mixed chemical compounds, occlusion and mechanical inclusion of small amounts of other phases. Sometimes, all these factors act simultaneously to some extent. Some of the applications of precipitation and co-precipitation methods for the removal of fluoride, boron and mercuric ions from aqueous streams are discussed in the following section.

1.2.1.1 Applications of precipitation and co-precipitation methods for removal of fluoride, boron and mercury

Precipitation method for defluoridation involves addition of chemicals and formation of fluoride precipitates. Lime and alum are the commonly used precipitating agents. Fluoride precipitates as insoluble calcium fluoride on addition of lime and thus can be removed from water. But the addition of lime raises the pH value of water to 11-12. Complete removal of fluoride is impossible by addition of lime and a residue of 8.0 mg L^{-1} is left so this method is always used in conjunction with alum treatment to ensure the proper fluoride removal [47]. The Nalgonda technique of defluoridation is based on combined use of alum and lime in a two-step process and it has been used as the most effective technique for fluoride removal [48,49]. But this commonly followed method has several limitations. The major limitations include daily addition of chemicals, large amount of sludge production and it is least effective with water having high total dissolved solids and hardness. Moreover, it converts a large portion of ionic fluoride into soluble aluminum complex and practically removes only a small portion of it (18-33%) [50]. Residual aluminum from 2.01 to 6.86 mg L^{-1} was also reported which is dangerous to human health as aluminum is a neurotoxin, concentration as low as 0.08 mg L^{-1} in drinking water has been reported to cause Alzheimer’s disease. Due to use of aluminium sulfate as coagulant, the sulfate ion concentration increases tremendously and in few cases, it crosses the maximum permissible limit of 400 mg/L, which causes cathartic effect in human beings. Use of alkaline oxides like MgO and CaO followed by the adjustment of pH with $NaHSO_4$ has also been used to remove fluoride [51]. Several other precipitating agents such as calcium hydroxide [$Ca(OH)_2$], calcium chloride [$CaCl_2$] and calcium sulphate [$CaSO_4$] have also been applied for the fluoride removal purposes [52,53]. Cement paste and combined use of calcium salts as precipitant and polymeric aluminium hydroxide as coagulant have also been studied for the fluoride removal by precipitation method [54]. But the method of precipitation yields results only at higher initial concentration of fluoride as it is easy to attain super saturation level. However, at lower concentration of fluoride precipitation methods become insufficient to remove fluoride [55]. So, to decrease the fluoride from 10-20 mg/L to drinking water level (1.5 mg/L) by precipitation method is itself a challenge.

The literature on the precipitation methods used for boron removal is very less because there is no known compound that can quantitatively precipitate boron [56]. Usually the secondary acid effluents are generally neutralized and then evaporated to dryness to obtain a solid product. This operation is tedious and expensive since it involves the necessity of totally evaporating the water. Powdered $Ca(OH)_2$ and $MgCl_2$ has been used for precipitating boron from aqueous solution in form of calcium and magnesium borate [57,58]. The flocks thus formed are separated by the means of physical sedimentation. However, reported boron precipitation methods using magnesium, aluminum and various other metal hydroxides typically require large volumes of adsorbent and produce large quantities of sludge, making them uneconomical for many industries [59-60]. Boron co-precipitation with calcium carbonate was researched by Kitano et al. in which calcium carbonate was added to solutions containing various ratios of sodium chloride, magnesium chloride, and boric acid [61].

The precipitation methods used for mercury treatment are based on precipitation of mercury compounds using hydroxides and sulfides [62]. Hydroxide precipitation is ineffective, with soluble levels exceeding 75 mg L^{-1} mercury over a pH range of 3.5 to 11.5. Sulfide precipitation is the most common method of removing mercury and yields more complete removal of mercury than hydroxide precipitation but it leaves the residue of toxic sulfides in solution. The method works on less than 85% acid concentrations, at higher acidity sulfur is oxidized to sulfur dioxide and the product contains the undesirable sodium sulfate. This method is much more expensive than hydroxide precipitation since the excess sulfides are usually regulated and the resulting sludge may be difficult to landfill. Therefore, it is not as widely used as hydroxide precipitation. Toho process of mercury removal involves the addition of KI which precipitates mercury as mercury iodide and precipitated mercury is removed by filtration [63].

1.2.2. **Liquid/Liquid extraction (Solvent Extraction)**

Solvent Extraction as a method of separation and preconcentration has been reviewed by Zolotov and Kuzmin [64]. The knowledge gained in this direction in subsequent years is summarized in several books, reviews and general papers [65,66]. Separation and preconcentration procedures using liquid/liquid extraction generally result in a high enrichment factor due to the difference between the volumes of aqueous and organic phases. Solvent extraction is distribution of a dissolved substance between two immiscible liquid phases- one of them is usually an aqueous phase and the other phase is an organic solvent. Extraction, being a heterogeneous process, is governed by the phase rule

$$P+F = C+2 \tag{1.1}$$

where P is the number of phases, F is the number of degrees of freedom and C is the number of components. If the number of phases is equal to two and one substance (C=1) is distributed then at constant temperature and pressure the system is univariant. In such cases, at equilibrium, the ratio of concentrations of the substance distributed in both the phases is a constant value and this is independent of total concentration of the substance.

This value, designated as distribution constant or partition constant is described as

$$D \text{ (Distribution or Partition constant)} = C_o/C_{aq} \tag{1.2}$$

where C_o and C_{aq} are the equilibrium concentrations of the substance in organic phase and aqueous phase respectively. This is known as Nernst distribution law.

Solvent extraction separations are mainly dependent for their successful operation upon the distribution ratio of the species between the organic and aqueous phase and the pH and salt concentration of the aqueous phase. Much of the selectivity which is achieved in liquid-liquid extraction is dependent upon adequate control of the pH of the solution. The addition of masking agents such as EDTA and cyanide can greatly improve selectivity, but they too are dependent upon the pH of the solution to exert their full effect. In many cases complete extractions and separations are obtained only in the presence of salting-out agent. There are some of the major disadvantages of liquid-liquid solvent extraction such as the process is cumbersome for a large number of samples or for large samples and often requires toxic or flammable solvents. It can be time consuming, especially if attainment of equilibrium is slow and can require costly amounts of organic solvents and generate large volumes of organic waste. Solvent extraction is affected by small impurities in the solvent(s) and multiple extractions might be required, thereby increasing time, consumption of materials, and generation of waste. Sometimes, the formation of emulsions can interfere with the phase-separation process and in addition to that, alteration of chemical form of the species to be extracted can change on going from one phase to the other, thereby altering the distribution coefficient and effectiveness of the extraction.

1.2.2.1 Applications of solvent extraction methods used for removal of fluoride, boron and mercury

The applications of solvent extraction method for fluoride removal are limited in literature however a few of the reports involves extraction of fluoride using trimethylchlorosilane (TMCS) in toluene to produce trimethylfluorosilane (TMFS) [67,68]. Solvent extraction method has been used for boron removal from concentrated boron liquors. Diols, triols and other polyols having long aliphatic chains with low solubility in water have been applied for extracting boron from waste effluents [69-74]. Based on the literature survey on solvent extraction of boron, the mechanism can be divided into three groups: simple extraction, extraction forming borate complex and extraction by forming non-ionic borate ester complex. Although a large number of extractants have been used, the extraction process suffers from the loss of extractants as these diol based extractants have appreciable solubility in water.

In the case of mercury, different amines and organophosphorus based extractants have been used for the removal of mercury(II) ions from aqueous streams. However, these extractants containing nitrogen or oxygen as donor atom show poor selectivity for mercury(II) over other metals. On the other hand the extraction reagents containing sulphur as donor (soft base) atom bind selectively with mercury because of the soft acid-soft base (SASB) principle [75]. In recent years, various sulphur containing reagents such as thiophosphorus, triisobutylphosphine sulphide (TffiPS), marketed under the trade name of CYANEX 471X by Cytec Canada Inc. have been used for the extraction of mercury(II) from from aqueous solutions [76-78]. Recovery of mercury from paper industry effluent using TffiPS as an extractant has been carried out by Singh and Tandon [77]. Extraction behaviour of mercury(II) from thiocyanate solutions using TffiPS in benzene as an extractant has been investigated [79]. Reddy et al. [80] have studied the extraction behaviour of mercury(II) from iodide solutions using bis-2-ethylhexyl sulphoxide (B_2EHSO) in benzene as an extractant and reported the extracted complexes as HgI_2, HgI_2,B2EHSO and $Hgh._2B_2$EHSO. Inoue et al. synthesised 2-ethyl-2-(isobutylthiomethyl)butane thiol (EIBTMT), 3,3-diethylthietane (DETE) and3,3-dibutylthietane (DBTE) [81] and utilized for the extraction of mercury(II) from acidic chloride solutions. Crown thioethers have been studied for the selective extraction of mercury from acidic solutions because of their high affinity towards Hg(II) as well as their resistance towards degradation under acidic conditions [82-84]. Tri-n-butyl phosphate(TBP) and tri-n-octylphosphine oxide (TOPO) have been reported as efficient extractants for mercury(II) [85,86]. Brewer et al. investigated the extraction of mercury from acidic aqueous solutions using the TRUEX process solvent, a mixture of n-octyl(phenyl)-N,N-diisobutylcarbamoylmethyl phosphine oxide (CMPO) and TBP in n-dodecane [87]. The most recent studies on the liquid-liquid extraction of mercury (II) are based on the use of calixarenes derivatives with different number of atoms and several structural modifications. p-tert-butylcalix[4]arene derivatives having S-containing functionalities in the upper and lower rim have also been studied for the extraction of mercury from aqueous phase [88-92]. The existing problems associated with solvent extraction as listed above makes above makes its use limited.

1.2.3. Solid phase extraction

Solid phase extraction (SPE) is highly useful separation/preconcentration method which eliminates many problems associated with liquid liquid extraction (LLE). SPE is more efficient than liquid-liquid extraction and yields quantitative extractions that are rapid, easy to perform and can easily be automated for analytical applications or integrated to water treatment plants. Consequently, in recent years SPE has been successfully used for the separation and sensitive determination of toxic ions in water samples.

The principle of solid phase extraction (SPE) is similar to that of Liquid-Liquid extraction, involving partitioning of solutes between two phases. However, instead of two immiscible liquid phases, as in LLE, SPE involves distribution between a liquid (sample matrix) and a solid phase. Partitining of a solute usually involves its sorption on a particular solid support known as sorbent. There are different ways in which a particular solute can interact with a sorbent surface. The different sorption mechanisms are briefly discussed below.

1.2.3.1 Sorption

Surface adsorption retains a major place in water treatment because of its greater accessibility and lower cost. Sorption is a process that occurs when a solute (the sorbate) accumulates on the surface of a solid sorbent, forming a molecular or atomic film. Both short range (repulsive) and longer range (attractive) forces between the solute and the sorbent become balanced, when adsorption occurs. Depending on the type of bonding involved, sorption can be classified as follows:

(a) **Physisorption** or physical adsorption is a type of sorption in which the sorbate adheres to the surface only through weak intermolecular van der Waals interactions. Physisorption is characterized by interaction energy comparable to heat of vaporization (condensation), and multiple layers may be formed, with approximately the same heat of sorption. The heat of physisorption is, at the most, a few kcal/mole, and, therefore, this type of sorption is stable only at temperatures below 150 °C, depending on the sorbate-sorbent pair.

(b) **Chemisorption** is a type of adsorption whereby a molecule adheres to a surface through the formation of a chemical bond, as opposed to the van der Waals forces which cause physisorption. Chemisorption is characterized by interaction energy between the surface and the sorbate to be comparable to the strength of a chemical bond (tens of kcal/mol), and, consequently, is much stronger, and more stable at high temperatures, than physisorption.

(c) Ion exchange

Ion exchange process involves exchange of counter ions at fixed sites by electrostatic interactions in the matrix. The negative or positive groups attached to the matrix are called fixed sites and available opposite sign ions are called counter ions. The selectivity of an ion-exchanger towards different ions is dependent upon the strength of their electrostatic binding.

An ion exchanger is characterized by its capacity, resulting from the effective number of functional groups per unit mass of material. Ion exchange resins are classified as cation exchangers, which have positively charged mobile ions available for exchange, and anion exchangers, whose exchangeable ions are negatively charged.

Both anion and cation resins are functionalized organic polymers. They differ in the ionizable group attached to the hydrocarbon network. It is this functional group that determines the chemical behavior of the resin. Resins can be broadly classified as strong or weak acid cation exchangers and strong or weak base anion exchangers.

Strong acid cation resins: Strong acid resins are so named because their chemical behavior is similar to that of a strong acid. The resins are highly ionized in both the acid ($R\text{-}SO_3H$) and salt ($R\text{-}SO_3Na$) form of the sulfonic acid group. The hydrogen and sodium forms of strong acid resins are highly dissociated and the exchangeable Na^+ and H^+ are readily available for exchange over the entire pH range. Consequently, the exchange capacity of strong acid resins is independent of solution pH.

Weak acid cation resin: In this the ionizable group is a carboxylic acid (COOH). These resins behave similar to weak organic acids that are weakly dissociated. The degree of dissociation of a weak acid resin is strongly influenced by the solution pH. Consequently, resin capacity depends on the solution pH.

Similarly there can be strong anion exchangers and weak anion exchangers dependent on the type of groups attached to it. Ion exchange process is usually reversible. This means that ion exchange is a physical separation process in which the ions exchanged are not chemically altered. Some commonly used ion exchangers used in water treatment are listed in the Table 1.1

Table 1.1 *Commonly use ion –exchangers with their exchange capacities*

Type	**Ionogenic group**	**Trade name**	**Exchange capacity (m equiv./g)**
Cation exchanger	$-SO_3H$	KU-2	4.9-5.1
	$-SO_3H$, -OH	Dowex 50	5
	-COOH	Amberlite IR-120	5
		KU-1	4.5-5.1
		KB-4	10
Anion Exchanger	$-N(CH_3)_3Cl$	AV-17	
		Dowex 1	4.3
		Amberlite	3
	=NH, ≡ N	IRA-400	3
	$-NH_2$, = NH	AN-2F	10.6
		AN-1	4

The ion exchangers are extensively used in wastewater treatment for the removal of hazardous ionic materials from the wastewater and some of their applications for the removal of chosen ions are given below.

1.2.3.3 Applications of solid phase extraction methods for removal of fluoride, boron and mercury

Applications of solid phase extraction methods usually employs the use of adsorption and ion-exchange processes involving the passage of water through a contact bed where desired analyte is removed by ion exchange or surface chemical reaction with the solid bed matrix. For defluoridation the use of powdered activated carbon was demonstrated by Mckee and Johnston as early as 1934 and the results were appreciable but the process needs adjustment of pH thus making it tedious [93]. Bauxite, magnetite, kaolinite, serpentine, various types of clays and red mud are some of the naturally occurring materials studied for defluoridation [94]. The general mechanism of fluoride uptake by these materials is the exchange of metal lattice hydroxyl or other anionic groups with fluoride. Fluoride uptake capacity can be increased by certain pre-treatments like acid washing, calcinations, etc. however none of the mentioned materials generally exhibits high fluoride uptake capacities.

Some of the other sorbents reported in literature for fluoride removal are activated alumina, activated carbon, activated alumina coated silica gel, calcite, activated saw dust, activated coconut shell carbon and activated fly ash, groundnut shell, coffee husk, rice husk, magnesia, tricalcium phosphate, bone charcoal, activated soil sorbent, are [95-107].

Among these activated alumina and activated carbon are the most commonly used adsorbents.

Activated alumina has been the sorbent of choice for defluoridation of drinking water in developed countries. Generally it is implemented on a large scale source community plants. Small defluoridation units employing activated alumina have been developed which can be directly attached to the tap. During recent years this technology is gaining wide attention even in developing countries. Domestic defluoridation units have been developed in India using indigenously manufactured activated alumina, which is commercially available in bulk quantities. Choosing the proper grade of activated alumina is important for its effective reuse in multiple defluoridation cycles. Around 500-1500 litres of safe water could be produced with 3 kg of activated alumina when the raw water fluoride is 11 and 4 mg/l respectively at natural water pH of 7.8-8.2. The frequency of regeneration is once in 1.5-3 months [108]. But there are certain limitations using these adsorbents. Hardness and surface loading (the ratio of total fluoride concentration to activated alumina dosage) affects the fluoride removing tendency of sorbents. In addition to this the pH of the solution should be between 5.0 and 6.0 because at pH > 7, silicate and hydroxide become stronger competitor of the fluoride ions for exchange sites on activated alumina and at pH less than 5, activated alumina gets dissolved in acidic environment leading to loss of adsorbing media. The adsorption process has a low adsorption capacity, it requires acidification and pretreatment and its effectiveness for fluoride removal reduces after each cycle of regeneration [109].

Anion-exchange resins containing quaternary ammonium functional groups can be used for the removal of fluoride from aqueous solution using simple ion exchange mechanism. The removal takes place according to the following reaction:

$$\text{Matrix- }NR_3^+Cl^- \; + \; F^- \longrightarrow \text{Matrix- }NR_3^+F^- \; + \; Cl^- \qquad (1.3)$$

The fluoride ions replace the chloride ions of the resin. This process continues until all the sites on the resin are occupied. The resin is then backwashed with water that is supersaturated with dissolved sodium chloride salt. New chloride ions then replace the fluoride ions leading to recharge of the resin and starting the process again. The driving force for the replacement of chloride ions from the resin is the stronger electronegativity of the fluoride ions. Alum treated ion exchange resins, polystyrene resins, sulphonated saw dust resin have been used in the defluoridating process [110-112]. Synthetic inorganic ion exchangers, eg. complex metal chloride silicates, formed from barium or ferric chloride with silicic acid, also showed selectivity for fluoride. Novel materials such as Indion FR 10 (IND), and Ceralite IRA 400 (CER) [111] have also been used for removing fluoride from aqueous medium. Though percentage removal is quantitative but the efficiency is reduced in presence of other ions. Regeneration of sorbed ion-exchanger leads to fluoride rich waste which again needs to be treated. Further, the pH of the treated water changes making it unfit for drinking purpose.

Magnetic materials as sorbents

Magnetic solid phase extraction (MSPE) using magnetic particles (MPs) as the adsorbents have aroused great interest in water treatment in recent years [113]. MSPE involves the use MPs or magnetic nanoparticles which are added into the aqueous solution where the target analyte is sorbed on the surface of the magnetic sorbent which are further separated from the aqueous solution by applying an external magnetic force. The target analyte is then either desorbed by using an eluent or directly quantified on the sorbent using a suitable analytical technique. Magnetic materials especially the class of magnetic nanomaterials represents an important class of compounds that are known for their unusual properties as well as multidiscipline applications [114-119].

Advances in nanoscale and engineering suggest that many of the issues involving water quality can be addressed by use of appropriate nanoparticles. The nano-sorbents have immense potential in water purification. The high surface area to volume ratio and particle size is some of the properties of nanoparticles that provide better kinetics for the sorption of contaminants from aqueous solution. However, success of nano-size particles in the application of water purification depends on their retrieval from water bodies. Incorporation of magnetic properties to nano-sorbents provides their easy retrieval from aqueous medium using external magnetic field. Hence, the magnetic nano-sorbents based aqueous treatment processes have become one of the promising methods for the removal of toxic metal ions from aqueous streams. This approach has become more useful when polluted water contains solid residues that lead to the risk of fouling of the columns used for purification. Water treatment is greatly simplified by the employment of MSPE considering that there is no need for packing of the column with the sorbent in the case of batch mode operation, since the phase separation can be quickly and easily accomplished by applying an external magnetic field. Fig 1.2 shows a general schematic diagram of

MSPE where the sorption and elution steps are shown using a magnetic sorbent along with its retrieval of from treated solution using an external magnet.

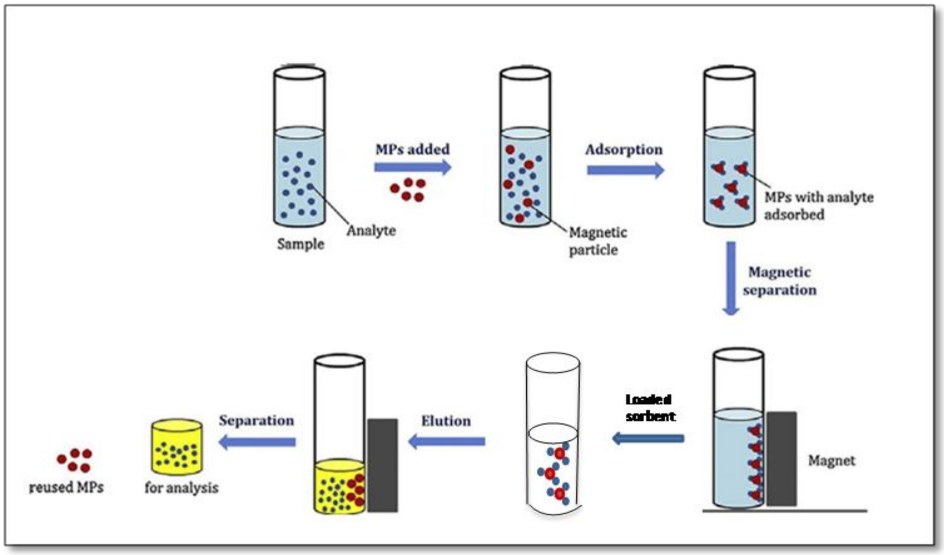

Fig. 1.2 *Schematic diagram of a magnetic solid phase extraction process*

Generally, MPs consist of magnetic elements such as iron, nickel, cobalt or their oxides and alloys having ferromagnetic or superparamagnetic properties. Ferromagnetic materials once magnetized behave like small permanent magnets and have a permanent magnetism whereas superparamagnetic particles are magnetized in a magnetic field but retain no residual magnetism after the field is removed. There are many magnetic nanoparticles which are used in MSPE. The size of the these magnetic particles varies from micro meter to nanometer. The nanometer-sized MPs (1–100 nm) have attracted a specific interest currently due to their superparamagnetic nature as well as their unique physical and chemical properties such as high dispersibility, relative large surface area and the high ratio of surface-to-volume resulting in a higher adsorption capacity [120,121].

In the recent years, Fe_3O_4 magnetic nanoparticles have attracted attention in the field of MSPE. However these magnetic iron oxide particles have some limitations such as difficulty of recycling the sorbent as Fe_3O_4 is highly susceptible to oxidation when exposed to the atmosphere and its hydrophobic surface properties which limit its dispersion into aqueous solutions and matrices [122,123]. Their lack of selectivity towards the targeted analyte in the complex matrices makes them unsuitable for real water samples.

In order to overcome such limitations, modification of existing magnetic particles with specific active groups has become a promising technique (Fig. 1.3). Modification is usually achieved by the attachment of inorganic components (e.g., silica or alumina) or organic molecules (e.g., modified with polymer or surfactant, etc.) on the surface of magnetic nanoparticles thereby improving their chemical stability by preventing their oxidation and selectivity for ion uptake. Further modification of polymer coated magnetic nanoparticles with various hydrophilic functional groups prevents the agglomeration of particles as well as provides an environment for transferring the hydrophobic iron oxide nano-particles into a hydrophilic system.

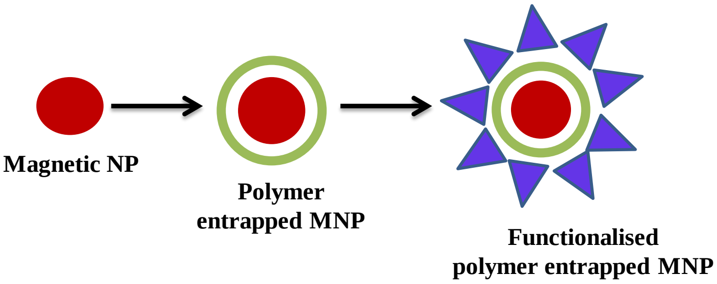

Fig 1.3 *Functionalization of magnetic nano-particles*

Most of the adsorbents used in the defluoridation of aqueous streams are in the form of powders or resins and have a tendency to block the sewer and as such are difficult to separate from the aqueous solution. Therefore, an ideal adsorbent with high surface area, good physical and chemical stability and ease of its removal should be developed for fluoride removal. The literature survey of few magnetic sorbents which have been synthesized for the removal of fluoride is discussed in the introduction chapter of the corresponding chapter.

The solid phase extraction methods for boron uptake are based on using boron selective ion exchange resins or adsorbents such as activated carbon impregnated with salicylic acid [124,125]. Several waste products of natural materials have been used as ion exchange material for removing boron. Cellulose and chitosan derivatives modified with NMDG were synthesized for boron uptake from aqueous streams [126,127]. Sawdust of several species of trees like pine, birch and oak has been used as adsorbents [128]. Tannin gel synthesized from tannin molecules, amine-modified tannin gel, calcined magnesite tailing are some of the lesser known adsorbents for boron removal [129-131].

Apart from using the natural available sorbents, there are some polymeric adsorbents which have been used for deboronation of aqueous feed. Glycidyl methacrylate (GMA)-methyl methacrylate (MMA)-DVB (divinyl benzene) terpolymer beads have been reported as an efficient method for boron removal from drinking water [132]. Several polymeric resins have been applied for the treatement of water. Diaion CRB02 and Dowex XUS 43594.00 boron selective resins have also been tested for boron removal from simulated seawater samples. A few commercial boron selective resins (BSRs) are macroporous crosslinked polystyrenic resins, functionalized with Nmethyl- D-glucamine (1-amino-1-deoxy-D-glucitol; NMG) group. The performance of these resins from model seawater was appreciable and it also eliminated boron from natural seawater reverse osmosis permeate [133,134]. There are some polymer bound sugar derivates like sorbitol and mannitol that have been widely employed for the removals of boron at trace levels but the major disadvantage is their high cost of regeneration [135-140]. For instance Amberlite IRA- 743 containing sorbitol functional groups reduces boron concentration below 1 mg L^{-1}. Despite high boron removal efficiency of 90%, this process is unsatisfactory because of expensive resin regeneration and the capacity loss during each step of regeneration [141].

The SPE method has also been applied for extracting mercury using different sorbents as extractants. Activated carbon is one of the most well-known adsorbents which have been mostly used for decontamination of mercury contaminated water [142-145]. While raw activated carbon can be effective in removing mercury at high sorbent to mercury ratios impregnation of functional groups, especially sulfur, can significantly improve the adsorption capacity. Although it was the widely used method but the high costs of the process has limited its use in real water situations. Alternative bio-materials, such as fern, fruit derived biomass and leaves of casto tree have also been investigated for mercury sorption with encouraging results [146-148]. Bark is available as a by-product of the timber industry and is effective because of its high tannin content. The polyhydroxy polyphenol groups of tannin are the active species in the adsorption process. Ion exchange takes place as mercury cations displace adjacent phenolic hydroxyl groups, forming a chelate [149-153].

Adsorbents containing sulfur-bearing groups have a high affinity for heavy metals like mercury. Some sulfur-bearing compounds include sulfides, thiols, dithiocarbamates and dithiophosphates which have been used for mercury sorption [154]. Zeolites, clay and fly ash were used for the uptake of mercury from aqueous solution [155,156]. Roberts and Rowland et al.[157] studied the removal of Hg using modified cotton. Masri et al. [158] presented mercury adsorption capacities for several natural materials but no information is given on the sorption mechanisms of these materials or their chemical constituents. Many researchers also have used natural or synthetic polymers to selectively remove Hg(II) from aqueous solution using batch process [159]. Although various conventional methods of extraction as described earlier are being used at present to solve the problem of groundwater pollution, none of them is user friendly due to some or the other limitations and has either no or very long payback period. In the recent years, membrane process has emerged as an alternative to provide safe drinking water as discussed below.

1.2.4. Membrane based methods

The use of membranes for the removal of contaminants from aqueous feed is increasing day by day because of the following advantages:

- ➢ Membranes provide an effective barrier to suspended solids, all inorganic pollutants, organic micropollutants, pesticides and microorganisms, etc.
- ➢ The process permits the treatment and disinfection of water in one step and ensures constant water quality.

- No chemicals are required and very little maintenance is needed.
- Life of membrane is sufficiently long, so problem of regeneration or replacement is encountered less frequently.
- It works under wide pH range and shows no interference from other ions.

Hence, membranes based methods are now supplementing the above listed methods that are widely used on industrial scale for the separation of targeted analytes from aqueous feed. Nowadays membrane based methods which were earlier limited to chemical laboratories as analytical tools have become an important part of industrial applications. They are used for water treatment, in packaging materials, sensors, ion-selective electrodes, fuel cells, battery separators, beverage industries and last but not the least in organic/inorganic separations. The pressure driven membrane processes have dominated the field of membrane separation till date.

Membrane is a thin sheet of natural or synthetic material that is permeable to certain substances and prevents the passage of others in solution. The first milestone of "**Synthetic Membrane**" was its application in the water softening during the Second World War [160]. The principal development in the 1980 was the emergence of industrial membrane gas separation processes e.g. Monsano prism membrane for hydrogen separation [161]. Today, membrane separation processes find wide ranging applications as discussed above.

Membranes can be divided into different types: homogeneous or heterogeneous, symmetric or asymmetric in nature, neutral membranes, ion-exchange membranes, functionalized membranes etc. Among all these the neutral membranes involve only physical interaction between diffusing species and membrane matrix. This class of membranes is generally used for water desalination as discussed in the underlying sections.

Apart from physical interactions, diffusing species can have electrostatic interactions (in ion-exchange membranes) or covalent interactions (functionalized membranes) with the membrane matrix. These interactions provide a basis for utilizing the membranes as sorbents. The use of membrane technology can provide an alternative to existing chemical processes such as distillation, extraction, fractionation and adsorption.

Membranes can in principle be used to carry out most of the separation processes and can be broadly used in two ways:

i. Membranes for filtration
ii. Membranes as sorbents

1.2.4.1. Membrane filtration

Membranes in filtration mode provide physical barriers that permit the passage of materials only up to a certain size and shape. Different membrane separation processes include micro-filtration, ultra filtration, nanofiltration and reverse osmosis.

Among these, micro filtration and ultra filtration are pressure-dependent processes, which remove dissolved solids and other substances from water to a lesser extent than nanofiltration and reverse osmosis. All these membrane based methods are used for physical separation. The extent to which dissolved solids, turbidity and microorganisms are removed by the membranes is determined by the size of the pores in these membranes. Substances that are larger than the pores are fully removed. Substances that are smaller than the pores of the membranes are partially removed, depending on the construction of a refuse layer on the membrane. All the four types of above listed membrane filtration processes are briefly described below.

Micro-filtration: Membranes with a pore size of 0.1 – 10 µm perform micro filtration. These membranes remove all the bacterial components from the solution. Micro filtration is usually implemented in different water treatment processes where particles with a diameter greater than 0.1 mm need to be removed from a liquid.

Ultra filtration: Ultrafiltration (UF) is a pressure-driven process that removes emulsified oils, metal hydroxides, colloids, emulsions, dispersed material, suspended solids, and other large molecular weight materials from water. UF membranes are characterized by their molecular weight cut-off. In ultra filtration, particles of 0.001 – 0.1 µm dimensions can be removed from the fluids.

Nano filtration (NF): Nanofiltration membranes have pore sizes from 0.0001-0.001 µm which are smaller than those used in microfiltration and ultrafiltration, but just larger than that in reverse osmosis.Nanofiltration (NF) is generally targeted to remove only divalent and larger ions. Monovalent ions such as sodium and chloride will pass through an NF membrane, thus many of the uses of NF involve de-salting of the process stream.

Reverse Osmosis (RO): The membrane with the smallest pore size comes under reverse osmosis (RO) category. These RO membranes involve reversal of the osmotic process of a solution in order to drive water away from the dissolved molecules. RO depends on ionic diffusion to effect the separation. A common application of RO is seawater and brackish water desalination. Below is the diagram outlining the process of RO (Fig 1.4). When pressure is applied to the concentrated solution, the water molecules are forced through the semi-permeable membrane whereas the contaminants are not allowed through.

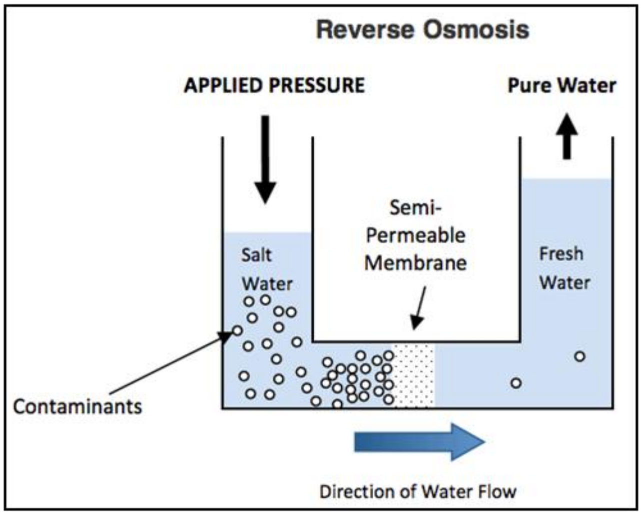

Fig. 1.4 *Typical diagram of Reverse Osmosis process*

In the recent years, RO membrane process has emerged as a preferred alternative to provide safe drinking water without posing the problems associated with other conventional methods. For proper water treatment in desalination plants a series of membranes has to be applied for water decontamination. Dialysis is another membrane treatment process which involves transport of solute from feed compartment to the receiver compartment using a membrane rather than retaining it in on membrane itself. The pores of the membrane used in dialysis are much less restrictive compared to NF and RO membranes. The solute is driven through the membrane either by Donnan effect or by an applied electric field. Electro-dialysis is another membrane based process which involves the removal of ionic components from aqueous solutions through ion exchange membranes under the driving force of an electric field.

1.2.4.2 Applications of membrane filtration methods for removal of fluoride, boron and mercury

Reverse osmosis and electrodialysis are two membrane filtration processes which are used for the removal of the above listed contaminants from aqueous feed. Defluoridation from effluents using RO technique was carried out by Ndiaye et al and it was observed that the rejection of fluoride ion was typically higher than 98% [162]. Work has been carried out by many researchers using NF and RO membranes to optimize both theoretical and experimental conditions for the retention of fluoride in the membrane system [163-172]. The removal of fluoride from diluted solution with Neosepta AHA anion-exchange membrane has been studied by Donnan dialysis and the transport efficiencies of different membranes have been compared [173]. It was observed that the transport of fluoride was maximum at pH 6 of feed phase and at pH 1 of receiver phase. Electrodialysis phenomenon has also been used for the defluoridation of aqueous streams by many research groups [174-176].

Combination of reverse osmosis with selective ion exchangers for selective removal of boron in the desalination of seawater and brackish water has been carried out [177-179]. These hybrid methods consisting of two step pathways are followed where borate is complexed using ion exchange resins and it is further separated using ultra filtration membranes [180-182]. This method is known as polymer enhanced ultra filtration method

(PEUF). The polymers used in PEUF method were: poly(vinyl alcohol) [183], glucoheptanamide derivatives of poly(amidoamine) and poly(ethyleneimine) [184], poly(glycidyl methacrylate) and poly(N,N′-diallylmorpholiniumbromide) modified with hydroxyethylaminoglycerol[185], hydroxyethylaminoglycerol functionalized to poly(glycidylmethacrylate) and poly(4-vinyl-1,3- dioxalan-2-one-co-vinyl acetate) [181], alkyl monol, diol, or triol containing polyethylenimines [186]. But usually the membrane fouling, high cost of regeneration of adsorbents and preparation of water soluble polymers for complexing boron are some of the major limitations of these hybrid methods.

Membrane filtration method has also been applied for mercury removal. Reverse Osmosis (RO) system for mercury removal consists of granular activated carbon pre-filters followed by a RO membrane. Thin Film Composite (TFC) and Cellulose Triacetate (CTA) are commonly used RO membranes for mercury removal. TFC membranes are relatively more efficient compared to CTA membrane. Both have a very high rejection rate for different forms of mercury.

However, there are certain limitations of using membranes in filtration mode such as it removes all the ions present in water, though some minerals are essential for proper growth. The water after treatment becomes acidic and needs pH correction therefore remineralization of the treated water is an added step. Lot of water gets wasted as brine and disposal of brine is a problem itself. In addition to this, the scaling up of membrane process is expensive in comparison to other methods such as adsorption based methods.

1.2.4.3 Membranes as sorbents

Membrane-based processes, with their inherent advantages, emerge as a highly competitive candidate for reclamation and reuse of water, owing to its efficiency, ease of implementation, cost, and low environmental impact. Furthermore, day by day the capital, operational, and maintenance costs for membrane systems continue to decline, making them increasingly attractive for water purification applications [187-189]. Separation using polymer membranes has become an effective technology for the removal and recovery of various metal ions. Selectivity in the membrane separation has become possible only by tailoring the existing membranes with various functional groups required for binding the ion of interest. Selectivity of a membrane towards a specific analyte is governed by many factors. Some of these are: (i) size exclusion, (ii) diffusivity, (iii) Donnan exclusion and electrostatic interactions of ions with fixed charges in the membrane, (iv) solubility/partition coefficients, (v) conditions at aqueous membrane interface and (vi) covalent interactions of desirable component (mostly metal ions) with the functional groups present in the membrane.

The physical structure of the selected membranes also plays an important role in the membrane process. Some of the parameters responsible for providing different physical structures in polymer membranes are: (a) primary structure of matrix polymers, (b) crosslinking and grafting, (c) crystallites (d) pore structure (e) connectivity of pores and (f) free volume. Pore size, pore size distribution, pore density etc. are usually controlled more precisely to improve membrane performance whenever they are to be used for any application.

Currently the membrane based separation methods are gaining attention in analytical applications because of the preconcentration step which is achieved simultaneously with separation, enhancement in the selectivity gained by using various selective functional groups, mechanical strength of the base membrane as a support, use of low concentrations of reagents and possibility of onsite application. However, use of membranes as a solid phase extractants for removal and detection of toxic ions is scarcely reported in literature. This is because the type of the matrix of the sample governs the choice of a proper type of membrane. Depending on the type of the matrix, different types of membranes are needed whose brief overview is as follows.

1.3. Types of polymeric membranes

1.3.1 Plasticized membrane

Plasticized membranes are also referred to as polymer inclusion membranes (PIM). Polymer inclusion membranes (PIMs) were first introduced by *Sugiura et.al* [190]. PIMs are prepared by the physical immobilization of a selective extractant into a plasticized polymer matrix (Fig. 1.5). Two of the commonly used polymer matrices are poly (vinyl chloride) (PVC) and cellulose triacetate (CTA) [191-192]. They are inert and highly hydrophobic polymers. The base polymer forms the skeleton of the PIM to provide mechanical strength. The chemical structure of the base polymer also plays an important role in transport of ions across the PIMs. These matrix forming polymers can be plasticized upto 70 – 80% by weight with a variety of plasticizers like 2-nitrophenyl octyl ether (NPOE), dioctyl phthalate (DOP), bis(2-ethyhexyl) terephthalate (DOTP), dioctyl sebacate (DOS) and tri-(2-ethylhexyl) phosphate (T2EHP). The network of overlapping chains of the polymer provides mechanical support to the PIMs.

The properties of these membranes can be tuned by appropriate selection of matrix forming polymer, plasticizer and extractant. Therefore, these membranes can be tailor made for a specific application without involving exotic synthetic chemistry. These membranes exhibit many advantages, viz. ease of operation, minimum use of hazardous chemicals and flexibility in membrane composition to achieve desired selectivity and separation efficiency [193,194].

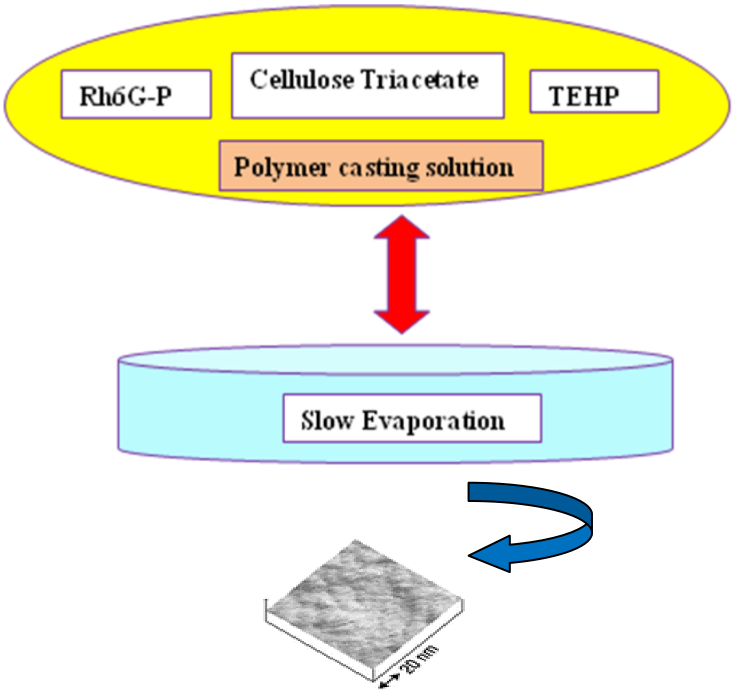

Fig 1.5 *Schematic diagram showing steps involved in the preparation of plasticized membrane*

The stability of these polymer inclusion membranes (PIMs) is amongst the major reasons for the recent rejuvenation of interest in carrier-mediated transport for selective separation and recovery of metal ions as well as numerous organic solutes. This is reflected by an increasing number of PIM investigations reported in the literature over the last two decades [195,196]. In addition to the use of the PIMs in the separation experiments a few reports in literature are also available on PIM based optical sensors for metal ion detection [197-202]. PIMs are usually preferred for making optodes for optical detection because of the high selectivity, flexibility, and chemical and mechanical stability offered by its matrix. In addition to this, the major advantage of using PIMs as optodes is based on their ease of synthesis. For the membrane type optical sensing layer, these PIMs not only act as the support for the immobilized reagent, but also enable permeation of the targeted chemical species. Therefore, researchers are focusing on the development of PIM based optodes which can be used for on-field detection of metal ions in natural waters.

1.3.2 Grafted membrane

Grafted polymer membranes are a class of membranes containing segmented copolymers with a linear backbone of one composite and randomly distributed branches of another composite (Fig 1.6). Grafting is an attractive method to impart desired functionality to any base polymer matrix. Grafting can be carried out in two ways either end-functionalized polymer chains can be grafted to the solid substrate (grafting to) or the grafting reaction can proceed by polymerization from the surface (grafting from). In both the cases a thin polymer brush layer on the solid surface is formed that determines the surface properties. The grafting mechanism is usually irreversible. Selectivity of the grafted membranes is achieved by incorporating various inorganic or organic groups that can bind to the desired analyte.

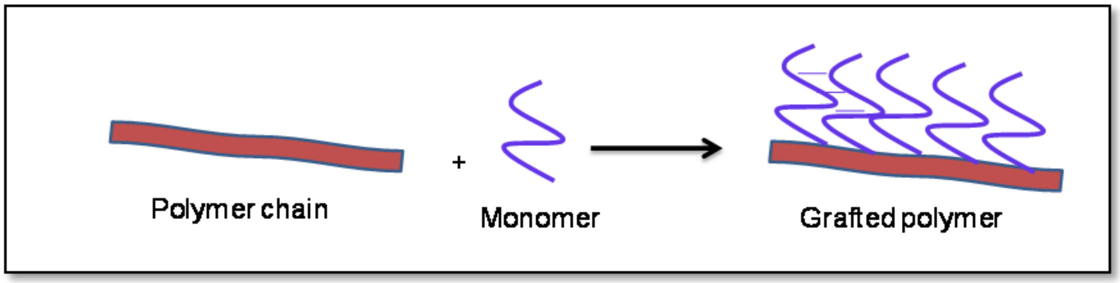

Fig 1.6 *Pictorial representation of grafted polymer*

Grafting of polymers as described above have a variety of potential applications resulting from the wide range of properties when different polymer chains are connected to form hybrid branched macromolecules. Graft polymers have been synthesized for many decades and are especially used as impact resistant materials, thermoplastic elastomers, compatibilizers, or emulsifiers for the preparation of stable blends or alloys. One of the more well known examples of a graft polymer is high impact polystyrene, which consists of a polystyrene backbone with poly butadiene grafted chains.

Crosslinking of the polymer network in the base matrix is another probability along with grafting. Formation of network structures using multidirectional chain extension is defined as crosslinking (Fig 1.7). Crosslinking may occur intramolecularly or intermolecularly.

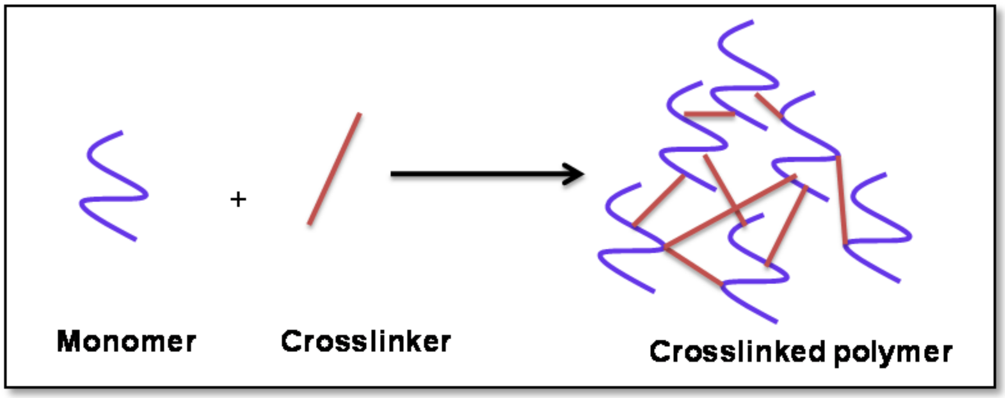

Fig 1.7: *Pictorial representation of crosslinked polymer*

Crosslinking of polymers enhances its stability, improves the mechanical characteristics and results in improved resistance to stress cracking and better fluid resistance. The grafted membranes can be synthesized using different methods of polymerization. Among various existing methods, radiation induced polymerization method has been used in the present work and hence it has been discussed in detail in the following section.

1.4 Methods of modification of polymer membranes

Depending upon the type of polymer, different techniques may be used to carry out its modification. Radiation induced method of grafting/crosslinking includes irradiation of polymeric materials with either high energy radiation (gamma rays, X rays, accelerated electrons, ion beams) or low energy U.V radiation. In all methods, the chemical structure of the polymer is altered either through the crosslinking or the grafting process as discussed above. Modification using high energy radiation such as gamma irradiation is usually most economical at lower doses (~80 kGy and below) and for large, high density parts whereas electron beam is commonly used for small parts, particularly low density parts. For easily degradable polymers, low energy UV irradiation method is used. In all these methods, the degree of crosslinking or grafting depends upon the type of base polymer and applied radiation dose. One of the benefits of using irradiation is that the degree of polymerisation can be easily controlled by the amount of dose. Both the high energy radiation and low energy UV-irradiation methods are discussed in what follows.

1.4.1 High energy radiation

High energy radiations like gamma rays or electrons interact with organic and other molecules in the polymerizing solution to create free radicals s precursors which will often chemically react in various ways. These precursor radicals thus formed results in formation of new bonds among the monomers or rearrangements in existing polymer chains. The degree of the rearrangements depends on the structure of the monomer and the conditions of treatment before, during and after irradiation. There are several advantages of high radiation grafting methods over commonly used chemical methods:

- ✓ Possibility of polymerizing monomers which are difficult to polymerize by conventional methods.
- ✓ Ease and high efficiency of polymerization with low power consumption.
- ✓ Purity of the initiators is not a concern because polymers form free radicals on its surface.
- ✓ High penetrating ability makes it appropriate for solid substrate grafting.
- ✓ Grafting of different monomers on different portions of the same polymer: mosaic grafting is possible.

Preirradiation, peroxidation, and simultaneous radiation are three different methods of irradiation of polymers which are briefly discussed below.

(a) Preirradiation technique

In this method the backbone of polymer is irradiated by high energy radiation in an inert gas atmosphere to form free radicals on its surface and then this is further reacted with a monomer at high temperature (Fig 1.8). As monomers are not involved during the radical generation stage, the possibility of homopolymerisation is negligible in this technique. The major disadvantage of this method is the formation of block polymers compared to graft polymers because of the scissoring of the direct polymer by using high energy radiation.

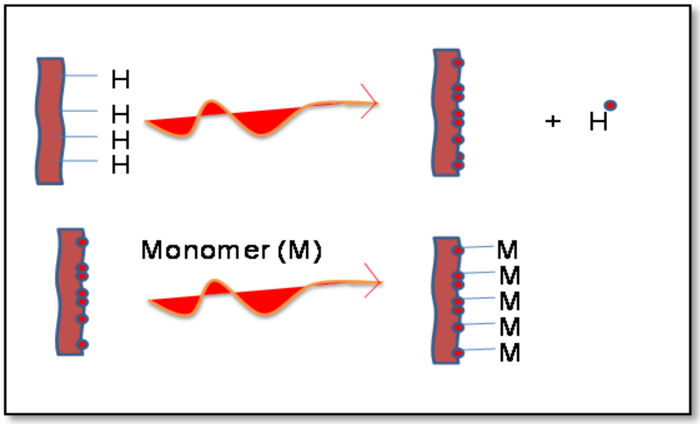

Fig 1.8 *Scheme showing preirradiation method of grafting*

(b) Peroxidation technique

In this the polymer is subjected to high energy radiation in the presence of air or oxygen. Formation of hydroperoxides/diperoxides depending on the nature of the polymeric backbone and irradiation conditions occurs on the polymer backbone. These stable peroxy products are then treated with the monomer at higher temperature, where the peroxides undergo decomposition to radicals (Fig. 1.9). The radicals thus formed are made to react with the monomer to be grafted on the polymer chain.

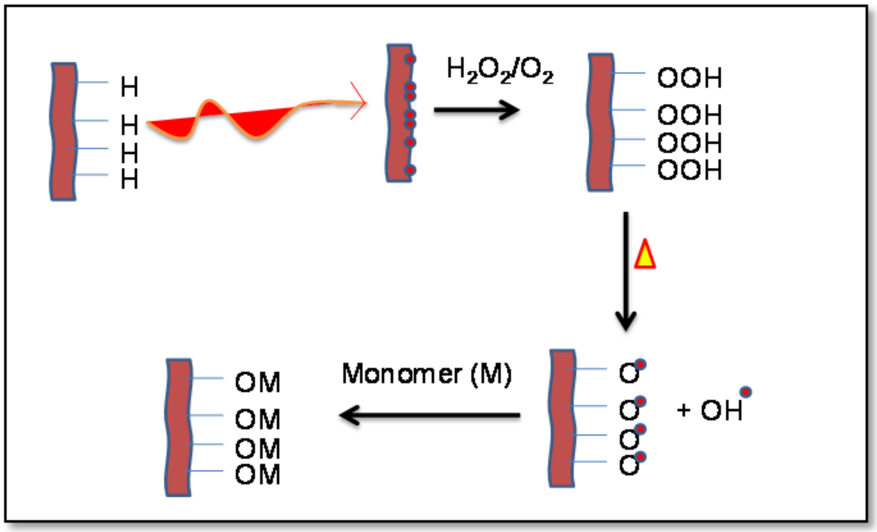

Fig. 1.9 *Scheme showing peroxidation method of grafting*

(c) **Simultaneous method**

This is the commonly used method and in this the polymer is irradiated simultaneously along with the monomer [203]. As both the monomer and substrate are exposed simultaneously to the radiation source, formation of active radicals occurs on both of them (Fig. 1.10). Further reaction is dependent on the generation of free radicals on the polymer/monomer in the reaction system. Homopolymer formation is favored over grafting if the monomer has high radiation yield. Radiation doses required to achieve graft polymerization in this method are lower than the other two methods described above.

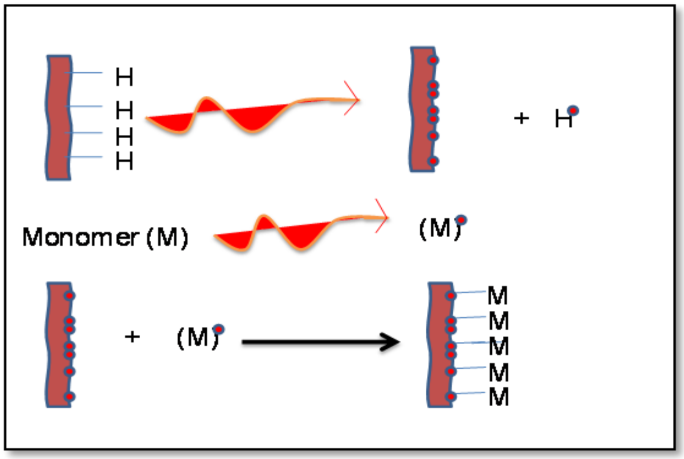

Fig 1.10 *Scheme showing simultaneous method of grafting*

1.4.2 Photoirradiation

Grafting and crosslinking using photo irradiation i.e with UV or lasers light is one of the other methods to generate radicals. In this method radicals are generated via photochemical reaction. Photoirradiation requires very low activation energy and it provides both spatial and temporal control of the reaction since light can be directed to locations of interest in the system. In addition to this, these reactions proceed under low or room temperature and grafting can be controlled on polymeric surface unlike in high energy radiation induced grafting where surface polymerization is not possible because of the penetrating nature of radiations [204,205]. There are two pathways for photoinitiator induced grafting; one is the direct method where photolysis of the chromophoric groups present on the surface occurs whereas the other one is an indirect way where radicals are generated by the photolysis of solvent or additive molecules.

The direct method shows that apart from the graft copolymer, the unwanted homopolymer is also formed if radical A• generated by the photolysis of side groups of the polymer (| - A) is reactive towards the monomer (Fig. 1.11). The chemical nature of the final product depends on the extent to which chain termination occurs via disproportionation versus combination. Combination of polymer chains usually leads to various crosslinks in the polymer matrix.

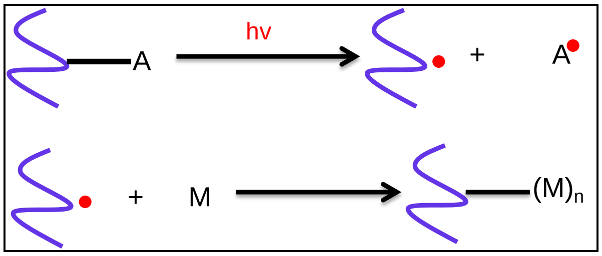

(M = Monomer; A= Photoactive group)

Fig 1.11 *Scheme showing direct method of photoirradiation*

The indirect method of photoirradiation is illustrated in the following routes (Fig 1.12). Route 1 shows the attack of free radicals on the monomer whereas route 2 illustrates the reaction of electronically excited photoinitiator molecules with the functional groups of the monomer. Usually photoinitiators are required in all those cases where the monomers have a low quantum yield.

Route 1:

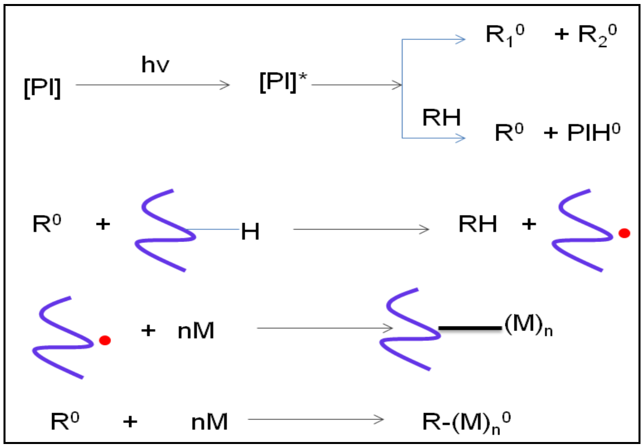

(PI: Photoinitiator, RH: Solvent, M: Monomer, R_1 nd R_2 are the fragments)

Route 2:

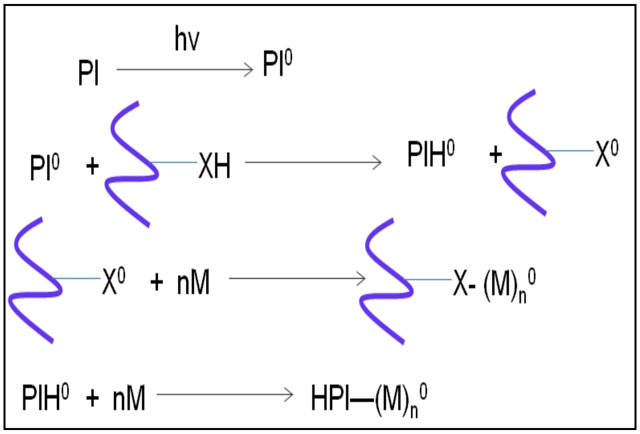

Fig 1.12 *Scheme showing in-direct method of photoirradiation*

The primary radicals thus produced react with the monomers to form graft polymers through the initiation, propagation, and termination reactions as in the usual free – radical polymerization. In the present thesis photo irradiation method has been used to introduce the required grafted monomer chains on the polymeric backbone of polypropylene sheets. The precursor grafted membranes thus formed are treated with specific organic groups or inorganic ions so as to generate selectivity towards the targeted ions.

1.5 Scope of the Thesis

Development of new separation methods for removal of targeted species is a very fascinating field in analytical chemistry. Though there are many existing separation methods as explained in the previous sections, a lot of scope exists in improving the sensitivity of existing methods and for developing better methods. The greatest of the scientific and technological challenges in removing toxic ions from different aqueous matrices lies in finding a technology that gives a net positive balance in terms of their selective removal and the other is their cost of production. Following factors has to be taken into account for developing any method for removing targeted ions from natural waters.

- ✓ The method should be capable of treating large volume of contaminated water.
- ✓ The sorbents should have high sorption capacity and kinetics.
- ✓ Chemical composition of the matrix to be treated cannot be altered therefore; sorbent has to be designed keeping in mind the targeted analyte.
- ✓ Sorbent production should not involve complicated synthetic route and the developed sorbent should be reusable making it more economical.

Functionalized inorganic-organic hybrid polymeric membranes are the new entrant in the field of membrane processes for water purification as discussed in the previous sections. Permeation selectivity of the membrane towards competing ions is an important factor for selective preconcentration of the target ions from the multicomponent aqueous feed. Generally, the selectivity is achieved by anchoring the target ions specific functional groups (receptors) in the membrane. The functionalized membranes are prepared by either physical containment or covalent attachment of the functional groups in a suitable organic or inorganic-organic hybrid matrix. The intrinsic multifunctional character of these membranes makes them potentially useful in multiple fields especially in water treatment as discussed above.

Keeping in mind the theme of the thesis, a different approach for the tailoring of existing organic polymers has been used to synthesize fixed site functionalized inorganic-organic polymeric sorbents. The fixed-site sorbents have been synthesized for the separation and preconcentration of fluoride, boron and mercuric ions from variety of aqueous matrices especially the ground-water and seawater. The mechanism of transport of ions across these fixed-site sorbents involves “ion jumping” from one site to the next. Facilitated diffusion of targeted ions in such sorbent can occur only if the “chained” carriers (fixed sites) are reasonably close to each other and have some limited mobility. Therefore, grafting/crosssinking of a desired monomer on the existing fixed-chains of a polymer base matrix was carried out. The advantages of using these fixed-site sorbents are: (1) the stability is improved; and (2) the transport of analyte is actually enhanced as these membranes are generally hydrophilic with a high functional group density.

The ion carrier complex formation involved in mass transfer of ions from aqueous to membrane matrix should have fast reaction kinetics. To achieve this, two types of the polymer base matrices: microporous and fibrous poly(propylene) sheet has been selected. The use of the fibrous base having larger void spaces within the fibers helped in providing higher accessibility of binding sites to the targeted ion.

These fixed-site membranes are most successful when ions interact with membrane through electrovalent interactions. However, the permeation selectivity of the target ions across the membrane cannot be achieved by only electrovalent interactions. The target ions should have covalent interactions with the fixed sites in the membrane for achieving desirable selectivity in facilitated transport of the target ions from aqueous phase to membrane phase. Therefore for fluoride, boron and mercury (II) sorption, study involves anchoring of optimized chemical composition of the hydrogel in the microporous poly(propylene) matrix and their further functionalization with various inorganic/organic groups for achieving desired selectivity. In addition to the fixed site-polymeric sheet sorbent for fluoride removal, a highly super-paramagnetic polymer sorbent has also been synthesized and optimized for various parameters under simulated groundwater and seawater conditions.

Similarly, the part of thesis focused on mercury uptake involves scanning of different types of functionalized membrane sorbents and optimizing their chemical composition in terms of sorption kinetics, capacity and selectivity in real water samples. The choice of poly(propylene) membrane base for the entire study was based on its inherited advantages as listed below.

- ✓ Reproducible geometrical form, simplicity and amenability to large volumes.
- ✓ Incorporation of functional groups by chemical bonds: Uniform material with high accessibility of binding sites.
- ✓ Non-interfering matrix and hence direct quantification using EDXRF.
- ✓ Applicability in wide pH range and salt concentration.

Comparison of all the sorbents synthesized in the present research work with the existing sorbents in terms of the key parameters that affect the sorption uptake of the desired analyte has been made. Along with the development of newer sorbents, the detection and monitoring of toxic elements at ultratrace concentrations in natural and waste waters is important. Therefore the last part of the study involves synthesis of a visual optode membrane based sensor for on-site detection of mercuric ions in natural waters. The flat sheet polymer sorbents having fixed binding sites are amenable for scaling up for water

Chapter -2

EXPERIMENTAL

2.1 Introduction
2.2 Materials
2.3 Apparatus
  2.3.1 UV Multi-Lamp Photoreactor
  2.3.2 Micrometer Screw Gauge
  2.3.3 pH Meter
2.4 Synthetic Strategies for Different Polymer Sorbents
  2.4.1 Synthesis of Polypropylene Sheet Sorbents
    2.4.1.1 In-situ UV Irradiation Method
    2.4.1.2 Room Temperature Crosslinking Method
  2.4.2 In-House Membrane Preparation by Solution Casting Method
  2.4.3 Synthesis of Magnetic Resin Sorbent
2.5 Characterization Techniques
  2.5.1 Degree of Grafting

2.5.2 Water Uptake Capacity
2.5.3 Scanning Electron Microscopy (SEM)
2.5.4 Infra-Red Spectroscopy (IR)
2.5.5 Energy Dispersive X-Ray Fluorescence Spectrometer (EDXRF)
2.5.6 UV-Visible Spectroscopy (UV-Vis)
2.5.7 X-Ray Diffraction (XRD
2.5.8 Vibrating Sample Magnetometer (VSM)
2.6 Analytical Instrumentation
2.6.1 Ion Exchange Chromatography (IC)
2.6.2 Inductively Coupled Plasma Mass Spectrometry (ICP-MS)
2.6.3 Cold Vapor Atomic Absorption Spectroscopy (CV-AAS)
2.7 **Calibration of Instrumental Methods**
2.7.1 Linear Calibration Method
2.7.2 Standard Addition Method
2.7.3 Internal Standard Method
2.8 Batch Sorption Studies
2.9 Sorption Isotherms
2.9.1 Langmuir Isotherm

	2.9.2	Freudlich Isotherm
2.10	Sorption Kinetics	
	2.10.1	Pseudo First-Order Kinetic Model
	2.10.2	Pseudo Second-Order Kinetic Model

2.1. Introduction

This chapter deals with the methods used for the synthesis of fixed site membranes for selective extraction of fluoride, boron and mercuric ions from aqueous solution. It also presents a method of synthesis of a magnetic polymer composite for fluoride removal.

The details of various apparatus, materials used during the entire course of the present work have been briefed in this chapter. Different techniques that were employed for the characterization of synthesized membranes/sorbent are discussed in this chapter. The chapter also deals with the details of the sorption studies, optimization of various sorption parameters and the methodologies used for the determination of fluoride, boron and mercury in aqueous matrices/ polymeric membrane.

2.2. Materials

All the reagents used in the present work were of A.R. grade. Nano pure water having 18.2 MΩ cm^{-1} of specific resistance (Bransted Easy pure RF compact ultra pure water system) was used throughout the experiments. Bis[2-methacryloyloxy)-ethyl] phosphate (MEP), N-N-methylene-bis-acrylamide (MBA), α,α’-dimethoxy-α’-phenyl acetophenone (DMPA), acrylamide, ammonium persulphate, boric acid, tetramethylethylene-diamine, poly(vinylbenzyl chloride) (60/40 mixture of 3- and 4- isomers with an average molecular weight M_n ca. 55,000 and M_w ca. 100,000) , piperazine, N-methyl-D-glucamine (NMDG), cellulose triacetate, rhodamine 6G, Tri-(2-Ethylhexyl) phosphate (TEHEP), hydrazine monohydrate, phenyl isothiocyanate were procured from Sigma-Aldrich (Steinheim, Switzerland). sodium borohydride ($NaBH_4$), silver nitrate salt ($AgNO_3$), dichloromethane, tetrahydrofuran (THF), methanol, zirconium oxychloride ($ZrOCl_2$) and

N,N’ dimethylformamide (DMF) were obtained from Merck (Mumbai, India) and were used as received. Fe_3O_4 nanoparticles (20-30 nm) were procured from J.K. Impex (Mumbai, India). Nitric acid and hydrochloric acid used were of supra pure grade procured from E. Merck, Germany.

pH of the solutions was adjusted by the addition of either 0.1 mol L^{-1} HCl or 0.1 mol L^{-1} NaOH (M) solutions. Aqueous stock solutions of 1000 mg L^{-1} of F^-, boric acid, Hg^{2+}, K^+, Na^+, Ca^{2+}, Mg^{2+}, Cd^{2+},Cr^{2+},Ni^{2+},Cu^{2+}, Pb^{2+} and Fe^{2+} were prepared from their respective salts.

Two types of polypropylene membranes were used as substrate for the synthesis of fixed site sorbents. These were thermally bonded non-woven polypropylene macroporous fibrous sheet (NK Filter Fabric, Mumbai, India) and microporous polypropylene flat sheet membrane (Accurel^R 1E R/P from Membrana) were used as substrates The fibrous substrate was having thickness of 2 mm. The microporous polypropylene flat sheet membrane (Accurel^R 1E R/P from Membrana) has a nominal pore size of 0.1 µm, porosity 80% and thickness of 92.5 µm.

2.3. Apparatus

2.3.1. UV Multi-Lamp Photoreactor

The UV multi-lamp photoreactor was procured from Heber Scientific (Model No. HML-SW-MW-LW-888, India). The photoreactor consisted of eighteen lamps (8 watt each) arranged in circular manner. These eighteen lamps were separated into six sets emitting a fixed wavelength (λ)(254, 312 and 365 nm). At a time, four membranes of 6x6 cm^2 can be irradiated by fixing them on a glass plate between polyester sheets followed by mounting them in the photoreactor. The irradiation time was optimized depending on the percentage grafting required and the wavelength of the irradiation was chosen depending on the photoinitiator used in the polymerizing solution. In the present work 365 nm wavelength was kept fixed for all the irradiation experiments. The schematic representation of UV photoreactor is shown in Fig. 2.1.

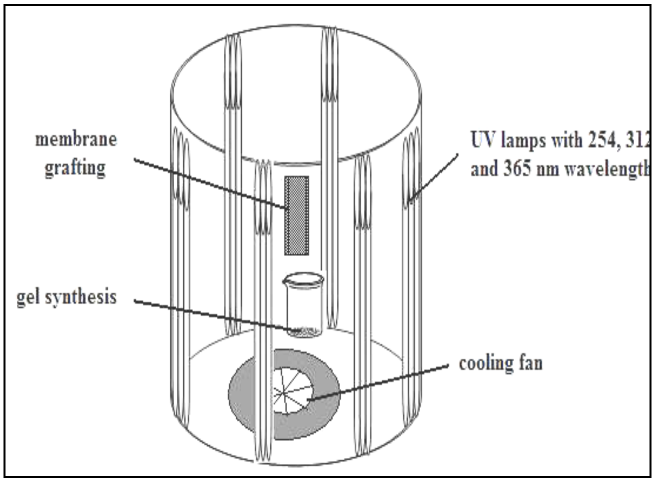

Fig. 2.1 *Schematic diagram of multi-lamp photo-reactor*

2.3.2. Micrometer Screw Gauge

The thickness of the nascent and grafted membrane samples was measured using a digital Micrometer Mitutoy (Tokyo, Japan) with a precision of ±1μm.

2.3.3. pH Meter

The pH of all the working solutions was measured using the pH meter (Metrohm 780,Germany). Before measuring, the pH meter was calibrated periodically using standard buffer solutions having pH 4, 7 and 9. The precision in the pH measurements was within the relative standard deviation of 2%.

2.4. Synthetic Strategies for different polymer sorbents

Polymer sorbents can be synthesized in different forms viz. gels, resins and membranes. In this work sorbents in the form of membranes and resin have been synthesized and the different methods of synthesis are described below.

2.4.1. Synthesis of polypropylene sheet sorbents

To synthesize various sorbents in the form of sheets two approaches were followed. The first approach is based on tailoring the properties of the commercially available microporous and fibrous polypropylene (PP) sheets using various polymerization techniques and the second approach is employing solution casting method for in-house synthesis of polymer inclusion membranes. Both of these approaches are discussed in the following section.

2.4.1.1 I*n-situ* UV irradiation grafting on the polypropylene membrane

UV-irradiation method has been used for developing the grafted sheet sorbents for solid phase extraction of fluoride and mercury. Depending upon the functionality required for selective extraction of these analytes various functional groups were grafted on the commercially available polypropylene as described below.

(i) For Fluoride sorption

Bis[2-methacryloyloxy)-ethyl] phosphate (MEP) grafted polypropylene membranes (MEP-PP)

The pictorial representation and the scheme employed for the synthesis of fixed site functionalized sorbents for selective fluoride extraction is given in Fig 2.2. Briefly, the monomer MEP (0.25 g) along with fixed amount of cross-linker MBA (0.00599g, 5 mol % of monomer) was dissolved in 1:1 mixture of DMF and methanol. The solution was kept for ultrasonication. After a clear solution was obtained, DMPA (0.005g) the UV-initiator was added to this solution. The amount of UV-initiator was taken as 1 wt % as this was found to be minimum quantity required to initiate the bulk polymerization. The host poly(propylene) microporous and fibrous host substrates (5×5 cm area) were immersed in 5 mL solution of ethanol for 5- 10 minutes before soaking them in the polymerizing solution. Host substrates were immersed in the solution for overnight so as to make sure that there pores are saturated with the polymerizing solution. The excess of polymerizing solution adhering on the surface was removed using tissue paper. The resultant solution filled substrates were sandwiched between two transparent polyester sheets to prevent any possible loss of solution filled in the pores. Care was taken to remove excess grafting solution and air bubbles trapped between the membrane and polyester sheets covering the membrane surface. Finally, the sandwiched substrates were exposed to 365 nm UV light in a multilamp photoreactor for a period of 15 min. After exposure in the photoreactor, the membranes were removed and washed thoroughly with hot DMF, methanol and distilled water to remove the un-polymerized components.

Continuous washing followed by weighing of the substrates was carried out till the constant weight of each membrane sample was obtained. Conditioning of the so obtained grafted samples was carried out by immersing them in aqueous solution having 0.25 M NaCl for 24 h.

Preparation of Th-MEP-PP fixed site membrane for fluoride sorption

To make them fluoride selective, the MEP grafted polypropylene substrates were equilibrated with 25 mL of $Th(NO_3)_4$ having 100 g L^{-1} concentration in 1 M HNO_3 for overnight with constant stirring. After equilibration, samples were washed thoroughly with 1 M HNO_3 and water, and used for the experiments.

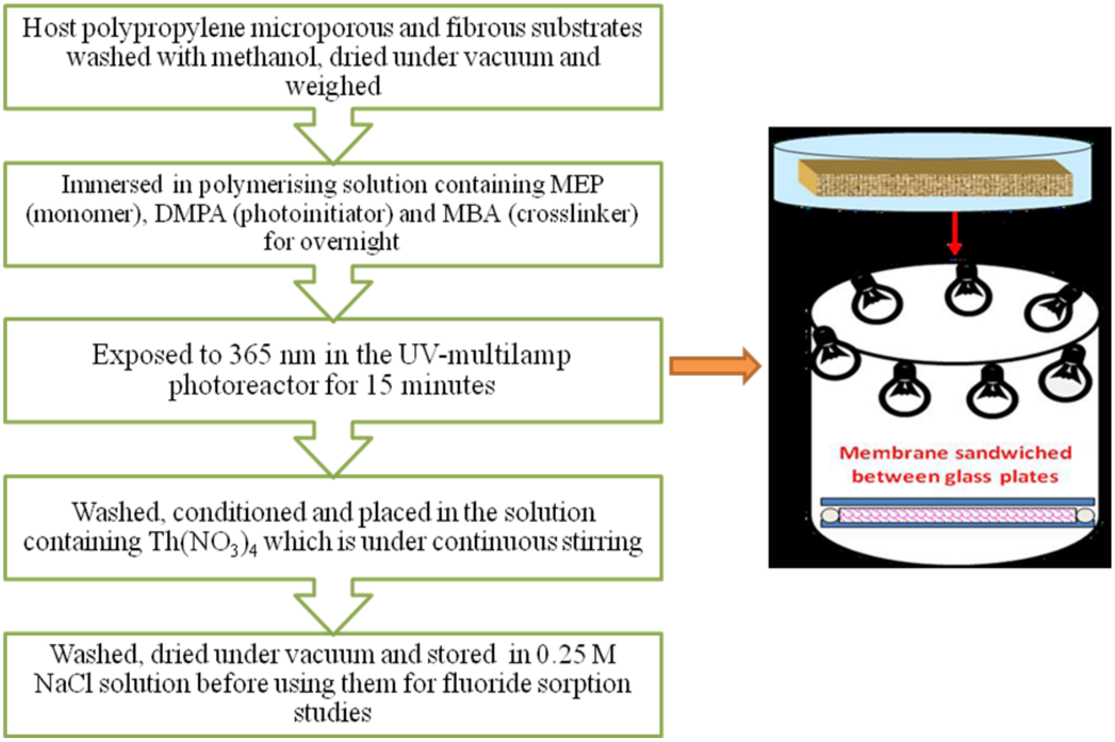

Fig 2.2 *Steps involved in the synthesis of tailored sorbents for fluoride*

(ii) For Mercury sorption

Synthesis of polyacrylamide grafted polypropylene membranes (PAM-PP)

Acrylamide (AM) was chosen as a monomer to be grafted in the host polypropylene (PP) membranes for the mercury sorption. For this the membranes (5x5 cm^2) were immersed in a 1 : 1 mixture of DMF and methanol containing 0.3g of monomer acrylamide, 0.006 g of UV initiator DMPA (1 wt% of monomer) and 0.0049 g of cross-linker MBA (5mol% of monomer) for 3 h. Excess polymerizing solution adhering on the surface was removed and membranes were irradiated using UV irradiation by sandwiching them in the polyester sheets as described above. Washing of the grafted membranes was carried out using a 1: 1 mixture of hot DMF and methanol followed by drying until constant weight is obtained. Fig. 2.3 shows the schematic representation of polymerisation of as taken acrylamide to form polyacrylamide in the pores of the host substrate.

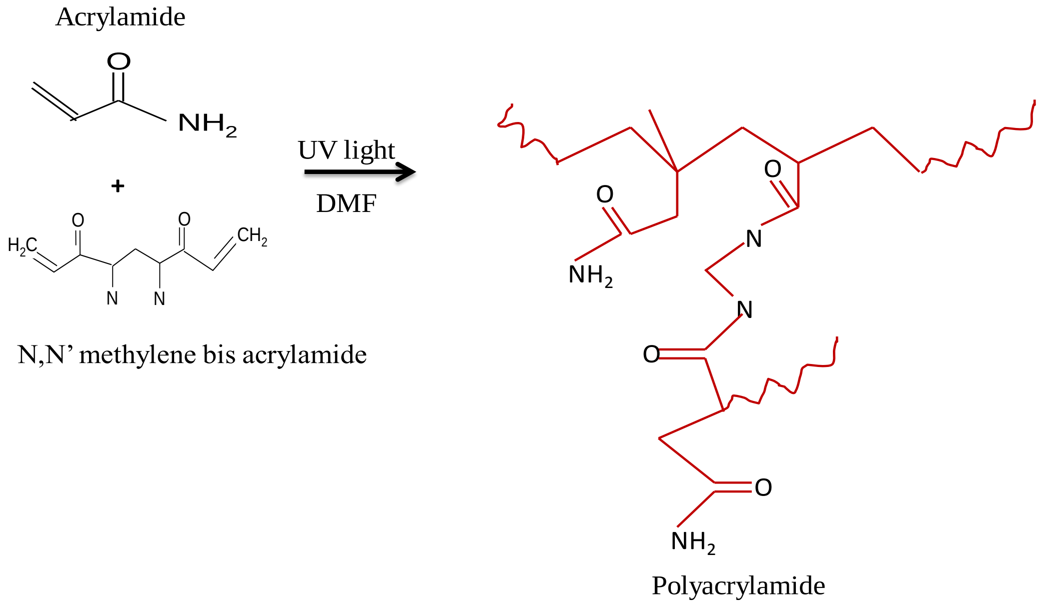

Fig. 2.3 *Synthesis of polyacrylamide in polypropylene substrate by in-situ UV grafting*

Preparation of Ag-PAM-PP fixed site membrane for mercury (Ag-PAM-PP)

The poly(acrylamide)-grafed substrates were further treated overnight with a 1 mmol L^{-1} solution of $AgNO_3$ at room temperature. The in situ reduction of Ag^+ ions incorporated in the poly(acrylamide) sheet samples was carried out by immersing them in 25 mL of well-stirred 0.01 M sodium borohydride solution for 30 min at 25^0 C. After reduction, the sorbent samples were washed with water. These Ag Np embedded sorbent sheets (Ag-PAM-PP) were further used for experiments by cutting them into a fixed size of 2x2 cm^2.

2.4.1.2 Room temperature crosslinking in the polypropylene membrane

(iii) For boron sorption

To synthesize the fixed site extractive sheet for extracting boron from natural waters, room temperature crosslinking method of polymerization was carried out. A preformed polymer polyvinylbenzyl chloride (PVBCl) was selected which can be easily polymerized in the pores of polypropylene sheet using a diamine based crosslinker.

Synthesis of poly(vinyl)benzyl chloride crosslinked polypropylene membranes (PVBCl-PP)

The poly(vinylbenzyl chloride) (PVBCl) was dissolved in N,N'-dimethyl formamide (DMF) to obtain concentration in the solution as 0.15g mL^{-1}. A solution of crosslinker piperazine (concentration determined by crosslinking ratio required) in DMF was prepared separately. Appropriate volumes of solution containing PVBCl and piperazine were rapidly mixed so that their ratio in the resultant mixture was 1:5 mole %. The solution was spread on a weighed piece of poly(propylene) microporous membrane (6cm x 6 cm) placed on a glass plate.. The excess solution was removed gently by a glass rod . Finally, the filled poly(propylene) membrane was left for 16 h at room temperature to allow crosslinking to occur. The pore-filled membranes were washed with methanol to remove unreacted PVBCl and piperazine. Washing was repeated till constant weights of membrane samples were obtained.

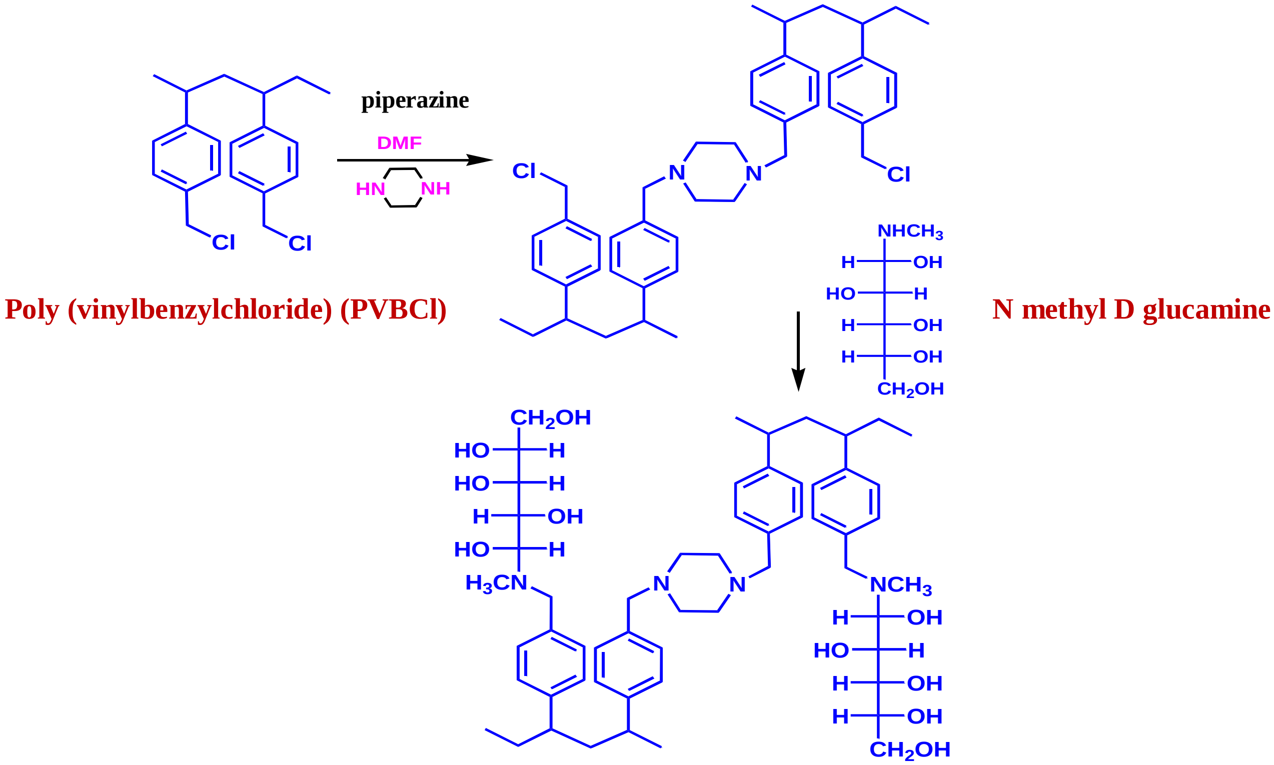

Fig. 2.4 *Reaction scheme involved in the synthesis of NMDG functionalized PVBCl sorbent*

N methyl D glucamine functionalized PVBCl crosslinked sorbent membrane

The PVBCl crosslinked membranes were further chemically modified with 1 % solution of N-methyl D glucamine (NMDG) in DMF for 8 h at 40^0 C. After equilibration, membrane based sorbents were washed thoroughly with deionised water, and used in the experiments. NMDG was cosen because of the presence of vicinal diols which can help in selective binding of boron present in its neutral form in natural waters. The scheme of crossinking of polymer along with its functionalization with the boron selective group - NMDG is shown in Fig. 2.4.

2.4.1.3 In-house membrane preparation by solution casting method

(iv) For mercury

A polymer inclusion membrane (PIM) for mercury detection and quantification was synthesized using solution casting method. Different types of extractants can be immobilized in the polymer solution to be casted as sheets depending on the targeted analyte. As aim was to develop an optode / optical sensor for mercury detection, phenylthiosemicarbazide based rhodamine 6g derivative was incorporated in the base matrix as explained below.

Rhodamine derivative incorporated cellulose triacetate (CTA) membranes

Cellulose triacetate (0.1 g) was dissolved in 6 mL of dichloromethane with continuous stirring using a magnetic stirrer. 0.05g of plasticizer tri-(2-ethylhexyl) phosphate (TEHP) with varying amount of synthesized Rhodamine-6G derivative from 0.001 to 0.007g were dissolved in 1 mL of dicholoromethane separately. Both the solutions were mixed and ultrasonicated for 5 min to form a solution. Resultant solution was poured into a 10.0 cm flat bottom petri dish and covered loosely with a lid. After 8 h, the membrane was casted with controlled evaporation of the dichloromethane and the transparent membrane was peeled off from the petri dish using water. The membrane thus prepared was thoroughly washed with distilled water to remove any soluble components. The synthesized membrane was further cut into 2x1 cm^2 size pieces and used in all the experiments.

2.4.2 Synthesis of magnetic polymer sorbent

(v) For Fluoride

For synthesizing a polymeric magnetic composite polyacrylamide was synthesized by bulk polymerization of acrylamide monomer along with crosslinker in the presence of Fe_3O_4 nanoparticles. 2.6 g acrylamide (AM), 0.31 g N,N'-methylene-bis-acrylamide (MBA), 0.2 mL of 2 wt. % ammonium persulphate (initiator) were mixed together in mL 10 mL de-ionized water in addition to the Fe_3O_4 nanoparticles. Different weight percentage of Fe_3O_4 nanoparticles (1 wt. %, 5 wt. % and 10 wt. %) were added keeping the other components fixed so as to vary the magnetisation required for magnetic separation .The mixture was sonicated for 10 min for better dispersion of nanoparticles into polymerizing solution. Tetramethylethylenediamine (0.02 mL of 1 wt. % solution) was added drop-wise to the above solution for catalysing the polymerizing reaction and the mixture was stirred at 40^oC for 30 min. The resulting gel was left undisturbed for 2 h for completion of polymerization reaction. Finally, the gel was washed repeatedly with distilled water to remove excess reactants if any. It was dried under IR lamp for 24 h and ground in a mortar with a pestle to a fine powder.

Zirconium incorporated polyacrylamide (Zr-PAM) magnetic sorbent

To achieve selectivity towards fluoride sorption, modification of the synthesized composite was done by equilibrating it with 5 wt. % zirconium oxychloride solution for 24 h (Fig. 2.5). The resultant magnetic composite so formed was filtered and washed repeatedly with de-ionized water and used for the experiments.

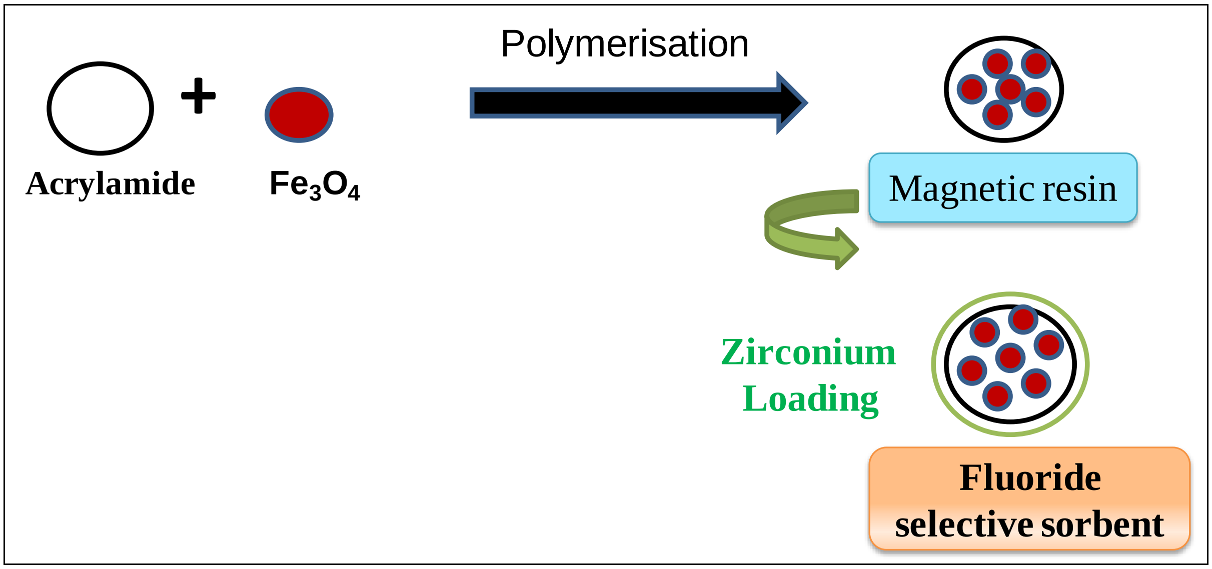

Fig. 2.5: *Pictorial representation of synthesis of magnetic composite for fluoride*

2.5 Characterization of sorbents

The above synthesized polymeric sorbents were characterised by different physical and chemical characterization techniques as given below.

2.5.1. Degree of Grafting

Degree of grafting is an important parameter for the characterization of fixed site membranes. The grafting yield gives an idea of the optimum concentration of various components entrapped in the polymer substrate.

In the present work, the degree of grafting of polymerization in the membrane samples was determined gravimetrically from the knowledge of weights of membrane sample before ($W_{nascent}$) and after grafting ($W_{grafted}$) using following equation:

Degree of grafting (%) = $(W_{grafted} - W_{nascent}) / W_{nascent} \times 100$ (2.1)

The composition of the polymerizing solution was optimized in such a way so as to obtain grafting percentage close to 100%. This was done to make sure that the grafting is limited to the pores of the substrate. Higher degree of grafting leads to the accumulation of grafted polymer on the surface of the polymer sheet which in-turns leads to its increased thickness. The increased thickness of the sorbent makes the binding sites less accessible to the targeted analyte. To confirm that the grafting is limited to the pores, thickness measurements of the membrane before and after grafting were carried out using digital micrometer.

2.5.2 Water uptake capacity

The water uptake capacity is another important property of the synthesized polymeric sorbents for deciding the hydrophilicity of the grafted substrates and hence the uptake of target analytes in the sorbents. It is also determined gravimetrically using following equation:

Water uptake capacity (%) = $(W_{wet} - W_{dry})/W_{dry} \times 100$ (2.2) where W_{wet} is the weight of wet sorbent sample equilibrated with deionized for overnight, and W_{dry} is the weight of the dried sample under vacuum until constant weight is obtained. The percentage water uptake gave an idea of the hydrophilicity of the synthesized polymer substrate. The as-such taken base (poly(propylene)) membrane was hydrophobic but the incorporation of the desired monomers gave a hydrophilic character to the polymerized substrates. The hydrophilicity of the substrates enables the easy access of the targeted analytes present in aqueous solution to the sorption sites available on the sorbent.

2.5.3 Scanning electron microscopy (SEM)

SEM technique is a versatile tool for studying the surface morphology, particle size, magnetic domains, and surface defects of materials. SEM can achieve higher magnifications than optical microscopes because unlike optical microscopy, one does not look through lenses at the actual sample, but observes images of the sample created by the instrument’s electronics. In a typical SEM, a source of electrons is focused into a beam of a very fine spot size of ~5 nm having energy ranging from a few hundred eV to 50 KeV, to examine a very small area of an object.

As the electrons strike and penetrate the surface, a number of interactions occur as shown in the Fig 2.6. These interactions give rise to different phenomena and hence different images. In addition to secondary electron signals, X-rays characteristic of the elemental composition of the sample can be mapped to sample images, and back-scattered electrons can also be collected and displayed. Secondary electrons having energy between 0-40 eV are easy to collect as they are created near the surface of the sample and are sensitive to the topography of the sample.

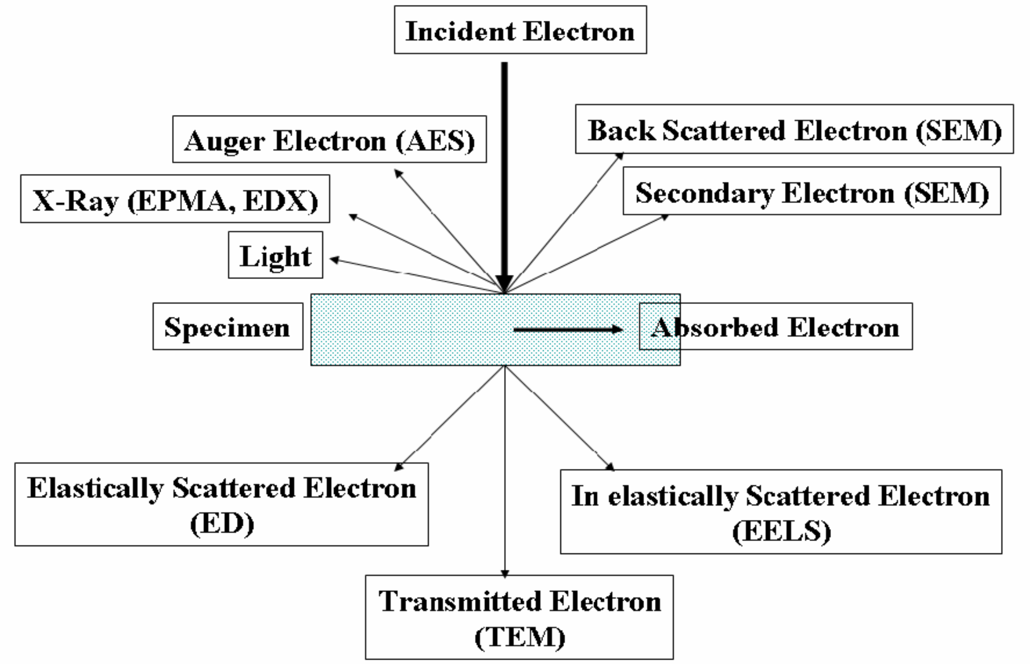

Fig 2.6 *Depiction of different phenomena occurring on interaction of electron beam with the specimen*

A typical instrumentation of SEM is shown in Fig 2.7. Depending on the type of interactions the emitted rays are detected by a silicon-lithium (Si(Li)) detector and separate signals are obtained due to high resolution of Si(Li). Each signal is collected, amplified and corrected for absorption and other effects to give an image. The collection of secondary electrons by the detector gives rise to the secondary /scanning electron image (SEM). SEM analyses are conducted in vacuum environments. All non-conductive samples must be coated with electrically conductive coatings before they can be observed in SEM It is also possible to carry out qualitative and quantitative analysis of various elements present (atomic number greater than 11) in the sample exposed to electron beam, using energy dispersive analysis of X-rays (EDAX or EDX).

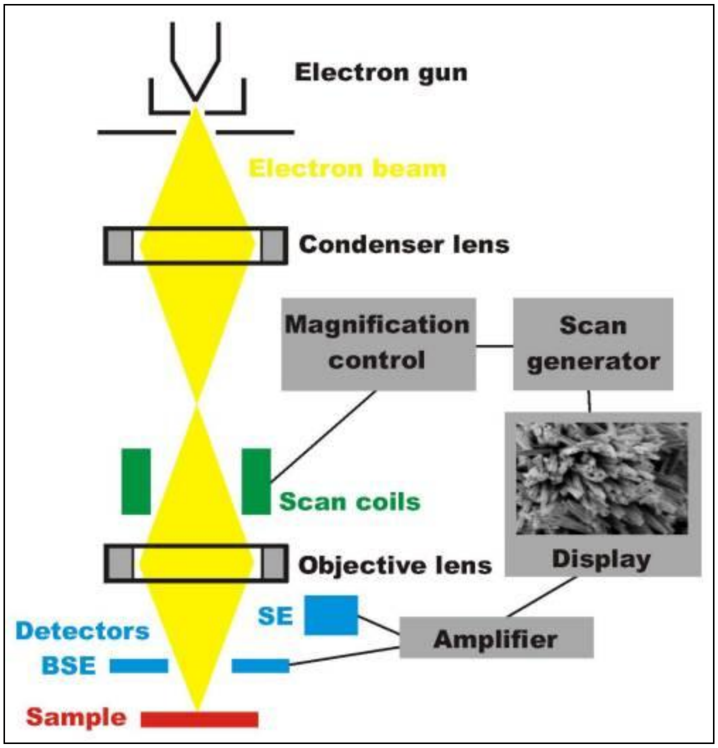

Fig. 2.7 *Various components of a typical Scanning electron micrograph (SEM)*

In the present study SEM was used to determine surface morphology of the polymer substrate before and after grafting. The EDX analysis was carried out for qualitative analysis of the analyte sorbed in the host membrane/sorbent material. The surface morphology of the synthesized membrane sorbents was analysed using AIS2100 SERON Tech. SEM, South Korea, equipped with energy dispersive X-ray (EDX) spectrometer.

A common problem encountered during recording of the SEM images for polymeric membrane samples is the destruction of the sample due to build-up of charges, or the strong electric currents produced by the electron beam. In order to avoid the charging effect on the samples during SEM/EDX measurements, a thin layer of gold was deposited on the samples by thermal evaporation using a tungsten filament at a base pressure of 2 x 10^{-6} Torr. Under these conditions it was possible to study the physical structures of the different grafted substrates. Images of the sample surfaces were recorded at different areas and magnifications.

2.5.4 Infra-red spectroscopy (IR)

IR is a technique used for identifying different functional groups present in the organic and inorganic materials and to determine the presence or absence of certain types of bonds. For example, double and single bonds associated with carbon-hydrogen and carbon oxygen bonding (=C-H,-C-H, C-O and C=O) can be distinguished by IR absorption.

When a sample is illuminated by IR radiation of the appropriate frequency, atoms, ions, and functional groups present in molecules starts vibrating about their bonds and the energy of the incoming radiation is absorbed. The absorbed energy will lead to either bending or stretching of the bonds present in the molecules. Each bending and stretching vibrational mode of a molecule or functional group will absorb at a particular frequency. Infra red spectroscopy measures the absorption of this incident infra-red radiation as it passes through the vibrating atoms of a molecule. IR sensitive vibrations are often associated with changes in dipole moments. A typical instrumentation of IR is shown in Fig 2.8.

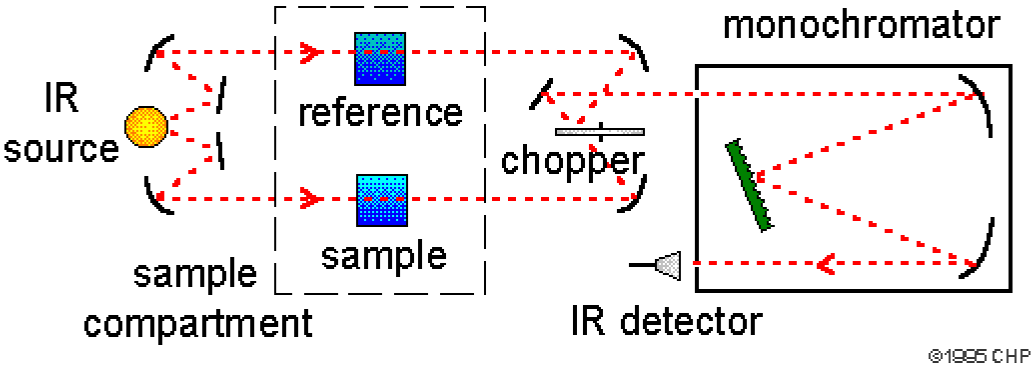

Fig 2.8 *Schematic diagram of Infrared spectroscopy system*

In the current research work, the presence of functional groups and the signature of chemical modification in the membranes/sorbent were confirmed by the presence of characteristic bands in their respective IR spectra. The IR spectra of the membrane samples were recorded using Diamond attenuated total reflectance (ATR) (IR Affinity, Shimadzu spectrophotometer). The spectrometer has a resolution of 4 cm^{-1}, and an average of 40 scans can be recorded. The spectrum of the magnetic polymer sorbent was recorded by powdering it in liquid nitrogen and mixing with KBr. The pellets were made by applying pressure of around 82 kg cm^{-2}. The pellets thus formed were subjected to the IR radiations in the IR spectrometer and the resultant data obtained was interpreted with the help of an-inbuilt library.

2.5.5 Energy Dispersive X-ray fluorescence spectrometer (EDXRF)

X-ray fluorescence technique (XRF) is a non-destructive technique used for the qualitative and quantitative detection of elements (At No. >11) in various materials. The elements can be detected upto a few ppm or above. In this technique material is exposed to X-rays of high energy. When X-ray photon strikes an atom in the sample the energy is absorbed by the atom. If the X-rays photon energy is high enough, a core electron is ejected out of its atomic orbital. An electron from an outer shell then occupies the hole left behind by emission of core electron. This transition gives off an X-ray of fixed, characteristic energy of the element/ in the sample that can be detected by a fluorescence detector. The energy needed to eject a core electron is equal to the binding energy and therefore is characteristic of each element. The transition of an L shell electron to the K shell is termed a K_α transition, while an M shell electron to the K shell is a K_β transition (Fig 2.9).

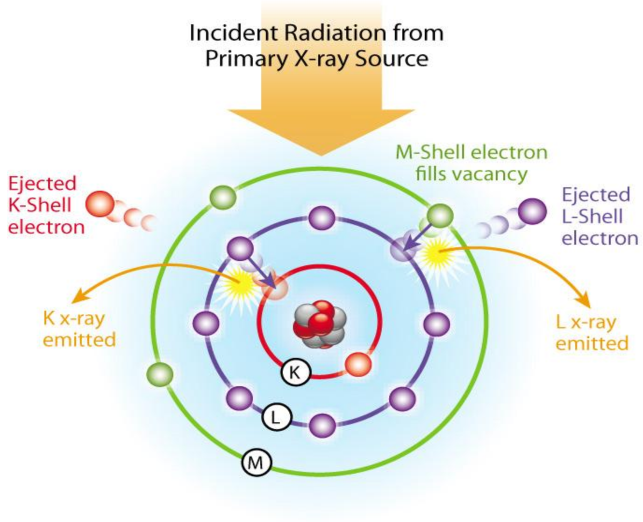

Fig 2.9 *Consequence of interaction of incoming X-ray radiation*

Two types of spectrometers are used for recording the emitted X-rays; Wavelength dispersive spectrometers (WDX) and Energy dispersive spectrometers (EDX). Both WDX and EDX employ an X-ray source for exciting the sample. Essentially, energy-dispersive X-ray spectrometry differs from wavelength-dispersive only in the means used to disperse (separate) the several spectral lines emitted by the specimen.

Wavelength dispersive spectrometers (WDX or WDS): The emitted photons are separated by diffraction on a single crystal before being detected and then energy and intensity of the dispersed X-rays are measured by a Si(Li) detector.

Energy dispersive spectrometers (EDX or EDS): the energy of the emitted photons are measured using a high resolution detector like Si(Li). The EDX spectrometers are usually smaller (even portable), cheaper and the measurement is faster, but the resolution and the detection limit are inferioras compared to the WDX spectrometers. The basic instrumentation of EDXRF is shown in Fig 2.10.

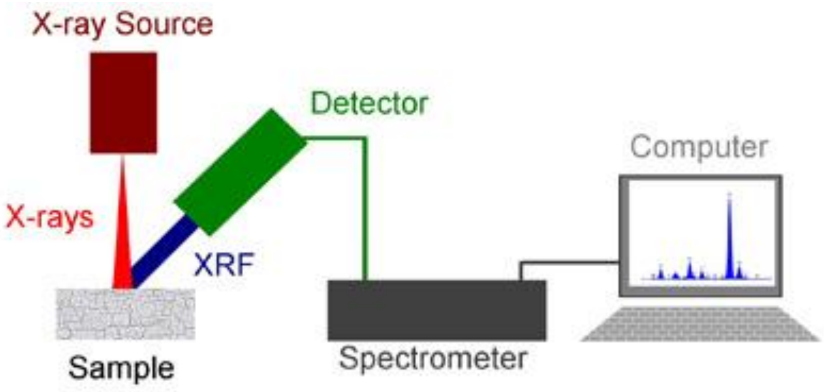

Fig 2.10 *Components of a typical XRF*

In the present work EDXRF measurements were carried out using an EX 3600-M spectrometer (Jordan valley AR Ltd. (Migdal Haemek Israel) equipped with a Rh source along with an assembly of six filters (Cu, Fe, Mo, Rh, Sn, and Ti) and a Si (Li) detector maintained at liquid nitrogen temperature was used. The resolution of the Si(Li) semiconductor detector is 139 eV at 509 keV Mn K_{α}. In the sample chamber, the samples were placed in teflon cup assemblies, whose bases were fitted with mylar film having thickness of 6.3 μm. The X-ray cross-sectional area available to the sample is circular with an internal diameter of 8mm at the base of the Teflon cup assembly. The entire fluorescence spectrum was recorded using a solid state detector which was then processed using a multichannel analyser to obtain the information on the energy scale. For each incident X-ray photon, the detector generated a pulse of electric current. The detector output is amplified and subjected to electronic pulse-height analysis to separate the pulses on the basis of their heights which are proportional to the incident X-rays energies. By appropriate setting of the operating parameters, the pulses of each line of interest can be measured individually. The integrated peak area for each X ray peak was calculated from the pulse height spectrum using the NEXT software. In the present work the EDXRF measurements were carried out for the qualitative and quantitative determination of various elements present in the membrane sorbents or the magnetic sorbent.

2.5.6 UV-visible absorption spectrometry (UV-Vis)

UV Vis spectrometers are the most important analytical instrument in the modern day laboratory. It is commonly used to determine the concentration of an absorbing species in a solution/solid. UV spectroscopy is used to study the molecules and their electronic excitations. When the energy of the incident photon matches with the energy of excited state of any atom/ molecule/ radical or an ion, resonance occurs and the intensity of the transmitted light is decreased. Depending on the energies of the excited states and the incident photons an absorption band is observed.

The principle of UV-visible absorption spectroscopy is based on the *"Beer-Lamberts Law",:* when a monochromatic light passes through an absorbing medium, the rate of decrease in intensity with the thickness of the medium is proportional to the intensity of the incident light and the concentration of the absorbing substance.

Mathematically it can be express it as

$-dI/dl \propto Ic$ (2.3)

or

$dI/I = kcdl$ (2.4)

where k is the constant of proportionality and is called absorption coefficient. One can integrate the above equation and the integrated form is given as

$\ln I_0/I = kcl$ (2.5)

or

$\log I_0/I = (k/2.303)cl$ (2.6)

$k/2.303 = \varepsilon$ (Extinction coefficient)

For any absorbing substance (solution/solid) absorbance 'A' is defined as

$\mathbf{A = \log I_0/I}$ (2.7)

A typical instrumentation of a double beam UV-Vis spectrophotometer is shown in Fig 2.11.

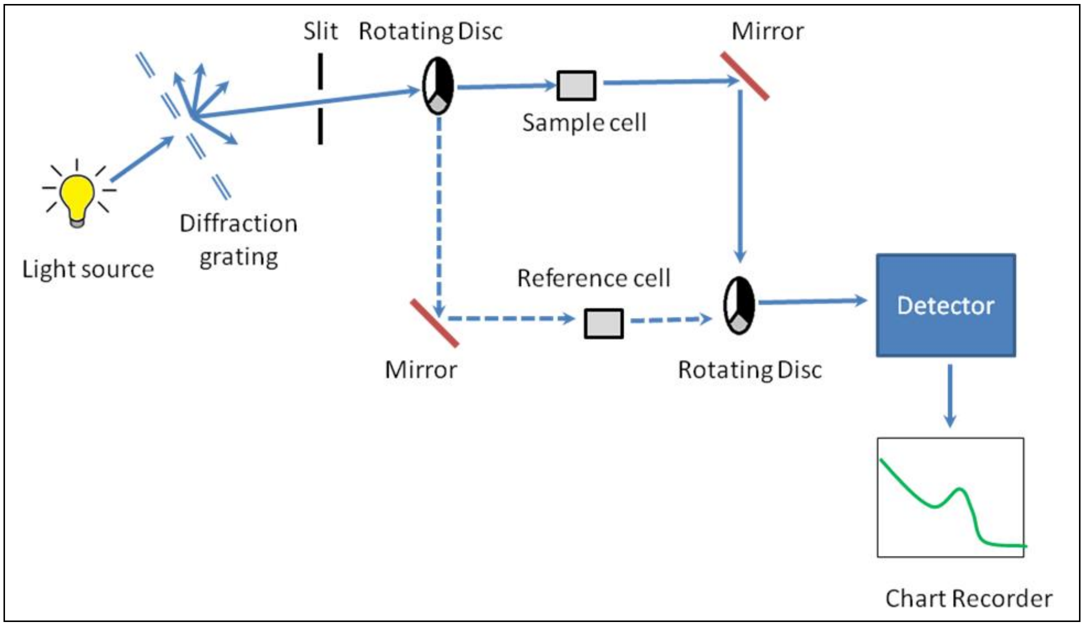

Fig 2.11 *A working schematic of the UV-visible spectrophotometer*

In the present studies, UV-visible optical absorption spectra of the membranes were recorded using USB4000-UV-VIS Miniature Fiber Optic Spectrometer, Germany. The membranes of 1x1 cm^2 size were placed under the optic fibre and the absorption data was recorded.

2.5.7 X ray Diffraction (XRD)

X-ray diffraction is a versatile analytical technique that is used to study crystalline solids, which include ceramics, metals, electronic materials, geological materials, organics, and polymers. These materials may be powders, single crystals, multilayer thin films, sheets, fibers, or irregular shapes, depending on the desired measurement.

X Ray diffractometers fall broadly into two classes: single-crystal and powder X-ray diffractometers. Single crystal diffractometers are most often used to determine the molecular structure of new materials. Powder diffractometers are routinely used for phase identification and quantitative phase analysis.

The three-dimensional structure of crystalline materials is usually defined by regular, repeating planes of atoms that form its crystal lattice. When an X-ray beam hits a sample it is diffracted and the diffraction of the beam is governed by Bragg's Law which is defined as

$$\mathbf{2d\ sin\theta = n\lambda} \qquad (2.8)$$

where the integer *n* is the order of the diffracted beam (n= 1,2,3….) , ***λ*** is the wavelength of the incident X-ray beam, ***d*** is the distance between adjacent planes of atoms (the *d*-spacings), and ***θ*** is the angle of incidence of the X-ray beam. When the path length in the crystal (*2dsin*θ) is a multiple of the wavelength (**λ**), constructive interference occurs and diffracted intensity is obtained. The d-spacing of a crystal is a function of the lattice parameters (a,b,c) and angles (α, β,γ) defining the unit cell, and the Miller indices (h, k, l) denoting a particular reflection. It is the geometry of the crystal lattice that determines the position of the peaks in an X-ray diffraction pattern. More symmetrical is the material, the fewer peaks are present in its diffraction pattern. **λ** of the incident X-rays is usually known and we can measure ***θ*** therefore the ***d***-spacings between the planes of the crystalline material can be calculated. A simplified diagram of XRD diffractometer is given in Fig. 2.12.

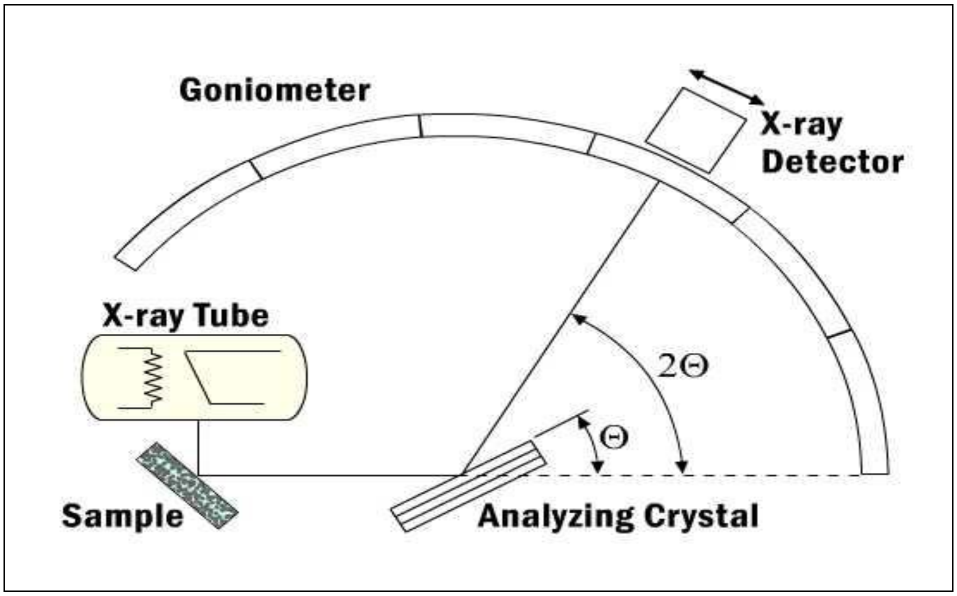

Fig 2.12 *A simplified diagram of the X-Ray diffractometer*

X-ray powder diffraction (XRD) data in the present work was collected on a Philipps X'Pert Pro diffractometer (PW-1710) using Cu Kα_1 radiation (λ=0.154nm). The Philips diffractometer has a proportional counter (Argon filled) for the detection of X-rays. The X-ray tube rating was maintained at 30 kV and 20 mA in the Philips unit.

2.5.8 Vibrating sample magnetometer (VSM)

The VSM, first developed by Foner in the late 1950s, is a research tool for determining magnetic properties in a variety of paramagnetic, ferromagnetic, antiferromagnetic, diamagnetic and ferrimagnetic materials. VSM is based on Faraday's law which states that an electromagnetic force is generated in a coil when there is a change in flux linking the coil [206].

VSM uses an induction technique to measure magnetic moment μ of a sample. If any material is placed in a uniform magnetic field, the induced dipole moment in the sample is proportional to the product of the sample susceptibility and the applied magnetic field. If the sample is made to undergo sinusoidal motion, the resulting magnetic flux changes near the sample, this change in magnetic flux induces an electrical signal in a set of suitable placed stationary coils. This signal generated is proportional to the moment, amplitude, and frequency of vibration.

In a typical VSM the sample is mounted at one end of a rigid rod which is driven by an oscillator (Fig 2.13). The oscillator provides a sinusoidal signal that is translated by the transducer assembly into a vertical vibration. The sample which is fixed to the sample rod vibrates with a given frequency and amplitude (60 Hz and 1 mm, respectively). The sample can be magnetized by a horizontal magnetic field generated by the two pole pieces of an electromagnet. Surrounding the sample is a set of stationary sensing coils mounted on the poles of the electromagnet. Their symmetry center coincides with the magnetic center of the sample. As the sample moves, its magnetic moment μ alters the magnetic flux through these coils. The induced AC voltage is directly proportional to μ and can be detected using a lock-in amplifier. In simple words the magnitude of this signal is dependent on the magnetic properties of the sample itself.

The measurement setup is sensitive even to very low magnetic moments. Currently available Vibrating Sample magnetometers are able to detect magnetic moments of down to the μ emu range, which corresponds to approx. 10^{-9}g iron [207]. Along with this the hysteresis loop of paramagnetic, superparamagnetic and super conductors are measured using VSM.

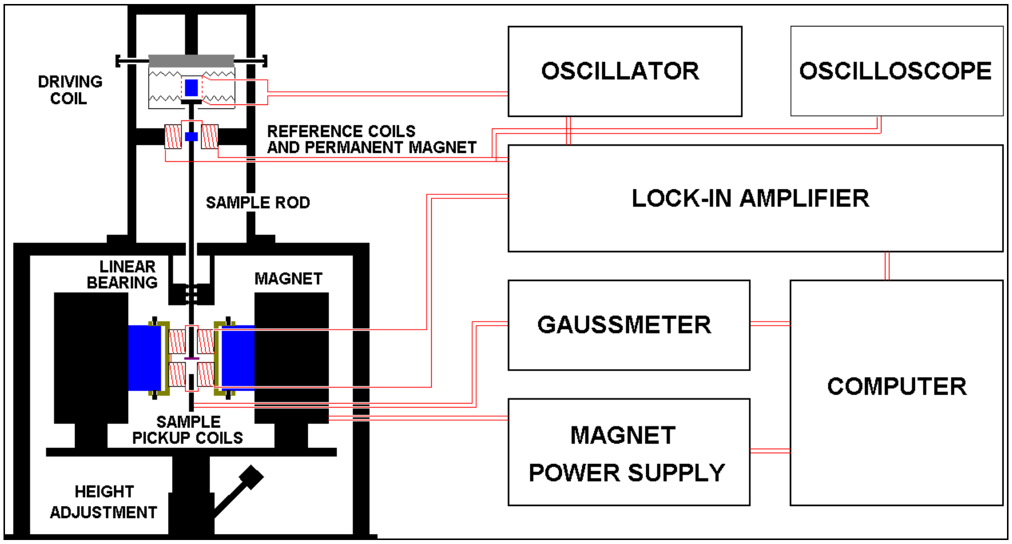

Fig 2.13 *Schematic representation of Vibrating sample magnetometer*

In the present work the magnetic hysteresis measurement of the synthesized magnetic sorbent was carried out using a vibrating sample magnetometer (VSM) (Cryogenic Ltd., UK) at room temperature (300 K) over applied magnetic fields of +9 to -9 Tesla.

2.6 Analytical Techniques

The quantification of targeted analytes in the aqueous solution after equilibration with the sorbent samples was carried out using different analytical techniques such as Ion chromatography, Inductively coupled plasma mass spectrometry and cold-vapor atomic absorption spectrometry. The working principle of all these instrumental techniques is briefly outlined as below. The choice of the technique was based on the analyte to be quantified.

2.6.1. Ion Chromatography

Ion chromatography is an important analytical technique for the separation and determination of ionic compounds [208-210]. The separation of different anions and cations is carried out using ion exchange column containing ion-exchange resins. Anions are separated using anion-exchange resin column and cations are separated using cation-exchange column. The main principle behind the separation of anions or cations is the difference in their affinities towards the resin packed in an analytical column. This affinity and hence separation of ions is governed by two factors

- Charge on the ions and size of the ions (hydrated)

Depending on the above factors, among the doubly charged species, sulphate and phosphate have stronger affinity towards the anion exchange resin than the singly charged ones like fluoride, chloride and nitrate and hence are held on the resin for a longer time. Among singly charged ions F^-, Cl^- and NO_3^- , fluoride has the largest hydrated radius due to high charge density therefore it has the least affinity towards the resin and hence will be eluted first followed by chloride (Cl^-) and then nitrate (NO_3^-). Once the components are separated, they are detected and measured by a conductivity detector.

The ion chromatography can be conducted in two modes

- Suppressed conductivity detection and non suppressed conductivity detection.

In this work, suppressed conductivity method was used where a suppressor column, installed after anion exchange resin column, is needed for removing the opposite ionic substance in the mobile phase. This helps in reducing the high conductivity of the mobile phase and to convert counter ions of analyte ions to a single ionic species with a higher equivalent conductivity.

For anion exchange separation, basic eluents ($Na_2\ CO_3$, $NaHCO_3$, or NaOH) are used to separate the anions on an anion exchanger whereas H_2SO_4 is used as an eluent for separating cations on a cation exchanger. A high pressure pump is required to force the eluent through the ion exchange column at typical flow rates of 1-2 ml min^{-1}. The sample to be separated is introduced into the mobile phase by an injection device, prior to the column and then it is fed to the main analytical column followed by the suppressor and the detector.

A typical instrumentation of Ion chromatography system is shown in Fig. 2.14.

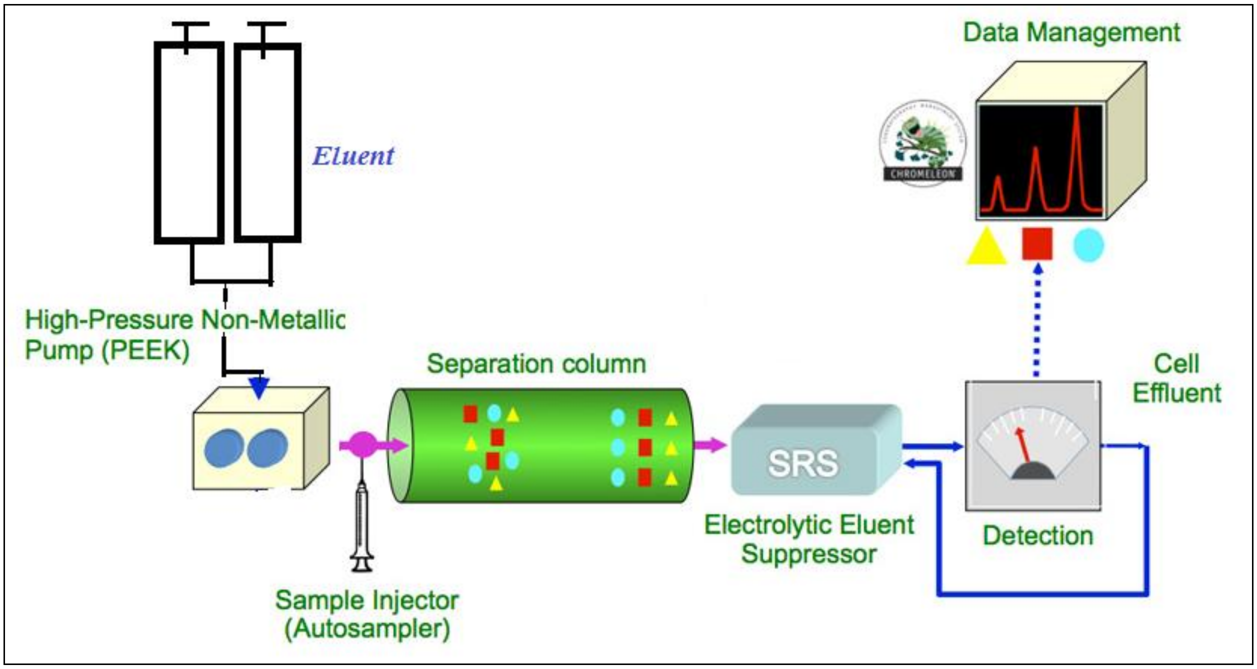

Fig. 2.14 *Schematic representation of an Ion chromatography system*

In the present research work, Dionex Ion chromatography system (ICS-5000) was used to determine the residual concentration of anionic components left in the solution after it has been equilibrated with the polymeric sorbent. The eluent used was 35 mM NaOH into auto suppression mode. The concentration of the eluent was further optimized for obtaining a clean separation with well resolved peaks. The column used was an anion exchange AS-20 column attached with an anion self regenerating suppressor (ASRS-3000, 4 mm). For analyzing the real water samples, they were filtered using 0.45 μm filter paper before injecting into the system for analysis.

2.6.2 Inductively Coupled Plasma Mass Spectrometer (ICP-MS)

ICP-MS is widely accepted as a powerful technique for elemental analysis. It provides rapid, multi-element analysis with detection limits at parts per trillion or below, for about 60 elements in solution with a dynamic range of 10^4 to 10^8 [211,212]. It has additional unique capabilities of detecting elemental isotope ratio measurements and carrying out convenient semi-quantitative analysis. A typical ICP-MS combines a high-temperature ICP (Inductively Coupled Plasma) source with a mass spectrometer. A block diagram of the same is shown in Fig 2.15.

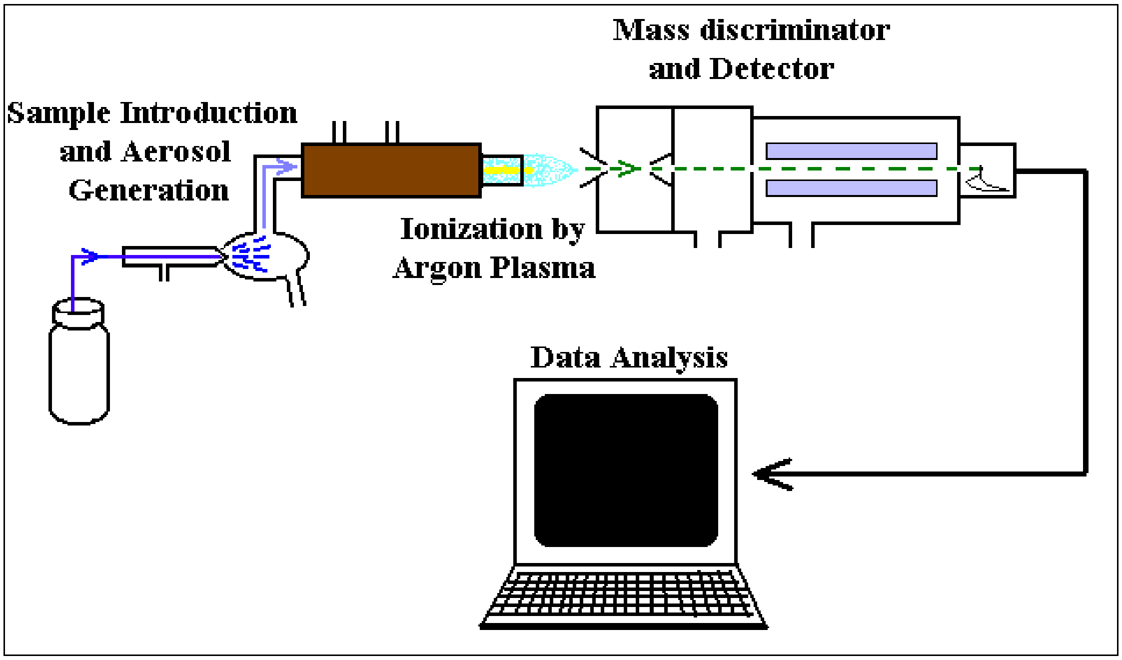

Fig 2.15 *Schematic of an ICP-MS system*

The plasma in ICPMS converts the atoms of the elements present in the sample to ionic form. The sample is typically introduced into the ICP plasma as an aerosol, by aspirating a liquid sample into a nebulizer. Once the sample aerosol is introduced into the ICP torch, it is completely desolvated and the elements in the aerosol are converted first into gaseous atoms and then ionized. The ions are then brought into the mass spectrometer via the interface cones. The interface region in the ICP-MS transmits the ions traveling in the argon sample stream at atmospheric pressure (1-2 torr) into the low pressure region of the mass spectrometer ($<1 \times 10^{-5}$ torr). This is done through the intermediate vacuum region created by the two interface cones, the sampler and the skimmer. In the mass spectrometer, ions are separated by their mass-to-charge ratio with the help of a quadrouple mass filter. The quadrupole mass filter is made up of four stainless steel rods which are mounted with stringent (10-µm) tolerances as shown in Fig 2.16.

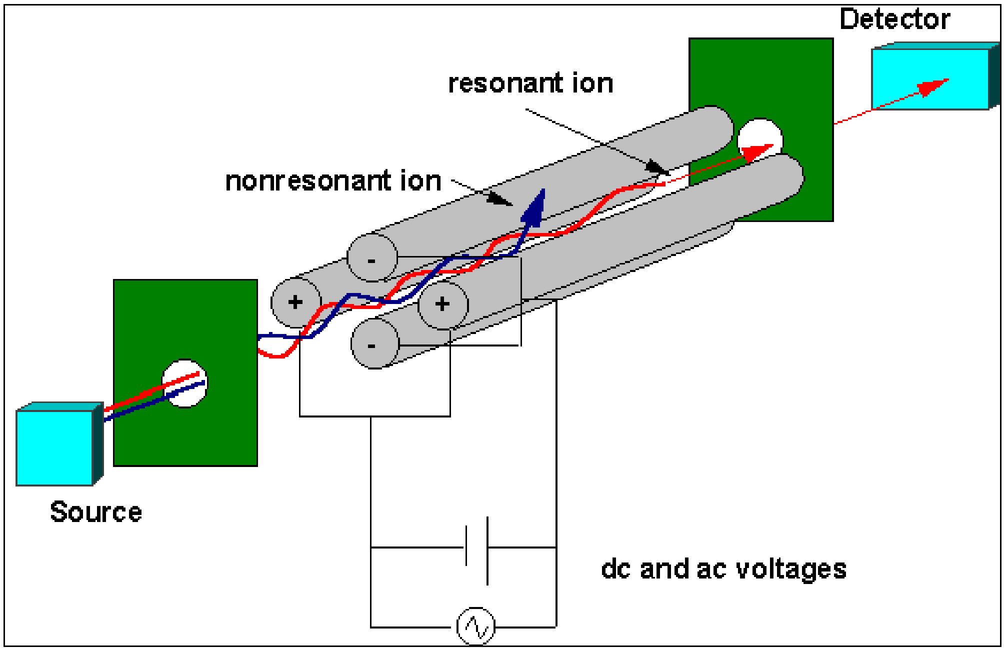

Fig 2.16 *Diagram of a quadrouple mass filter*

Opposing pairs of rods are connected to radio frequency (RF) power supply with a direct current (DC) offset. The voltage applied on one pair is opposite to the polarity of the other pair. These voltages are then rapidly switched along with an RF-field. The result is that at any instant of time only ions of a particular mass-to-charge ratio (m/e) are allowed to pass through the rods to the detector. So, the quadrupole mass filter is really a sequential filter, with the settings being change for each specific m/e value at a time.

The detector used in ICP-MS is a channeltron detector. It is a continuous dynode based electron multiplier in which a high voltage is applied between the input and output ends of the detector. When an ion strikes the detector, secondary electrons are produced and accelerated. These electrons in turn strike the wall of the dynode, generating more electrons. Up to 108 electrons are produced and collected at a collector electrode at the output end of the detector for each incident ion, depending on the applied voltage. Components such as the nebulizer, spray chamber, plasma torch, interface, and detector are common to any ICPMS system but can differ significantly in the design of the mass spectrometer and in particular the mass separation unit.

In the present work analysis of various ions in aqueous solution was carried out using VGPQ Ex cell (Thermo Elemental) inductively coupled mass spectrometry (ICP-MS) model. The instrumental operating conditions are given in Table 2.1. Prior to the analysis X, Y, and Z positions of torch, RF power, the nebuliser gas flow, and lens voltages were optimized using a 10 ng mL^{-1} multielement standard solution containing Li, Be, Bi, Co, Ce, In, Ba, Pb, and U.

Table 2.1 *Typical operating conditions of ICP-MS*

Plasma conditions		
Incident power	**:**	1.33 kW
Reflected Power	**:**	0.8 W
Coolant gas flow rate (Ar)	**:**	131 L min^{-1}
Auxiliary gas flow rate (Ar)	**:**	0.88 L min^{-1}
Sample gas flow rate (Ar)	**:**	1.05 L min^{-1}
Sampling depth	**:**	8 mm
Sample Introduction System		
Nebulizer	:	Concentric Nebulizer
Spray Chamber	:	Peltier cooled cyclonic spray chamber at $4^{o}C$

Sample uptake rate	:	1 mL min^{-1}
Uptake Time		60 s
Wash time		90 s
Data acquisition		
Scanning Mode	:	Continuous mass scan
Number of points per peak	:	10
Number of replicates	:	10
Detector mode	:	Pulse counting
Detector dead time	:	15 ns
Dwell time	:	200

2.6.3 Cold Vapor Atomic Absorption Spectroscopy (CV-AAS)

Atomic absorption spectrometry (AAS) is a technique capable of determining trace (μg/mL) and ultratrace (sub μg g/mL) levels of elements or metals in a wide variety of samples, including biological, clinical, environmental, food, and geological samples.

The principle of AAS is based on the absorption of a monochromatic light of the chosen wavelength of initial intensity, I_0, by the atoms present in the gaseous state. The incident light is focused on the flame cell containing ground state atoms. Some of the atoms absorb the light and the initial intensity is decreased by an amount proportional to the atom concentration in the flame cell. The light is then directed onto the detector where the reduced intensity, I, is measured (Fig 2.17). The amount of light absorbed is determined by measuring the incident power intensity (I_o) with the transmitted power intensity (I_t) in form of absorbance which is defined as

$$A = \log(I_o / I_t) \qquad (2.9)$$

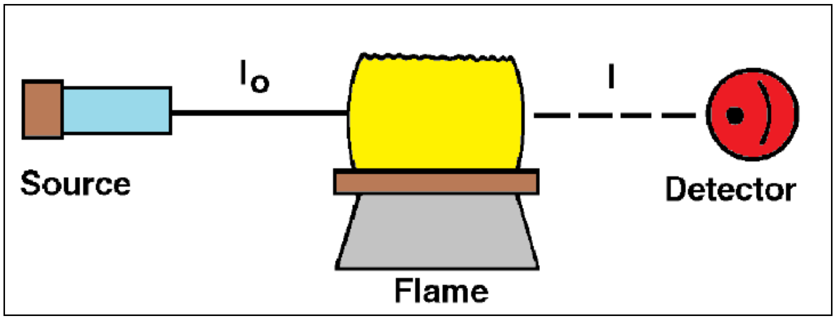

Fig 2.17 *The atomic absorption process*

Cold vapor atomic absorption spectrometry (CV-AAS) has the same principle as that of AAS but it is limited only to the determination of mercury, due to it being the only metallic element to have a large enough vapor pressure at ambient temperature. It has a high vapor pressure of about 0.0016 millibars at 20 degree centigrade, that is, room temperature which corresponds to about 14 milligrams per cubic meter, given the environmental pollution potential of mercury.

CVAAS method of determining mercury in any sample initiates by converting mercury present in the solution to be analysed into Hg^{2+} by oxidation using nitric acid, followed by its reduction with tin(II)chloride. After reduction the mercury vapors thus formed are swept into a long-pass absorption tube by bubbling a stream of inert gas like (argon or nitrogen) through the reaction mixture. The mercury vapors when present is the absorption cell absorbs the incident light of wavelength 253.7 nm. The intensity of the transmitted light decreases after passing through the absorption cell and the decrease in the intensity is measured using the absorbance relationship given in equation 2.9. Once the absorbance is measured, concentration of mercury present in the sample can be calculated using Beer’s Lambert Law. Detection limits for this technique are in the parts-per-billion range making it an excellent mercury detection atomization method.

In the present work determination of mercury concentrations after equilibration with the membrane sorbent were determined using a Mercury analyser CV-AAS unit (Model no. MA 5800E, ECIL, Hyderabad, India). It consists of a low pressure mercury lamp emitting a 253.4 nm line, an absorption cell, a filter, a detector with associated electronics and a vapor generation system containing a reaction vessel with a magnetic stirrer (Fig 2.18).

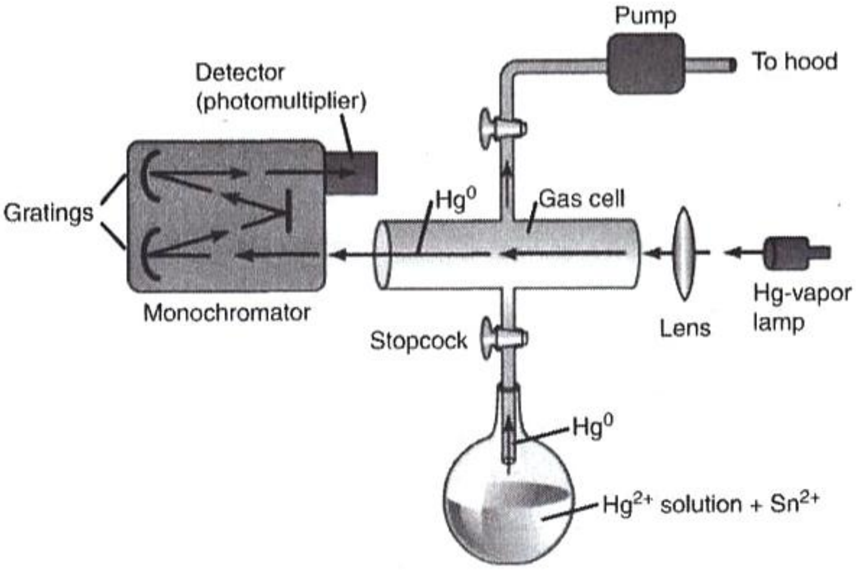

Fig 2.18 *Schematic Diagram of a typical CV-AAS*

Residual mercury after sorption studies in aqueous samples was determined by taking an aliquot of the sample in the reaction vessel followed by stirring for 10 minutes with 10% HNO_3 and 20% $SnCl_2$. The carrier gas system carries elemental mercury thus formed through the system and passes to the absorption cell. Mercury is quantitatively determined from the absorbance obtained at a wavelength of 253.7 nm at room temperature. The direct determination of mercury sorbed on the membrane was carried out by placing the membrane in the reaction vessel containing HNO_3 and $SnCl_2$ and the same steps as listed for solution samples were repeated.

2.7. Calibration of Instrumental Methods

Measured analytical signal is related to the concentration of the analyte by several calibration methods. Three most common calibration methods are the standard calibration curve, the standard addition method, and the internal standard method. Standard calibration curve method and the standard addition method both are used for calibrating the instruments as well as for carrying out the spike recovery measurements in real samples. Therefore these methods are discussed in the following sections.

2.7.1. Standard Calibration Method

To use the calibration curve technique, several standards containing exactly known concentrations of the analyte are introduced into the instrument, and the instrumental response is recorded. Generally, this response is corrected for the instrument output obtained with a blank. Ideally, the blank contains all of the components of the original sample except the analyte. The resulting data are then plotted to obtain a graph of corrected instrument response *vs.* the analyte concentration. The plot should be linear over a significant concentration range (the dynamic range). The success of the calibration curve method is critically dependent upon how accurately the analyte concentrations of the standards are known and how closely the matrix of the standards resembles that of the samples to be analyzed.

2.7.2. Standard Addition Methods

Standard addition methods are particularly useful for analyzing complex samples in which the likelihood of matrix effect is substantial. A standard addition method can be carried out in different ways. One of the most common forms involves spiking the sample aliquots with one or more increments of a standard solution. Each solution is then diluted to a fixed volume before measurement. It should be noted that when the amount of a sample is limited, standard additions can be carried out by successive introduction of increments of the standard to a single measured volume of the unknown. Measurements are made on the original sample and on the sample plus the standard after each addition.

In most versions of the standard addition methods, the sample matrix is nearly identical after each addition, the only difference being the concentration of the analyte or, in cases involving the addition of an excess of an analytical reagent, the concentration of the reagent. This method is frequently used in the current work.

2.7.3. Internal Standard Methods

An internal standard is a substance that is added in a constant amount to all the samples, blanks and calibration standards in an analysis. The internal standard must be known to be absent from the sample matrix so that the only source of the standard is the added amount. For example, lithium is a good internal standard for the determination of sodium or potassium in blood serum because the chemical behavior of lithium is similar to both analytes, but it does not occur naturally in blood. Calibration then involves plotting the ratio of the analyte signal to the internal standard signal as a function of the concentration of the standards. This ratio for the samples is then used to obtain analyte concentrations from a calibration curve.

A major difficulty in applying the internal standard method is that of finding a suitable substance to serve as the internal standard and of introducing that substance into both samples and standards in a reproducible way. The internal standard should provide a signal that is similar to the analyte signal in most ways but sufficiently different so that the two signals are readily distinguishable by the instrument.

2.8. Batch Sorption Studies

Sorption is a mass transfer process by which a substance is transferred from the liquid phase to the surface of a solid and becomes bound by physical and /or chemical interactions. To obtain the optimum sorption conditions for the sorbents batch experiments were carried out for the sorption of each targeted analyte onto the fixed site membranes/sorbent. Effects of all the parameters affecting the sorption process like pH, contact time, concentration and interference of co-exiting ions were investigated. The efficiency of any sorption process can be judged by the capacity of the sorbent material. For this purpose it is necessary to calculate the uptake capacity of the developed sorbents. The uptake capacity can be calculated by two methods as discussed below.

The first method is based on the analysis of the sorbent material before and after equilibration with a solution of increasing analyte concentration, the difference of the amounts gives the amount of sorbate loaded on the sorbent. After a particular concentration, the amount of sorbate on sorbent becomes constant because of the saturation of the available binding sites. Beyond that concentration there is no uptake by the sorbent. The amount of analyte sorbed on the sorbent divided by the weight of sorbent taken gives the maximum uptake capacity (mg/g).

The second method involves determination of sorbate concentration in the solution before and after equilibration. Equilibrium sorption capacity, q_e, is determined, using equation

$$q_e = (C_o - C_e) * V/m \tag{2.10}$$

where C_o and C_e are the initial and the equilibrium concentrations, respectively, of the sorbate in the solution, m is the mass of the sorbent and V is the volume of solution. The second method of analysis of residual sorbate concentration is generally preferred due to the convenience in the analysis.

Sorption studies using synthesized polymeric sorbents were carried out, by adding a fixed amount of the sorbent or a weighed membrane sample of a fixed size 1x1 cm^2 into a fixed volume of the sorbate solution of varying concentrations. After a particular time of equilibration, a aliquot of the aqueous phase was drawn, and analyzed for sorbate concentrations using various instrumental techniques described above. The experiments were carried out by varying different parameters and the experimental data was fitted to different kinetic and equilibrium models. Mathematical modeling of sorption offers an extremely powerful tool for understanding the mechanism of interaction of analyte with sorbate. It is also essential for knowing the optimized conditions for any process to be designed. The various mathematical models applied to the experimental data are discussed below.

2.9. Sorption isotherms

Surface adsorption to a solid falls into two broad categories; physisorption and chemisorption as discussed in the introduction chapter of this thesis. Both these processes are governed by different isotherm models as explained below.

Sorption isotherms are mathematical models that describe the distribution of the sorbate specie among liquid and solid phases, based on a set of assumptions that are related to the heterogeneity/homogeneity of the solid surface, the type of coverage, and the possibility of interaction between the sorbate specie and the sorbent. The analysis of the sorption equilibrium data by fitting them into different isotherm models is an important step to find the suitable model that can be used for designing any batch process.

A sorption isotherm is a curve relating the equilibrium concentration of a solute on the surface of an sorbent, q_e, to the concentration of the solute in the liquid, C_e, with which it is in contact. It also relates the amount of solute adsorbed and the equilibrium concentration of the solute in solution at a given temperature.

There are several models for predicting the equilibrium distribution. In the present work, sorption isotherm study was carried out using two isotherm models, namely the Langmuir and Freundlich isotherms. The applicability of the isotherm equation to describe the adsorption process was judged by the correlation coefficients, R^2 values.

2.9.1. Langmuir Isotherm

Langmuir's isotherm describing the adsorption of Adsorbate (A) onto the surface of the Adsorbant (S) has three assumptions:

- The surface of the adsorbant is in contact with a solution containing an adsorbate which is strongly attracted to the surface.
- The surface has a specific number of sites where the solute molecules can be adsorbed.
- The adsorption involves the attachment of only one layer of molecules to the surface, i. e. monolayer adsorption**.**

The chemical reaction for monolayer adsorption can be represented as follows:

$$A + S \rightleftarrows AS$$

where AS represents a solute molecule bound to a surface site on S. The equilibrium constant K_{ads} for this reaction is given by:

$$K_{ads} = [AS]/ [A] [S] \qquad (2.11)$$

[A] denotes the concentration of A, while the other two terms [S] and [AS] are two-dimensional analogs of concentration and are expressed in units such as mol/cm^2. The complete form of the Langmuir isotherm considers in terms of surface coverage θ which is defined as the fraction of the adsorption sites to which a solute molecule is attached. An expression for the fraction of the surface with unattached sites is therefore equal to (1 - θ). The term [AS]/[S] is rewritten as

$$[AS]/ [S] = \theta/(1 - \theta) \qquad (2.12)$$

and

$$K_{ads} = \theta/ (1 - \theta)*C \qquad (2.13)$$

Rearranging, the final form of the Langmuir adsorption isotherm is obtained as

$$\theta = K_{ads}\, C / (1 + K_{ads}\, C)$$

This is known as Langmuir sorption equation. θ can be expressed in terms of equilibrium sorption capacity, q_e, and maximum monolayer capacity, q_m,

$$\theta = q_e/q_m \tag{2.14}$$

Substituting θ and rearranging, eqn 2.14 is obtained as

$$q_e = q_m K_L C_e / (1 + K_L C_e) \tag{2.15}$$

The linearised form of the above equation is

$$1/ q_e = 1/ q_m + 1 / K_L C_e q_m \tag{2.16}$$

By plotting a graph between $1/ q_e$ and $1/ C_e,$ the values of the constants can be calculated from the slope and intercept of the graph. The variation of surface coverage θ with the concentration is shown in Fig 2.19.

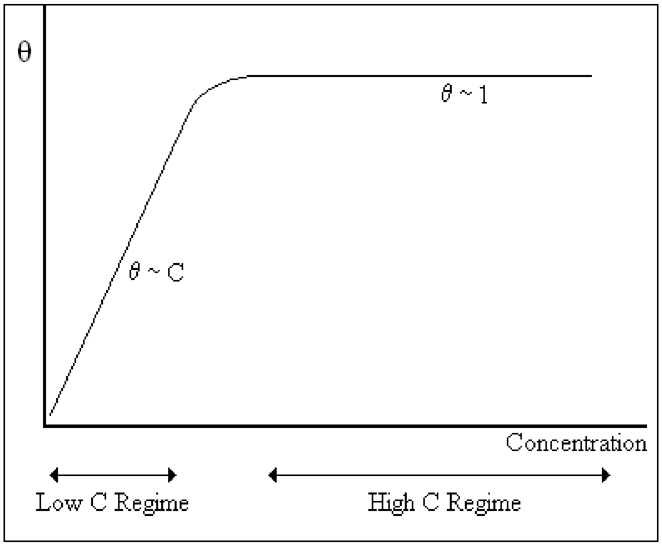

Fig 2.19 *General form of Langmuir isotherm*

2.9.2. Freundlich isotherm

In 1909, Freundlich gave an empirical expression representing the isothermal variation of adsorption of a quantity of gas adsorbed by unit mass of solid adsorbent with pressure.

Although the isotherm was given for gases, it is widely used for the sorption phenomenon in solution form too. In contrast to the Langmuir equation, the Freundlich isotherm assumes sorption onto sorbent surfaces, which are characterized by heterogeneous sorption sites. It also assumes that the stronger binding sites are occupied first, and that the binding strength decreases with increase in the degree of site occupation.

At low concentration, amount of sorption is directly proportional to concentration (raised to power one).

$$q_e \propto C_e \tag{2.17}$$

At high concentration, extent of sorption is independent of concentration (raised to power zero).

$$q_e \propto C_e^0 \tag{2.18}$$

Therefore at intermediate value of concentration, sorption is directly proportional to the concentration raised to power 1/n .Here n is a variable whose value is greater than one. Using constant of proportionality, k, also known as adsorption constant equation 2.18 is obtained as

$$q_e = K_F C_e^{1/n} \tag{2.19}$$

The above equation is known as Freundlich adsorption equation (2.19)

The linearised form can be written as

$$\text{Log } q_e = \text{Log}K_F + 1/n \text{ Log}C_e \tag{2.20}$$

On ploting log q_e versus log C_e a slope of 1/n and an intercept of log K_F is obtained. Larger value of n (smaller value of 1/n) implies stronger interaction between the sorbate and the sorbent, while 1/n equal to 1 indicates linear sorption, leading to identical sorption energies for all the sites. A favorable sorption tends to have the value of n between 1 and 10.

2.10. Kinetic steps

The kinetics of sorption of any batch process is very crucial for knowing the optimum time required for quantitative sorption. Usually the mass transport of the sorbate in the sorbent can be divided into four consecutive steps until it reaches the interior surface of the pores and attains equilibrium as shown below.

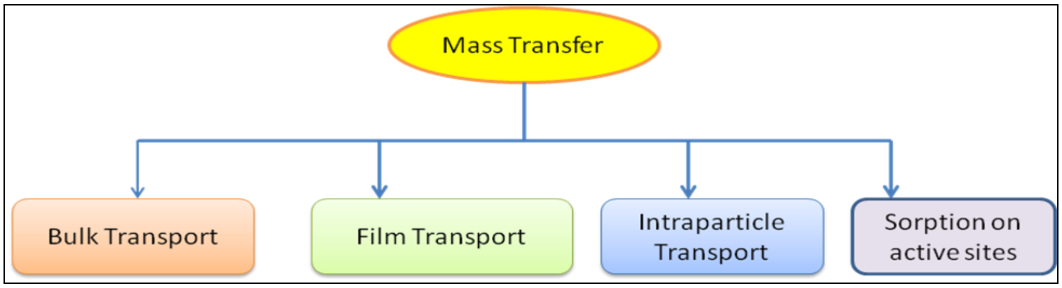

Bulk transport is transport of the sorbate from the solution phase to the subsurface, which is built up around the sorbent i.e near to the boundary layer of the sorbent. This step is usually very rapid due to mixing of the flow by usual stirring or shaking.

Film transport involves diffusion of the solute across the so-called liquid film/sub surface surrounding the sorbent membrane/particles. The step is also known as external diffusion.

The ***intraparticle*** diffusion step in sorption involves the transport or diffusion of the solute in the liquid contained in the pores of sorbent particle, and along the pore walls.

The final step of ***sorption*** which is itself a fast step involves sorption of the solute molecules on the sorbent surface. The total sorption process is governed by combination of one or more steps listed above and as clearly shown in Fig 2.20.

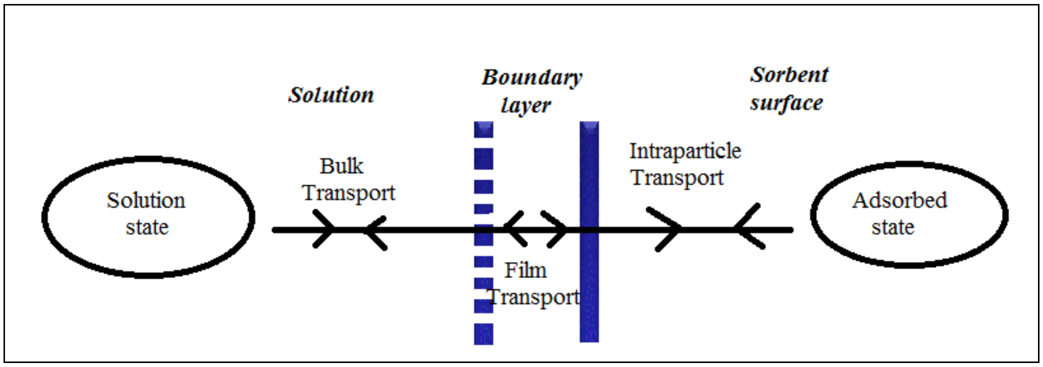

Fig 2.20 *Schematic of mass transport steps involved in sorption process*

The first step is usually neglected while considering the sorption as the system under rapid mechanical mixing. Thus, the sorption rate is governed by external diffusion or internal diffusion [213]. Internal diffusion step actually involves intraparticle diffusion and intercrystalline diffusion, or the sorption of the solute on the active sites.

All of these steps may or may not occur simultaneously, which makes the determination of the rate determining step difficult. In order to determine the contribution of the steps involved, numerous kinetic models have been compared to predict the behavior of the experimental data and the models used in the present work has been explained in the following section.

Kinetic models

Kinetic tests show the time- concentration profile for the sorption system. In order to investigate the mechanism of sorption and potential rate controlling step, kinetic models are generally used to test experimental data. Moreover, the information on the kinetics of the sytem is required for selecting optimum operational conditions for full batch scale process. Among the most popular kinetic models/equations are the so-called “first-order” and “second order” rate expressions. These models are explained in detail as follows.

2.10.1. Pseudo first-order kinetic model

The pseudo-first order rate equation or Lagergren first order equation has been applied to describe the sorption rate. It is given as:

$$dq/dt = k_1 (q_e-q) \qquad (2.21)$$

where q (mg/g) is the amount of adsorbed analyte ion on the adsorbent at time t and k_1 (min^{-1}) is the rate constant of the first –order adsorption. The integrated form of the above equation can be written as:

$$\log(q_e-q) = \log q_e - k_1/2.303 * t \qquad (2.22)$$

where q_e is the equilibrium sorption uptake, is obtained by extrapolation of the experimental data at infinite time. A straight line of $\log(q_e-q)$ vs t suggests the applicability of this kinetic model. q_e and k_1 can be determined from the intercept and the slope of the plot respectively. In many sorbate-sorbent interactions, the chemisorption is slow, after the initial fast response and it is difficult to ascertain whether equilibrium is reached or not. Therefore determining q_e accurately becomes a difficult task. It has been reported that, many sorption processes follow Lagergren pseudo first-order model only for the initial 20 to 30 min of interaction. Value of k_1 can be dependent or independent of the working experimental conditions. Its value depends on the initial concentration of the sorbate and usually decreases with the increasing initial sorbate concentration in the bulk phase [214]. Therefore to get exact value of k_1 at higher concentrations higher order kinetic models are employed to analyze the experimental results.

2.10.2. Pseudo second-order kinetic model

The pseudo second order model is expressed as

$$dq/dt = k_2 (q_e-q)^2 \qquad (2.23)$$

where k_2 (g/mg.min) is the rate constant of the second order adsorption. The integrated form of the above equation can be written as :

$$1/(q_e-q) = 1/q_e + k_2 t \qquad (2.24)$$

Above equation can be linearised to obtain

$$t/q = (1/k_2)*q_e^2 + (1/q_e)*t$$

The plot of t/q vs t should be a straight line for the system to follow second order kinetics and the value of q_e and k_2 can be determined from the slope and intercept of the plot, respectively. Many reports are available in literature, indicating that the value of k_2 has strong dependence on the applied operating conditions, such as the initial solute concentration, pH of solution and temperature, etc. The value of k_2 is usually strongly dependent on the applied initial solute concentration, and it decreases with the increase in C_o, i.e., the higher is the C_o value, the longer time is required to reach an equilibrium [215-219].

CHAPTER 3

DEVELOPMENT OF POLYMER SORBENTS FOR SOLID PHASE EXTRACTION OF FLUORIDE

Section 3A

POLYMERIC SHEET SORBENT FOR FLUORIDE

3A.1 Introduction
3A.2 Experimental
  3A.2.1 Synthesis of Sheet Sorbents
  3A.3.2 Stability of thorium in Polymeric Matrix
  3A.3.3 Sorption Studies
3A.3 Results and Discussion
  3A.3.1 Characterization of the sorbents
  3A.3.2 Sorption and Desorption Studies
  3A.3.3 Kinetic Models
3A.4 Mechanism of Fluoride Sorption
3A.5 Comparison of the Sheet Sorbents With Existing Sorbents
3A.6 Application to Real Samples
3A.7 Conclusions

3A.1. Introduction

Occurrence and uses of fluoride

Fluorine is the first element of Halogen group (Group 17) of periodic table. It is also the 17th most abundant element in the earth's crust. It is the most electronegative of all the elements and never occurs in its free state in nature. Soil contain approximately 330 mg L^{-1} of fluorine, ranging from 150 to 400 mg L^{-1}. Some soils can have as much as 1000 mg L^{-1} and contaminated soils have been found with 3500 mg L^{-1}. In the atmosphere 0.6 μg L^{-1} of fluorine are present as salt spray and organo-chloride compounds [220]. Fluorine readily forms compounds with most other elements, even with the noble gases krypton, xenon and radon. It is so reactive that glass, metals, and even water, as well as other substances, burn with a bright flame in a jet of fluorine gas. In aqueous solution, fluorine commonly occurs as the fluoride ion (F^-).

Fluorides are compounds that combine fluoride with some positively charged counterpart. In nature it is widely distributed in the form of various minerals like fluorite, cryolite and topaz [221]. Slow weathering of rocks containing fluorite releases fluoride in the water sources. There are many commercial applications of fluorine. Atomic fluorine and molecular fluorine are used for plasma etching in semiconductor manufacturing, flat panel display production, semiconductor manufacturing, electroplating, coal fired power stations, glass and ceramic industries, aluminium smelters and beryllium extraction plants [222,223]. Crystals of calcium fluoride are used to make lenses that focus infrared light. Fluorine is indirectly used in the production of low friction plastics such as teflon and in halons such as freon, in the production of uranium. Fluorochlorohydrocarbons are used extensively in air conditioning and in refrigeration. Fluorides are often added to toothpaste and, somewhat controversially, to municipal water supplies to prevent dental cavities.

Due to the slow and continuous release of fluoride in water resources by both natural and anthropogenic sources, fluoride has become a major source of human intake especially in the developing countries like India where groundwater is a major source of drinking water. The concentration of fluoride in the released effluents from above listed industries ranges from ten to thousands of mg L^{-1} [224]. Worldwide more than 250 million people rely on drinking water with fluoride concentrations that exceed the WHO guideline of 1.5 mg L^{-1} [225].

Health Effects of Fluoride

A small concentration fluoride is required to strengthen the tooth enamel. It displaces the hydroxide ions from hydroxyapatite, $Ca_5(PO_4)_3OH$, the principal mineral constituent of teeth (in particular the enamel) and bones, to form the harder and tougher fluoroapatite, $Ca_5(PO_4)_3F$. However, fluoroapatite is an order of magnitude less soluble than hydroxyapatite, and at high fluoride concentration the conversion of a large amount of the hydroxyapatite into fluoroapatite makes the teeth and the bones denser, harder and more brittle and leads to dental fluorosis which causes embrittlement of teeth [226,227]. It has been reported in literature that there are many deleterious effects of consuming fluoride contaminated water depending on its concentration. With prolonged exposure at higher fluoride concentration this dental fluorosis progresses to skeletal fluorosis. The various health issues caused by different concentration of fluoride are listed in Table 3.1.

Table 3.1 *Concentration of fluoride and its biological effects*

Fluoride concentration in water (mg L^{-1})	Health outcome
< 0.5	Dental carries
0.5-1.5	Optimum dental health
1.5-4.0	Dental fluorosis
4.0-10	Skeletal fluorosis
>10.0	Crippling fluorosis

The limit set for fluoride in drinking water as 1.5 mg L^{-1} as can be seen from the Table 3.1. In addition to the above mentioned effects, excess fluoride concentration can interfere with the metabolism rate of carbohydrates, lipids, proteins, vitamins and minerals [228]. Because of the high reactivity of fluoride it initially acts locally on the intestinal mucosa, later on forming hydrofluoric acid in the stomach, which leads to gastro-intestinal irritation. Functions of various enzymes are also disrupted by the presence of fluoride in the human system e.g. oxidative phosphorylation, glycolysis, coagulation, and neurotransmission are some of the activities of various enzymes distrupted by high fluoride consumption. The ability of fluoride to interfere with the functions of the brain and pineal gland is well reported. Pineal gland is a major site of fluoride accumulation within the body, with higher concentrations of fluoride than either teeth or bone. It secretes a harmone called melatonin, which regulates the circadian rhythm, or sleep cycle. Bladder cancer and thyroid activity is also known to be influenced by continuous accumulation of fluoride in the body system [229-232].

There are more than 20 developed and developing nations that are endemic for fluoride related disease typically called fluorosis. Argentina, U.S.A., Morocco, Algeria, Libya, Egypt, Jordan, Turkey, Iran, Iraq, Kenya, Tanzania, S. Africa, China, Australia, New Zealand, Japan, Thailand, Canada, Saudi Arabia, Persian Gulf, Sri Lanka, Syria, India, etc. are some of them [233-235]. A considerable work has been carried out in different parts of the world to determine the fluoride in water sources and their impact on human as well as to evolve methods to reduce high concentration of fluoride [236-239].

Fluoride poisoning can be minimized in a community drinking fluoride contaminated water by using alternate water resources for daily use, by improving the nutritional status of community at risk or by removing excess fluoride using different methods of defluoridation. Surface water, rainwater and low fluoride groundwater are some of the alternate water sources which can be used. Rain water is a cleaner source of water compared to surface water which is highly polluted with chemical pollutants thus rain water can serve as a better and low cost source. But the uneven distribution and limited storage facilities make this measure a limiting one. Measures to improve the nutritional status of population might be an effective supplement but it is practically difficult to follow this. Defluoridation of drinking water is the only practicable option to overcome the problem of excessive fluoride in drinking water, where alternate source is not available. The different methods used for the defluoridation of contaminated water streams are described below.

Literature survey on existing methods of defluoridation

During the past few years extensive research has been done on various methods for the removal of fluoride from groundwater and wastewater. The most commonly used methods for the defluoridation of contaminated waters till date can be divided into four different categories:

1. Precipitation
2. Adsorption and ion-exchange
3. Membrane filtration processes
4. Distillation.

Although there are a large number of methods, the surface adsorption retains a major place in defluoridation research and practice because of its greater accessibility and lower cost. Activated alumina and activated carbon are the most commonly used adsorbents as discussed in the introduction chapter of the thesis. But there are certain limitations using these adsorbents. Hardness and surface loading (the ratio of total fluoride concentration to activated alumina dosage) affects the fluoride removing tendency of sorbents. In addition to this the pH of the solution should be between 5.0 and 6.0 because at pH > 7, silicate and hydroxide becomes stronger competitor of the fluoride ions for exchange sites on activated alumina and at pH less than 5, activated alumina gets dissolved in acidic environment leading to loss of adsorbing media [108,240]. The alumina based adsorption process has a low adsorption capacity, it requires acidification and pretreatment and its effectiveness for fluoride removal reduces after each cycle of regeneration.

In the recent years, RO membrane process has emerged as a preferred alternative for defluoridation in many parts of the world. Applied pressure, temperature, characteristics of the membrane and characteristics of the feed water govern the overall efficiency of the membrane defluoridation process. Membrane based methods offers the advantages of removal of inorganic and organic pollutants along with fluoride [165,241-243]. Very little maintenance is required because there are no chemicals involved and as life of membrane is sufficiently long so the problem of regeneration is less. Unlike other methods, this method is free of interference. But apart from these advantages, the membrane based methods have certain limitations such as the process is expensive and the water becomes acidic and need pH correction. All the other ions are also removed although some minerals are essential for proper growth therefore remineralization is also required after treatment. Distillation units have also been used for treating the fluoridated water. Large scale electrodialysis plants are already used for making drinking water out of brackish water with high fluoride concentrations [244].

Although there has been much advancement in the above stated methods, the development of low-cost and effective adsorbents and to improve efficiency of all the adsorbents has been a major area of research for defluoridation of aqueous streams [47, 245-250]. Adsorption methods based on solid phase extraction (SPE) is advantageous over other sample pretreatment techniques like liquid-liquid extraction, precipitation, co-precipitation, etc. in terms of simpler and faster operation, higher enrichment factors with better recoveries, quicker phase separation, lower cost and reduced consumption of organic solvents as well. In SPE, the sorbent material is a key factor regarding the fact that the extraction depends on the partition coefficient of analytes between a solid and a liquid phase. Therefore, the current research in SPE is oriented on the development of novel sorbents with high adsorption capacity, good regenerability and surface area accessibility.

The selection of an appropriate adsorbent is one of the prime factors governing the performance characteristics of any solid phase extraction (SPE) process. An efficient adsorbent should consist of a stable and insoluble porous matrix with suitable active groups which can interact with target ions. With the advancement in technology, development of new composite polymers having high selectivity for a particular analyte in terms of both the structural and functional properties is at par. The main advantage of the polymeric composite materials resides in the possibility of combining the physical properties of the constituents to obtain new structural or functional properties. Polymeric composites can be shaped into desired form viz., beads, resins, membranes and candles. Due to the possibility of designing properties, polymeric composite materials have been used for various field applications.

Considering the facts stated before, we have developed two different types of polymer composite sorbents for solid phase extraction of fluoride, by using two different approaches.

- One of the sorbent is an inorganic-organic hybrid polymers sheet sorbent whereas the other one consist of a super paramagnetic resin sorbent. Therefore, the current chapter is being divided in two sections. Studies on various experimental parameters and adsorption isotherms were carried out in order to know the feasibility and to understand the sorption process. The potential of the developed polymeric sorbents for removal of fluoride from real samples collected from different regions was also evaluated.

3A.2. Experimental

In the present work an inorganic-organic hybrid polymer sorbent in form of a flat sheet has been synthesized. Two types of poly(propylene) host substrates : microporous sheet and thermally bonded fibrous sheets having different surface morphology has been chosen for carrying out the grafting of a desired monomer. In order to achieve chemically and mechanically uniform sorbent material all the components have been incorporated in the polypropylene base matrix by chemical bonds. In-situ method UV irradiation has been used for the chemical bonding. The chosen host for the irradiation i.e. the poly(propylene) base provides the mechanical integrity for using them as the flat sheet sorbents or membranes in flow cells.

Photo-initiator induced graft-polymerization of a precursor monomer bis[2-methacryloyloxy)-ethyl] phosphate (MEP) on poly(propylene) chains has been carried out. Precursor monomer was selected based on its ability to form highly stable complex with thorium [Th(IV)] ions. The choice of thorium was based on its high affinity towards fluoride in any media and in addition to this, the work on thorium incorporated sorbents for defluoridation is limited in literature [251] therefore an attempt was made to synthesize a fixed-site thorium loaded sorbent for highly selective uptake of fluoride.

The chemically modified inorganic-organic sheet sorbents have been characterized in terms of parameters that influence the defluoridation of aqueous streams like pH, loading capacity, contact time, effects of competing ions, reusability and chemical stability of thorium complex in the host matrix. Physical characterization of the sorbents has also been carried out using SEM and EDXRF. After optimizing the sorbent for maximum fluoride sorption it has been further examined for its efficacy for defluoridation of real water samples.

3A.2.1 Synthesis of polymeric sheet sorbents

The pictorial and chemical representation of the synthesis is given in the Fig. 3.1 whereas the detailed experimental synthesis is discussed in chapter 2.

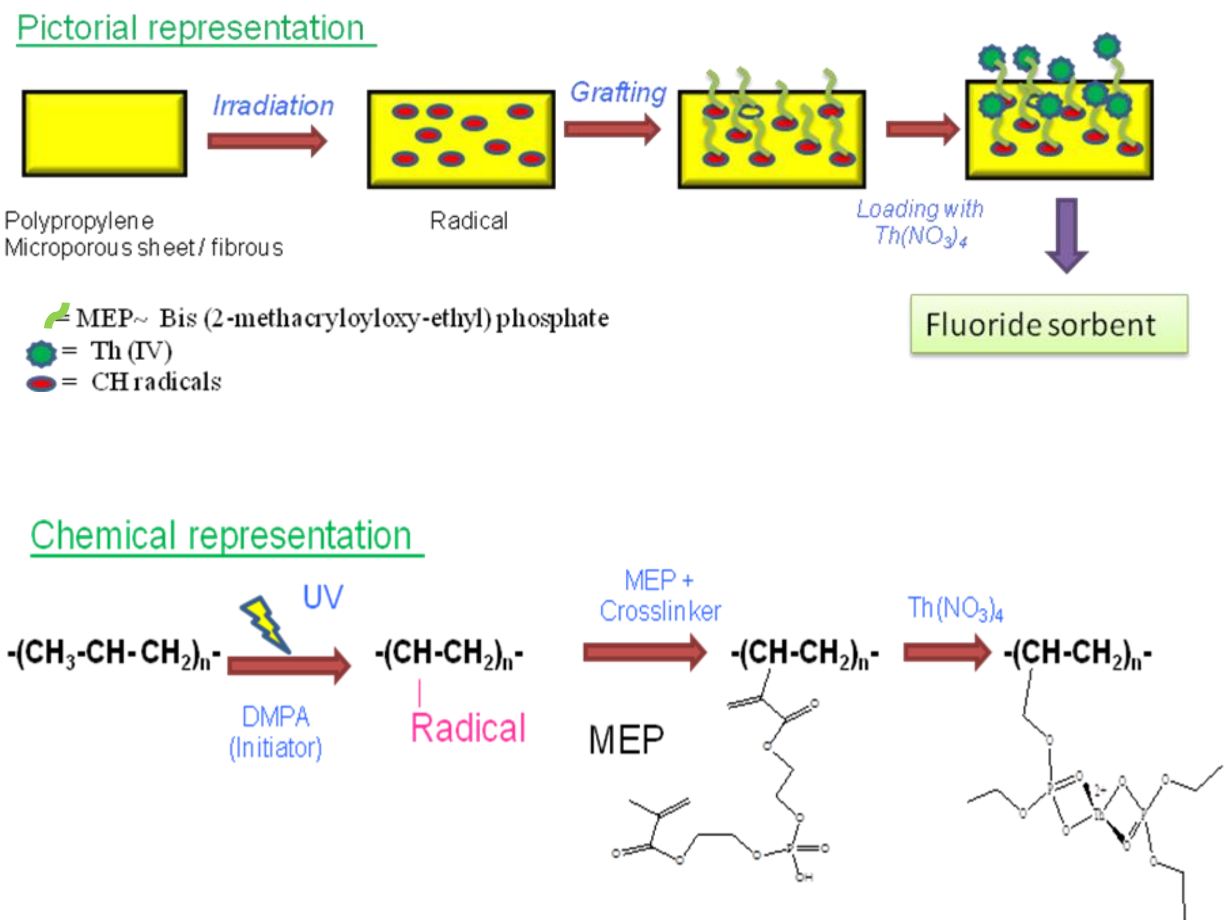

Fig. 3.1 *Schematic representation of PP membrane grafting followed by chemical treatment to prepare fluoride selective sorbent*

3A.2.2 Stability of thorium in polymeric matrix

Th(IV) ions in the sorbent samples were loaded from 1 mol L^{-1} HNO_3 containing excess of Th(IV) ions as described in experimental section 2.4.1.1. The stability of thorium-complex in the sorbent was tested by experimentally studying the leaching of thorium from the sorbents under different conditions. Sorbent samples were equilibrated with aqueous solutions containing varying acidities for one week to examine the extent of leaching out of Th from the sorbent. The amounts of Th leached out in the equilibrated solutions were measured by ICP-MS. Analyses of the solution after removing the sheet sorbents confirmed that there was no leaching of thorium from the sorbent in the treated aqueous samples.

3A.2.3 Sorption studies

The synthesized sorbents were cut into fixed size of 1×1 cm^2 area and were used for the sorption studies. Preliminary experiments were carried out by taking 25 mL solution of 1mg L^{-1}, 5 mg L^{-1} and 10 mg L^{-1} fluoride concentration. The solutions were equilibrated with the sheet sorbents under continuous stirring using a magnetic stirrer. After continuous equilibration with stirring for a predetermined time interval, the sorbent samples were taken out and fluoride concentrations left in aqueous samples were determined by Metrohm Ion Chromatograph. All the experiments were carried out at ambient temperature (25±2 ◦C).

Tolerance of the synthesized sorbent towards co-existing ions in the real water samples was carried out by repeating the sorption experiments in the presence of known concentration of certain competing ions like chloride, nitrate, sulphate, bicarbonate and phosphate along with fixed concentration of fluoride. All the samples, especially the samples from the tolerance studies were diluted prior to the fluoride determination in Ion Chromatograph so as to prevent column overloading.

Desorption experiments were carried out by equilibrating fluoride loaded sample in 20 mL NaOH solution at pH ≥10 for a period of 24h. Resultant solutions were analyzed for fluoride concentrations before and after removing the sorbents using Ion Chromatography system.

3A.3 Result and Discussion

3A.3.1 Characterization of the sorbents

The grafted sheet and fibrous sorbents were characterized, using various techniques such as percentage grafting and SEM studies.

Grafting percentage and SEM studies

The initial studies of the synthesis of the membrane sorbent were carried out by varying the composition of polymerizing solution in six different batches (Table 3.2).

Appropriate amount of the monomer MEP along with required amount of crosslinker and initiator was taken and one membrane of 5x5 cm^2 each was dipped in the solution as explained in the experimental section. Percentage grafting calculated gravimetrically of six membranes are given in Table 3.3. The extent of grafting of monomer MEP along with cross-linker MBA in the microporous poly(propylene) host substrates varied in the range of 95-400%. To limit the amount of grafting to the pores of the membrane, the composition having grafting % close to 100-150 % was fixed in rest of the experiments.

Table 3.2 *Composition of six different set of membranes (membrane size = 5x5 cm^2)*

Membrane	MEP (g)	MBA (g)	DMPA(g)	DMF (mL)	Methanol(mL)
MEM-1	0.50	0.00196	0.010	0.06	0.06
MEM-2	0.25	0.00598	0.005	0.06	0.06
MEM-3	0.15	0.00359	0.003	0.06	0.06
MEM-4	0.50	0.01196	0.010	0.06	0.06
MEM-5	0.75	0.0179	0.015	0.06	0.06
MEM-6	1.0	0.0239	0.020	0.06	0.06

Table 3.3 *Grafting yield obtained from six different set of membranes*

Membrane	$W_{Initial}$ (g)	W_{Final}(g)	Grafting yield (%)
MEM-1	0.065	0.201	209
MEM-2	0.065	0.132	103
MEM-3	0.066	0.116	82.4
MEM-4	0.107	0.362	238
MEM-5	0.101	0.232	139
MEM-6	0.113	0.199	76.2

It was found that the percentage grafting of the synthesized sorbents came out to be 130±10 wt.% which was further confirmed by SEM. To see the water uptake capacity, the grafted membranes were equilibrated with de-ionised water overnight and then weighed. All the grafted substrates prepared in the present work were found to sorb water up to 40-45 wt.% providing the required hydrophilic character to the sorbent. The scanning electron microscopic (SEM) images of both types of blank and the grafted substrates are shown in Fig 3.2.

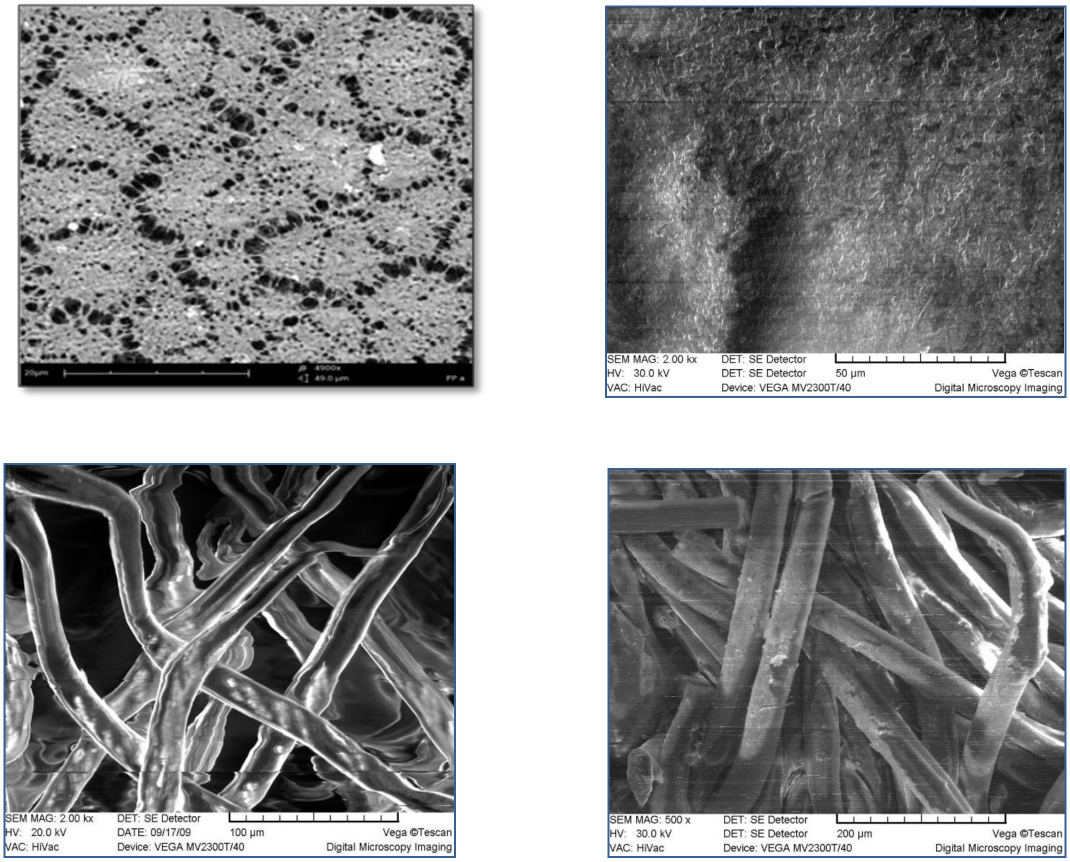

Fig. 3.2 *Scanning electron micrographs of sorbents: Sheet sorbents (a) before and after grafting (b) Fibrous sorbent before (c) and after grafting (d)*

When blank microporous sheet (Fig. 3.2.a) was compared with the grafted sheet it was found that the pores of grafted sheet were completely blocked (Fig. 3.2.b). For fibrous substrate the grafting yield calculated gravimetrically was 100±10 wt. %. In fibrous substrates void spaces between the fibers were not much affected even after the grafting (Fig. 3.2.d) when compared to the blank fibrous substrate (Fig. 3.2.c). However, the size of fibers in grafted fibrous substrate ranged from 20 to 30 μm. Thus, as can be clearly seen from the SEM images, the physical structures of these two grafted substrates were quite different suggesting that the exchange sites were more accessible in fibrous substrate than the densely blocked microporous host substrate.

EDXRF Analysis

Thorium is responsible for selective extraction of fluoride from the aqueous solution. To confirm the presence of Th(IV) in the sorbents, EDXRF analysis of the sorbent was carried out. A typical EDXRF spectrum of the sheet substrate is shown in Fig.3.3. Th L_α at 12.96 keV and Th L_β at 16.199 keV confirmed the presence of thorium in the sorbent. La, Lb, Lc notations in the figure stands for L_α, L_β and L_γ X-rays of thorium where as La1, Lb1, Lc1 denotes $L_{\alpha1}$, $L_{\beta2}$ and $L_{\gamma3}$ X-rays. The measurement was carried out for 50 sec with 100 μA current. The obtained counts were converted to cps as shown on the y-axis of the Fig 3.3.

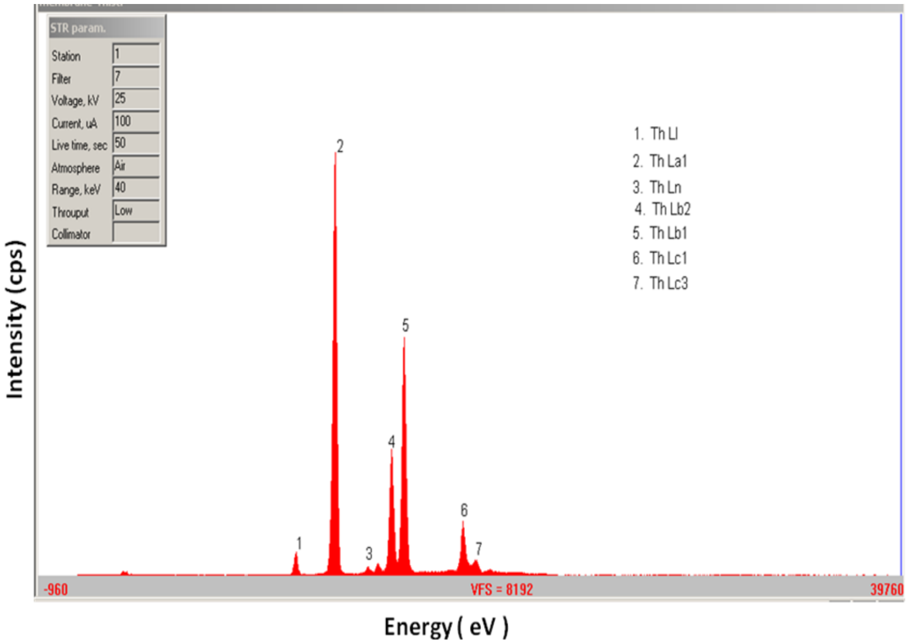

STR param.

Station: 1
Filter: 7
Voltage, kV: 25
Current, uA: 100
Live time, sec: 50
Atmosphere: Air
Range, keV: 40
Throuput: Low
Collimator:

Fig. 3.3 *EDRXF Spectrum of thorium-loaded MEP sorbent*

3A.3.2 Sorption and desorption studies

Effect of concentration

The residual fluoride concentration left in the solution after equilibration with the sorbent was measured by ion exchange chromatography. Fluoride uptake by the sorbent was calculated from the difference of fluoride concentration before and after equilibration and the results thus obtained were plotted as a function of concentration in Fig. 3. 4. It can be seen from the figure that with the increase in the fluoride concentration the percentage uptake showed a gradual decrease. Upto a concentration of 6-7 mg L^{-1} the sorption is quantitative (>80%) beyond which it decreases abruptly. The decrease in the uptake can be attributed to the saturation of available binding sites in the sorbent. Similar observation was obtained by using fibrous sorbent.

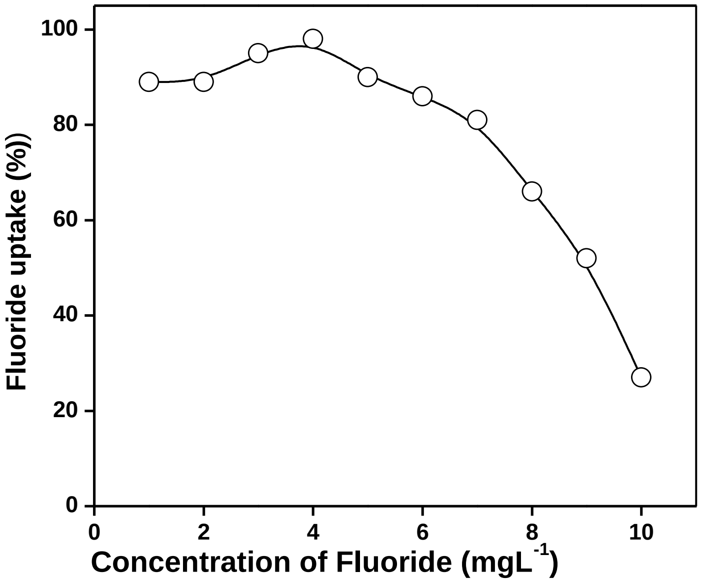

Fig. 3.4 *Uptake of fluoride ions in fixed size (1x1 cm^2) Th-MEP sheet sorbent*

The fluoride loading capacities of both the sheet and fibrous sorbent was experimentally calculated by equilibrating a known weight of sample with 25 mg L^{-1} solution of fluoride. The fluoride uptake capacities in the sheet and fibrous sorbents when calculated were found to be 0.24 meq g^{-1} and 0.09 meq g^{-1}, respectively.

Effect of pH

pH is one of the chemical conditions of aqueous media which may influence the uptake of fluoride. Therefore, uptake of fluoride in Th-MEP sorbent (1x1 cm^2) from 25 mL solution having fluoride concentration of 5 mg L^{-1} was studied as a function of pH of equilibrating solution(Fig. 3.5) .

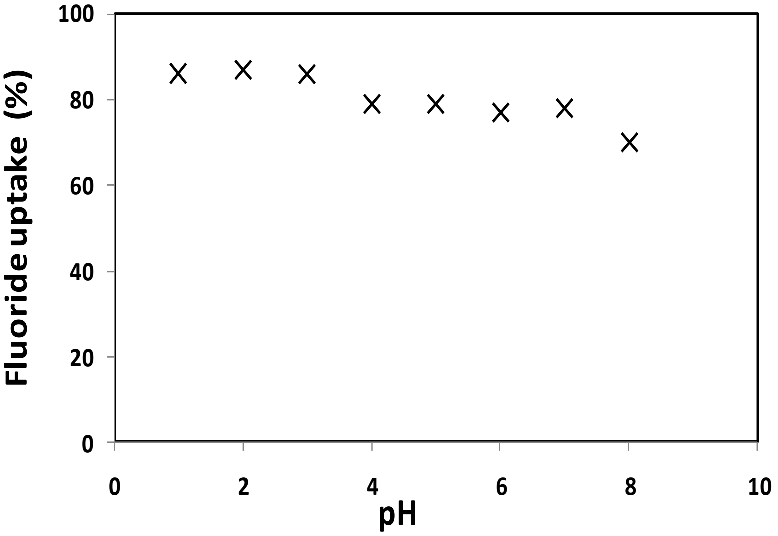

Fig. 3.5 *Uptake of fluoride in Th-MEP sheet sorbent as a function of pH of equilibrating solution*

The results showed that the uptake in the sorbent remained fairly constant with a value of 86 ±2%from pH 1 to 3 and 77±2% from pH 4 to 7. The free anions concentration in aqueous solution is governed by the dissociation constant of the acid. HF is a weak acid having pK_a values of 3.14. Thus, the change in degree of dissociation of HF is expected on increasing pH from 3 to 4. Thus, it appears from the variation of fluoride removal efficiency of the Th-MEP sorbent as a function of pH of equilibrating solution that fluoride exchange equilibrium shift to membrane side at lower pH. This is due to complexation of HF with neutral Th-MEP binding sites as it does not require electrostatic charge neutralization. Thus, the Th-MEP sites that did not have +ve charge as shown in Fig. 3.10 (b) could act as the binding sites for un-dissociated fluoride.

However, the Th-MEP sites without residual positive charge in the sorbent should be small in number due to the geometrical constraint of the cross-linked polymer chains.

This explains why there is fixed 10% decrease in fluoride removal efficiency of Th-MEP sorbent from pH ranging from 4 to 7. It is also reported in the literature that the high degree of association (low dissociation) of the acid favors its transfer in the membrane phase [252]. The uptake of fluoride in the sorbent sample was found to decrease with increase in the pH above 7. This may be due to the increased OH^- concentration with the increase in pH that competed with the fluoride. However, the wide range of pH (1-7) for fluoride uptake is good enough to make it applicable for a variety of aqueous feed ranging from natural water to industrial acidic waste streams.

Desorption studies

Desorption of fluoride from the sorbent were studied by equilibrating fluoride loaded sorbent with NaOH solution of pH > 10. The higher range of pH is based on the results obtained from pH studies. As the pH increases the percentage uptake decreases showing that the sorbent has less affinity for fluoride ions at higher pH. The results obtained in desorption experiments are plotted in Fig. 3.6. It can be clearly seen in the figure that the desorption process was not quantitative up to pH 11. However, more than 70% of fluoride was desorbed from the sorbent by onetime equilibration with a solution having pH 13. To get the complete desorption of fluoride, the same desorbed sorbent was equilibrated thrice with 0.1 M NaOH solution which in-turn led to 90% regeneration of the sorbent. This indicates that the sorbent developed in the present work is reusable.

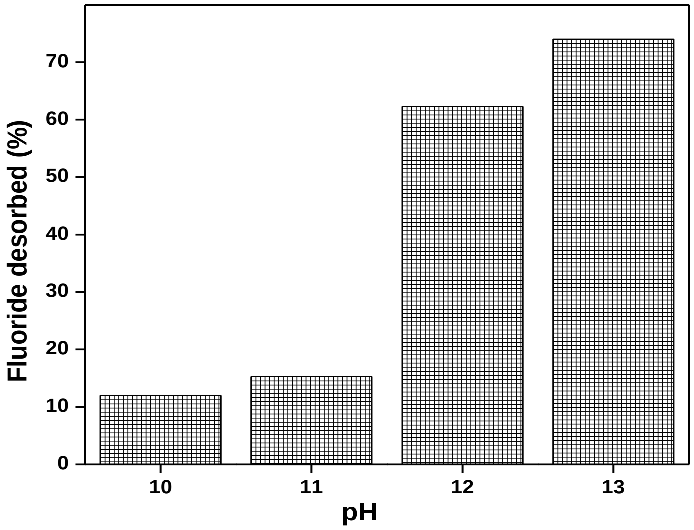

Fig. 3.6 *Desorption of fluoride from the sorbent in aqueous solution having basic range of pH*

Tolerance studies

Ground water samples usually contain several other anions along with fluoride such as chloride, nitrate, phosphate, sulphate and bicarbonate. These anions can compete with fluoride for the available binding sites in the sorbents. Therefore, tolerance of the sorbent towards existing ions was studied by equilibrating the sorbent samples with solution containing binary mixture of fluoride and one of the competing anions. The initial concentration of fluoride was fixed at 5 mg L^{-1} while for other ions two concentrations i.e. 20 mg L^{-1} and 150 mg L^{-1} were used. Fig. 3.7 shows the results obtained. It can be seen from the above figure that all other competing anions like Cl^{-}, NO_3^{-} and SO_4^{2-} have negligible effect on fluoride sorption at a concentration of 20 mg L^{-1} except PO_4^{3-} and HCO_3^{-}. For an initial concentration of PO_4^{3-} and HCO_3^{-} of 20 mg L^{-1} and 150 mg L^{-1}, defluoridation capacity of the sorbent was reduced by ~30-35% and by ~40-45%

respectively. The anions NO_3^- and SO_4^{2-} also affect fluoride sorption by about ∼20% at 150 mg L^{-1} concentration of these ions.

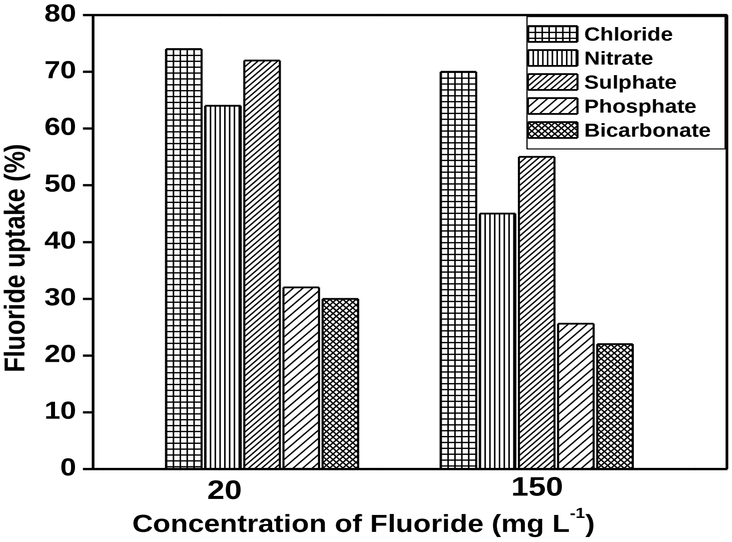

Fig. 3.7 *Effect of different competing anions on fluoride uptake in Th-poly(MEP) sheet sorbent at fixed fluoride concentration (5 mg L^{-1}) in solution*

The decrease in the sorption capacity can be due to the affinity of phosphate and bicarbonate towards thorium complexed with poly(MEP) in the sorbent. Fig. 3.7 shows that the sorbent has high affinity towards fluoride with respect to Cl^- ion therefore can be easily applied to contaminated seawaters samples where fluoride is usually accompanied with high concentration of chloride.

Sorption kinetics

For selecting optimum operating conditions for a full scale batch process kinetics of sorption is an important parameter. The uptake of fluoride by these Th(IV) ions loaded sorbents as a function of equilibration time were studied in the well stirred solution having a fixed initial concentration of fluoride as 5 mg L^{-1}. In microporous sheet sorbent it was observed that 60% of fluoride was removed in 180 min and equilibrium uptake (≈90%) was obtained only after 9 h of equilibration (Fig. 3.8a).

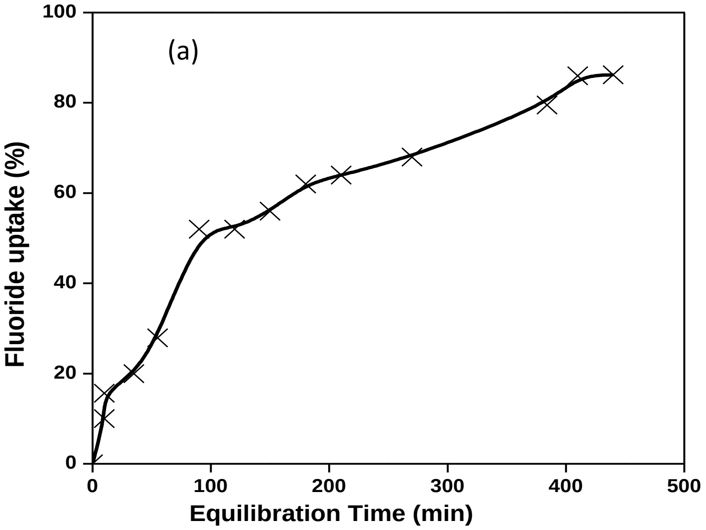

Fig. 3.8 (a) *Fluoride uptake as a function of time in sheet Th-MEP sorbent at a fixed fluoride concentration*

As accessibility of binding sites in densely grafted microporous sorbent is limited at its surface, the initial fluoride uptake might be faster whereas it slowed down as surface binding sites were saturated. In the fibrous Th-poly(MEP) sorbent ∼76% of the fluoride sorption took place in first 15 min and reached to ∼90% within 50 min of equilibration time (Fig. 3.8 b) suggesting that **the** fibrous Th-poly(MEP) sorbent having wider pore size behaves as a better sorbent compared to sheet sorbent in terms of its sorption kinetics.

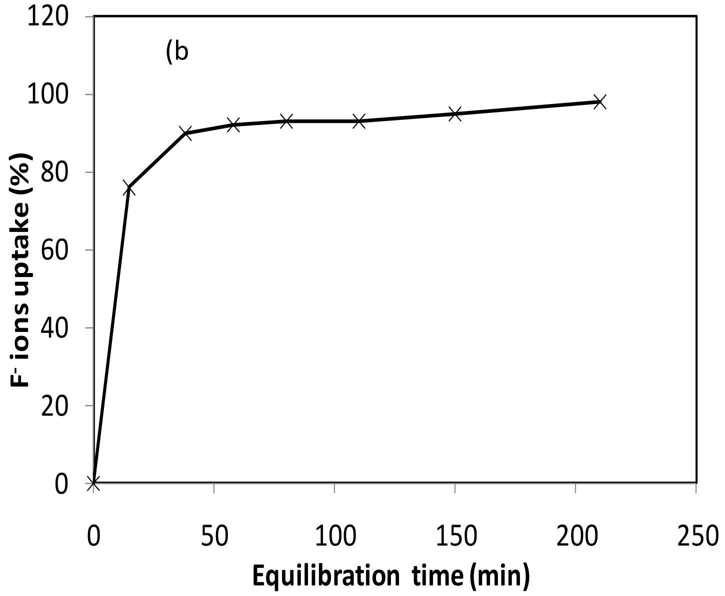

Fig. 3.8 (b) *Fluoride uptake as a function of time in fibrous Th-MEP sorbent at a fixed fluoride concentration: 5 mg* L^{-1}

3A.3.3 Kinetic models

To test whether the removal process followed first order or second order kinetics, the fluoride sorption data were analyzed using two mass transfer models. These models are Lagergren's pseudo first order rate equation and pseudo second order rate equation. The theory of these models is explained in chapter 2.

The mathematical equations used for plotting the kinetic data for first order and second order model are given below:

$$\text{Log}\ (q_e - q_t) = \text{Log}\ q_e - k_1\ (t / 2.303) \qquad (3.1)$$

$$t / q_t = (1/k_2) * q_e^2 + (1/q_e) * t \qquad (3.2)$$

where q_e and q_t are the amount of fluoride adsorbed at equilibrium and at time 't', respectively, q_o is the maximum adsorption capacity. Fig. 3.9 (a) shows the plots for the pseudo first order rate equation whereas Fig. 3.9 (b) shows the pseudo second order rate equation graphs for both the Th-poly(MEP) sorbent substrates i.e the sheet and fibrous.

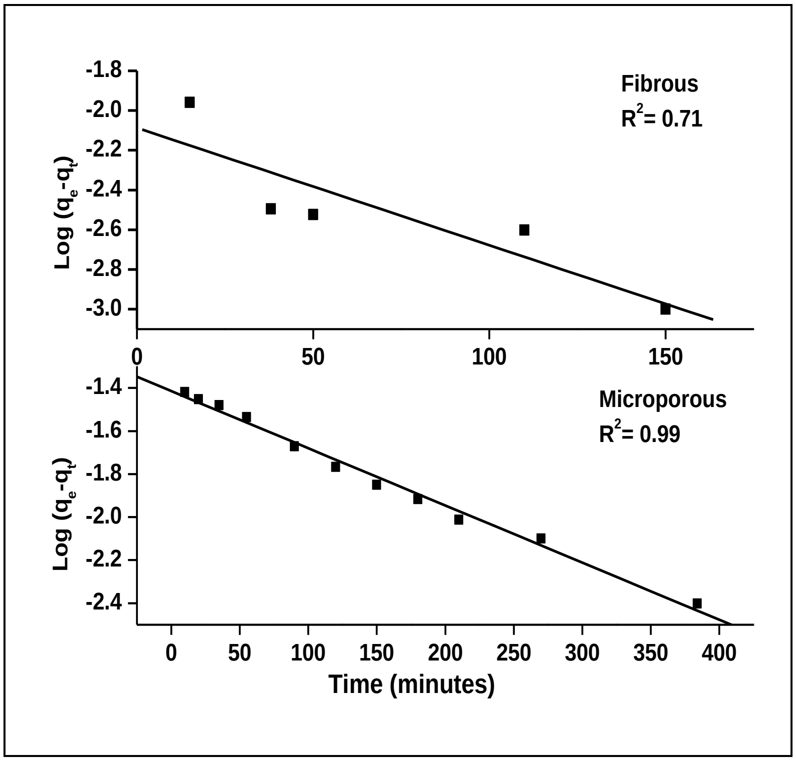

Fig. 3.9 (a) *Comparison of fluoride sorption kinetics data fitted with pseudo first order rate equations for the sheet and fibrous sorbents*

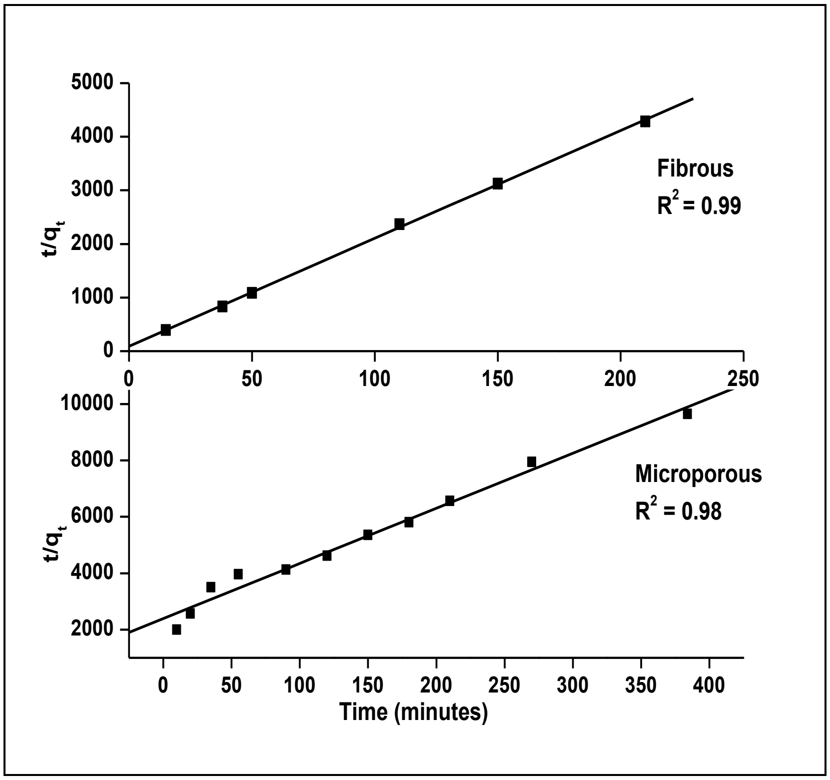

Fig. 3.9 (b) *Comparison of fluoride sorption kinetics data fitted with pseudo second order rate equations for the sheet and fibrous sorbents*

The plot of t/q_t against ‘t’ as a function of time has better linearity than that obtained from pseudo first order rate equation for fibrous sorbent indicating the validity of Lagergren’s second order equation for fluoride sorption kinetics in fibrous sorbent. However, it is reversed in the case of sheet sorbent indicating that pseudo first order rate equation better represents the kinetic data. This may be attributed to different physical structures of these sorbents. According to the pseudo first- order and pseudo-second-order kinetics models, the sorption process obeys pseudo-first-order kinetics at high initial concentration of solute and pseudo-second-order kinetics at lower initial concentration of solute [253]. The mechanisms of fluoride sorption differed in both the substrates because of the different accessibility of the binding sites. The fibrous sorbent has large spaces between fibers which provided higher accessibility of binding sites to fluoride as clearly seen in the SEM images of the grafted fibrous substrate (Fig. 3.2. (d)). Therefore, the kinetics of fluoride sorption was also governed by the fluoride concentration in aqueous phase adjacent to surface of the fibers in the sorbent leading to fast but pseudo-second-order kinetics. In case of sheet sorbent, only limited binding sites were accessible for fluoride present in the equilibrating solution (Fig. 3.2. (b). As binding sites start saturating at the surface of the sorbent, further sorption of fluoride would be dependent on its transfer from surface binding sites to interior binding sites. The transfer of fluoride to interior matrix of the sorbent would be the rate determining step in the sheet sorbent as Th-MEP binding sites have strong affinity towards fluoride. The overall result of this was slow and pseudo-first-order kinetics for fluoride sorption in the sheet sorbent. Therefore, change in surface concentration of binding sites may be responsible for switching of fluoride sorption profile from pseudo-first-order in sheet sorbent to pseudo-second order in fibrous sorbent. The adsorption rate constant (k_1 and k_2) and correlation coefficient (R^2) were calculated from the plots by fitting the experimental data and are given in Table 3.A.3.

Table 3.4 *Rate constants obtained from the graphs for Th-poly(MEP) sheet and fibrous sorbents*

Sorbent	First order rate parameters		Second order rate parameters	
	k_1	R^2	k_2	R^2
Fibrous	1.4×10^{-1}	0.717	4.36	0.99
Sheet	6.58×10^{-3}	0.99	1.28×10^{-1}	0.98

3A.4 Mechanism of fluoride sorption

The chemical structure of the monomer MEP grafted in the two types of the substrates along with their probable interaction with thorium is shown in the Fig. 3.10.

The chemical structure of MEP, given in Fig. 3.10 (a), shows that the sorbents have fixed mono-acidic phosphate groups. It is well known that phosphate groups have high affinity towards Th(IV) ions. Thus, Th(IV) ions can be strongly bound in the MEP-grafted poly(propylene) sorbents. However, it is difficult to neutralize all the four positive charges on Th ions in the sorbents due to geometrical constraint of cross-linking. This may result in one or two positive charges due to non neutralization of charge on the complex of Th-phosphate in the sorbent as shown in Fig. 3.10 (b). Since Th(IV) has affinity towards fluoride, the fixed positive charges on complexed Th(IV) ions provide binding sites for fluoride ions. Thus, the fluoride removal by the thorium loaded membrane appears to be controlled by electrostatic and complexation as shown in Fig. 3.10(c).

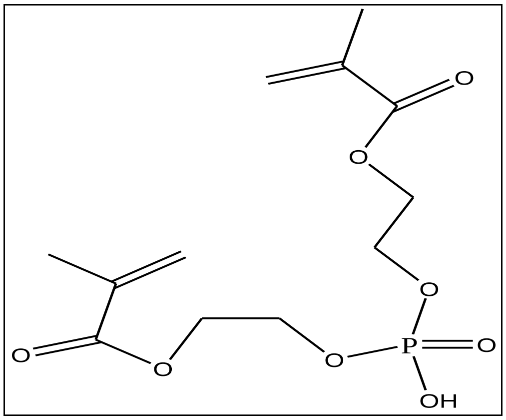

(a)

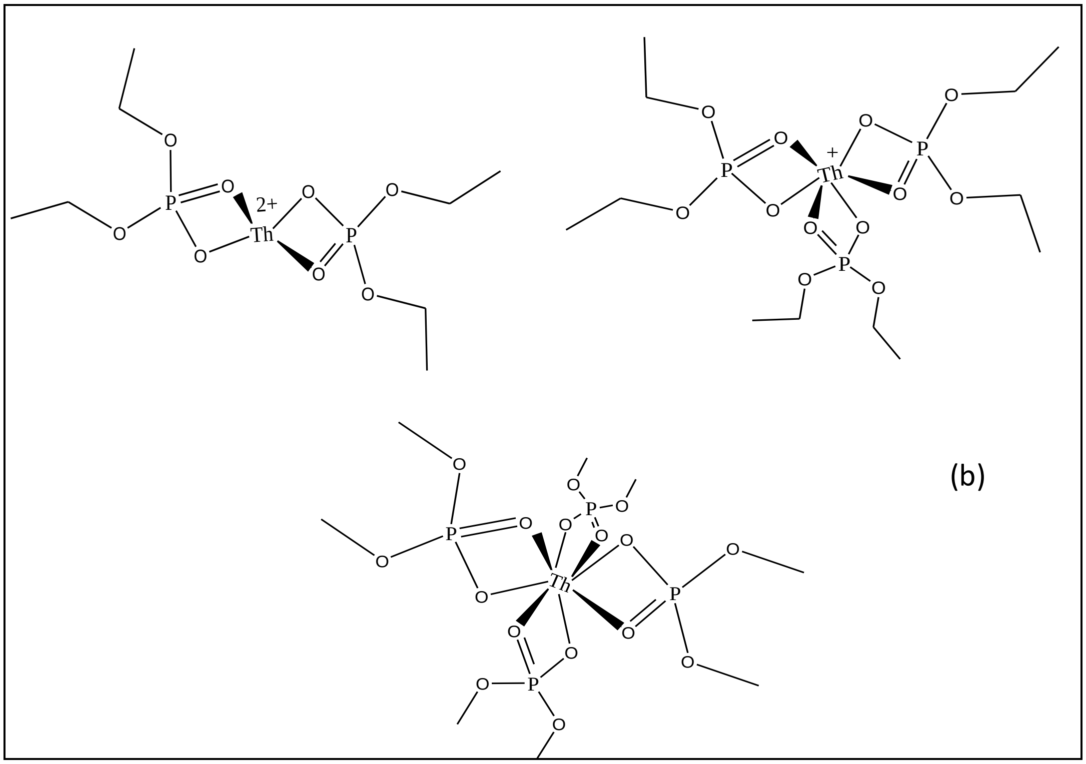

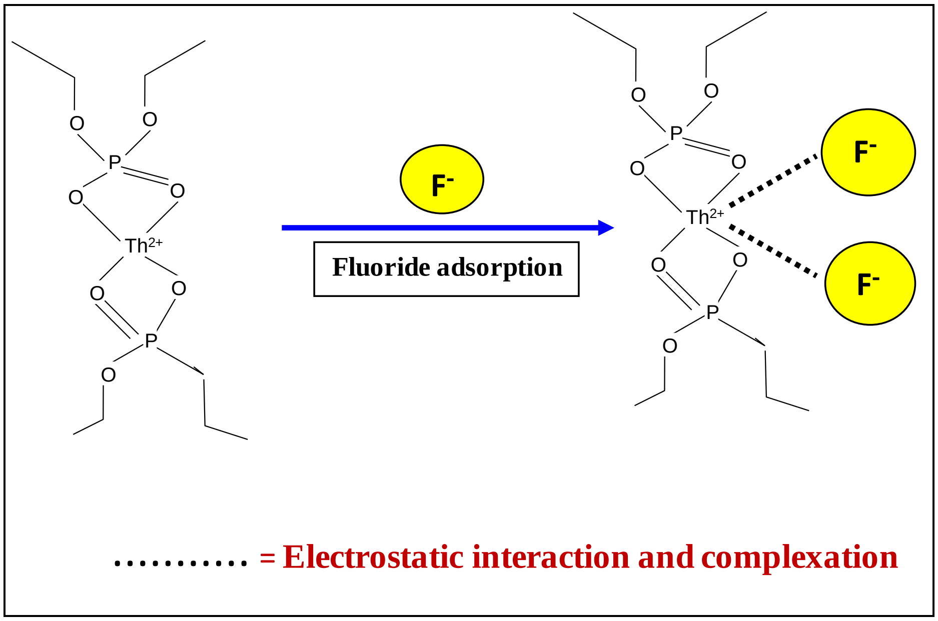

Fig. 3.10 *Chemical structures of MEP grafted (a) and different possible complexes of Th(IV)-phosphate sites(b)Mechanism of fluoride interaction with sorbent (c) in the poly(propylene) sorbents*

3A.5 Comparison of the synthesized sheet sorbents with the existing sorbents

The defluoridation capacities of the sorbents reported in the literature were compared with the capacity of the sorbents synthesized in the present work Table 3.5.

Table 3.5 *Comparison of fluoride loading capacities in different sorbents*

Sorbents	**Defluoridation capacity** (mg F^- Kg^{-1})	**Ref.**
Th-MEP grafted in fibrous poly(propylene)	1620	**Present work**
Th-MEP grafted in sheet poly(propylene)	4320	**Present work**
Alumina/chitosan composite	3809	254
Nano-hydroxyapatite/chitin composite	2840	255
Polyacrylamide Ce(IV) phosphate	2290	256
Polyacrylamide Zr(IV) phosphate	2166	256
Polyacrylamide Al(III) phosphate	2144	256
Activated Alumina	2136	257
Zirconium (IV) tungstophosphate / chitosan composite	2025	258
Nano-hydroxyapatite/chitosan composite	1560	259
Nano-hydroxyapatite	1296	260
Protonated chitosan beads	1664	261
Carboxylated chitosan beads	1385	262
Pumice	310	263
Modified kaolinite clay	105	264
Commercial ion-exchange resin	97	112

It is evident from this comparison that sheet sorbent developed in the present work has maximum fluoride loading capacity (4320 mg kg^{-1}) among the sorbents reported in literature [256-264] and fibrous sorbent has comparable fluoride loading capacity (1620 mg kg^{-1}). This is because of the fact that MEP grafted on fibrous substrate may have close proximity of the phosphate groups that may neutralize +ve charges on Th(IV) ions compared to that in the pores of sheet sorbent. The higher fluoride loading capacity of the sorbent developed in the present work can be attributed to high +ve charge density obtained by high degree of grafting of MEP that have phosphate groups for complexation with Th(IV) ions. Also, the high degree of cross-linking prevents neutralization of +ve charge on thorium ions in the complex as shown in Fig. 3.10 (b). The higher fluoride loading capacity of the sorbent developed in the present work would lead to lower inventory of the sorbent for defluoridation of aqueous streams. It is also important to note that the sorbents developed in the present work is in the form of sheets and therefore they have better mechanical integrity and are more amenable to use for defluoridation. Using bulk polymerization, the Th-poly(MEP) can be made in the bead forms for using it in the ion-exchange column.

3A.6 Application to real water samples

To see the efficacy of the developed sorbents in the real water samples, the groundwater samples collected from Punjab, India (channu area) were treated with the thorium (IV) phosphate fibrous membrane. The concentration of different cations and anions present in the original groundwater sample are presented in Table 3.6.

Table 3.6 *Composition of ground water sample collected from Channu, Punjab, India.*

Ions	Concentration (mg L^{-1})
Fluoride	3.0
Chloride	200.7
Sodium	350.0
Magnesium	33.0
Calcium	18.4
Potassium	14.0
Phosphate	ND
Bicarbonate	47

1x1 cm^2 Th-loaded fibrous membrane was dipped in 10 mL solution of these samples without any pH adjustment. After an equilibration period of 6 h the sorbent was taken out and residual fluoride concentration was measured. These samples were further filtered using 0.45 μm filter paper prior to their injection in the ion-chromatography system.

Table 3.7 *Removal of fluoride from ground water samples collected from Channu, Punjab, India using Th-poly(MEP) fibrous sorbent*

Water quality parameters	Treatment	
	Before	After
Fluoride (mg L^{-1})	3	0.3
pH	6.5	3.8

The initial fluoride concentration of 3 mg L^{-1} was reduced to 0.3 mg L^{-1} (Table 3.A.6). Thus, the final concentration left after uptake was well below permissible limit. The pH of aqueous sample was also changed to 3.8 from 6.5 that can be attributed to exchange of H^+ ions from residual un-complexed phosphate groups of MEP with cations in the ground water.

3A.7 Conclusions

To conclude, fluoride ion selective tailored polymer sheet sorbents with different surface morphologies were synthesized by in-situ UV irradiation method. The high selectivity towards fluoride was achieved by chemically modifying the polymer grafted sheets with thorium ions. The so formed Th-poly(MEP) sorbents developed were found to be robust, chemically stable and effective for the removal of fluoride from a wide variety of aqueous matrices having pH ranging from 1 to 7.

The fluoride sorption capacity and kinetics were found to be dependent on the physical architecture of poly(propylene) host substrate used for anchoring Th-poly(MEP). The two types of substrates used had different porosity and hence their fluoride sorption capacity varied depending on the ease of access of fluoride ions to the sorption sites. The sorption capacity of microporous sheet Th-poly(MEP) was found to be 4320 mg kg^{-1} compared to the fibrous substrate (1620 mg kg^{-1}) , which was highest among the sorbents reported in the literature so far. However, Th-poly(MEP) anchored on fibrous substrate was found to have very fast fluoride sorption kinetics. For example, 76% of the fluoride was sorbed in fibrous sorbent within 15 min of equilibration time. However, the fluoride loading capacity of fibrous Th-poly(MEP) sorbent was significantly lower than that of the sheet sorbent. Thus, this sorbent might be preferred when initial concentration of fluoride in aqueous medium is not very high. Most of the common interfering anions have shown insignificant effect on fluoride sorption in the sorbents. This seems to suggest that this sorbent can be used for defluoridation of natural waters as well as industrial aqueous wastes streams.

Both the sorbents developed in the present work were found to be reusable as fluoride could be desorbed quantitatively by single equilibration in solution having pH 13. Finally, the sorbents were found to have efficacy for defluoridation of ground water having higher fluoride concentration.

The developed sorbents are in the form of sheets which can further be applied in the flow cells to treat large volume of fluoride contaminated water. Along with this the sheet sorbents does not pose the problems associated with other conventional methods. Hence the use of sorbents in form of sheets provides a user-friendly and cost-effective method for fluoride decontamination.

Section 3B

MAGNETIC POLYMERIC COMPOSITE FOR FLUORIDE

3B.1 **Introduction**
3B.2 **Experimental**
  3B.2.1 **Synthesis of Magnetic Composite**
  3B.3.2 **Stability of Zirconium in Polymeric Matrix**
  3B.3.3 **Sorption Studies**
3B.3 **Results and Discussion**
  3B.3.1 **Characterization of Magnetic Sorbent**
  3B.3.2 **Sorption and Desorption Studies**
  3B.3.3 **Sorption Isotherms**
  3B.3.4 **Kinetic Models**
3B.4 **Mechanism of Fluoride Sorption**
3B.5 **Comparison studies of Magnetic Sorbents with Existing Sorbents**
3B.6 **Real Sample Analysis**
3B.7 **Conclusions**

3B.1 Introduction

Magnetic SPE (MSPE), a novel mode of SPE based on magnetic or magnetizable adsorbents, has emerged recently as a promising technique for removal of toxic ions from aqueous solution [265,266]. The targeted analytes are adsorbed onto the magnetic sorbents, and then separated from the sample solution using an external magnetic field as discussed in the introduction chapter. The analytes are consequently eluted from the adsorbents for further analysis [267-271].

Compared with conventional SPE techniques, MSPE avoids the time-consuming column passing or filtration operations because the adsorbents do not need to be packed into SPE cartridges [272-274]. Moreover, by employing magnetic separation, instead of filtration or centrifugation, MSPE obviously enhances the extraction efficiency and simplifies the pretreatment procedure [275-278]. Furthermore, the dispersive extraction mode increases the interfacial area between sorbents and analytes, and most magnetic adsorbents can be readily recycled and reused afterwards [279-281]. MSPE presents a comprehensive advantage of simplicity, time- and labor-saving, which renders it a prospective technique for sample pretreatment. Because of its several advantages, magnetic separation has become one of the promising methods of the removal of pollutants from contaminated water sources. An overview of separation by magnetically stabilized beds is proposed by Hristov and Fachikov [282]. The recent review of Ambashta and Sillanpaa [283] brings out a series of information about water purification technique using magnetic assistance.

In the recent years use of magnetic particles in the form of nanosorbents has emerged as an efficient technology in analytical community [114-119]. The application of magnetic nanoparticles (MNPs) as MSPE adsorbents has received considerable attention mainly due to its convenience and compatibility when used in complex sample matrices. Among the widely used MNPs absorbents, Fe_3O_4 nanoparticles are most popular due to their low price and toxicity. For analytical purposes, Fe_3O_4 nanoparticles have always been modified and functionalized with different materials to improve their stability and introduce new surface properties [284]. A series of substances have been used to functionalize Fe_3O_4 to achieve designed nanocomposites, such as polymers, silica, carbon, metal oxides, and ionic liquids [285-287].

Various natural and synthetic materials that have been studied as adsorbents for fluoride uptake from waste waters have low adsorption capacities, poor adsorption kinetics and high cost which make them to be not considered for full-scale water treatment. Furthermore, most of the adsorbents are powders, which would block the sewer and as such are difficult to separate easily. Therefore, an ideal adsorbent with high surface area, good physical and chemical stability and ease of its removal should be developed for fluoride removal.

The use of magnetic sorbents has not left even the field of fluoride sorption untouched. A few magnetic sorbents have been synthesized for the selective removal of fluoride. Some of the magnetic sorbents reported in literature are nano-sized super paramagnetic zirconia material ($ZrO_2/SiO_2/Fe_3O_4$), magnetic-chitosan particles, lanthanum loaded chitosan magnetic microspheres, sulfate-doped Fe_3O_4/ Al_2O_3 nanoparticles, iron oxide-hydroxide nanoparticles, bayerite/SiO_2/Fe_3O_4, hydrous aluminum oxide embedded with Fe3O4 nanoparticle, polypyrrole/Fe_3O_4 magnetic nanocomposite, and zirconium (IV)-metalloporphyrin grafted Fe_3O_4 nanoparticles [124,224,288-297]. Bhaumik et al. has also synthesized Polypyrolle/Fe_3O_4 nanocomposites with magnetic behavior for the removal of fluoride ions from aqueous solution [294]. Most of these sorbents have low fluoride sorption capacities and slow sorption rates, which lead to higher amounts of the sorbent being required in order to decrease the fluoride concentration below WHO limits. Therefore, there is a need to develop low-cost and effective sorbents with higher defluoridation capacities as well as better sorption kinetics.

As a typical kind of functionalized magnetic sorbent, magnetic polymers have been widely used for sorption studies due to their abundant adsorption sites, high pH stability as well as flexibility for modification [298] Polymer-coated MNPs are generally composed of spherical Fe_3O_4 cores with polymer coating on the surface [299]. The exterior coating can be chemically anchored on MNPs and protect the magnetic cores from oxidization and coagulation [300]. Many kinds of polymers have been used as the coating materials for MSPE adsorbents such as polyaniline (PANI), polypyrrole (PPy) and polystyrene (PS) [301]. The magnetic polymer nanomaterials can be applied to extract various organic and inorganic contaminants from environmental samples.

In the present work the main objective was to synthesize an inorganic-organic hybrid superparamagnetic polymer sorbent for fluoride removal in terms of better sorption capacity, simple preparation method and fast sorption kinetics. The commonly available acrylamide was chosen as a precursor monomer which was further polymerized along with iron oxide nanoparticles using heat induced polymerization. The as synthesized polyacrylamide was made specific for fluoride by loading it with zirconium. The developed Zr- PAM/ Fe_3O_4 magnetic composite has been characterized for its physical, chemical and magnetic properties. Various experimental conditions such as contact time, initial fluoride concentrations, pH and the presence of competing anions affecting performance of the magnetic sorbent in defluoridation have been examined. Finally the developed sorbent has been applied to real waters samples and advantage of paramagnetic nature of the sorbent has been exploited for its removal from aqueous solution by applying magnetic field.

3B.2 Experimental

3B.2.1 Synthesis of Zr-PAM/Fe_3O_4 composite

For the synthesis of magnetic polymeric sorbent, heat induced polymerisation method was used. Bulk polymerization of acrylamide monomer along with crosslinker in the presence of Fe_3O_4 nanoparticles was carried out by varying the proportion of magnetic nanoparticles in the polymerising mixture. In a typical polymerization procedure, 2.6 g acrylamide (AM), 0.31 g N,N'-methylene-bis-acrylamide (MBA), 0.2 mL of 2 wt. % ammonium persulphate (initiator), Fe_3O_4 nanoparticles (10 wt. %) in 10 mL de-ionized water were ultrasonicated for 10 min. for better dispersion of nanoparticles into polymerizing solution. Tetramethylethylenediamine (0.02 mL of 1 wt. % solution) was added drop-wise to catalyse the polymerizing reaction and the mixture was stirred at 40^o for 30 min.

Polyacrylamide is formed by copolymerization of acrylamide and N,N'-methylene-bisacrylamide via a vinyl addition polymerization reaction initiated by a free radical-generating system. Polymerization is initiated by ammonium persulfate and TEMED accelerates the rate of formation of free radicals from persulfate and these in turn catalyze polymerization. The persulfate free radicals convert acrylamide monomers to free radicals which react with unactivated monomers to begin the polymerization chain reaction. The Fe_3O_4 nanoparticles gets physically trapped in the polymer gel so formed and thus a coating of polyacrylamide on the entrapped nanoparticles prevent them from coagulation. The resulting polymer gel was left undisturbed for 2 h for completion of polymerization reaction. Finally, the gel was washed repeatedly with distilled water to remove unreacted components if any, dried under IR lamp for 24 h and ground in a mortar to a fine powder. The synthesized magnetic composite was equilibrated with 5 wt.% zirconium oxychloride solution for 24 h, and thereafter filtered and washed repeatedly with de-ionized water. The washed powder was then air-dried overnight and used for the experiments.

3B.2.2 Stability of Zirconium in polymeric matrix

Zr (IV) leaching from the sorbent was studied in aqueous solutions having varying acidity to test stability of the Zr-PAM/ Fe_3O_4 composite. 0.2 g of the synthesized magnetic composite was equilibrated with 10 mL solution solutions containing varying acidities for one week. The amounts of zirconium leached out in the equilibrated solutions was measured by ICP-MS.

3B.2.3 Sorption studies

Batch mode experiments were carried out by equilibrating a fixed amount of Zr-PAM/Fe_3O_4 composite with a known concentration of fluoride. About 0.2 g of composite was equilibrated with 25 mL of fluoride solutions of known concentrations for a predetermined time using a shaker. An external magnetic field was applied to remove the sorbent and decant the solution as shown in Fig. 3.11. The fluoride concentration in the decanted solution was measured using ion chromatograph. The variation of the percentage uptake with pH was investigated by adjusting pH of the fluoride solution of fixed concentration (5 mg L^{-1}) in the range 1-11 using 0.1 mol L^{-1} HCl and 0.1 mol L^{-1} NaOH.

The adsorption isotherm experiments were carried out by varying the initial fluoride concentration from 5 mg L^{-1} to 50 mg L^{-1}. For kinetic experiments, the fluoride concentration was fixed at 5 mg $L^{-1}$and aliquots were withdrawn at regular time intervals and were injected in Ion chromatograph for measuring residual fluoride concentration. To test the selectivity of the sorbent towards fluoride, the sorption experiments were carried out in the presence of known concentration of commonly occurring competing anions like chloride, nitrate, sulphate, bicarbonate along with fluoride. For the desorption studies, fluoride loaded sorbent was treated with 20 mL aqueous solution adjusted to different values of pH from 10-13 for 2 h. Cycles of sorption/desorption studies were carried out to check the reusability of the sorbent.

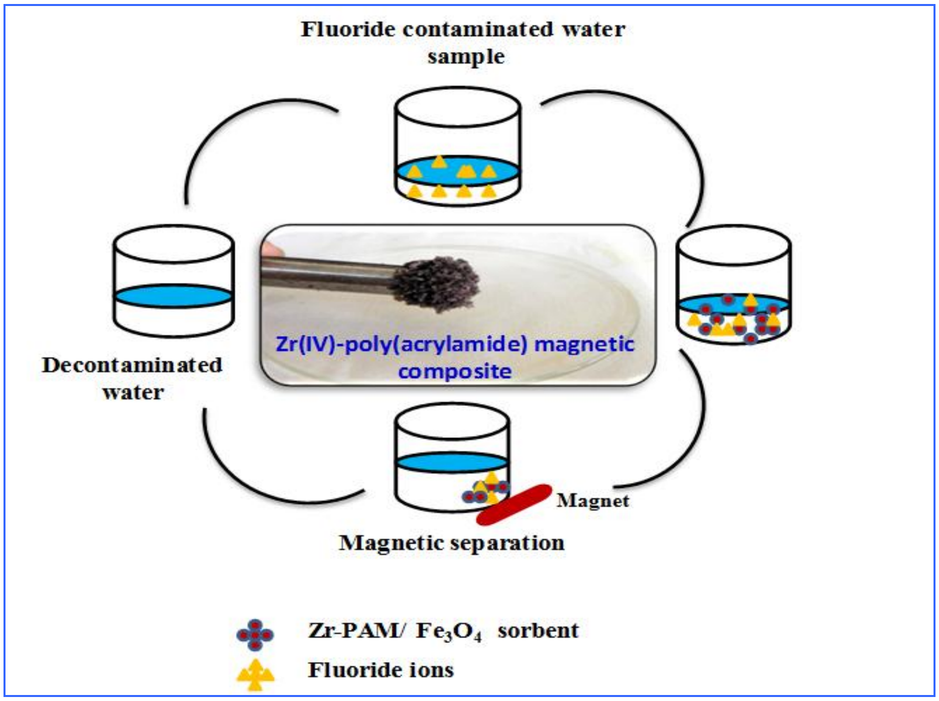

Fig. 3.11 *Defluoridation scheme using synthesized magnetic composite*

3 B.3 Results and discussion

3B.3.1 Characterization of magnetic sorbent

SEM studies

To examine the surface morphology of the synthesised magnetic composite, SEM images of the as synthesised magnetic composite before and after fluoride sorption were taken which are shown in Fig 3.12. The images were taken by sticking the sample on a conducting carbon tape and placing them in the direction of incoming electron beam.

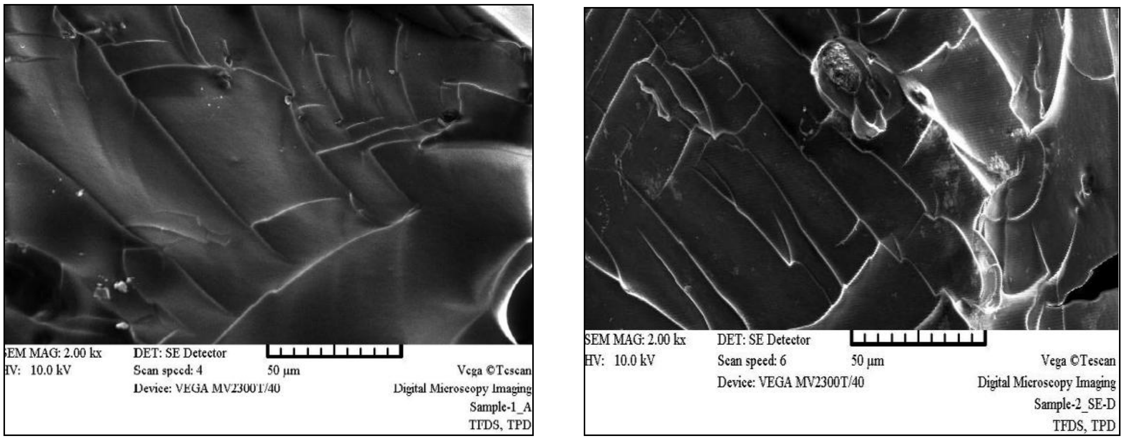

(a) (b)

Fig. 3.12 *SEM images of the magnetic sorbent before (a) and after (b) fluoride sorption*

As can be seen from the SEM figures, the sorbent developed in the present wok is a dense polymer without microporosity and has an irregular pattern. The surface morphology of the sorbent remained unchanged before and after fluoride sorption. The water content, defined as the amount of water absorbed per unit dry weight of the membrane, was determined from the difference between the weight of wet sample (W_m) and weight of dry membrane sample (W_d).

The water content of the Zr-PAM/Fe_3O_4 composite equilibrated with de-ionized water for overnight was found to be 98±10 wt. %. This suggests that the Zr-PAM/Fe_3O_4 composite has reasonably good hydrophilicity and free volume which is important for exhibiting sorption properties as the Zr-PAM/Fe_3O_4 does not have micrporous structure as seen from SEM images.

EDXRF analysis

The presence of Zr(IV) in the PAM/ Fe_3O_4 composite was confirmed by EDXRF analysis and a typical EDXRF spectrum of the composite is shown in Fig. 3.13. The K_α and K_β X-rays of zirconium in the spectrum confirmed its presence in the composite.

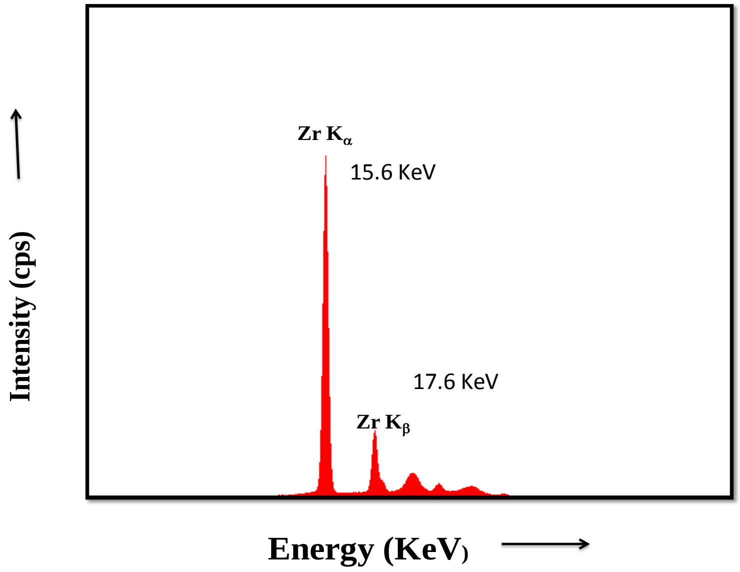

Fig. 3.13 *EDXRF spectrum of Zr(IV)-loaded polyacrylamide/Fe_3O_4 composite*

IR studies

FTIR spectra of the magnetic composite were recorded in order to identify the functional groups present in it. It is seen from the FT-IR spectra given in Fig. 3.14 that several peaks corresponding to chemical structure of PAM are present. The FT-IR spectrum (a) taken before loading shows the major bands for the PAM at 1660 cm^{-1} (–CO stretching vibration –$CONH_2$), 1652cm^{-1} (–NH_2 bending vibration), 1428 cm^{-1} (–CN stretching vibration in – $CONH_2$), 1367 cm^{-1} (-CH_2 wagging vibration), 1120 cm^{-1} (C-C stretching vibration), and 3300–3500 cm^{-1} (–NH_2 and -OH stretching vibration). The diminishing of the broad band at 3300–3500 cm^{-1} and 1660 cm^{-1} in the spectrum of Zr(IV) loaded PAM could be attributed to the complexation of zirconium with the amide groups of polyacrylamide composite.

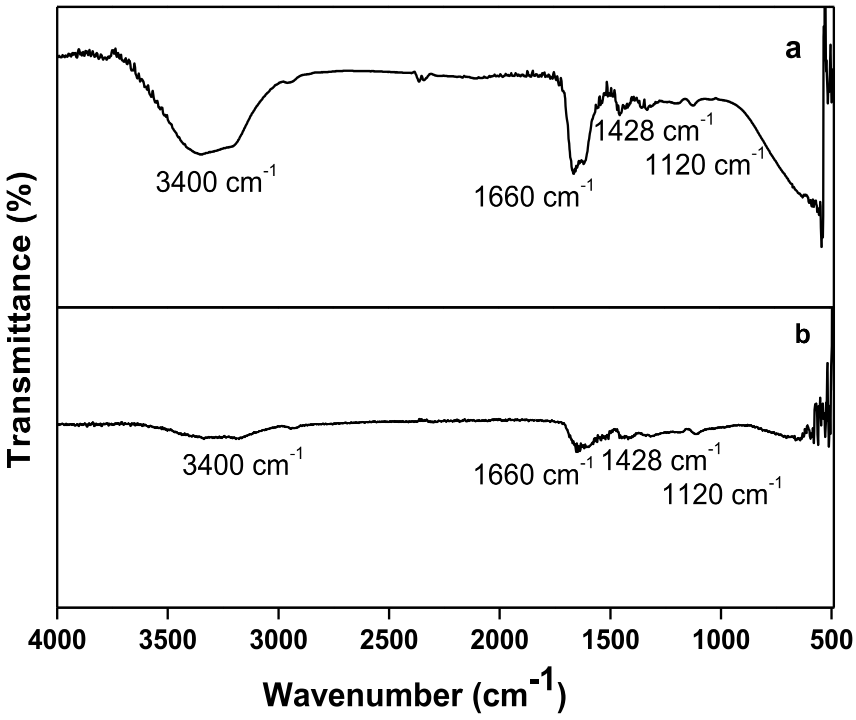

Fig. 3.14 *FTIR spectra of the composite sorbent before (a) and after (b) fluoride sorption*

Magnetic characterization

To study super paramagnetic properties of the synthesised Zr-PAM/Fe_3O_4 composite, the variation of magnetization (*M*) vs magnetic field (*H*) curves for the Zr-PAM/Fe_3O_4 samples with different mass ratio of Fe_3O_4 to Zr-PAM (2:1, 5:1 and 10:1) at room temperature (300 K) were obtained (Fig 3.15).

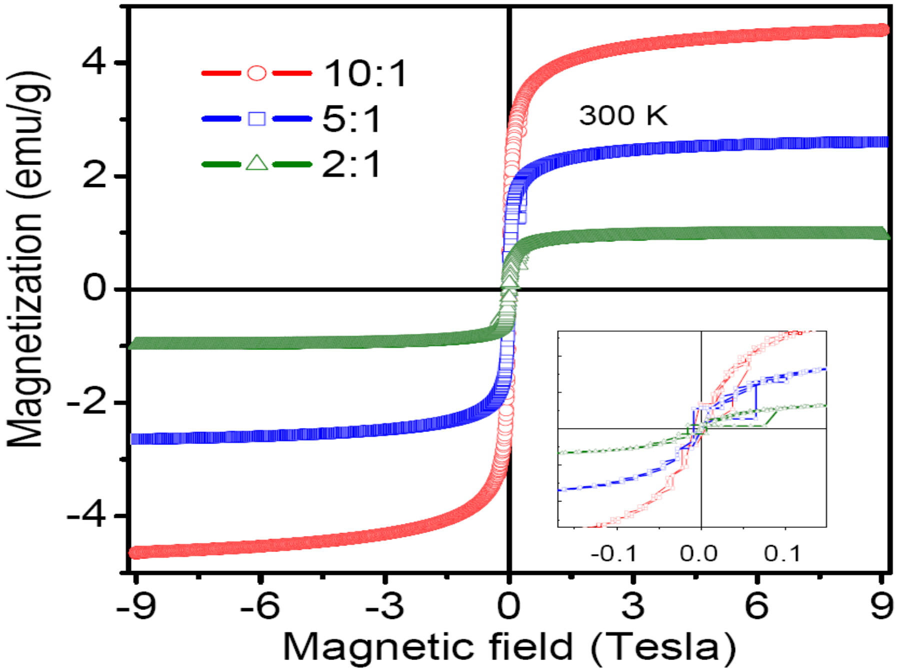

Fig. 3.15 *VSM magnetization curves of the Zr-PAM/Fe_3O_4 samples with varying mass ratio of Fe_3O_4 to Zr-PAM*

It is clear from Fig. 3.15 that the Zr-PAM/Fe_3O_4 samples exhibit typical behaviour of super paramagnetic compounds characterized by zero coercivity, zero remanence and *s* shape like hysteresis curves with high value of saturation magnetization. The negligible coercivity and zero remanence can be seen in the inset of Fig. 3.15 for all the the Zr-PAM/Fe_3O_4 samples having different amount of Fe_3O_4. As expected, the saturation magnetization, a measure of the maximum magnetic strength, increased linearly with increase in weight fraction of Fe_3O_4 nanoparticles in the Zr-PAM/Fe_3O_4 composites. The saturation magnetization is a key factor for successful magnetic separation. The saturation magnetization of 2:1, 5:1 and 10:1 compound is found to be 1, 2.6, and 4.5 emu/g, respectively at 9 Tesla. The saturation magnetization of 4.5 emu/g of the Zr-PAM/Fe_3O_4 composite with 10 wt.% was high enough for magnetic separation.

Stability of zirconium in polyacrylamide matrix

Zr (IV) leaching from the sorbent was studied in aqueous solutions having varying acidity to test stability of the Zr-PAM/Fe_3O_4 composite. It was observed from ICP-MS analysis that there was no leaching of Zr(IV) ions from the sorbent in the treated aqueous samples (Fig. 3.16). This indicates strong chemical binding of Zr(IV) ions with functional groups of PAM.

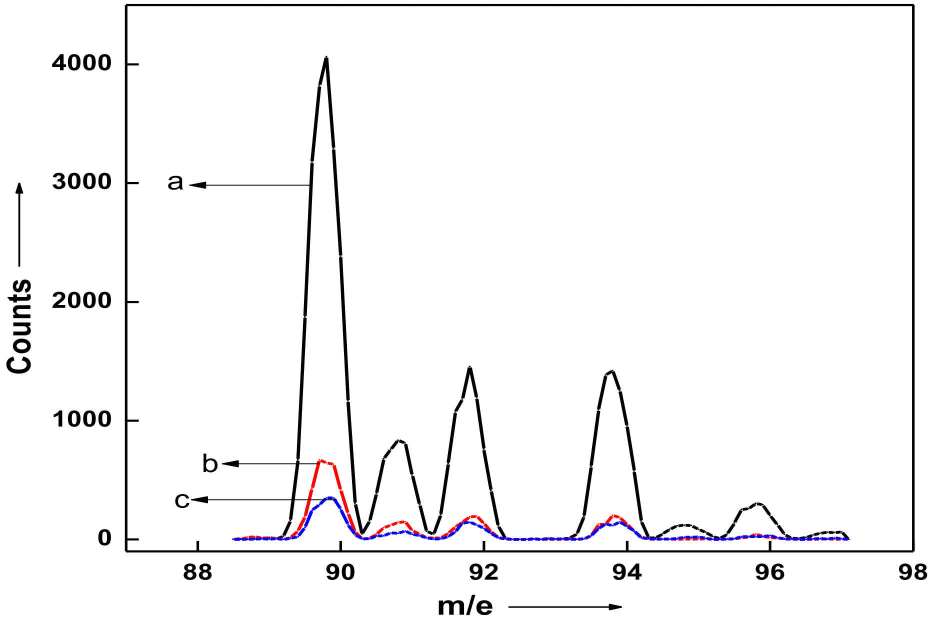

Fig. 3.16 *ICPMS spectra of leached sorbent showing absence of zirconium.-(b and c are the sorbent treated aqueous samples at pH 2 and pH 4 and a - 2 μgL^{-1} Zr standard)*

3B.3.2 Sorption and desorption studies

Effect of pH

The effect of pH on the removal of fluoride by the sorbent was studied by varying pH of the solution and the results are shown in Fig. 3.17.

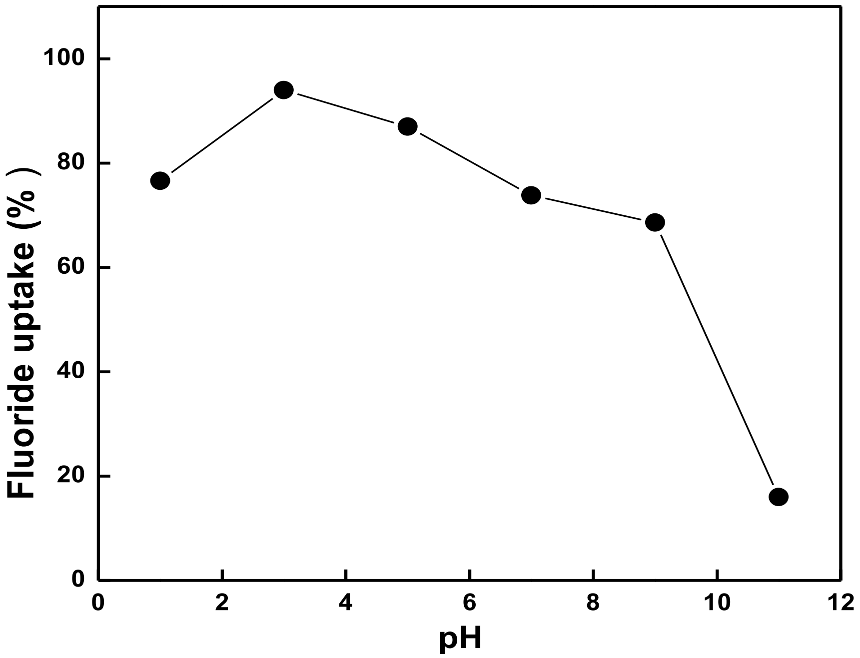

Fig. 3.17 *Uptake of fluoride by the sorbent as a function of pH of equilibrating solution*

The sorbent showed about 80 % fluoride uptake in the pH range of 1-8 with maximum of 93 % at pH 3. These results suggest that the composite is effective in a broad pH range. The maximum uptake at pH 3 is attributed to the fact that HF is a weak acid (pKa = 3.14). The free anions concentration in aqueous solution is governed by dissociation constant of the acid. The degree of dissociation of HF is expected to increase with increase in pH from 1 to 3 [302]. The presence of higher concentration of free fluoride ions at pH 3 leads to higher uptake. Low sorption at pH < 3 can be attributed to the formation of electrically neutral hydrofluoric acid. This would reduce the electrostatic attraction between fluoride and the sorbent surface whereas the hydroxyl ions compete with the fluoride ions for the available binding sites on the sorbent in alkaline medium. Therefore, the uptake decreases at higher pH.

Optimization of sorbent dosage

Study of the effect of sorbent dosage gives an idea of the effectiveness of a sorbent. Herein, the sorption of fluoride using Zr-PAM/Fe3O4 composite has been analyzed by varying the sorbent dosage in the range of 0.1-0.25 g. The percentage removal of fluoride with different sorbent dosages is shown in Fig. 3.18.

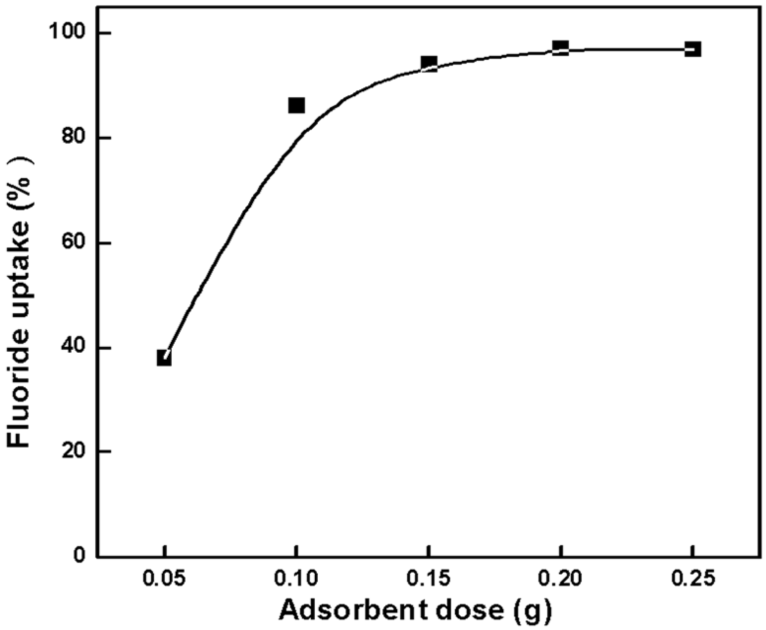

Fig. 3.18 *Effect of dosage of the sorbent on the uptake of fluoride (Fluoride concentration: 5 mg* L^{-1}*; volume of solution : 25 mL)*

Initially the percentage removal increased with the increase in the dosage and then it remained almost constant with further increase in the sorbent dose. The increase in the number of the active adsorption sites of the sorbent with increased dose explains the initial increase in percentage uptake. At the sorbent dose of 0.15 g the uptake became constant because the available sites on the composite are more than needed for a fixed amount of fluoride (5 mg L^{-1}). To ensure the complete removal of fluoride from the solution 0.25 g of sorbent was fixed as an optimum dosage of sorbent for rest of the experiments.

Effect of competitive anions

In order to study the possible interference of these ions in the fluoride uptake, tolerance studies of the sorbent were carried out. The variation of defluoridation capacity of Zr-PAM magnetic composite in the presence of co-anions viz., Cl^- , SO_4^{2-} , NO_3^- and HCO_3^- with a fixed initial concentration of 200 mg L^{-1} and fluoride concentration of 10 mg L^{-1} is shown in (Fig. 3.19).

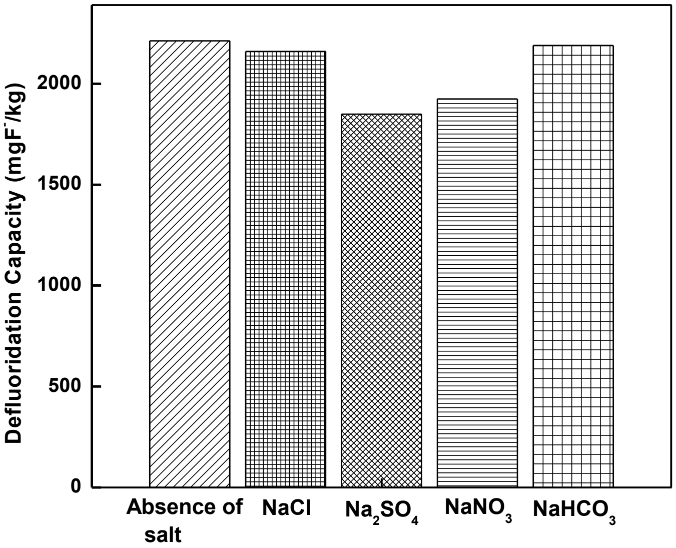

Fig. 3.19 *Effect of different co-existing anions on fluoride uptake in magnetic sorbent (Fluoride concentration = 10 mg L^{-1} and concentration of co-existing ions = 200 mg L^{-1})*

It was observed that the presence of sulphate and nitrate decreased marginally (~ 5%) while other anions (chloride and bicarbonate) have no significant effect on the fluoride removal efficiency. This clearly shows that the developed sorbent can selectively preconcentrate fluoride due to the complex formation with zirconium in the sorbent.

Desorption studies

As the uptake of fluoride is reduced at higher pH, desorption was studied by equilibrating the fluoride loaded Zr-PAM/Fe_3O_4 sorbent with NaOH solution of different pH. The fluoride loaded sorbent was transferred to 20 mL of water and pH was adjusted to different values from pH 1 to pH 13. After equilibrating for 30 min, the supernatant was monitored for fluoride concentration and the results are shown in Fig. 3.20.

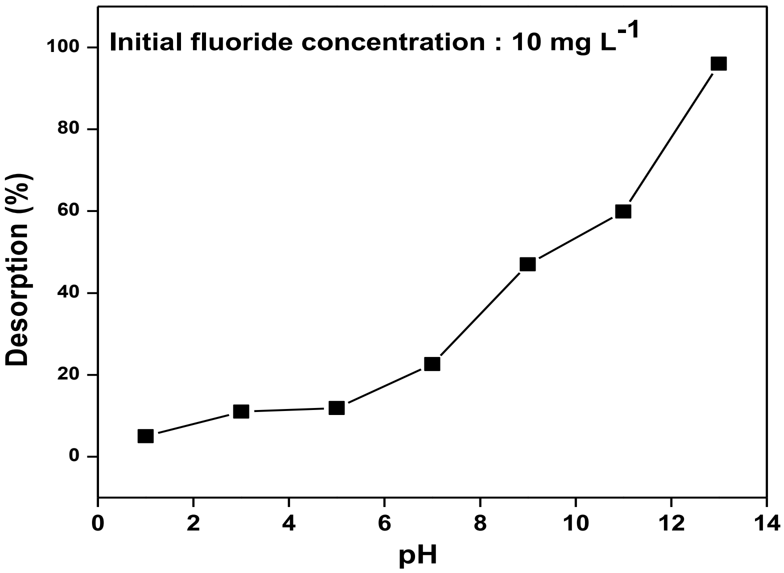

Fig. 3.20 *Desorption profile of fluoride sorbed Zr-PAM magnetic nanocomposite under different pH values.*

It can be clearly seen from the figure that up to pH 11, desorption was only 60 %. However, fluoride desorption was increased to 96% with the increase of pH to 13. Fluoride sorption tests with the regenerated sorbent showed no decrease in the sorption capacity of the sorbent upto 6 cycles but after 6th cycle the kinetics of desorption became slower thus the results indicate that the composite sorbent is reusable upto five cycles.

Effect of initial concentration

Sorption equilibrium is established when the ratio of concentration of sorbate in the bulk solution and that on the solid- liquid interface is constant. Equilibrium data are a perquisite to calculate sorption capacity of the sorbent and are needed to operate a sorption process efficiently. The specific amount adsorbed in the sorbent is calculated from the following equation

$$Q_e = \frac{(C_0 - C_e)}{W} \times V \tag{3.3}$$

where Co, Ce, W and V are initial concentration, equilibrium concentration, weight of sorbent and volume of solution, respectively. The sorption isotherm between fluoride concentration on the sorbent (Qe) and that remained in the solution (Ce) is shown in Fig. 3.21. An exponential isotherm indicates that the equilibrium fluoride sorption capacity increased significantly followed by a gradual increase in sorption which finally resulted in a plateau as the surface binding sites were saturated at fluoride concentration of 24 mg L^{-1} (Fig. 3.21). The fluoride sorption capacity obtained experimentally using equation 3.3 was 124.5 mg g^{-1}. The initial increase in the fluoride sorption capacity with increase in the fluoride concentration is due to the concentration gradient across the surface of the sorbent.

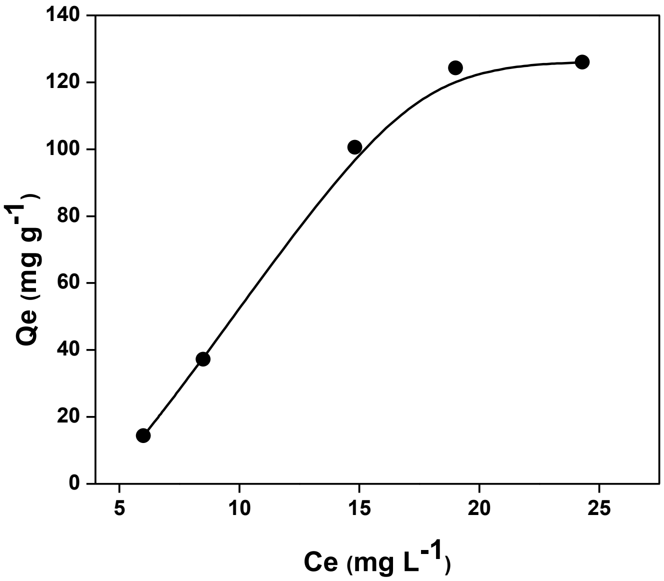

Fig. 3.21 *Uptake of fluoride by the magnetic sorbent as a function of concentration of equilibrating solution*

3B.3.3 Sorption isotherms

Langmuir and freundlich isotherm models were used to evaluate the maximum sorption capacity of the synthesised magnetic sorbent. The sorption of fluoride on the sorbent can be considered as a monolayer or multilayer. Among the two models, the freundlich isotherm model is based on the assumption that the ratio of solute sorbed to that in the solution is a function of solute concentration. The data obtained was analyzed using the linear form of Freundlich isotherm which is given by eq. 3.4.

$$\text{Log } q_e = \text{Log}K_F + 1/n \text{ Log}C_e \qquad (3.4)$$

where K_F and n are Freundlich constants representing adsorption capacity and adsorption intensity, respectively, Qe is the equilibrium adsorption capacity (mg g^{-1}) and Ce is the equilibrium concentration (mg L^{-1}). The plot of ln Qe vs. ln Ce was a non linear graph (Fig. 3.22(a)).

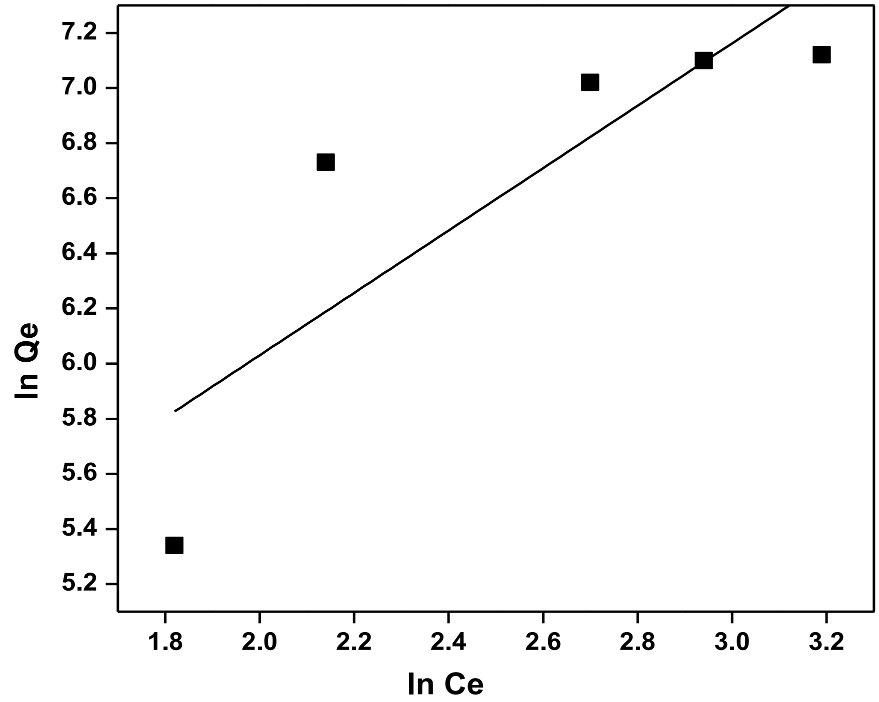

Fig. 3.22 (a) *Freundlich isotherms for the uptake of fluoride by magnetic sorbent*

Langmuir isotherm as explained in the chapter 2, indicates that the interaction between sorbate and sorbent is through chemical bonding. The linear form of the Langmuir equation was applied to calculate adsorption capacity and is given by following eq.:

$C_e/ Q_e = 1/ Q_o K_L + C_e / Q_o$ (3.5)

where Ce is the equilibrium concentration (mg L^{-1}), Q_e is the equilibrium adsorption capacity (mg g^{-1}) ,Q_o and K_L are Langmuir constants representing adsorption capacity(mg

g^{-1}) and energy of adsorption (L mg^{-1}), respectively. The plot of C_e/Q_e and C_e obtained was a straight line as shown in (Fig. 3.22(b)) indicating that the sorption system followed Langmuir model. The value of Q_o and K_L were calculated from slope and intercept of the straight line. Higher correlation coefficient was obtained with Langmuir model compared to Freundlich suggesting its validity for the present sorption system.

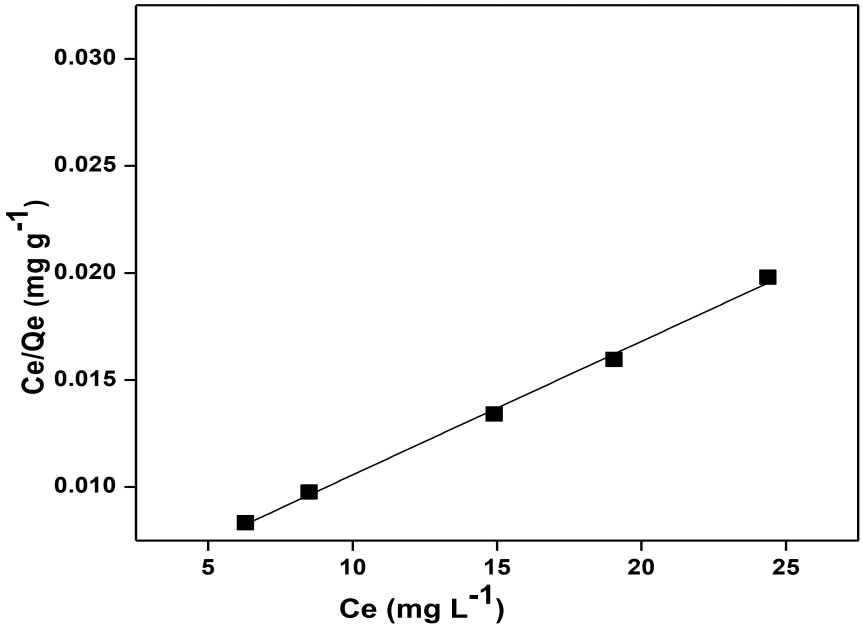

Fig. 3.22 (b) *Langmuir isotherms for the uptake of fluoride by magnetic sorbent*

The values of all the constants derived from the isotherms are given in Table 3.8.The experimentally determined uptake capacity (124.5 mg L^{-1}) was found to be comparable with that obtained by the analysis of Langmuir plot (123.9 mg L^{-1}) confirming that the interaction between sorbate and sorbent is through chemical bonding. The R_L (separation factor) which can be calculated from Langmuir data as $R_L = 1/ (1+ K_L C_i)$ was 0.41 (< 1) suggesting favourable adsorption as the value of R_L lies between 0 and 1.

Table 3.8 *Values of the constants derived from Freundlich and Langmuir isotherms*

Freundlich			Langmuir		
K_F	n	R^2	K_L (L mg^{-1})	Q_o ($mg\ g^{-1}$)	R^2
42	0.88	0.69	0 .14	123.9	0.99

3B.3.4 Kinetic models

Kinetics of sorption is one of the important parameter to be studied for designing any sorbent system. The uptake of fluoride as a function of equilibration time was studied in well stirred solution having a fixed initial concentration of fluoride as 5 mg L^{-1} (Fig. 3.23).

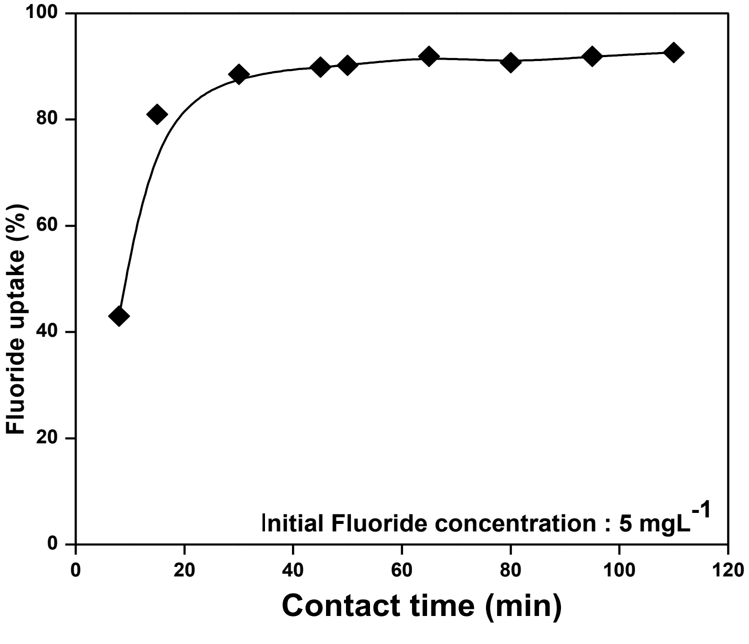

Fig. 3.23 *Fluoride uptake in the Zr-PAM/Fe_3O_4 as a function of time*

It can be seen from the sorption profile given in Fig. 3.23 that within 15 min 81% of fluoride was sorbed equilibrium (≈92%) was attained after 50 min. The time to reach equilibrium was shorter as compared to most of the sorbents listed in Table 3.10. This could be attributed to the reduction in diffusion path and increase in exposed surface area that has facilitated the fast sorption rate. Time required for the uptake beyond 85% is longer i.e. > 30 min for 92% sorption. This could be due to the saturation of the available binding sites at the sorbent surface, and further sorption of fluoride in the Zr-PAM matrix would be dependent on the diffusion of fluoride to the interior sites in the sorbent leading to slower sorption.

To study the order of kinetics, the sorption profiles were tested with pseudo first order and pseudo second order kinetic models as explained in section 3A. Linear plots suggested the applicability of Lagergren equations (Fig. 3.24).

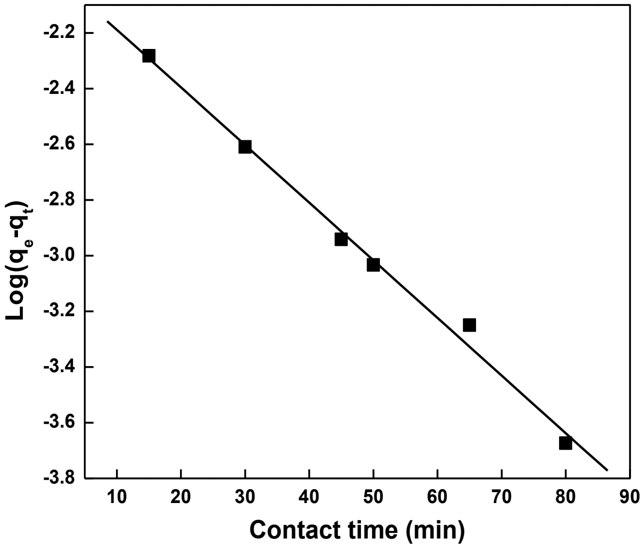

Fig. 3.24 (a) *Fluoride sorption kinetics data fitted with pseudo first order rate equations*

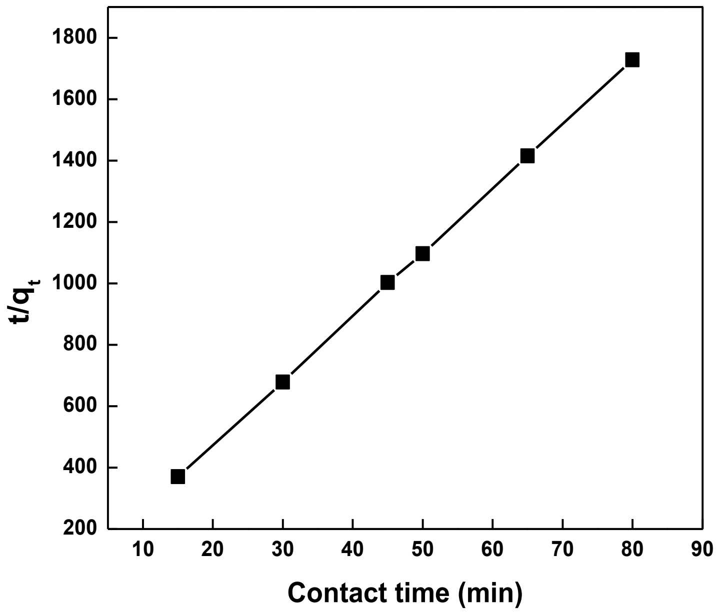

Fig. 3.24 ***(b)*** *Fluoride sorption kinetics data fitted with pseudo second order rate equations*

The plot t/q_t vs t gives a straight line with a higher correlation coefficient than that observed from pseudo first order plot. This suggests the applicability of pseudo - second order process. The value of adsorption coefficient (k_{ad}) and correlation coefficient (R^2) computed from these plots of the sorbent are given in Table 3.9.

Thus, kinetics of fluoride sorption was governed by the binding sites on the composite as well as the fluoride concentration in aqueous phase adjacent to surface of the sorbent leading to fast pseudo-second-order kinetics. In addition to this, applicability of pseudo - second order model supports the results obtained from the Langmuir isotherm suggesting that the interaction of fluoride is via chemisorption and it is the rate determining step for the sorption system.

Table 3.9 *Rate constants obtained from the graphs for the sorbent. (Fluoride concentration: 5 mg L^{-1}; volume of solution : 25 mL)*

F^- conc.	**Pseudo first order**		**Pseudo second order**	
	k_1	R^2	K_2	R^2
5 mg L^{-1}	$4.7x10^{-2}$	0.98	$0.79x10^{-1}$	0.99

3B.4 Mechanism of fluoride sorption

The fluoride removal by the zirconium loaded magnetic composite appears to be controlled by both electrostatic interaction and complexation mechanism. It has been reported in the literature that the carbonyl group of amide binds with the metal ions therefore zirconium binds to polyacrylamide irreversibly as shown in the figure. Since PAM is neutral polymer, the positive charge on zirconyl ions provide binding sites for anions particularly F^- ions that has strong affinity towards Zr(IV). The removal of fluoride may also be controlled by ion exchange with chloride ions in addition to the electrostatic attraction as shown below.

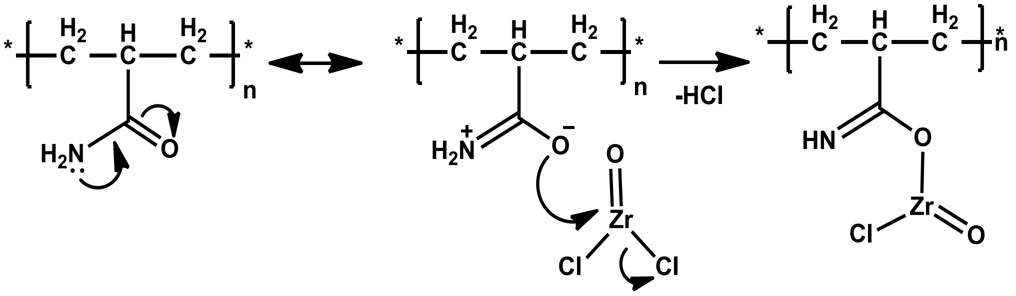

3B.5 Comparison studies of magnetic sorbent with existing sorbents

In order to see the performance of the developed sorbent in terms of its capacity, fluoride sorption capacities of different magnetic and non-magnetic sorbents reported in literature were compared with the Zr-PAM/ Fe_3O_4 sorbent as shown in Table 3.10.

Table 3.10 *Comparison of Fluoride loading capacity of various adsorbents*

Sorbents	**Defluoridation capacity ($mg\ F^- g^{-1}$)**	**Reference**
Zr- Polyacrylamide magnetic nanocomposite	124.5	**Present study**
Polyacrylamide Zr(IV), Al(III) phosphate	2.17, 2.14	256
Zirconium (IV) tungstophosphate / chitosan	2.03	258
Nano-hydroxyapatite/chitosan	1.56	259
Nano-hydroxyapatite	1.29	260
Protonated chitosan Carboxylated chitosan	1.66, 1.38	261
Activated Alumina	3.86-5.0	303
Aligned carbon nano tubes	4.1	304
Polypyrrole/Fe_3O_4 magnetic nanocomposite	17.63–22.31	294
Fe_3O_4@$Al(OH)_3$ magnetic nanoparticles	88.48	293
Aluminum-type superparamagnetic adsorbents	38	292
Magnetic chitosan	20.96–23.98	288
Superparamagnetic zirconia material	14.7	124
Iron Oxide-Hydroxide Nanoparticles	1.66	291
Sulfate-doped Fe_3O_4/Al_2O_3 nanoparticles	70.4	290
Aluminium hydroxide lime stone waste	84.03	305
Nanomagnesia	20.66	295
Calcined layered double hydroxides	80.00	296
MgAl-CO_3 double hydroxides	213.8	297
Fe–Al–Ce trimetal oxide	178.0	224

It can be seen from this comparison that the F^- sorption capacity of the Zr-PAM/ Fe_3O_4 is significantly higher than the sorbents listed in Table 3.10. Such high F^- sorption capacity of the Zr-PAM/ Fe_3O_4 can be attributed to the high loading of ZrO^{2+} ions in the polyacrylamide matrix as well as availability of all the positive charges for neutralization with F^- ions. This clearly shows that the super paramagnetic sorbent synthesized in this study offers a great potential in the sorption process not only due to its high adsorption capacity but also the ease of separation, which can overcome the difficulties in case of polluted water containing solid suspensions for e.g. in brackish water streams.

3B.6 Application to Real Samples

The field applicability of the Zr-PAM/Fe_3O_4 sorbent was evaluated using real samples collected from Punjab state, India. The samples were collected from the groundwater of Channu district of Punjab. The fluoride content of the real sample was investigated before and after the sorption study. The results are listed in Table 3.11. The fluoride concentration left after uptake was well below the permissible limit, where as chloride concentration was reduced marginally (~ 10 %).

Table 3.11 *Removal of fluoride from ground water samples collected from Channu, Punjab, India using Zr- PAM/Fe_3O_4 sorbent*

Water quality parameter	Before treatment	After treatment
pH	8.5	7.8
F^- mg L^{-1}	4.2 ± 0.2	0.1 ± 0.8
Cl^- mg L^{-1}	61.0 ± 1.1	53.4 ± 0.7

3B.7 Conclusions

To conclude, a fluoride selective magnetic composite in the form of a polymeric resin was synthesised using heat induced polymerisation method. In situ polymerization of acrylamide was carried out in presence of Fe_3O_4 nanoparticles followed by chemical treatment with zirconium oxychloride to form Zr-PAM/Fe_3O_4 composite.

The synthesised composite was found to be effective for the removal of fluoride from aqueous samples having pH ranging from 1 - 9. This seems to suggest that this sorbent can be used for the defluoridation of natural waters as well as industrial aqueous wastes streams. The sorption kinetics was found to be rapid as 81% fluoride from aqueous solution was removed in 15 min. The equilibrium data fitted well to the Langmuir model with an sorption capacity of 124.5 mg g^{-1} which is quite higher when compared to the sorbents reported in literature. Different interfering anions commonly present in the ground waters did not show any significant effect on fluoride sorption suggesting its applicability to treat groundwater samples. In addition to this, the Zr(IV)-PAM/Fe_3O_4 composite was found to be reusable during the fluoride soption-desorption cycles. The sorbent's high fluoride selectivity and suitability in practical situations permits the removal of fluoride from water in a single step using its magnetic behaviour thereby ensuring constant water quality.

Chapter -4

DEVELOPMENT OF POLYMERIC SHEET SORBENT FOR SOLID PHASE EXTRACTION OF BORON

4.1	**Introduction**	
4.2	**Experimental**	
	4.2.1	**Synthesis of boron selective sheet sorbent**
	4.2.2	**Sorption Studies**
4.3	**Results and Discussion**	
	4.3.1	**Characterization studies**
	4.3.2	**Sorption and Desorption Studies**
	4.3.3	**Sorption Isotherms**
	4.3.4	**Kinetic Models**
4.4	**Mechanism of Boron Sorption**	
4.5	**Comparison of the Extractive Sheet Sorbents with Existing Sorbents**	
4.6	**Real Sample Analysis**	
4.7	**Conclusions**	

4.1 Introduction

Occurrence and uses

Boron is the first element in IIIA group of periodic table having symbol B and atomic number 5. It occurs as a trace element in the soil and is estimated to constitute 0.001% of the earth's crust [306,307]. Boron is found in nature often associated with other elements as in form of different oxides. More than one hundred borate minerals are found in the earth crust. A few examples are kernite, borax $Na_2B_4O_5(OH)_4{\cdot}8(H_2O)$, ulexite $NaCaB_5O_6(OH)_6{\cdot}5(H_2O)$, colemanite $CaB_3O_4(OH)_3{\cdot}(H_2O)/2CaO{\cdot}3B_2O_3{\cdot}5H_2O$, and boracite $Mg_3B_7O_{13}Cl$ [308,309]. These minerals usually occur as white crystalline deposits in desert areas. Boron's presence in water is often a result of weathering of boron-containing minerals and soils [310]. Another significant source of boron is boric acid, which is released through volcanic eruptions [311]. Concentrations of boron in groundwater throughout the world range widely, from 0.3 to 100 mg L^{-1}. The amount of boron in fresh water depends on factors such as the geochemical nature of the drainage area, proximity to marine coastal regions, and inputs from industrial and municipal effluents [312]. Its concentration in the oceans ranges between 1-10 mg L^{-1}, with an average of 5 mg L^{-1}.

Boron compounds find application in several industries. Borax, the most common natural form of boron is used in various household laundries and cleaning products as well as is present in some tooth bleaching formulations [309,313]. Borax is also used in manufacturing glass and ceramics and in the industries of fertilizers, papers, paints, fire retardants, in enamels covering the steel of refrigerators, washing machines. Amorphous boron is used in pyrotechnic flares to provide a distinctive green colour, and in rockets as an igniter. Agriculture also consumes significant quantities of boron as fertilizer. In 2007, 4.3 million tons of boron as boric oxide was produced in the United States [314]. Boric acid, one of the most important compounds of boron, is widely used as a mild antiseptic. In addition to this boron carbide and boron nitride are used in making abrasive tools. Being hard, strong and light weight element boron is also added to steel for extra hardness and strength at high temperatures. Boron plays a very important role in the nuclear power industry, because of its high neutron-absorption cross-section. Boron carbide is used as the control rods in nuclear reactors to control the neutron flux and also as shielding material. In Canadian deuterium-uranium pressurized heavy water (CANDUPHW) type reactors, boron compounds also serve as readily removable neutron poisons added to the moderator (heavy-water) system for reactivity control. Boron as BF_3 is also used in the detectors to detect, and count neutrons.

Effects of boron

Boron also plays an important role in agriculture. It is required for maintaining the integrity of cell walls by forming borate esters [315]. However, both high and low boron exposure can harm plant growth. The tolerance limit of plants varies with their types. Some plants are more and some are less sensitive [316]. Above a particular concentration of 1.8 mg L^{-1} all the plants start showing the symptoms of boron toxicity. The visible effects of its toxicity can be clearly seen in the form of thickening of leaves, bark cracking, poor budding, excessive branching, yellowing of tips of leaves, fall of unripe fruit and reduction of germination [317,318]. An example of excess boron effect on a plant leaf is depicted below in Fig 4.1.

Fig 4.1 *White Mulberry tree exhibiting signs of boron toxicity*

Tu et al. [319] collected data about the tolerable doses of boron for many agriculture crops and it was found that the critical plant level for toxicity ranges from 10 - 50 mg L^{-1} in sensitive crops such as small grains and garden beans, to as high as 200 mg L^{-1} in tolerant crops such as sugar beets, cucumbers, and conifers. Blackberries starts to show boron poisoning symptoms with less than 0.5 mg L^{-1} and are considered very sensitive, whereas cotton is very tolerant and can be exposed to concentrations as high at 10 mg L^{-1}.

Elemental boron, boron oxide, boric acid, borates, and many organo-boron compounds have low toxicity to humans and animals. The LD_{50} (dose at which there is 50% mortality) for animals is about 6 g per kg of body weight. Boron that enters the soil, surface waters and ground waters forms complexes with different heavy metals and these complexes are more toxic than the heavy metals. These complexes then enter the human food chain through their diet and drinking water. Due to its wide use, water contamination by boron has become a widespread environmental problem.

The World Health Organization (WHO) guideline for boron in drinking water is revised to 2.5 mg L^{-1}, which is incorporated into the Guidelines for Drinking-water Quality (4th edition) published in 2011 compared to the earlier value of 0.5 mg L^{-1} [309].The new change in the permissible limit seems more relaxed for drinking water but for irrigation water the requirement of 0.5 mg L^{-1} is still there since boron produces the herbicidal effect. Therefore, the problem of removing boron from water is not only related to the countries with natural deposits of this element but it has also become the critical issue for highly developed countries.

Literature survey on boron removal

The current research focuses on the development of effective technologies for the removal of boron. Selection of a suitable method for boron removal is difficult because of the fact that it exists in different forms and its concentration varies from place to place. At low concentration of < 200 mg L^{-1} , dissolved boron is present mainly as mononuclear boron species, $B(OH)_3$ and $B(OH)_4^-$ whereas with the increase in concentration, polynuclear species $B_2O(OH)_6$, $B_3O_3(OH)_4$ etc. are formed [320]. As the concentration of boron in seawater is around 4.8 mg/L [321], it is acceptable that most of it exists in form of mononuclear species $B(OH)_3$. Boric acid $B(OH)_3$ as such is a very weak acid with a pK_a value of 9.2 and its dissociation can be described as follows:

$$B(OH)_3 + H_2O \rightleftharpoons B(OH)_4^- + H^+ \quad (4.1)$$

The exact percentage of boric acid and borate in any aqueous system is basically dependent on pH. When pH is increased above pK_a value, most borate anions can be found. The fraction of boric acid and borate as a function of pH is presented in Fig 4.2 [322].

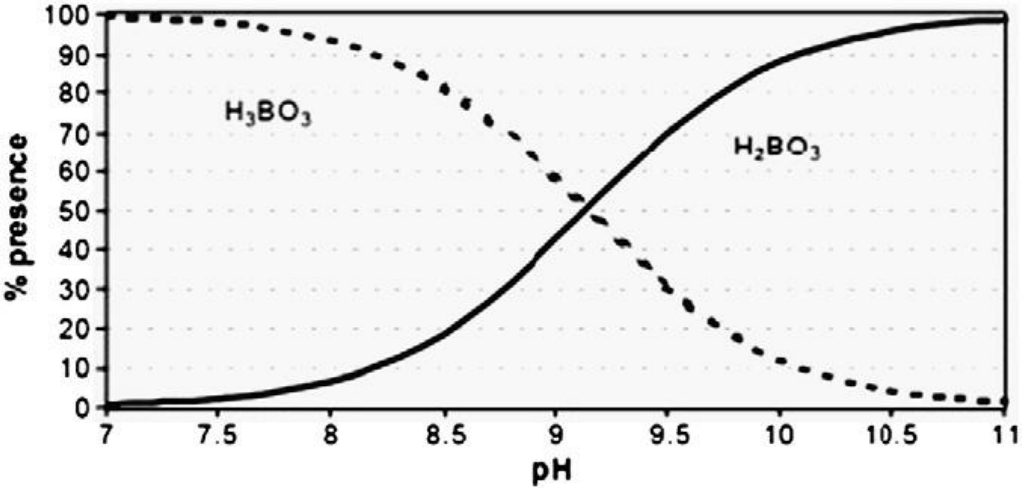

Fig 4.2 *Distribution of* $B(OH)_3/[B(OH)_4]^-$ *as a function of pH* [322]

Many methods have been reported in literature which aims at reducing the present boron concentration in seawater to an acceptable level. The commonly reported methods for boron removal from aqueous solution are based on the adsorption technique which aims at removing the charged species via ion-exchange mechanism. Some of the other methods are reverse osmosis, nanofiltration, polymer enhanced ultrafiltration, use of a specific ion exchangers, sorption and electrodialysis (ED) [323-336]. The available literature on these methods is already discussed in the introduction chapter of the present thesis. Though these methods are widely used, they are generally associated with certain limitations, especially when boron is present in its neutral form at very low concentration. One such limitation is the dependency of the removal efficiency on the pH of the solution to be treated. For example the removal of boron by electrodialysis is dependent on pH and degree of desalination of treated water and ranges between 42 and 75% [337]. Recently, a large number of water desalination plants using reverse osmosis (RO) have been set up to produce drinking water from seawater or brackish water. RO technology is an efficient and reliable membrane technology for the production of drinking water from seawater as it rejects most of the ions efficiently. However, some serious limitations had recently been discovered during the field practice of RO. Boron problem is one of them because the rejection of undissociated species, such as boric acid is poor. Most of the membranes presently used for desalination remove only 60-70% of boron in its first pass. This means the permeate still contains 0.9-1.8 mgL^{-1} of boron depending on the conditions of the water to be treated. To reduce the concentration below 0.5 $mg\ L^{-1}$ a second pass operating at pH 10 is required because boric acid is not ionised at lower pH values. This in turn requires the use of caustic soda which results in higher salinity of treated water, scaling, corrosion and high cost [58,338]. Another approach for effective boron removal from the treated solution is the use of effective and low-cost sorbents or using boron selective ion exchangers for the purification purposes. Among the different adsorbents used, the one containing vicinal polyalcohol groups have shown high selectivity towards boron. The use of chelating resins with vicinal polyalcohol groups has proved to be more efficient for trace concentration boron removal.

The vicinal polyalcohol groups tend to bind with boron forming esters of boron or borate anion complexes with proton as a counter ion [339]. Glycidyl modified resins and the resins grafted with sorbitol are some of the resins used [340,341]. Synthesis of terpolymer of glycidylmethacrylate/methyl methacrylate/ethylene glycol dimethacrylate (GMA/MMA/EGDMA) modified with diallylamine that removed boron from aqueous solution was carried out. A hybrid gel prepared with tetraethoxysilane (TEOS), (3-glycidoxypropyl)trimethoxysilane (GPTMS), and precursor synthesized from GPTMS and N-methyl-D-glucamine that had a good mechanical strength and affinity to boron was also synthesized for boron removal. Grafting of NMG onto silica-polyallylamine composites (SPC) was carried out to have a material that has a high capacity towards boron even in seawater spiked with high concentration of other ions [140,342-345]. Among these, sorbitol and mannitol have been successfully employed for the removals of boron at trace levels but they suffer from high cost of regeneration [138-140,346]. For instance, Amberlite IRA- 743 containing sorbitol functional groups reduces boron concentration below 1 mg L^{-1}. Despite high boron removal efficiency of 90%, this process is unsatisfactory because of expensive resin regeneration and the capacity loss during each step of regeneration [141]. Surface modification of natural polymers like chitosan and the synthesized copolymers of styrene divinylbenzene are widely used to make them selective for boron but the kinetics of developed sorbents and the hydrophobicity of copolymers limits their applicability in the aqueous solution.

Therefore, development of cost effective adsorbents having high efficiency of sorption is a major area of research. In our work we have focused on synthesising the polyol-functionalised sorbent in form of a polymeric sheet for the boron removal. The motivation of the current work was to develop a fixed-site polymer sorbent in a sheet form for the selective and efficient extraction of boron from natural waters. Polymer sorbent in the sheet form offers several advantages due to its well defined reproducible shape, geometry and large surface area. Additionally, the functional groups for the selective uptake of boron in form of boric acid can be incorporated in the sorbent by chemical bonds thus leading to chemically and mechanically a uniform material having high accessibility of binding sites for selective sorption through complex formation.

The boron selective functionalized sheet sorbent was synthesized by crosslinking a preformed polymer in the pores of commercially available polypropylene membrane and subsequently generating required functional group by chemical modification of the precursor crosslinked polymer chains [347].

Crosslinking was carried out by using a cyclic diamine i.e. diethylenediamine (piperazine) as a crosslinking agent. The resultant crosslinked membranes were subjected to chemical modification with N-methyl D- glucamine (NMDG) having vicinal diol groups thus making it selective for boron. Parameters that influence the boron uptake from aqueous streams like pH, uptake capacity, contact time, effect of competing ions and reusability have been evaluated. Finally the optimized conditions were examined for boron removal efficacy from real water samples. As ionization of boric acid is not required for its complexation with NMDG, these NMDG- functionalized membranes are effective for boron removal from natural water conditions. Further, the functional groups of the developed sheet sorbent are present on its surface which provides high accessibility of the functional groups and thus fast sorption rate is achieved.

4.2 Experimental

4.2.1 Synthesis of boron selective polymer sheet sorbent

Room temperature crosslinking method was used to synthesize the pore filled polymer sheet as explained in the experimental chapter of this thesis. Two set of polymer sheets with two different types of crosslinkers were synthesized. Piperazine (Diethylenediamine) and DABCO (1,4 diazabicyclo[2.2.2]octane) were the two different crosslinkers which were chosen to have different amount of crosslinking gel in the pores of the polymer matrix. Piperazine (PIP) is the simplest cyclic member of the ethyleneamines family. The product has two secondary amine groups whereas DABCO has two tertiary amine groups (Fig 4.3). Due to the difference in the availability of the lone pairs of nitrogen on both the crosslinkers, the percentage crosslinking is expected to vary and hence the variation in boron uptake. The other components of the polymerizing solution were kept fixed for both the sets and the resultant pore-filled substrates were synthesized.

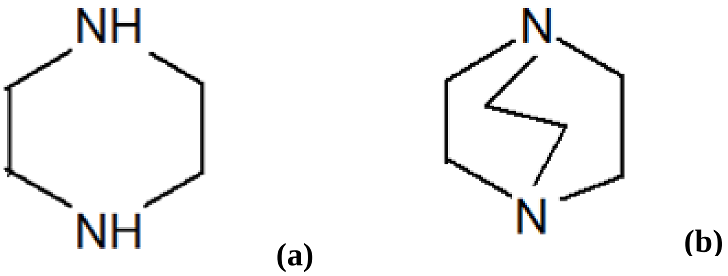

Fig 4.3: *Chemical structures of piperazine (a) DABCO (b) used as crosslinkers*

The procedure for the synthesis of NMDG functionalised membranes has been discussed in details in Chapter 2.

4.2.2. Sorption studies

Boron sorption experiments were carried out by equilibrating fixed size of NMDG functionalised sheet sorbent with 1, 5 and 10 mg L^{-1} boron standard solutions. The volume of the solution as fixed to 25 mL for all the experiments. All the sorption experiments were carried out at ambient temperature and uniform mass distribution in the solution was ensured throughout the experiment by continuous stirring of the solution using a shaker at about 300 rpm. After continuous equilibration with stirring using a magnetic stirrer for a predetermined time interval sorbent sheet was removed from the solution and residual boron concentration was determined using ICP-MS.

Selectivity of the NMDG-sheet sorbent towards boron in form of boric acid was tested by repeating the above experiments in the presence of a known concentration of competing anions like chloride, nitrate, sulphate and phosphate along with boron. The samples were diluted prior to the ICPMS determination of boron by applying proper dilution. Desorption of the boron from sorbed samples was carried out by equilibrating boron loaded sorbent with varying concentration of HCl. The solutions were analyzed for boron by ICPMS concentrations before and after removing the sorbents.

Hyphenation of developed sheet with curcumin method allowed boron determination on the sheet in the presence of ions like nitrate which otherwise was not feasible. Fig. 4.4 shows the steps involved in the hyphenated method of boron determination via curcumin method.

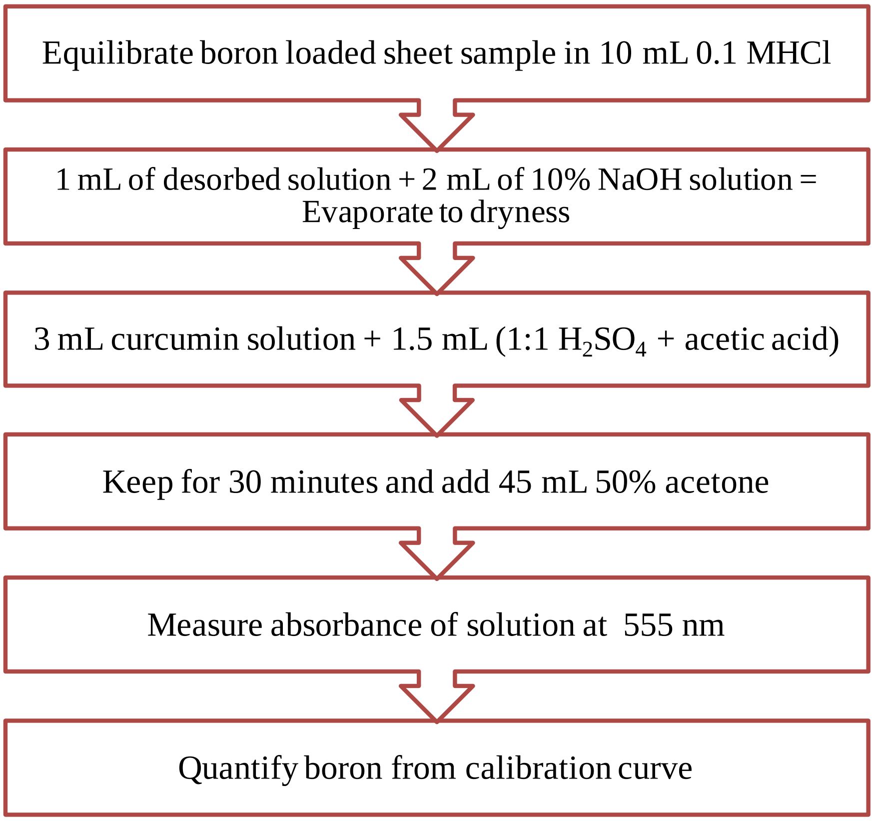

Fig. 4.4 *Steps involved in quantification of boron preconcentrated in sheet sorbent by curcumin method*

4.3 Results and Discussion

4.3.1. Characterization studies of sheet sorbent

Characterisation of the developed sorbent was carried out using various techniques as listed below. The extent of cross-linked PVBCl polymer anchored in the pores of piperazine crosslinked polypropylene was determined gravimetrically and was found to be 86±10 wt%. The extent of cross-linked PVBCl polymer anchored in the pores of DABCO crosslinked polypropylenewas determined gravimetrically and was found to be 48 ±13 %.

SEM studies

The SEM images of the host substrate polypropylene before and after pore-filling of PVBCl with piperazine as crosslinker are shown in Fig. 4.5 (a) and (b) respectively. Comparison of both the SEM images indicated that the majority of pores of the base substrate were filled while some pores were partially filled. Since the thickness of microprous sheet did not change as measured by the digital micrometer, it was confirmed that the crosslinking of the polymer was mostly confined to the pores of the host substrate.

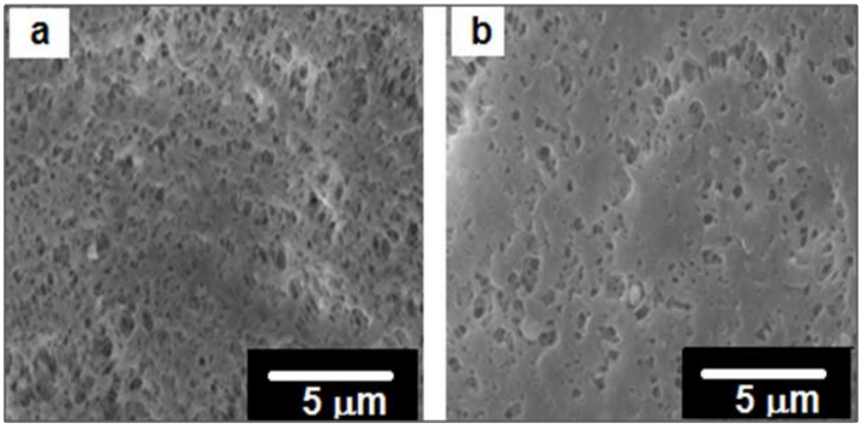

Fig 4.5 *SEM images of host poly(propylene) microporous substrates (a) blank membrane and (b) after anchoring PVBCl*

EDX studies

In addition to the surphace morphology obtained via SEM, EDX spectra of the sheet sorbent before and after equilibration with boron is shown in Fig 4.6 (a) and (b). The EDX spectra of boron sorbed sheet shows the X-ray peaks of boron confirming its sorption on the sheet sorbent. The functionalized sheet sorbents prepared in the present work were found to sorb water readily upto 45-55 wt% as confirmed by the water uptake capacity measurements done gravimetrically.

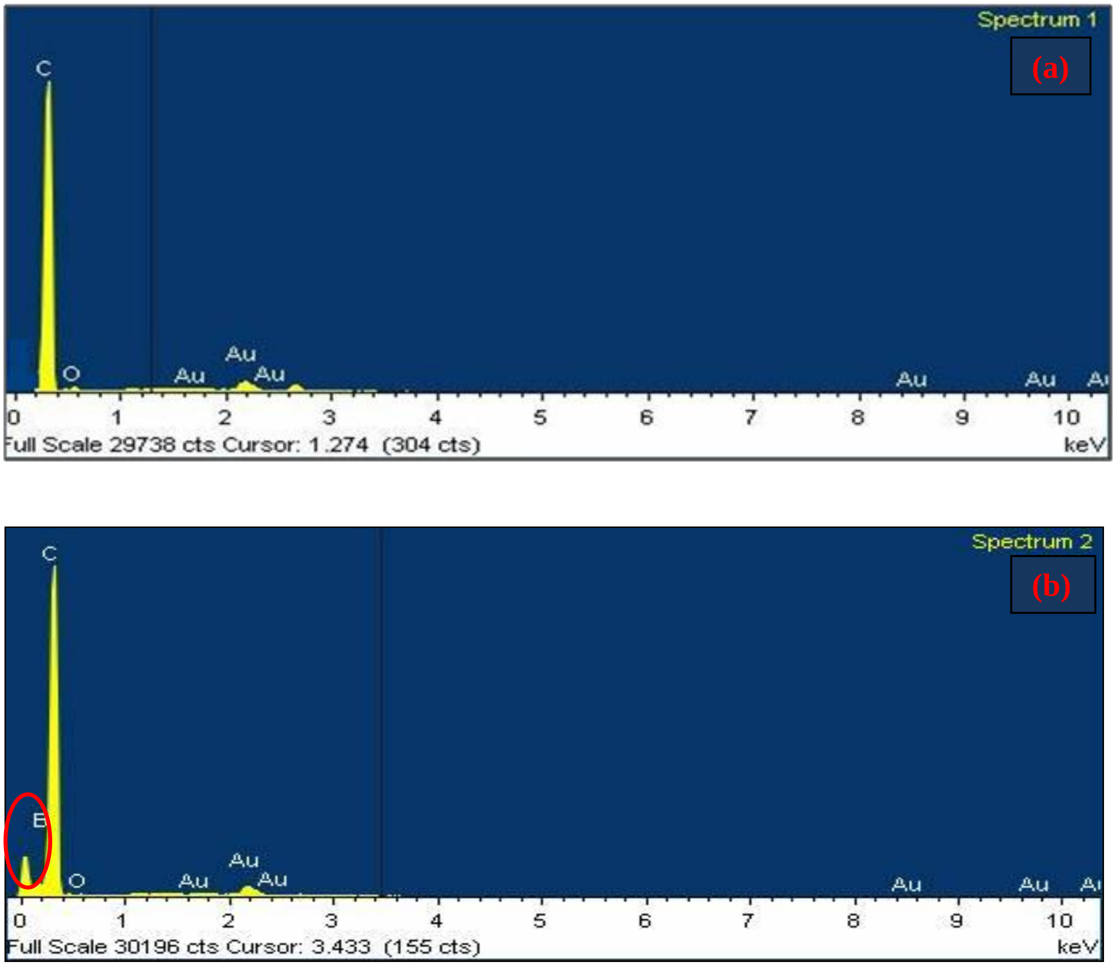

Fig. 4.6 *EDX images of NMDG functionalized sorbents (a) before boron sorption and (b) after boron sorption*

FTIR studies

FTIR spectrum of the PVBCl crosslinked precursor sheet sorbent before and after functionalization with NMDG were recorded, in order to identify the functional groups present and confirm the functionalization. Spectra of precursor PVBCl membrane showed a sharp band at 800 cm^{-1} which could be assigned to the stretching vibrations of C-Cl group Fig. 4.7 (a). The bands at 1213 cm^{-1} - 1440 cm^{-1} and 1250 cm^{-1} could be assigned to the C-N stretching vibrations of piperazine, and $-CH_2$ modes of benzyl group of PVBCl. In Fig. 4.7 (b) the diminishing of sharp bands of C-C stretching vibrations at 2875-2950 cm^{-} and the appearance of broad stretching vibrations of –OH and -NH groups are attributed to the binding of NMDG to the entrapped polymer. The presence of sharp peak at 1190-1210 cm^{-1} could be assigned to the stretching vibrations of C-N group present in NMDG.

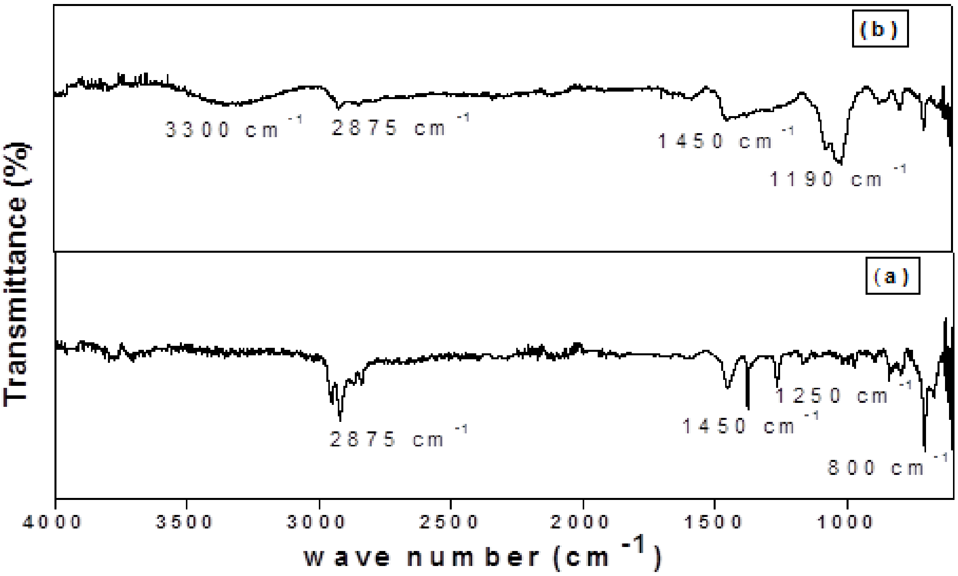

Fig. 4.7 *FTIR spectra of the polymer membrane (a) PVBCl crosslinked membrane (b) and its modified form with NMDG*

4.3.2 Sorption and desorption studies

Preliminary experiments of boron sorption were carried out by taking two sets of the pore filled membranes. i.e. PVBCl –Piperazine –NMDG modified sheet substrates and PVBCl

–DABCO –NMDG substrates. The initial boron concentration of equilibrating solution was fixed to 5 mg L^{-1}. Table 4.1.shows the residual boron concentration left in the solution after equilibration with both the substrates. It was experimentally found that the boron uptake in DABCO crosslinked substrates was lower compared to the piperazine crosslinked substrates. The lower uptake in the former can be attributed to the lower entrapment of polymer as can be experimentally seen from the percentage crosslinking obtained. Therefore piperazine was the choice of crosslinker for pore-filling the PVBCl polymer in the pores of polypropylene substrate effectively and these crosslinked substrates were used for rest of the experiments.

Table 4.1 *Effect of the choice of crosslinker on boron uptake (Volume of solution=25 mL)*

Substrate	Initial boron concentration (mg L^{-1})	Residual boron concentration (mg L^{-1})	%uptake
Piperazine crosslinked	5	2.3	82
DABCO crosslinked	5	0.9	54

Further the chemical conditions of aqueous media influence the uptake of boron. Therefore, to optimize various chemical conditions for maximum sorption the effects of underlying parameters were studied.

Effect of pH

One of the important parameters is the pH of aqueous streams. Fig 4.8 shows the percentage uptake of boron in the 2 x 2 cm^2 sheet sorbent from 25 mL solution having boron concentration of 5 mg L^{-1} obtained at different pH values. The percentage uptake increases upto pH 7 and thereafter decreases. The pH dependence may be interpreted by taking into account the formation of tetradentate complex of boric acid with the NMDG group of the sorbent (Fig. 4.13) and the dissociation process of boric acid. The increasing pH facilitates the formation of tetradentate complex and thus increases the percentage uptake. With the further rise in pH beyond 7 the concentration of –OH$^-$ ions also increases which leads to strong competition between available binding sites thus boron uptake decreases slowly after pH 7.

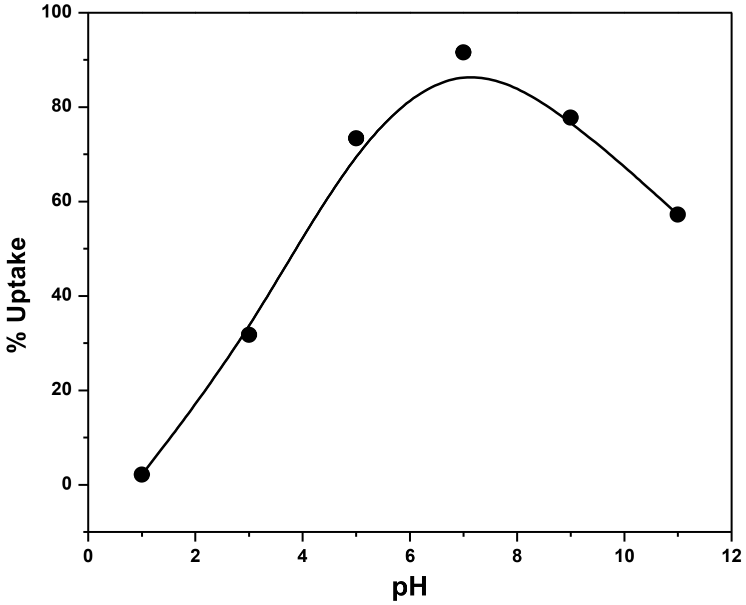

Fig. 4.8 *Uptake of boron in NMDG microporous sheet sorbent as a function of pH of equilibrating solution (boron concentration: 5 mg L^{-1})*

Regeneration of sheet sorbent

For reusability, the sorbed boron should be easily and quantitatively desorbed. As uptake of boron is reduced at lower pH, desorption was studied by equilibrating boron loaded sheet with aqueous solution of varying pH. The microporous sheet samples were equilibrated in solutions having pH 1-3 for overnight with constant stirring. The results showed that desorption was not quantitative upto pH 2 (Fig 4.9). However, more than 96% of the sorbed boron was desorbed by one time equilibration of the sheet sorbent with 0.1M HCl (pH=1) solution. Therefore 0.1 M HCl was used for the desorption of sorbed boron.

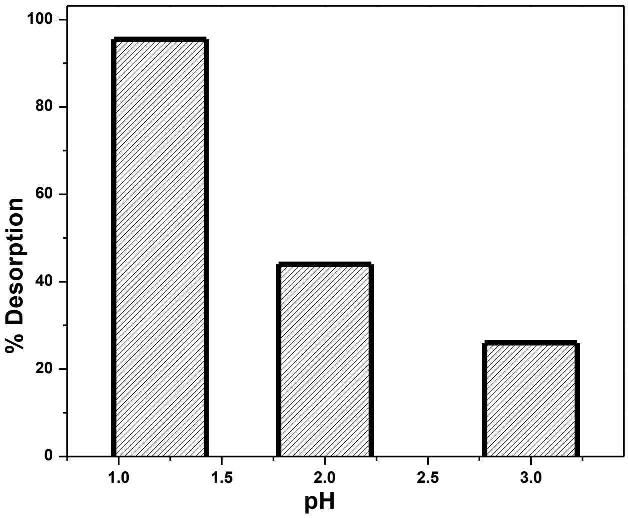

Fig.4.9 *Desorption of boron from NMDG microporous sheet sorbent as a function of pH*

In addition to this, a series of sorption/desorption experiments were performed to understand the reusability of the developed sheet sorbent. After each desorption step, sorbent was reconditioned with 0.01 M NaOH and then washed with ultra pure water. The studies showed that during six cycles there was no decrease in the uptake capacity of the regenerated sorbent however after that there was a steady decrease in the uptake capacity of the regenerated sorbent. This indicates that the NMDG-sheet sorbent developed is reusable upto 6 cycles of continuous boron sorption and desorption.

Tolerance studies

The ground water and seawater contain several other competing anions such as chloride, nitrate, phosphate, sulphate. These anions can compete with boric acid for the available binding sites in the sheet sorbent. To study the effect of these ions on the uptake of boric acid, the sheet was equilibrated with solution containing binary mixture of boron and one of the competing ions listed in Table 4.2.

Table 4.2: *Effect of different competing anions on boron uptake in NMDG-membrane*

Foreign ion	**Percentage removal of Boron**		
	5 mgL^{-1}	**20 mgL^{-1}**	**350 mgL^{-1}**
Cl^-	86± 0.42	79±0.33	73±0.27
NO_3^-	83±0.65	80±0.43	71±0.11
PO_4^{3-}	87±0.91	86±1.1	81±0.67
SO_4^{2-}	86±0.47	85±.96	84±0.72

The initial concentration of boron was fixed at 5 mg L^{-1} while for other ions three concentrations, 5, 20 and 350 mg L^{-1} were used. The interference studies showed that there is negligible effect of PO_4^{3-} and SO_4^{2-} on the sorption ability of the sorbent for boric acid even at high concentration of 350 mg L^{-1}. Percentage boron sorption was reduced from 80% to 71% with an increase in the concentration of NO_3^- from 20 mg L^{-1} to 350 mg L^{-1} whereas in case of Cl^- there was only 6% decrease at higher concentration of 350 mg

L^{-1}. This indicates that the developed sorbent is highly selective for boron due to its chelate formation with vicinal diols of NMDG functionalized sheet sorbent.

4.3.3 Sorption isotherms

The equilibrium uptake of boron was investigated at different initial concentrations by keeping the size of sorbent fixed. Fig 4.10 shows the results obtained.

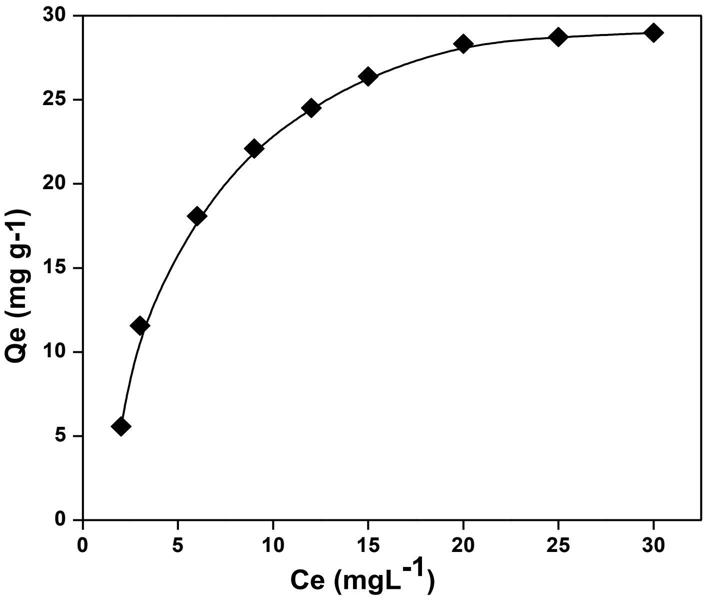

Fig.4.10 *Uptake of boron in NMDG microporous sheet sorbent as a function of concentration of equilibrating solution*

An ascending convex isotherm indicates that the sorption process is favorable. An initial increase in the boron sorption capacity with increase in the boron concentration is due to the concentration gradient across the sheet sorbent.The equilibrium boron sorption capacity increased drastically with increasing boron content in the solution and gradually approached a plateau at 28.99 mg g^{-1} as surface binding sites were saturated.

The sorption isotherm is important for description of how the sorbate will interact with the functionalized sorbent and determine its sorption capacity. The relationship between the amount of boron sorbed and the boron concentration remaining in the solution is described by the Langmuir and Freundlich isotherms as shown in Fig 4.11. The Freundlich isotherm equation used is given by eqn (3):

$$\text{Log } Q_e = \log K_F + 1/n \log C_e \quad (4.1)$$

where K_F and n are Freundlich constants representing adsorption capacity (mg g^{-1}) (L $mg^{-1})^{1/n}$ and adsorption intensity, respectively, Q_e is the equilibrium adsorption capacity (mg g^{-1}) and Ce is the equilibrium concentration (mg L^{-1}). The plot of Log Q_e *vs.* log C_e is shown in Fig 4.11(a) and from the slope and intercept of the line, value of 1/n and K_F were determined. The following linear form of the Langmuir equation was applied to calculate sorption capacity.

$$C_e/Q_e = 1/Q_oK_L + C_e/Q_o \quad (4.2)$$

where Ce is the equilibrium concentration (mg L^{-1}), Q_e is the equilibrium adsorption capacity (mg g^{-1}) ,Q_o and K_L are Langmuir constants representing adsorption capacity(mg g^{-1}) and energy of adsorption (L mg^{-1}), respectively.

The data fitted in Langmuir isotherm models indicated a linear plot for C_e/Q_e and C_e as shown in Fig 4.11(b). The value of Q_o and K_L can be calculated from slope and intercept of the straight line and are given in Table 4.3. Also the value of separation factor R_L (separation factor) = 1/ (1+ K_L C_i) obtained was 0.32 which is less than 1 indicating a favourable sorption.

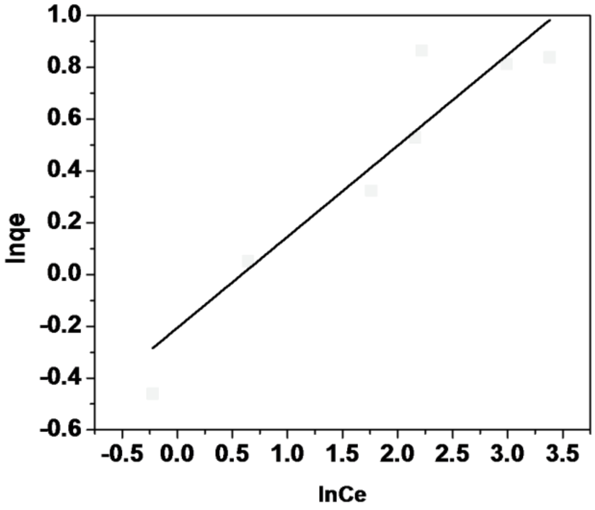

Fig. 4.11 (a) *Freundlich isotherm for the uptake of boron by NMDG functionalized sheet sorbent*

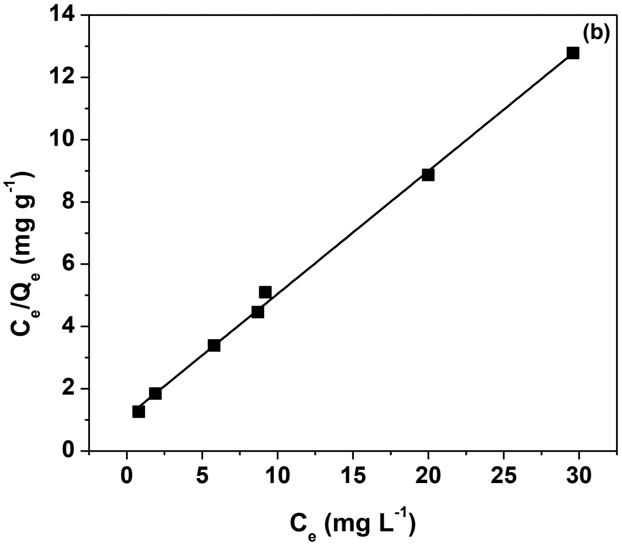

Fig. 4.11 (b) *Langmuir isotherms for the uptake of boron by NMDG functionalized sheet sorbent*

According to the correlation coefficients of both the models, experimental data exhibited higher correlation coefficient with Langmuir model representing the best equilibrium. The values of all the constants derived from the isotherm are given in Table 4.3. The experimentally determined uptake capacity was found to be comparable with that obtained by analysis of Langmuir plot confirming that the interaction between sorbate and sorbent is through chemical bonding.

Table 4.3: *Values of the constants derived from Freundlich and Langmuir isotherms.*

Freundlich			**Langmuir**		
K_F	**R^2**	**n**	**K_L (L mg^{-1})**	**Q_o (mg g^{-1})**	**R^2**
5.84	1.99	0.92	0 .41	28.25	0.99

4.3.4 Kinetic models

Sorption kinetics is one of the most important characteristics which represent the sorption efficiency. Kinetic models are used to determine the sorption rate of sorbate and the rate determining step. Rate determining step and rate of sorption is very crucial for a full batch scale process. The sorption rate of boron on the sheet sorbent, as a function of time is shown in Fig 4.12. It was found that the percentage uptake increases with increasing contact time. 80% of the boron sorption took place within 3 h and equilibrium (92%) was attained in 4 h. The kinetics of developed sheet was faster compared to many other sorbents reported in literature [133]. This can be attributed to the ease of the accessibility of the binding sites on the fixed site flat sheet sorbent. In addition to this, the porosity of the sorbent also plays an important role as sorption of boron occurs through complex formation. The high porosity of the developed fixed-site sheet sorbent provides larger contact area and better accessibility of binding sites which does not require hopping of boron from one site to another and hence the fast sorption kinetics. The kinetic experiments indicate that the sorption by the sheet followed three step processes: a rapid initial sorption followed by a slower uptake and finally equilibrium uptake. The first step is attributed to the instantaneous utilisation of the most readily available sites on the sheet (bulk diffusion). Second step, exhibiting additional sorption is attributed to diffusion of boron from surface into the pores of the sheet sorbent (pore diffusion). The last stage resembles the equilibrium stage of boron sorption.

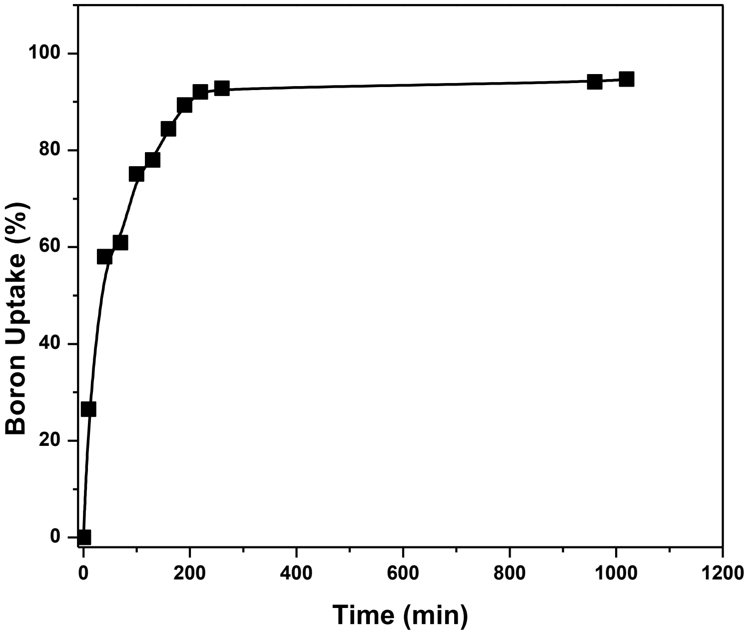

Fig 4.12 *Boron uptake as a function of time (Concentrations of boron in well stirred 25 mL solutions was kept as 5 mg L^{-1}throughout the experiments)*

In order to investigate the rate controlling step and to find the adsorption parameters Lagergren's pseudo first order model and pseudo second order model was applied to the data obtained by kinetic experiments as shown in Fig 4.13 (a) and (b).

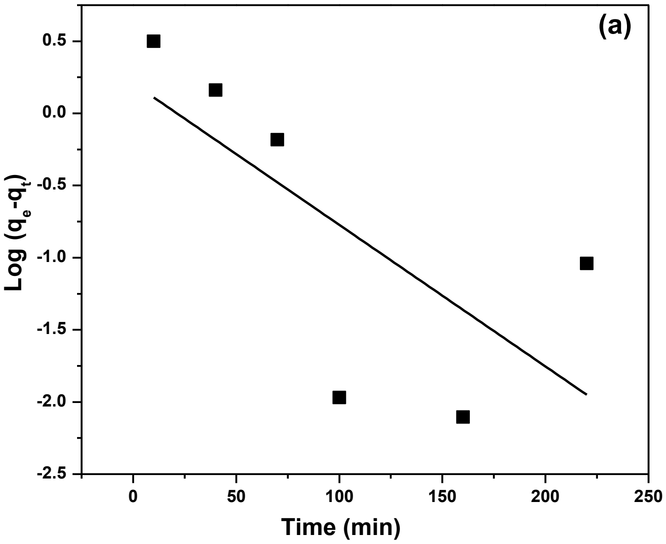

Fig 4.13 (a) *Boron sorption kinetics data fitted with a) pseudo first order rate equation.*

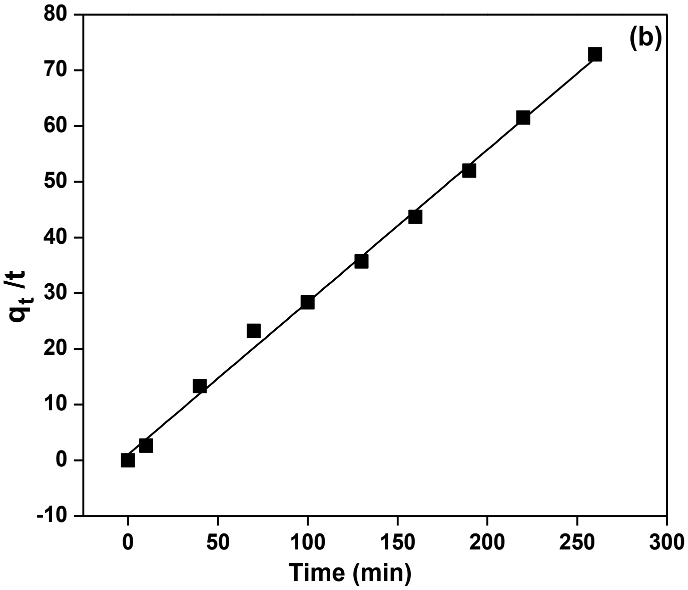

Fig 4.13 (b) *Boron sorption kinetics data fitted with pseudo second order rate equation*

The adsorption rate constants (k_1 and k_2) and correlation coefficients (R^2) were calculated from the plots (Fig. 4.13 (a) and (b)) and are given in Table 4.4. The correlation value obtained from pseudo first order rate equation is low, showing the bad quality of linearization. So the reaction cannot be classified as pseudo first order rate equation. The value of the correlation coefficient for the plot of t/q_t against 't' as a function of time was extremely high exhibiting a better linearity. This indicates that the sorption process in sheet sorbent followed Lagergren's second order equation. Thus experimental results supports the assumption behind the model that the rate limiting step in the sorption is chemisorption i.e the sorption of boron occurred via chemical bonding between the sorbate and sheet surface. The results obtained from the second order kinetics model also supported the results obtained by Langmuir isotherm model.

Table 4.4: *Rate constants obtained using pseudo first order and pseudo second order rate equations*

Boron Concentration	**First order rate parameters**		**Second order rate parameters**	
	k_1 (min^{-1})	**R^2**	**k_2 ($g\ mg^{-1}\ min^{-1}$)**	**R^2**
5 mg L^{-1}	2.1×10^{-2}	0.35	1.4 X 10^{-1}	0.99

4.4 Mechanism of boron sorption

The NMDG functionalized sheet has fixed vicinal diol groups and an amine functional group as shown in the figure below. The interaction mechanism of boric acid with the diol group in the sorbent is shown in Fig. 4.14. The molecules with vicinal diols are capable of forming tetraborate complexes, even in aqueous solutions.

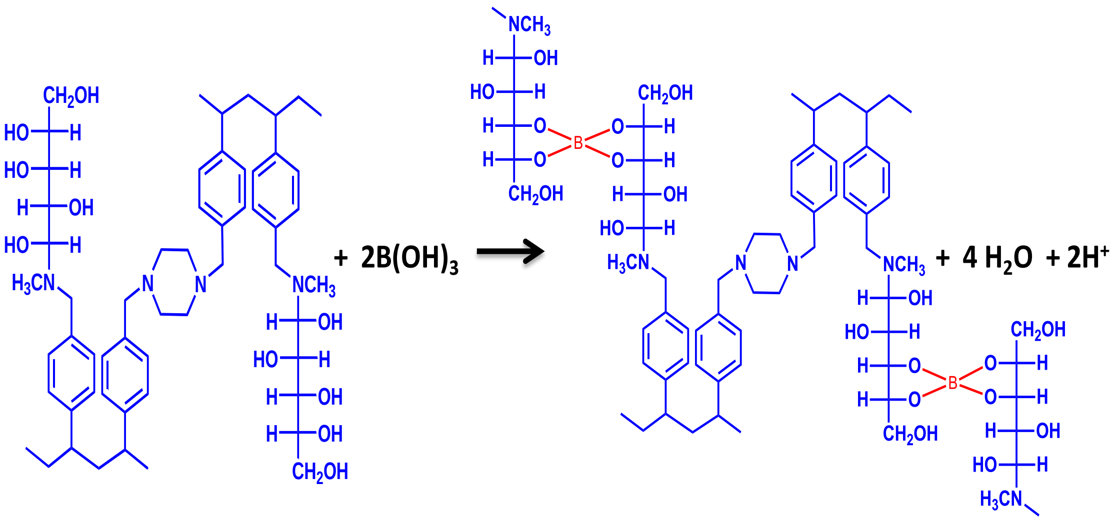

Fig. 4.14 *Interaction mechanism of boron with the NMDG functionalized sorbent*

The specific affinity between the vicinal diols of NMDG and the boric acid leads to the formation of highly stable tetradentate complex. The presence of an amine functional group helps in efficient chelating of boric acid by neutralizing the protons released in the formation of tetradentate complex during complexation thus leading to increase in sorption [344]. This confirms that the mechanism of boron uptake in NMDG- sheet sorbent involves reactive complexation mechanism with the diol groups present on the substrate.

4.5 Comparison of extractive sorbent with existing sorbents

Table 4.5 compares the boron sorption capacities of the existing sorbents with the one synthesised in present work. The developed sorbent for boron when compared with the existing sorbents showed higher sorption capacity and better kinetics of boron sorption. It can be seen that the developed sheet sorbent outperforms most of the sorbents reported in literature in terms of the sorption capacity.

Table 4.5: *Comparison of boron sorption capacities in different sorbents*

Sorbents	Sorption capacity (mg g^{-1})	Reference
PVBCl-NMDG Fixed-site sheet sorbent	28	Present work
NMDG type cellulose derivatives	11	126
CCTs-NMDG	21	127
CTS-MG	32	133
Amberlite IRA-743	7	133
Polymer supported 2-hydroxyethylamino glycol	18	344
Poly(styryl sulfonamide) resin	23.6	348
NMDG- MCM-41	8	349
Polyol grafted SBA-15	6.3	350

NMDG : N-methyl D-Glucamine, SBA : silica mesoporous materials, CTS-MG : NMDG modified crosslinked chitosan beads

4.6 Real sample analysis

The boron content of ground water samples collected from Bangalore and seawater samples collected from Thirumangalam area, Madurai,Tamilnadu was determined. The concentration of boron in these samples was found to be less than 0.5 mg L^{-1}. Therefore, the solutions were spiked with 2 mg L^{-1} and 5 mg L^{-1} boron standard and then uptake studies were carried out. It was found that the boron concentration after sorption was reduced to 0.11 mg L^{-1} and 0.33 mg L^{-1} respectively (Table 4.6) which is well below permissible limit of WHO confirming the suitability of the sorbent for desalination purposes.

Table 4.6 *Removal of Boron from ground water and seawater samples collected from Thirumangalam area, Tamilnadu and Bangalore, India using fixed-site sorbent*

B spiked (mg L^{-1})	**Ground water** [a]	**Seawater** [a]
	Residual B (mgL^{-1})	**Residual B (mgL^{-1})**
2.0	0.11	0.21
5.0	0.33	0.47

a-Initial and final volumes were 10 mL, Values are presented as (mean ± 1s), n=5

Analytical application of developed sorbent

Due to matrix elimination in the sorption process, these studies were extended for its applicability in the determination of boron in curcumin method. The developed sheet sorbent takes up boron selectively in presence of ions like nitrate and hence was hyphenated with spectrophotometric curcumin method of boron determination. Determination of boron in real samples by curcumin method is not possible without matrix removal because of the interference from the concomitants e.g presence of nitrate oxidises curcumin as well as destroys the curcumin-boron complex formed. The existing spectrophotomeric procedures used to eliminate nitrate interference by chemical treatment are tedious and complicated [351,352]. Since the developed NMDG membrane selectively binds boron in presence of nitrate, it can be used to separate boron selectively from the matrix. Extraction of boron by its preconcentration on the sorbent followed by desorption makes quantification feasible in the presence of nitrate (Fig 4.4). Table 4.7 compares the boron concentration in the desorbed solution as obtained by curcumin method of spectrophotometric analysis and ICP-MS analysis. The results obtained by two methods were comparable with a RSD of ±2 %.

Table 4.7 *Comparison of spectrophotometric and ICP-MS analysis of boron*

Initial concentration (mg L^{-1})	**Final concentration (mg L^{-1})**	**Uptake (mg L^{-1})**	**Desorbed Concentration (ICPMS)**	**Desorbed Concentration (Curcumin)**
1	0.13	0.87	0.84 ± 0.2	0.79 ± 1.4
2	0.34	1.66	1.59 ± 0.5	1.51 ± 0.7
5	0.80	4.20	4.01 ± 0.8	3.9 ± 1.7

Values are presented as (mean ± 1s), n=5.

4.8 Conclusions

N-methyl- D-glucamine (NMDG) functionalized, poly(propylene) sheet sorbent has been developed for selective extraction and determination of boron from various aqueous streams. The developed sorbent was found to be chemically stable and effective for the removal of boron from aqueous solutions over a wide pH range (4-8). It was found that equilibrium sorption capacity of boron was 28 mg g^{-1}. The kinetic studies confirmed that the sorption of boron occurred through chemical bonding between sorbate and sheet surface. Hence, most of the common interfering anions have no effect on boron sorption in the NMDG-sheet sorbent.

The extractive flat sheet sorbent developed in the present work for selective separation of boron was found to be better than those reported in literature in terms of high sorption capacity and reusability. The sorbent developed in the present work is in the form of sheet and therefore it has better mechanical integrity and is more amenable to use for desalination of sea water where continuous effort of harnessing potable water with desired salinity is a challenge.

Chapter 5

DEVELOPMENT OF POLYMER SHEET SORBENTS FOR MERCURY (II) DETECTION AND QUANTIFICATION

Section 5A

POLYMERIC SHEET SORBENT FOR DETECTION AND QUANTIFICATION OF MERCURY (II)

5A.1 Introduction

5A.2 Experimental

- 5A.2.1 Synthesis of Polymer Sheets
- 5A.2.2 Sorption Studies

5A.3 Results and Discussion

- 5A.3.1 Comparison of Sheet Sorbents
- 5A.3.2 Characterization of Sheet Sorbent
- 5A.3.3 Tolerance Studies

5A.4 Mechanism of Mercury Sorption

5A.5 Real Sample Analysis

5A.6 Analytical Application of Developed Sheet Sorbent

5A.7 Conclusions

5A.1. Introduction

Occurrence and uses of mercury

Mercury has a symbol of Hg with an atomic number 80. It is a transition element that is very unique because it is the only metal element that exists in a liquid form at room temperature. It is rarely found in nature as the pure, liquid metal, but rather as compounds and inorganic salts. It can be bound to other compounds as monovalent or divalent mercury (also expressed as Hg(I) and Hg(II) or Hg^{2+}, respectively). Many inorganic and organic compounds of mercury are formed from Hg(II). Inorganic mercuric compounds include mercuric sulfide (HgS), mercuric oxide (HgO) and mercuric chloride ($HgCl_2$). Some mercury salts (such as $HgCl_2$) are sufficiently volatile and may exist in the atmosphere.

Naturally occurring mercury has been widely distributed by natural processes such as volcanic activity. The use of mercury in industrial processes significantly increased following the industrial revolution of the 19th century. There are many applications of mercury and majority of them deal in electrical equipments and in control devices, where the fluidity, stability, high density and electrical conductivity are essential. It is used mainly in many temperature measuring instruments. Mercury vapors are used in making fluorescent lamps. It also finds applications in the field of agriculture (as fungicide and bactericide), in dental preparations and in the electrolytic preparation of chlorine and alkalis [353]. The mercurous chloride (calomel) is one of the oldest known pharmaceuticals and it is still used as antiseptic. The red mercury oxide is used in mercury batteries, developed during II World War, which are compact and stable energy sources. The organic compounds that contain mercury are important as microbial agents. At times liquid mercury was also used for the cooling purposes in nuclear reactors but it has been replaced by sodium these days due to the high density of mercury which in turn needs more power to circulate it as a cooling medium. However, mercury's industrial uses are decreasing because of environmental concerns and environmental legislation in many countries.

Mercury is released in the environment by both natural and anthropogenic sources. The natural sources of mercury include volcanoes which produce half of the mercury emissions released in the atmosphere. The rest half being generated by human activities as discussed above for example the major sources of mercury release are from chlor-alkali industries which serve as threat to aquatic life as well as for drinking water.

The solubility of mercury compounds in water varies: elemental mercury vapour is insoluble, mercury(II) chloride is readily soluble, mercury(I) chloride is much less soluble and mercury sulfide has a very low solubility. In aqueous environment, mercury does not occur in the form of free Hg(II) ions but as a mixture of compounds as hydroxyl and chloro complexes in varying proportions depending on pH and the concentration of chloride ions. At low pH, soluble mercury compounds, such as $HgCl_2$ and CH_3Hg^{2+} are the dominant species whereas in mild alkaline conditions Hg° and $(CH_3)_2Hg$ dominate [354]. On the other hand chlorine complexes are the dominant mercury compounds in marine water. Depending on the type of mercury species, the lifetime of mercury in water can last from a few minutes to many years.

A wide range of mercury species exists within our environment and the chemical form of mercury controls its bioavailability, transport, persistence and impact on the human body, with methylmercury being the most toxic species. Mercury cycling pathways in aquatic environments are very complex. Interconversion between various forms of the mercury occurs and the extents of mercury poisoning depend on its type of species. It can be seen from the mercury aquatic cycle (Fig 5.1) that all the forms of mercury are finally converted to methyl mercury, its most toxic form. Atmospheric elemental mercury settles in water, where it is converted by microorganisms into organic mercury, that is ingested by smaller creatures which are eventually consumed by larger fish. Fish at the top of the food chain (e.g., tuna, swordfish, or shark) may concentrate considerable mercury in their tissues. Because of the mercury contamination caused by continuous consumption of fish more than 3000 lakes have been closed in the United States [355-358].

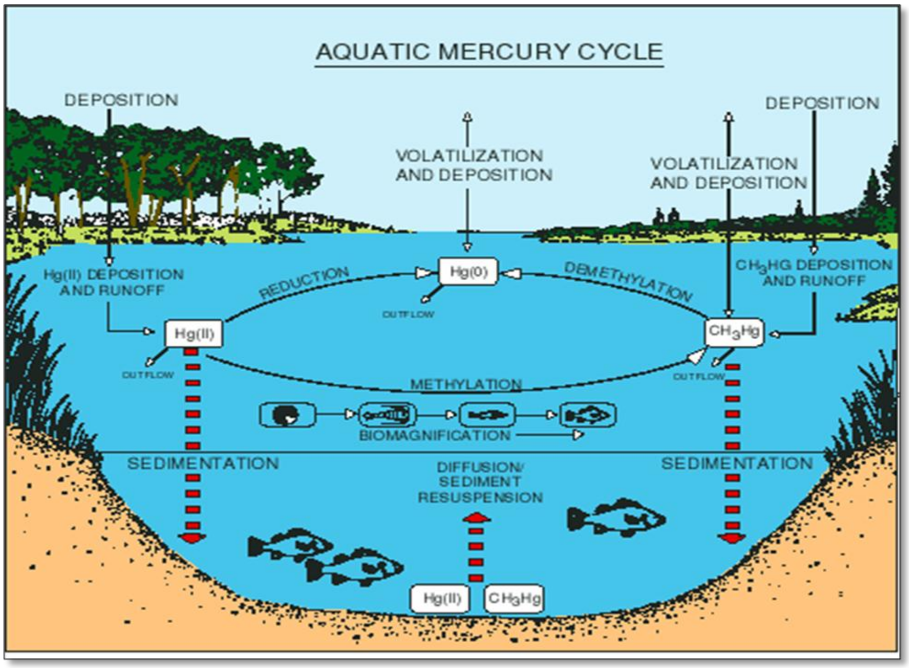

Fig. 5.1 *Aquatic mercury cycle showing interconversion of different forms of mercury*

Because of its high bioaccumulation, mercury concentrations escalate up the food chain e.g. predatory fish can have up to 106 times higher mercury concentrations than the ambient water and up to 95% of this mercury can be in the form of methylmercury. This bioaccumulation of the mercury was the cause of the well documented events in Minamata Bay in Japan in 1953, where over 2000 people, the majority of whom died, were affected by mercury poisoning due to the consumption of methylmercury contaminated fish. Another poisoning incident due to organic mercury occurred in Iraq in 1972 where grain treated with organomercury fungicides was consumed [359-362]. The effects of the mercury varies with its speciation as discussed below.

Health Effects of Mercury

Mercury in its different forms has varied toxicity. Inhaled elemental mercury vapor is easily absorbed through mucus membranes along with lungs leading to the symptoms of mercury poisoning namely shock, cardiovascular collapse, acute renal failure and severe gastrointestinal damage. Acute oral poisoning also results in haemorrhagic gastritis and colitis; with the ultimate damage to kidney. Swelling of the salivary glands, stomatitis, loosening of the teeth, nephritis, anuria and hepatitis are some of other symptoms with the increased dose of mercury [363-365]. Various cellular functions of the body are also altered by binding of inhaled mercury with sulfhydryl and selenohydryl groups of the enzymes [366-370]. Organic mercury in the form of methyl and dimethyl mercury is easily absorbed through the gut and deposits in many tissues, but does not cross the blood-brain barrier as efficiently as elemental mercury. However, on entering the brain it is progressively demethylated to elemental mercury [371-373]. Many reviews highlighting the toxicity of mercury are available in the literature [374-376].

Among all the species of mercury species, divalent mercuric ion (Hg^{2+}) is the most common and stable form of mercury in water. Environmental Protection Agency (EPA) has set the limit for Hg^{2+} in drinking water as 0.002 mg L^{-1} [377]. Inorganic mercury compounds are rapidly accumulated in the kidney, the main target organ for these compounds. The biological half-time of accumulated Hg(II) species is very long, probably years, in both animals and humans. Almost all the mercury present in drinking water is thought to be in the form of mercuric ions [378]. Thus, it is unlikely that there is any direct risk of the intake of organic mercury compounds, and especially of methyl-mercury, as a result of the ingestion of drinking water. In view of the reported disastrous consequences of mercury even at ultra trace levels [379], there is a need to develop new methodologies for separating and pre-concentrating mercury at low levels and to modify the existing sorbents for better efficiency and selectivity.

In recent years, considerable research efforts by numerous investigators has been made on the removal of Hg(II) from water by various methods. An exhaustive summary of existing methods of mercury sorption has been discussed in the introduction chapter. Recent reports estimate total mercury concentration in natural waters ranges from 0.2 to 100 ng L^{-1}[380]. Such low concentrations of mercury in the presence of high salt content demands the use of a preconcentration step prior to its determination by various instrumental techniques. In addition to this, various analytical methods for mercury determination like Cold Vapor Atomic Absorption Spectrometry (CV-AAS), Energy

Dispersive X Ray Fluorescence (EDXRF) requires an efficient preconcentration step not only to enhance their detection limit but also for the removal of the matrix. In view of this, there is a need to develop a simple preconcentration methodology for the selective determination of mercury in natural waters [381-394]. Till date many approaches have been developed for selective preconcentration and subsequent determination of mercuric (II) ions in aqueous solution. A schematic diagram showing commonly applied techniques for sample pre-treatment, pre-concentration, separation and quantification of mercury in waters is given in Table. 5.1. For sample pre-treatment several of the listed techniques are often combined whereas for pre-concentration, separation and quantification a particular technique is usually chosen.

Table 5.1 *General techniques for sample pre-treatment, pre-concentration, separation and quantification of total mercury and its species in waters*

Pre-treatment	Preconcentration	Separation	Quantification
Extraction (Liquid-Liquid, Solid phase micro-extraction) Derivatisation (Hydride generation, alkylation) Cold Vapour generation (Chemical, ultrasound) Distillation,Complexation	Solid phase micro-extraction Amalgamation Cryo trapping	High performance liquid chromatography Gas Chromatography Capillary Electrophoresis Non Chromatographic techniques	Inductively coupled plasma atomic emission spectrometry Inductively coupled plasma mass spectrometry Atomic fluorescence spectrometry Graphite furnace atomic absorption spectrometry

Solid phase extraction has been widely used in the separation and preconcentration of various species of mercury from aqueous streams [395,396]. There are many advantages to this technique, such as simplicity, reliability, reduction in analysis time, reduction or elimination of the use of organic solvents and a high potential for automation. Added advantage of this approach is that the mercury species are adsorbed on a solid phase in the field rather than stabilized in a liquid sample for transport and storage. Therefore, loss of mercury by evaporation is minimized and at the same time the risk of contamination from storage vessels is reduced, because a “solid sample” has less contact with the vessel walls. In addition, the absence of stabilizing reagents reduces the risk of contamination. However, complexation or derivatisation is often necessary prior to extraction [397,398].

There are many solid phase extractants which have been used for selective preconcentration of metal ions which are based on impregnation of the solid surface with certain donor atoms such as oxygen, nitrogen and sulfur containing compounds. For mercury sulfur containing compounds are mostly preferred. Sulfur containing dithiocarbamate derivatives were used for the selective extraction of mercury (II) [399,400]. Various other solid phase extractants used for on line and off line preconcentration of mercury include cystine, 4-(2-Pyridylazo)-resorcinol, dithioacetal derivatives and Schiff bases. However the main problems associated with these materials are their time consuming preparation, high cost and operational difficulties. Exploring new functional materials is still necessary because of the analysis demand and the complexities associated with real samples. At present nano-material based sorbents have gained popularity because of their special properties. Ion adsorption onto solid chelating nano polymer materials is now considered as one of the most promising techniques for selective concentration, removal and recovery of metal ions from a wide variety of sources.

Metal nanoparticles with their unique properties are promising materials for selective sorption of mercury. Typically based on their surface plasmon resonance absorption they have also been applied for the calorimetric detection of Hg(II) in aqueous solution [401,402]. Most of the work of nanosorbents is focused on calorimetric detection of mercury using silver or gold nanoparticles. To the best of our knowledge there have been a very few methods for preconcentration of mercury from aqueous solution using nanosorbents [403]. Silver and gold nanoparticles incorporated in beads have been reported for the removal of Hg^{2+} ions from water [404,405]. Optical detection of lead, mercury by mercaptoundecanoic acid functionalized gold nanoparticles has been carried out [406]. However most of these approaches are cumbersome, need surface modification and elution of sorbed mercury for its determination. Hence there is a need for developing simpler methods for rapid preconcentration and direct determination of Hg (II) in aqueous samples.

The main objective of the present work was to develop a composite sorbent having Hg(II) specific functional groups as well as metal nanoparticles. The functionalized polypropylene sheet sorbents consisting of silver nanoparticle embedded in poly(acrylamide) (Ag-PAM-PP) and gold coated 1,8-octanedithiol (HS-Octyl-S-Au-PP) have been synthesized. Characterization of silver incorporated poly(acrylamide) sheet using UV-Vis spectroscopy, field emission scanning electron microscope (FESEM) and X-ray Diffraction (XRD) have been carried out and the possible uptake mechanism for mercury has been proposed. The sorbent was amenable for solid-phase preconcentration and direct quantification by EDXRF and CVAAS. The use of sheet sorbent enhanced the analytical detection limits and also led to the safe handling of Hg(II) ions. The developed sheet sorbents has been applied to ground water and seawater samples.

5A.2 Experimental

5A.2.1 Synthesis of polymer sheets

Nano-silver embedded polyacrylamide sorbent (Ag-PAM-PP) and 1,8-octanedithiol functionalized gold coated polypropylene sheet (HS-octyl-S-Au-PP) polymer sorbents for preconcentration of mercury were synthesised and compared for their preconcentration efficiency of mercury from aqueous streams. The synthesis of nano-silver embedded polyacrylamide sorbent (Ag-PAM-PP) is discussed in the experimental section. 1,8-octanedithiol functionalized gold coated polypropylene sheet (HS-octyl-S-Au-PP) was synthesized using a two step process. In the first step, polypropylene sheet was coated uniformly with a thin layer (15nm) of gold using argon sputtering for 20 min. In the second step, gold coated sheet was immersed in 1% solution of 1,8-octanedithiol in ethanol for 24 h. The resultant sheet sorbent was washed thoroughly with deionised water, and used in the experiments. The chemical structures of various components used in the synthesis of sheet substrates are shown in Fig. 5.2.

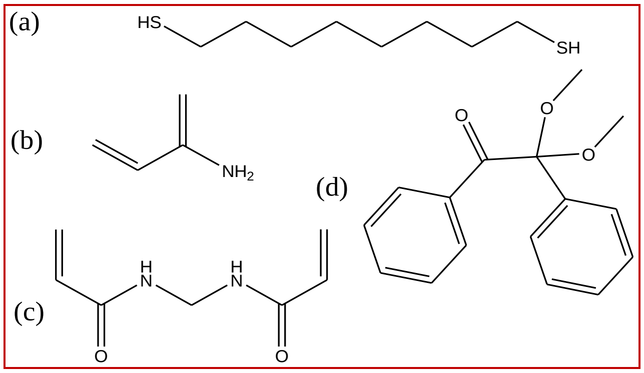

Fig. 5.2 *Chemical structures of components (a) 1,8-octanedithiol, (b) acrylamide (AM), (c) N-N'-methylene-bis-acrylamide (d) α,α'-dimethoxy-α'-phenyl acetophenone (DMPA)*

5A.2.2 Sorption studies

Preliminary experiments were carried out to evaluate the mercury uptake by different sheet sorbents. For this 1x1 cm^2 size of different synthesized sorbents were equilibrated for a predetermined time interval with 10 mL of solutions containing 2 mg L^{-1} of mercury under continuous stirring. The Hg^{2+} concentrations after equilibration were determined using CV-AAS unit. Effect of solution pH on the equilibrium uptake of Hg^{2+} (2 mg $L^{-1,}$ Volume = 25 mL) was investigated in the pH range of 1-9. For studying sorption kinetics, the Ag Nps incorporated poly(acrylamide) sheet and 1,8-octanedithiol functionalized gold coated sheet of a fixed size (1×1 cm^2) were equilibrated with 25 mL of 2 mg L^{-1} Hg^{2+} solution separately. At predetermined time intervals, aliquots were withdrawn and analyzed for the residual Hg^{2+} concentration using CV-AAS. All the experiments were carried out at ambient temperature (25 ± 2°C). From the experimental data, percentage uptake by the sorbent samples was calculated by using the following equation:

$$\text{Uptake (\%)} = (C_i – C_r)/C_i \times 100 \qquad (5.1)$$

where C_i is the initial mercuric ions concentration before equilibration and C_r is the residual mercuric ions concentration after equilibration.

Direct determination of mercury sorbed on the polymer sheet was also carried out using EDXRF and CV-AAS. In the case of Ag Nps embedded poly(acrylamide) (Ag-PAM-PP) sheet, the Hg^{2+} loaded sorbent was excited using low power Rh X-ray tube. The characteristic X-rays of Hg^{2+} sorbed on the sheet were measured using a LEO Si(Li) detector coupled to a 2 K Channel Analyser (MCA) and nEXt software. The overlapping X-rays of gold (Au, L_α X-ray = 9.78 KeV) and mercury (Hg, L_α X ray = 9.98 KeV) in

HS-octyl-S-Au-PP sheet sorbent made the direct quantification of mercury difficult. Therefore, Ag-PAM-PP sorbent was chosen for a direct EDXRF determination of mercury. The sorbed mercury in the Ag-PAM-PP sheet sample was also directly determined using CV-AAS.

To evaluate the tolerance of Ag-PAM-PP sorbent towards other co-existing ions, the Hg^{2+} sorption experiments were performed in the presence of a known concentration of common ground water and seawater matrix elements like Na^+, K^+, Ca^{2+}, Mg^{2+}, NO_3^-, PO_4^{3-} and SO_4^{2-} along with a fixed concentration of Hg^{2+}.

For tolerance studies, the salts used were $NaNO_3$, KNO_3, $CaCl_2$, $MgCl_2.6H_2O$, Na_3PO_4 and Na_2SO_4. The initial concentration of Hg^{2+} was kept fixed at 5 mg L^{-1} while three different concentrations of the interfering ions viz.; 100 mg L^{-1}, 200 mg L^{-1} and 500 mg L^{-1} were used. After continuous equilibration with stirring using a magnetic stirrer for a predetermined time interval, the Ag-PAM-PP sorbent samples were taken out and residual Hg^{2+} concentration was determined by CV-AAS.

5A.3 Results and discussion

5A.3.1 Comparison of sheet sorbents

The different functionalized sorbents were equilibrated with solutions containing mercury at pH 6 as described in experimental section. As can be seen from Table 5.2, the gold coated polypropylene (Au-PP) showed the least sorption of Hg^{2+} ions. The efficiency improved considerably in the 1,8-octanedithiol functionalized gold coated sorbent (HS-octyl-S-Au-PP). The *in-situ* poly(acrylamide) grafted sorbent (PAM-PP) showed better mercury uptake compared to the Au-PP sorbent. To further enhance the uptake, Ag NPs were incorporated in the polymer substrate. It can be seen that incorporation of Ag NPs in the PAM sorbent increased the Hg^{2+} sorption efficiency to 96%. Hence, further studies were carried out using Ag-PAM-PP and HS-octyl-S-Au-PP sheet sorbents.

Table 5.2 *Sorption efficiency of functionalized polypropylene (PP) sheet sorbents for Hg^{2+} in solution having pH 6*

Membrane	**Initial Concentration ($mg\ L^{-1}$)**	**Final Concentration ($mg\ L^{-1}$)**	**Uptake (%)**
Au-PP	2.00	1.60	20.0 ± 3
HS-octyl-S-Au-PP	2.00	0.53	63.6 ± 1.3
PAM-PP	2.00	0.78	61.0 ± 0.8
Ag-PAM-PP	2.00	0.08	96.0 ± 0.6

The chemical conditions of aqueous media also influence the uptake of mercury. One of the important parameters is pH of the aqueous solutions. The uptake profiles of both the sorbents for Hg^{2+} as a function of solution pH are shown in Fig. 5.3. As can be seen from the plots, the uptake followed a similar pattern for the sorbents but sorption of Hg^{2+} in Ag-PAM-PP was higher than that in HS-octyl-S-Au-PP at a given pH. Mercury was sorbed quantitatively in Ag-PAM-PP sorbent (> 95%) in the pH range of 4-6. Below pH 3, there is a competition of H^+ ions with the Hg^{2+} ions for the available binding sites that results in a lower uptake of Hg^{2+}. The reduction in the uptake at higher pH can be attributed to the formation of stable mercuric hydroxide. The higher percentage uptake by Ag-PAM-PP sorbent over a wide range of pH (3-9) makes it suitable for the selective mercury preconcentration from the contaminated waste and natural water samples.

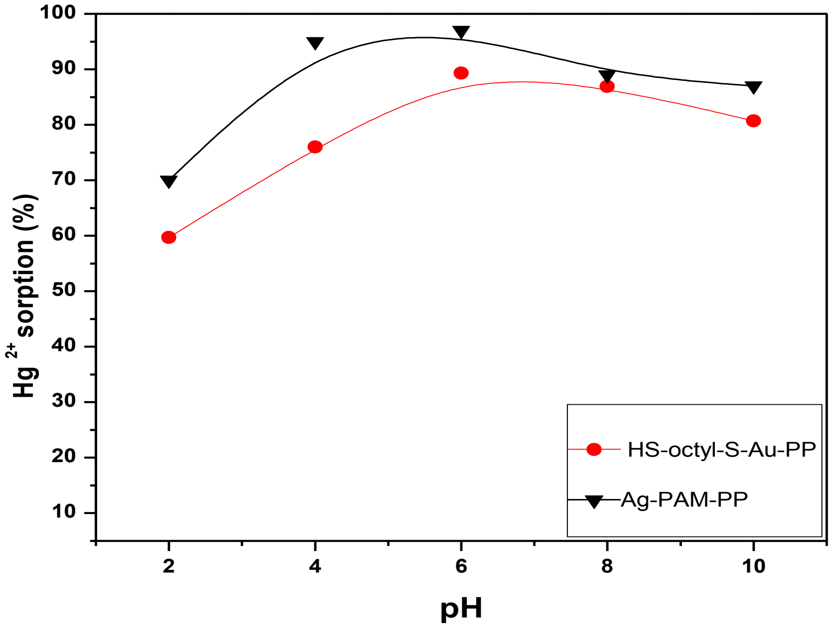

Fig. 5.3 *Sorption of* Hg^{2+} *in HS-octyl-S-Au-PP and Ag-PAM-PP sorbents as a function of pH of equilibrating solution (1×1* cm^2 *size of sorbents were equilibrated with 25 mL* Hg^{2+} *standard solution*

Another factor which is important in determining the efficiency of the sorption process is the kinetics. The uptake of Hg^{2+} by both these sorbents as a function of equilibration time were studied in the well stirred solution having a fixed initial concentration of Hg^{2+} as 2 mg L^{-1} at pH=6. It is clear from Fig. 5.4 that the equilibration time required for optimum Hg^{2+} uptake was about 250 min for Ag-PAM-PP compared to 340 min for HS-octyl-S-Au-PP sorbent sample. Thus, the rate of Hg^{2+} sorption was also faster in the case of Ag-PAM-PP sorbent as compared to the thiol functionalized sorbent. Hence, Ag-PAM-PP was the sorbent of choice for SPE of mercury. Therefore, it was characterized further for different physical parameters.

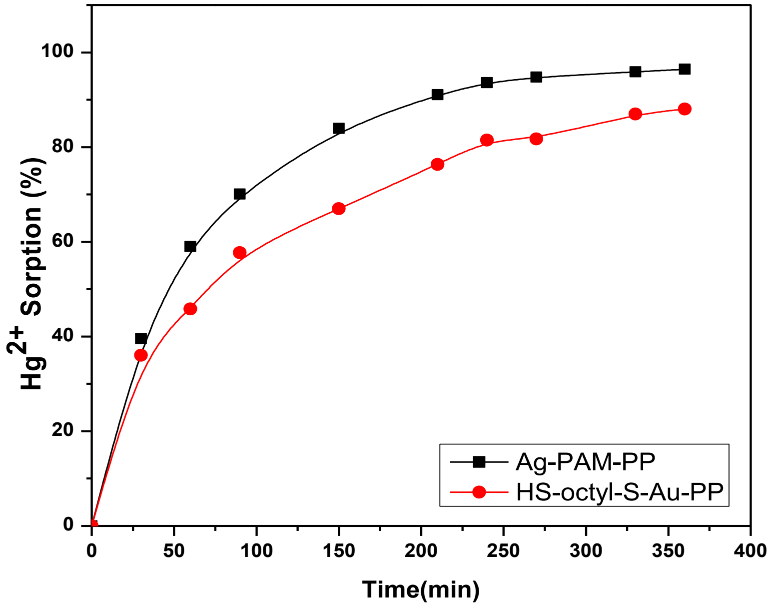

Fig. 5.4 *Sorption of Hg^{2+} in the sorbent sheets as a function of equilibration time (1×1 cm^2 sheet sorbents were equilibrated with 25 mL Hg^{2+} standard solution)*

5. A.3.2. Characterization of Ag-PAM-PP sheet

The Ag Nps embedded poly(acrylamide) (Ag-PAM-PP) sorbent was characterized using FE-SEM, UV-Visible spectrophotometry and XRD. The performance of a sorbent with functional groups grafted in its matrix depends mainly upon the extent and stability of grafting. The extent of grafting of monomeric acrylamide along with the cross-linker MBA in the microporous poly(propylene) host substrates was found to be 120±10 wt% gravimetrically. The grafted sorbent was found to sorb water up to 45 wt%, indicating that the Ag-PAM-PP sorbent was hydrophilic.

Silver was loaded in the poly(acrylamide) grafted samples by treating it with 1 mmol L^{-1} $AgNO_3$ solution followed by reduction with $NaBH_4$ to form Ag nanoparticles throughout the PAM-PP matrix. The in-situ formed Ag-NPs showed a surface plasmon resonance

(SPR) absorption peak around 395-410 nm (Fig. 5.5(a)) which is characteristic of Ag Nps as reported in the literature [407,408]. Although the peak appears at 405 nm, it shows a broad line shape, which might be an indication for larger particle size distribution in the sample. In order to confirm this assumption, XRD analysis of Ag-PAM-PP was carried out. The prominent peaks at respective 2θ values are known for zero valent silver (FCC), representing (111) and (200) crystal planes due to Braggs reflection at 2θ=37.06° and 42.2° respectively (Fig. 5.5(b)). XRD line broadening was used for the analysis of crystallite size using Debye-Scherrer formula [408].

$$D = 0.9\ \lambda/\beta\cos\theta \qquad (5.2)$$

where D is the crystallite size of Ag Nps, λ is the wavelength of the X-ray source (1.5406 A^o) used in XRD, β is the full width at half maximum at the diffraction peak and θ is the Bragg angle. The average particle size was found to be about 35 nm. The lattice constant calculated from this pattern is in agreement with the published results [409,410].

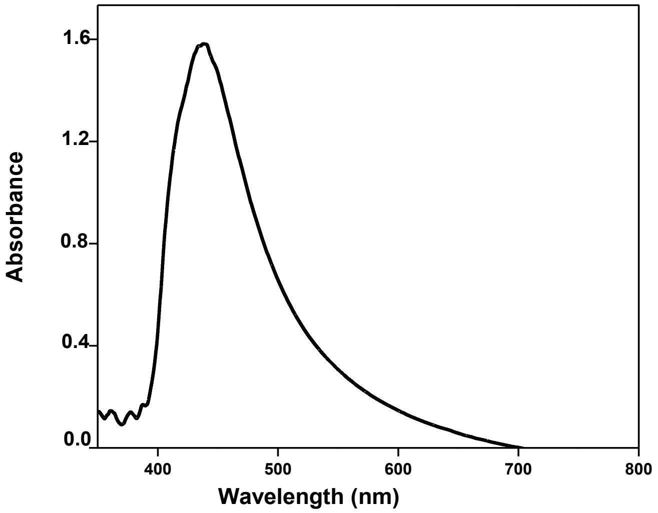

Fig. 5.5 (a) *UV – Vis absorption spectrum of Ag-PAM-PP sorbent showing characteristic SPR peak of Ag Nps*

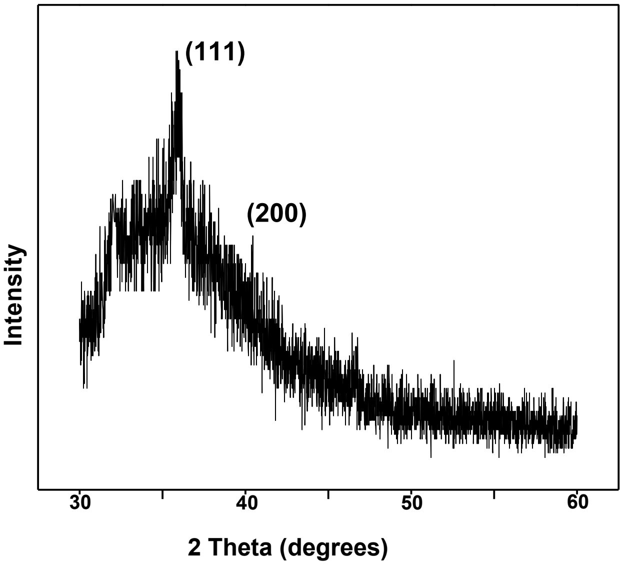

Fig. 5.5 (b) *X-ray Diffraction pattern of Ag-PAM-PP sorbent*

The Field Emission Scanning Electron Micrograph (FESEM) image of Ag-PAM-PP sorbent shows the morphology of Ag Nps (Fig.5.6). The sheet sample was imaged using both secondary electron signals (SEM) (Fig. 5.6(a)) and a backscattered electron signals (BSE) (Fig. 5.6(b)).

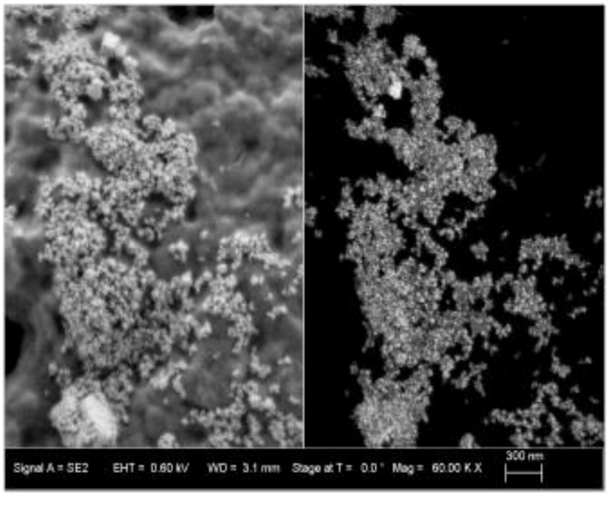

Fig. 5.6 *SEM image (a) and BSE image (b) of Ag Nps in Ag-PAM-PP sheet*

Both the figures show the formation of small size clusters of Ag nanoparticles which have non-uniform spatial distribution. The nanoparticles are not entirely spherical in shape and have diameters varying between 20 to 70 nm, with an average diameter of 40 nm.

5A.3.3 Tolerance studies

Ground water and seawater have a complex matrix due to the presence of a number of cations like Na^+, K^+, Ca^{2+}, Mg^{2+} and anions like NO_3^-, PO_4^{3-} and SO_4^{2-} that can interfere with the uptake of Hg^{2+}. Therefore, tolerance studies of these ions were carried out for Ag-PAM-PP sorbent.

Table 5.3 *Tolerance of co-existing ions in Ag-PAM-PP sorbent at fixed mercury concentration (5 mg L^{-1}) in solution*

Competing ions	**Mercury removal efficiency (%) of in the presence of a competing ions having different concentration**		
	100 mg L^{-1}	**200 mg L^{-1}**	**500 mg L^{-1}**
Na^+	94 ± 1	93 ± 3	93 ± 2
K^+	98 ± 3	94 ± 2	91 ± 1
Mg^{2+}	91 ± 6	88 ±1	71 ± 3
Ca^{2+}	87 ± 3	79 ± 4	60 ± 8
NO_3^-	96 ± 7	91 ± 1	93± 6
PO_4^{3-}	90 ± 1	88 ± 4	86 ± 0.9
SO_4^{2-}	94 ± 0.5	93 ± 1	91± 1

The Ag-PAM-PP sorbent was found to be unaffected in the presence of Na^+, K^+, NO_3^-, PO_4^{3-} and SO_4^{2-} up to 500 mgL^{-1} and from Ca^{2+} and Mg^{2+}, up to 200 mgL^{-1} for an initial Hg^{2+} concentration of 5 mg L^{-1} (Table 5.3). Above 200 mg L^{-1}, the mercury uptake was reduced to 60% in the case of Ca^{2+}. In the presence of Mg^{2+}, the uptake was reduced to 70%. These observations are in accordance with the complexing abilities of various metal ions. The monovalent ions have lowest complexing ability as compared to multivalent ions and, therefore, their high concentration can easily be tolerated. Among the divalent ions, Mg^{2+} being the smaller compared to Ca^{2+} forms less stable complex in a sterically restricted environment of the sorbent with respect to the former. Therefore the reduction in the mercury uptake was less in the presence of Mg^{2+} compared to Ca^{2+}.

5. A.4 Mechanism of Hg^{2+} sorption on Ag-PAM-PP sorbent

The mechanism of sorption of Hg^{2+} on Ag-PAM-PP sorbent is governed both by the complexation of mercury with the amide groups of poly(acrylamide) grafted on poly(propylene) substrate and the galvanic reaction of Ag Nps (formed *in situ* by sodium borohydride reduction) with the sorbed Hg^{2+}. The amide compounds are selective reagents for binding mercury as has been reported in literature [411].

$$2\mathrm{R}-\mathrm{CONH}_2+\mathrm{Hg}^{2+}\rightarrow(\mathrm{R}-\mathrm{CONH})_2-\mathrm{Hg}+2\mathrm{H}^{+} \qquad (5.3)$$

The amide nitrogen forms a covalent bond with the Hg^{2+} ions present in aqueous solution leading to 60% uptake but further enhancement in the uptake (~96%) is attributed to the presence of Ag Nps. The standard redox potiential of Hg^{2+}/Hg^0 (+0.85V) and Ag^+/Ag^0 (+0.80V) are close to each other. Therefore their reactivity is similar and the galvanic reaction is not feasible. However, it has been shown theoretically and experimentally that the standard redox potential of metal nanoparticles decreases with decreasing size. For example, Henglein predicted large negative shifts in the redox potential for small Ag_n

clusters (n = 1 to 15) as the number of atoms in the cluster decreases [412]. Similarly in the case of Ag Nps, it is known that the electrochemical potential of the Ag^+/Ag^0 becomes negative due to the high reactivity of the small size of the nanoparticles leading to the feasibility of following galvanic reaction in the sorbent [413].

$$2\,Ag^0 + Hg^{2+} \rightarrow 2Ag^+ + Hg^0 \qquad (5.4)$$

The formed Hg^0 gets trapped on the sorbent surface in the form of silver amalgam. It was observed that the increase of Hg^{2+} sorption on Ag-PAM-PP sorbent led to a decrease in the intensity of the surface plasmon absorption band (SPB) of AgNps. It was observed that there was a steady decrease in the intensity of SPB band at 405 nm with the increase in Hg concentration from 0.1 mg L^{-1} to 5 mg L^{-1} (Fig.5.7).

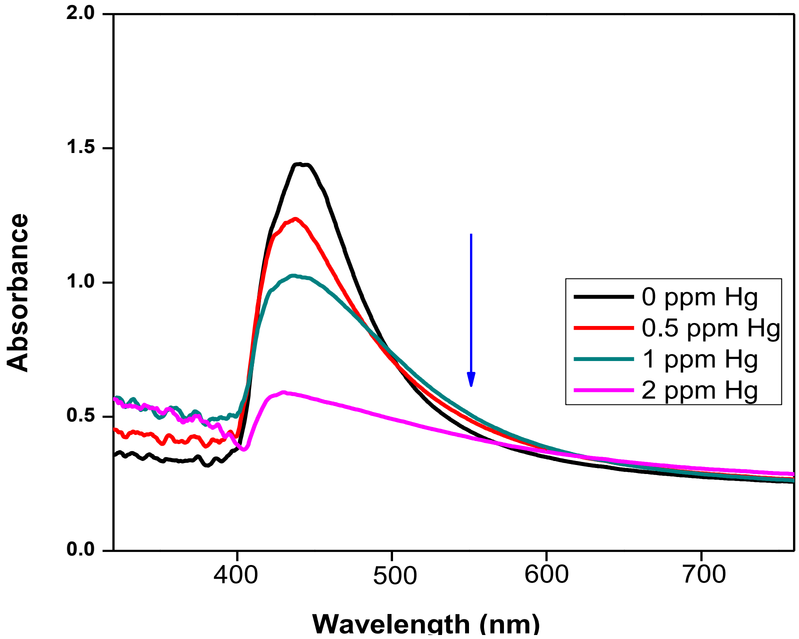

Fig. 5.7 *Change in SPB of Ag Nps embedded in PAM substrate as a function of* Hg^{2+} *concentration*

The decrease in SPB also led to a change in the color of sorbent (Fig. 5.8). Since the color change of the sheet sorbent was proportional to the amount of sorbed Hg^{2+}, a qualitative estimate for sorption could be made with naked eyes prior to the measurement by EDXRF/ CV-AAS.

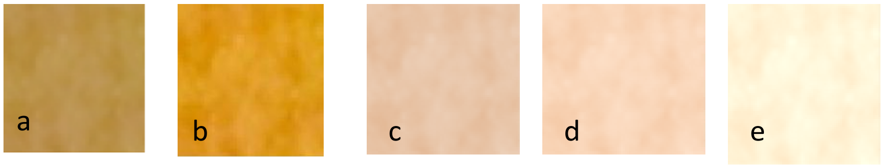

Fig. 5.8 *Variation of color in* Hg^{2+} *equilibrated Ag-PAM-PP sorbent (a) Blank , (b) 0.5 mg* L^{-1}*, (c) 1 mg* L^{-1}*, (d) 2 mg*L^{-1}*, (e) 5 mg* L^{-1} Hg^{2+}

5A.5 Real sample analysis

This study was undertaken so as to evaluate the potential of the developed sheet substrates for the preconcentration of trace levels of Hg^{2+} in natural water samples. The ground water samples were collected from Bangalore and seawater samples were collected from Thirumangalam area, Tamilnadu. The solutions were spiked with 2 mg L^{-1} Hg^{2+} standard solution and were equilibrated with 1x1 cm^2 sheet sorbent. The Hg^{2+} preconcentrated on sheet sorbent was determined by CV-AAS (Table 5.4).

Table 5.4 *Uptake of Hg(II) by sheet substrates from the ground-water and seawater samples*

Spiked Sample	Spiked Hg^{2+} (mgL^{-1})	Sample Volume (mL)	Sample Size (cm^2)	% Uptake (HS-HS-octyl-S-Au-PP)	% Uptake (Ag-PAM-PP)
GW	2	25	1 x1	67 (± 0.3)	94 (± 0.2)
SW	2	25	1 x 1	59 (± .9)	83 (± 1.3)

The results demonstrate the validity of these sorbents for the preconcentration of Hg^{2+} from the real sample solutions. The percentage uptake for Hg^{2+} was found to be high for Ag-PAM-PP sorbent (85-93%) compared to HS-octyl-S-Au-PP sorbent (59-67%). This clearly shows a better selectivity of Ag NPs embedded sorbent towards Hg^{2+} in the presence of a wide range of interferents in the real samples compared to dithiol functionalized gold coated sorbent. However, the preconcentration factor is also an important parameter for performance evaluation of such solid sheet sorbents. As such direct calculation of preconcentration factor is difficult. Hence, these calculations were performed by measuring the mercury desorbed from Ag-PAM-PP sorbent in 2 mL solution of 10% HNO_3. It was observed that the preconcentration factor of 12 can be achieved in the 1x1 cm^2 Ag-PAM-PP sample.

5A.6 Analytical application of developed sheet sorbent

Preconcentration not only helps in enhancing the detection limits of the method but also eliminates the spectral interference caused by undesirable components in the matrix. The preconcentrated trace mercury ions on Ag-PAM-PP sorbent can be quantified either by eluting it from the sorbent with subsequent solution phase determination or by direct solid phase determination of the sorbent using a technique like EDXRF.

In the present work, both the techniques were used for the quantification of Hg^{2+} depending on Hg^{2+} concentration in the sample. EDXRF can be used to determine elements of interest directly in solid matrix. Direct solid phase measurement offers advantages like high preconcentration factor, uniform and homogeneous reproducible matrix and short analysis time. The Ag-PAM-PP sheet sorbent developed in this work was used for direct quantification of preconcentrated Hg^{2+}. The EDXRF spectrum of the Ag-PAM-PP sorbent treated with Hg^{2+} showed both L_{α} and L_{β} (9.98 and 11.8 KeV) X ray peaks of mercury (Fig 5.9).

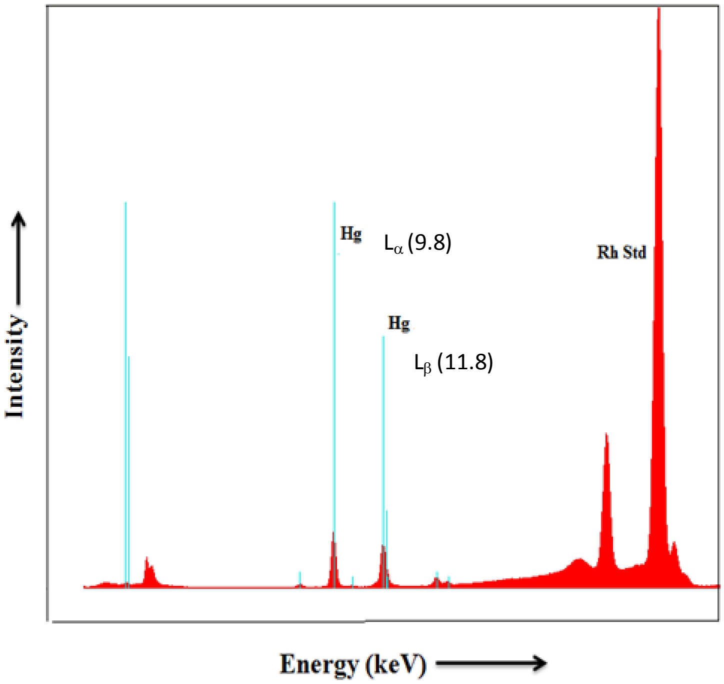

Fig. 5.9 *EDXRF spectrum of* Hg^{2+} *sorbed Ag-PAM-PP sorbent*

To establish a calibration range, 25 mL solution with initial Hg^{2+} concentration varying from 100 to 10000 ng mL^{-1} were equilibrated with 1x1 cm^2 Ag-PAM-PP sorbent for overnight. Calibration plot of increasing concentration of Hg^{2+} versus intensity of X-rays was obtained (Fig. 5.10). It was found that the percentage uptake was quantitative between 100 to 10,000 ng $mL^{-1}$and a correlation coefficient close to 1 was obtained. Beyond this upper limit, the sorption of Hg^{2+} reduces due to the saturation of the available binding sites on 1x1 cm^2 sorbent. Limit of detection (LOQ, 3σ) was found to be 30 ng mL^{-1} with a RSD of 5% for EDXRF.

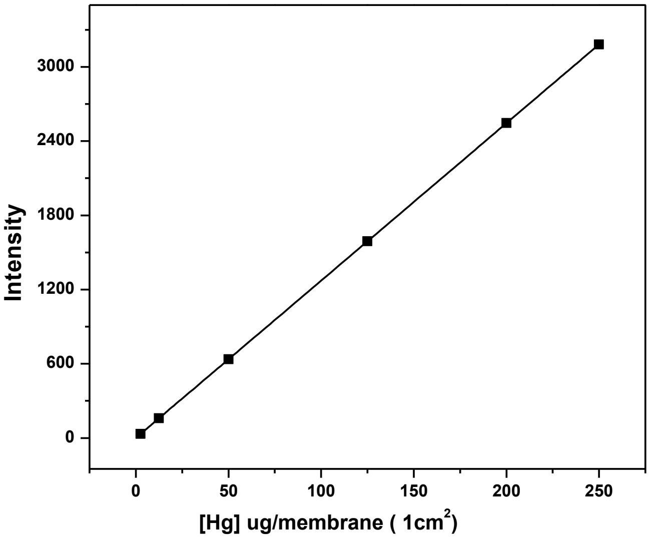

Fig.5.10 *EDXRF Calibration plot of Hg^{2+},1×1 cm^2 Ag-PAM-PP was equilibrated with 25 mL Hg^{2+} standard solutions and measured by EDXRF*

Direct quantification by CV-AAS was done by desorbing Hg^{2+} from the sorbent directly in the reaction vessel by HNO_3 (Fig 5.11). In 0.1 M nitric acid, the sorbed mercury on the exhausted sorbent gets oxidised to mercuric ions and hence gets desorbed in the solution.

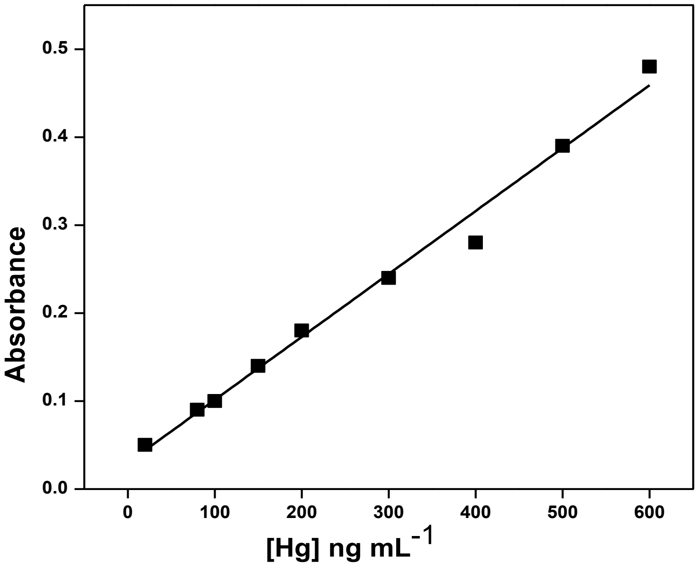

Fig. 5.11 *Calibration curve obtained by CV-AAS of desorbed Hg from the Ag-PAM-PP sorbent (Size of Ag-PAM-PP = 1×1 cm^2, Volume of desorbed solution = 15mL)*

A linear response in the concentration range of 20 ng mL^{-1} to 400 ng mL^{-1} for desorbed mercury was obtained. The limit of detection (LOD, 3σ) by CV-AAS was 6 ng mL^{-1} with a RSD of 2%.

Thus, it can be concluded that direct determination of Hg^{2+} is possible by EDXRF if the initial concentration of Hg^{2+} is in the range of 100-10000 ng mL^{-1} and for still lower concentration CV-AAS can be performed down to 20 ng mL^{-1} (Table 5.5). The detection limits can be further enhanced by increasing the sample volume from 25 to 100 mL.

Table 5.5 *Comparison of the lowest detection limits for the quantification of Hg^{2+}*

Technique	LOD (ng mL^{-1})	R.S.D (%)
EDXRF	30	5
CV-AAS	6	2

5A.7 Conclusions

In the present work, two types of polymeric sheet sorbents viz. Ag nanoparticles embedded poly(acrylamide) grafted poly(propylene) sorbent (Ag-PAM-PP) and 1,8-octanedithiol functionalized gold coated polypropylene sorbent (HS-octyl-S-Au-PP) were synthesized and applied to preconcentrate Hg^{2+} from aqueous solution. Among the two, Ag-PAM-PP has shown superior performance for the uptake of mercury from natural water samples in terms for sorption capacity, sorption kinetics and working pH range.

Further probing into the underlying sorption mechanism in the case of Ag-PAM-PP, revealed that complexation of mercury with the amide groups of Ag-PAM-PP substrate and the galvanic reaction of Ag Nps with the sorbed Hg^{2+} are the two mechanisms involved in the Hg^{2+} sorption.

Quantitative determination of preconcentrated Hg^{2+} was possible in the range 20 ng mL^{-1} to 10 mg L^{-1} using EDXRF and CV-AAS techniques. The tailored Ag-PAM-PP sheet sorbent was found to be amenable for Hg^{2+} removal and quantification from routine aqueous samples. The direct determination of preconcentrated Hg^{2+} in the sheet sorbent not only enhances the existing analytical detection limits of EDXRF but also leads to the safe handling of mercury solutions. In addition, the incorporation of Ag NPs in the sorbent facilitates its color change upon Hg^{2+} sorption, which can be utilized for qualitative screening of Hg^{2+} with naked eye at the site before its analysis using EDXRF/ CV-AAS in the laboratory later.

Section 5B

DEVELOPMENT OF VISUAL OPTODE SENSOR FOR MERCURY (II)

5B.1 **Introduction**
5B.2 **Experimental**
  5B.2.1 **Synthesis of Sensor Molecule**
  5B.2.2 **Fabrication of Optode**
  5B.2.3 **Optimization of Experimental Parameters**
5B.3 **Results and Discussion**
  5B.3.1 **Optimised Composition of Optode**
  5B.3.2 **Analytical Parameters of Optode**
5B.4 **Sensing Mechanism of Optode**
5B.5 **Application to Real Samples**
5B.6 **Conclusions**

5B.1 Introduction

The monitoring of heavy metals within the environment, drinking water, food, and biological fluids has become essential due to the increasing environmental awareness and stringent regulations for pollution control. Standard methods for heavy metal determination covers a wide range of laboratory-based techniques such as atomic absorption spectroscopy (AAS), inductively coupled plasma-atomic emission spectroscopy (ICP-AES), inductively coupled plasma-mass spectrometry (ICP-MS), and X-ray fluorescence spectroscopy (XFS) [414-420]. Although these techniques provide sensitive and precise detections, they require time-consuming sample pretreatments, sophisticated equipments and are unsuitable for on-site detection. The necessary collection, transportation and pretreatment of a sample is time consuming and a potential source of error. However, in the last years smaller and portable and less expensive devices have been brought to the market. On the other hand, the last years have seen a growing development of chemical sensors for a variety of applications. The toxicity posed by heavy metals even when present in ultra-trace concentration makes a continuous supervision of drinking or ground water sources necessary. Chemical sensors enable on-line and field monitoring and therefore can be a useful alternative tool.

A chemical sensor can be defined as "*a portable miniaturized analytical device, which can deliver real-time and on-line information in presence of specific compounds or ions in complex samples*" [421]. Chemical sensors can be categorized into electrochemical, optical, mass-sensitive and heat-sensitive, according to the types of transducer [422].

Over the past few years efforts are continuously being made to develop various optical sensors for on-site detection of heavy metal ions.

An optical sensor device consists of the following components. (a) the recognition element, where specific interaction and identification of the analyte takes place; (b) the transducer element that converts the recognition process into a measurable optical signal; (c) an optical device (process unit) which consists of at least a light source (in the simplest form a LED) and finally (d) a detector (in the simplest form a photodiode), which detects and converts the change of optical properties, after amplification of the primary signal, into a unit readout [423-425]. The optical properties measured can be absorbance, reflectance, luminescence, light polarization, Raman and other. The use of optical sensors offers potential advantages over conventional instruments such as electrical isolation, reduced noise interference, the possibility of miniaturization and remote sensing [426]. In addition, they are often inexpensive and can be mass-produced as disposable materials [427]. Being highly compact these optical sensors offers the advantage of using them in on-site measurements.

Considering the diverse sources of mercury and its high toxicity, highly sensitive and selective Hg^{2+} sensors are in high demand for understanding its distribution and pollution [428-432]. Most of the sensors for mercury detection are optical sensors which are based on the on-off fluorescence mechanism to develop colorimetric or fluorescent molecular probes [433-443]. Some of the sensors are based on proteins, oligonucleotides, genetically engineered cells, conjugated polymers and nanomaterials [444-452].

Colorimetric sensors based on the fluorescence properties of organic molecules usually work in organic media and therefore do not meet the selectivity and sensitivity requirements for the detection of mercury in aqueous solutions [453,454]. The strong hydration of mercury ions and the lack of solubility of synthesized organic derivatives lead to poor solid phase extraction of mercury from aqueous solutions. This poses a challenge for the development of optical sensors for the detection of mercury ions in the aqueous medium.

Development of optode sensors also known as optochemical sensors for mercury detection has recently gained interest among chemists [455-459]. The commonly used optodes consist of a plasticized polymeric membrane containing a molecular sensor which is responsible for targeting the desired analyte. The sensor molecule is immobilized by either physical or chemical methods. On interaction of the sensor with the analyte, a distinct change in the absorbance or fluorescence of the sensing layer is obtained which is responsible for the optical signal. The choice of molecular sensor responsible for generating the optical signal plays an important role in the design of optodes [460].

Recently rhodamine framework has attracted wide attention in the field of constructing fluorescent chemosensors, owing to its excellent photophysical properties such as higher absorption and emission wavelengths, high absorption coefficient, and high fluorescence quantum yield [461]. The rhodamine derivatives usually display a color change and strong fluorescence in acidic solution due to a carbonyl group in its spirolactone or spirolactam moiety as shown in Fig. 5.12. Similarly, on the addition of metal ions spirolactam ring can cause color as well as fluorescence changes depending on the solvent system [462,463]. Colorimetric determination of various metals (e.g. antimony, zinc, silver, osmium) in biological samples is being carried out using rhodamine derivatives since the middle of the 20th century [464-466].

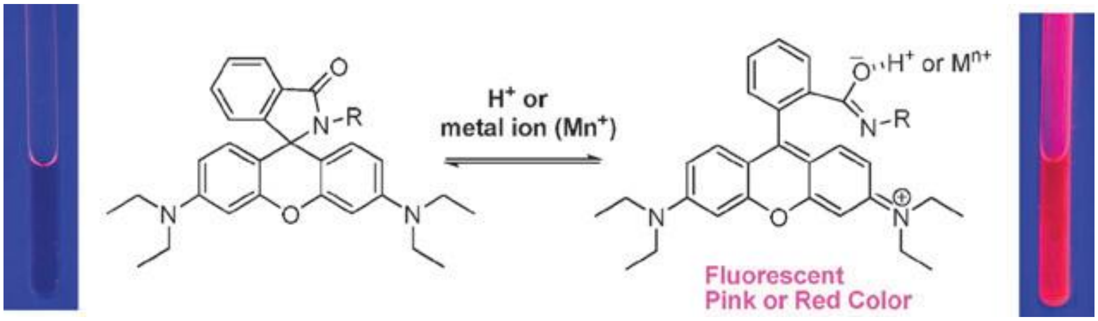

Fig. 5.12 *Spirolactam ring-opening process of rhodamine derivative*

There has been significant development in the synthesis of various rhodamine derivatives for mercury ions detection. Kim et al. has reported rhodamine-based tren(triethylenetetramine) and diethylenetriamine derivatives with tosyl groups, in which the Hg(II) was entrapped by diethylenetriamine groups [467]. The addition of Hg(II) ions to the CH_3CN solutions produced a color change with enhanced fluorescence intensity. Duan et al. reported a Hg(II) probe -based on rhodamine containing a carbohydrazone unit in DMF solution [468]. Yoon et al. reported rhodamine-urea based derivatives in acetonitrile solution. A multisignaling optical–electrochemical sensor based on a rhodamine - ferrocenyl derivative and an 8-hydroxyquinoline moiety for sensing Hg(II) in ethanol–HEPES (4-(2-hydroxyethyl)-1-piperazineethanesulfonic acid) buffer solution was synthesized by Huang et al [469]. Ma and Shi et al. and Xu et al. [470,471] reported a rhodamine-B thiolactone derivative as a sensor for Hg^{2+}. Most of the reported derivatives as stated above are applicable for Hg(II) detection in the non-aqueous media. Therefore, the current research is focused on developing chemical sensor for the detection of mercury ions in the aqueous medium. Recently, Yang et al. have developed a rhodamine-6G phenylthiosemicarbazide derivative, which works as a highly selective and sensitive chemodosimeter for Hg^{2+} in aqueous solution [435]. In our work we have selected this derivative to be incorporated in an optically transparent solid matrix to form a Hg(II) selective optode. Although a large number of molecular probes are reported for Hg^{2+} detection in solution phase, only a few examples of membrane/optode probes are found in literature. The major reason for this lies in the problems encountered during the synthesis of any solid phase reagent immobilized sensors. Agglomeration and leaching of the incorporated indicator reagent from the matrix are some of the common problems. The covalent linkage of the incorporated reagent to a suitable matrix appears to be an efficient method to overcome the leaching but most of the time it is accompanied by the decreased activity of the sensing site.

In the present work, the main objective was to synthesize a polymeric membrane based optode sensor for selective and sensitive on-site detection of Hg (II) present in the natural waters. Rhodamine-6G phenylthiosemicarbazide derivative (Rh6G-P) was immobilized in a plasticized polymer matrix as it binds with Hg(II) ions. The binding of Hg(II) followed by ring opening and cyclization reactions in the rhodamine derivative leading to the development of pink color. Based on the preliminary experiments, cellulose triacetate (CTA) matrix has been selected due to its optical quality and the ease with which signal generating molecule (rhodamine-6G phenylthiosemicarbazide) can be immobilized in it. The conditions for the synthesis of the optode were optmised to obtain maximum analytical signal for Hg(II) ions. The tolerance of the synthesized optode sensor towards co-existing ions in ground water has been studied. The optode showed high reproducibility and selectivity towards Hg(II) ions. Therefore it was applied for the detection of mercury in ground water samples in the presence of high concentration of interfering ions.

5B.2 Experimental

5B.2.1 Synthesis of sensor molecule (Rh6G-P)

Phenylthiosemicarbazide Rhodamine 6G derivative was synthesized following a detailed two step procedure described by Yang et al [435]. In the first step rhodamine 6G chloride (300 mg) was dissolved in 20 mL methanol and to this hydrazine monohydrate (0.2 mL) was added. The reaction mixture was refluxed for 6h until the pink color disappeared. The resultant solution was diluted with 30 mL ethyl acetate and then washed with water and 1N NaOH (10 mL). This organic phase was dried over magnesium sulphate, concentrated and was purified using silica-gel column with a mixture of hexane: CH_2Cl_2: MeOH = 10:2:1 as an eluent. The yield of rhodamine 6G hydrazide obtained was 250 mg (94%). In the second step, rhodamine 6G hydrazide (200 mg) was added to a solution of 0.65 mmol phenyl isothiocyanate (0.1 mL) in DMF (3 mL). The reaction mixture was stirred for 6 h at room temperature. After the solvent was evaporated under reduced pressure, the crude product was column purified on silica-gel (elution with hexanes/EtOAc/CH_2Cl_2 = 4:1:1) to give 250 mg (91.5%) of desired derivative. The reaction steps involved in the synthesis of the Rh6G-P derivative are shown in Fig. 5.13. . The characterization studies showed that Rh6G-P derivative is similar as expected from the procedure followed from literature [435].

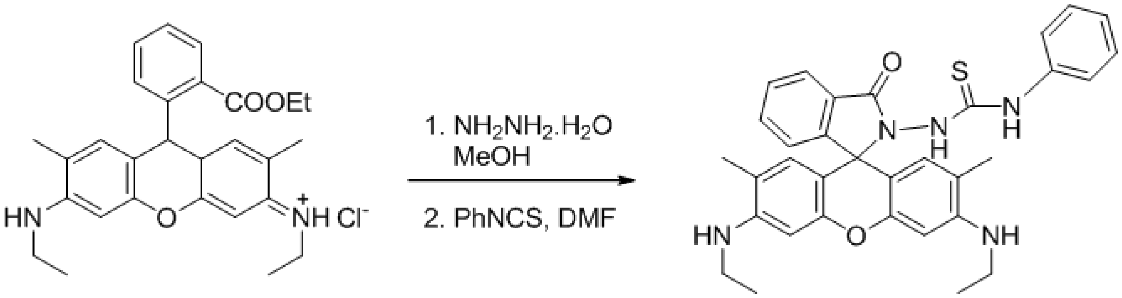

Fig. 5.13 *Two step reaction involved in synthesis of Rh6G-P derivative from rhodamine 6G*

5B.2.2 Fabrication of optode

The fabrication of the optode sensor is explained in the experimental section of this thesis. The transparent membrane obtained was further cut into 2x1 cm^2 size pieces and used in all the experiments. The chemical structure of the components used for the synthesis of optode membrane i.e cellulose triacetate (CTA), tri-(2-ethylhexyl) phosphate (TEHP) and phenylthiosemicarbazide rhodamine 6G derivative (Rh6G-P) are given in Fig. 5.14. To obtain the best sensing membrane in terms of uniformity and maximum sensitivity towards Hg(II), it is necessary to optimize various experimental conditions. The amount of Rh6G-P derivative was optimized by varying its concentration from 1 mg to 7 mg in the casting solution before synthesizing the membrane. The resultant membranes thus obtained were equilibrated with 10 mL standard solution of 2 mgL^{-1} Hg(II) and the absorbance values at λ_{max} were measured. The amount of derivative in the membrane which gave the maximum absorbance signal was fixed for rest of the experiments.

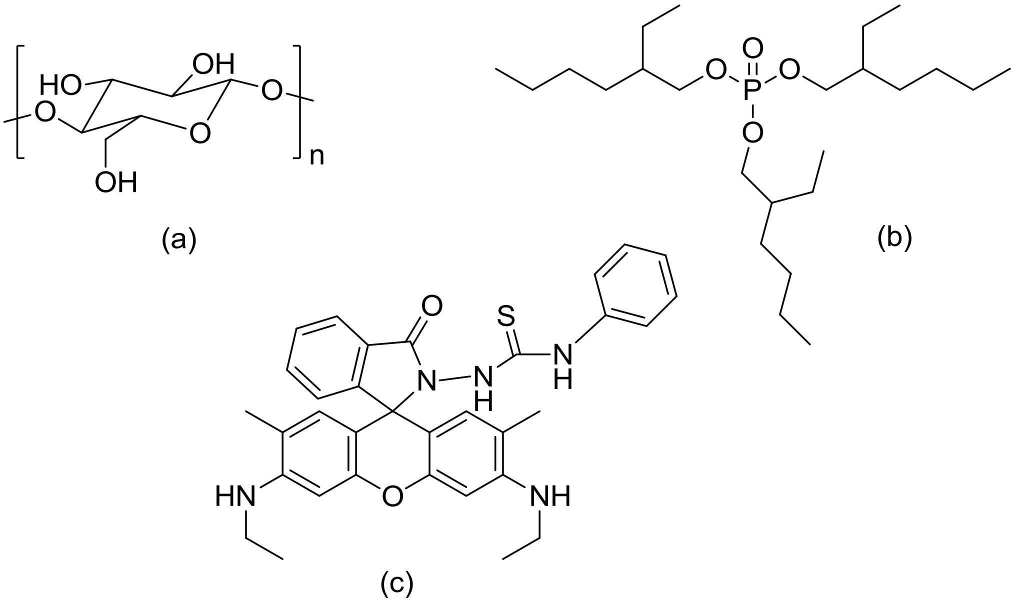

Fig. 5.14 *Chemical structures of components (a) Cellulose Triacetate (CTA), (b) Tri-(2-Ethylhexyl) Phosphate (TEHP), (c) Rhodamine 6G derivative (Rh6G-P) used in the synthesis of optode.*

5B.2.3 Optimization of experimental parameters

For quantitative measurement of the signal, the synthesized optode of 2x1 cm^2 size was placed under an optic fibre and absorbance was measured at λ_{max} = 535 nm. This was treated as blank reading. Similar measurements were performed out after equilibrating the optode with varying concentrations of Hg(II). To obtain the best measurement conditions for detecting Hg(II), the effect of pH, time taken to obtain maximum absorbance and tolerance of synthesized optode towards others cations were evaluated.

The surface morphology of the synthesized optode film was studied by atomic force microscopy (AFM) studies. The tapping mode AFM measurements were performed at ambient temperature conditions using a Nanosurf easy Scan 2 AFM (Nanosurf, Switzerland) with 10 μm scanner head. The cantilevers used were NCLR-10 (Nano World) with a resonance frequency of 190 kHz and force constant of 48 N/m. The AFM data was analyzed using Nanosurf Report 4.1 software. Membranes of 2 x1 cm^2 size were equilibrated with 2 mgL^{-1} Hg(II) solution adjusted at different pH values in the range of 4 to 10. Hg(II) was quantified in the sample by measuring the absorbance at λ_{max}. Hg(II) ions sorption kinetics (2x1 cm^2) was carried out by varying the contact time between the sensing membrane and Hg(II) solution of 2 mg L^{-1} from 5 min to 24 h at optimized pH. The membranes were taken out of the equilibrating solution after a predetermined time interval and the absorbance was measured using an optical fibre spectrophotometry. This was continued until a constant absorbance value was obtained. Tolerance studies were carried out by equilibrating 2x1 cm^2 membranes with various cations which are known to interfere with Hg(II) detection. In all the tolerance experiments the concentration of Hg(II) was fixed at 5 mg L^{-1} whereas the concentration of commonly occurring alkali and alkaline earth metal cations Na$^+$, K$^+$, Mg^{2+} and Ca^{2+} was about 500 mg L^{-1} and transition metal ions such as Cd^{2+},Cr^{3+},Ni^{2+},Cu^{2+}, Pb^{2+}, Fe^{2+}, Fe^{3+}, Al^{3+} and Zn^{2+} was about 1mg L^{-1}. All these experiments were carried out at pH 7.

5B.3 Results and Discussion

5B.3.1 Optimised composition of optode

A comparative study on the effect of different matrix materials on the performance of sensor has been made. Several optode membranes were prepared using polystyrene and cellulose triacetate plasticized with TEHP. It was found that the immobilized Rh6G-P derivative leached from films containing different compositions of polystyrene and TEHP on equilibration with Hg(II) solutions (2 mg L^{-1}). The leaching of the derivative could be attributed to the high hydrophilicity of the polystyrene based membrane as has been reported in the literature [472,473]. Therefore, in the following studies cellulose triacetate (CTA) having low hydrophilicity due to high interchain interactions has been used to entrap the derivative. There was no leaching of the sensing molecule from CTA membranes.

Several thin membranes containing different amounts of CTA, TEHP and Rh6G-P derivative were prepared by the solution casting method using dicholoromethane as a solvent as explained in experimental section. The synthesized optode membrane showed visual color change upon equilibration with Hg(II) standard solution of varying concentrations.

The composition of the optode with respect to Rh6G-P was optimized by preparing several membranes with different amounts of Rh6G-P. It was observed that on increasing its amount from 1 to 7 mg, the absorbance of the optode increased upto 5 mg and thereafter the change in the absorbance was insignificant (Fig. 5.15). Therefore, the amount of the derivative in the optode was fixed to 5 mg for further studies. Thus, optimized composition of the optode was found to be: 100 mg CTA, 50 mg TEHP and 5 mg Rh6G-P.

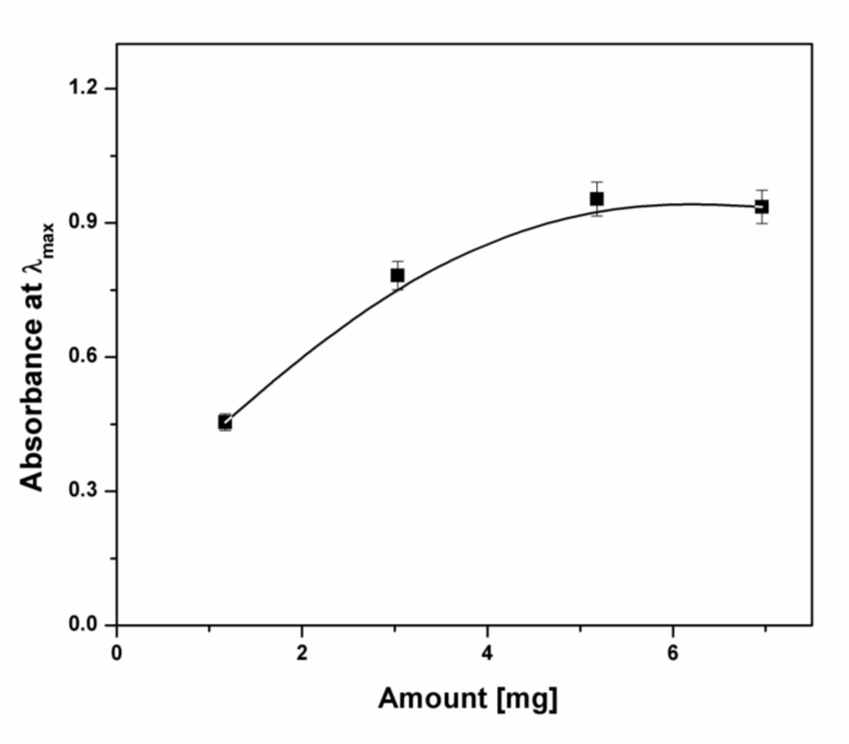

Fig. 5.15 *Absorbance as a function of the amount of Rh6G-P in the optode membrane (CTA (100 mg) and TEHP (50 mg) were kept constant)*

The AFM image of optode film with optimized composition in a two-dimensional form with the format 5.0 x 5.0 µm is shown in Fig. 5.16. The root-mean-square roughness (Sq) of the optode film calculated using AFM was 12.1 nm. The image shows that surface of the optimized optode is non-porous with occasionally pore-like defects. Therefore, the

Hg(II) ions enter the optode matrix with interactions with sensing Rh6G-P molecules. The homogeneity in the color formation on Hg(II) ions loading indicated that Rh6G-P molecules were uniformly distributed throughout the optode matrix.

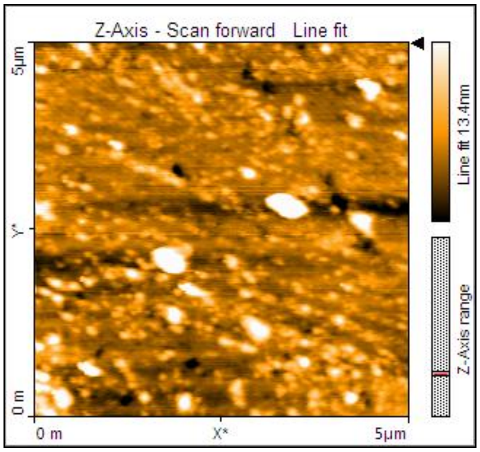

Fig. 5.16 *Atomic force microscopic image of an optode sample*

Optimization of analytical conditions

The pH of the test solution influences the sensor selectivity and its linear dynamic range. Therefore, influence of pH of the test solution on the absorbance of the proposed Hg^{2+} sensor was studied. At pH < 4, the optode showed high absorbance due to proton assisted ring-opening of rhodamine derivative which occurs under acidic conditions [474,475]. Therefore, the sensing range of the optode was studied only at higher pH from 4 to 12 as displayed in Fig. 5.17. It is clear from the Fig. that, there was an increase in the absorbance from pH 4 to pH 8 followed by a slow decrease. The decrease in the absorbance at higher pH values can be attributed to the formation of stable mercuric hydroxides. Therefore, pH 7.5 was selected for rest of the experiments.

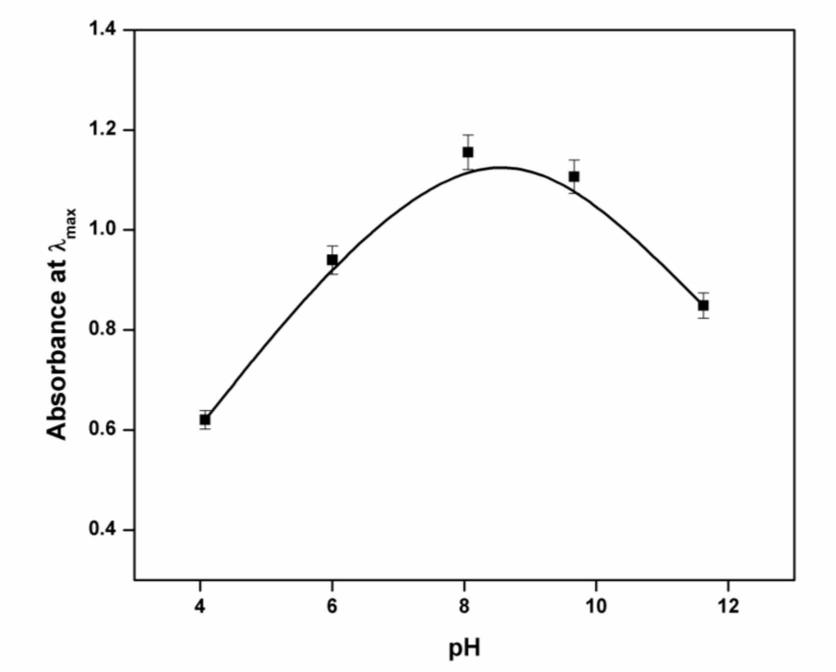

Fig 5.17 *Absorbance of the optode (2x1 cm^2) equilibrated with the solution having 2000 ng mL^{-1} Hg(II) and varying pH*

Response time is one of the important factors for consideration of a sensor. To determine the optimum response time to get a constant absorbance value, kinetic experiments using the optode were conducted up to a contact time of 24h as explained in the experimental section. Absorbance of the optode as a function of equilibration time is shown in Fig. 5.18. It can be seen from Fig. 5.18 that the equilibrium was attained in 160 minutes. However, the equilibration time of 20 min gave a measurable absorbance of 0.13 for 2 mg L^{-1} Hg(II). Therefore equilibration time of 20 min was fixed for rest of the experiments.

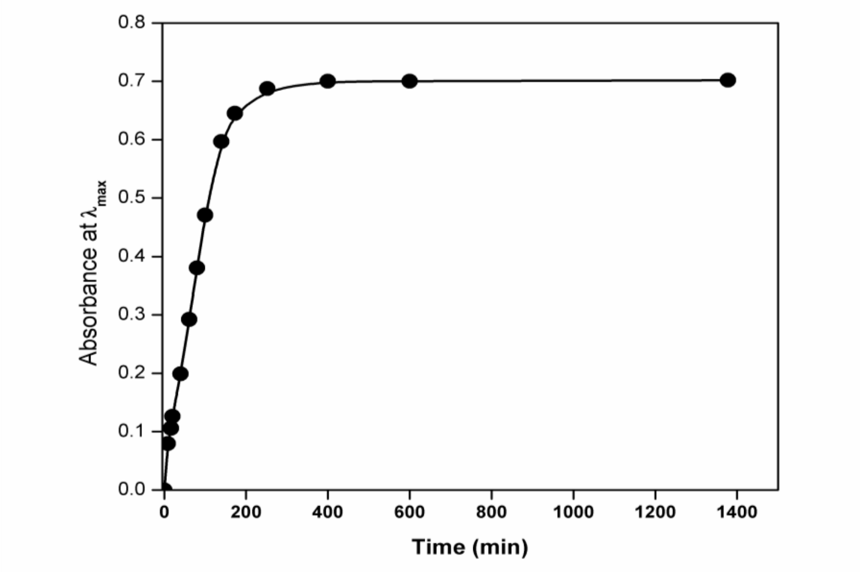

Fig 5.18 A*bsorbance as a function of equilibration time (optode membrane equilibrated with 10 mL of 2mgL^{-1} Hg(II) solution for different time intervals)*

To obtain the lowest mercury concentration that could be detected, the 2x1 cm^2 size optode samples were equilibrated with different concentrations of Hg(II) ranging from 10 to 5000 ng mL^{-1}(Fig 5.19(a)). It can be seen from the Fig. 5.19(a) that the absorbance increased with the increase of Hg(II) concentration. The absorbance at peak maximum was plotted against concentration of Hg(II) and the obtained plot has two different slopes as shown in Fig. 5.19 (b). The inset of Fig. 5.19 (b) shows a linearity ranging from 10 ng mL^{-1} to 60 ng mL^{-1} of Hg(II) with a 0.99 correlation coefficient (R^2 value). A minimum of 10 ng mL^{-1} could be detected by naked eye as shown in Fig. 5.20. The detection limit calculated using the 3s/S criterion, where 's' is the standard deviation of the absorbance of blank optode and 'S' is the slope of the linear calibration plot in lower concentration range was 1.3 ng mL^{-1} which is lower than the limit prescribed by the World Health Organization (WHO) for mercury in potable water (2 ng mL^{-1}). At higher concentration of Hg(II) ions, optode color changes to dark pink which gave an additional advantage for on-site detection of mercury prior to its analysis in the laboratory(Fig. 5.20).

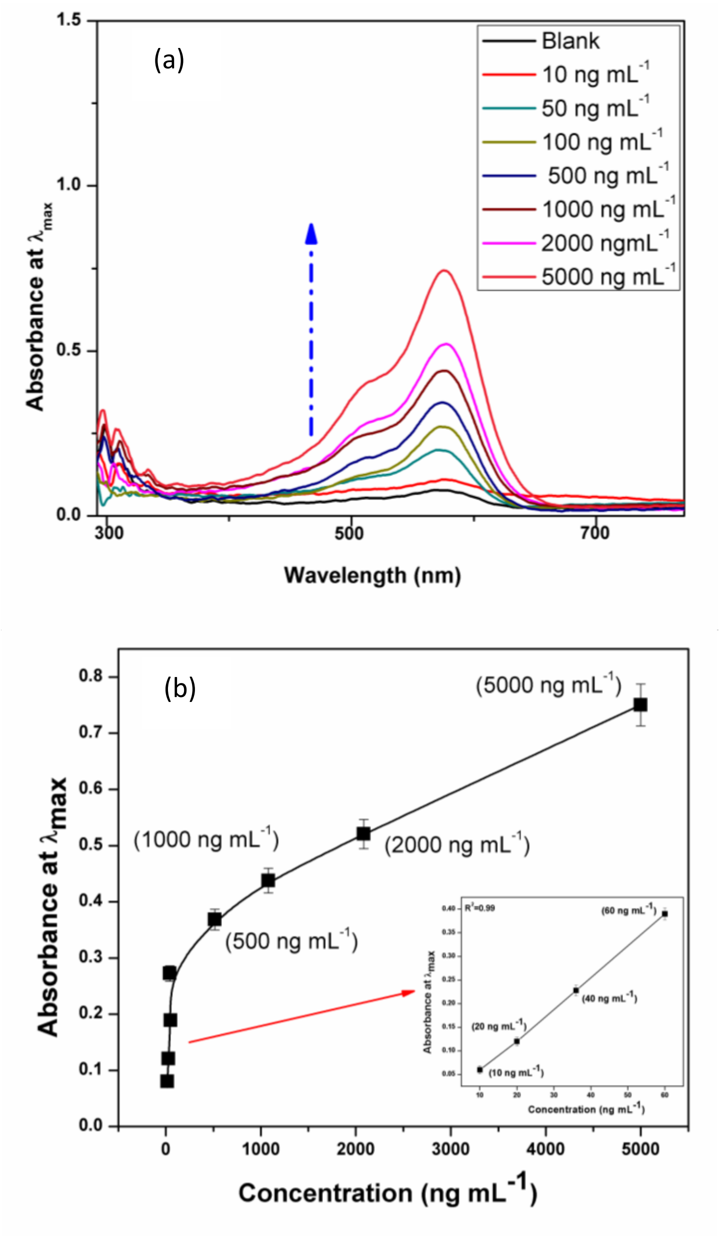

Fig 5.19 *Absorbance spectra of the optode for different concentrations of Hg(II) (10 ng mL^{-1} to 5000 ng mL^{-1} under the optimized conditions.)* ***(b)*** *Optode absorbance Vs concentration of Hg(II) plot ((10 ng mL^{-1} to 5000 ng mL^{-1})*

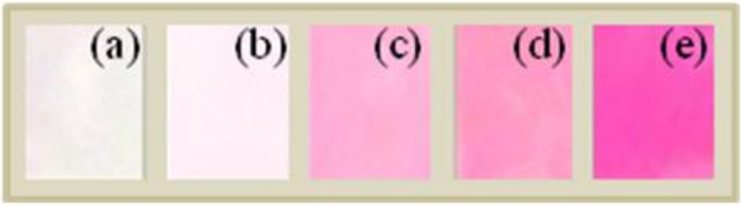

Fig. 5.20 *Change in the color of the optode with different concentration of Hg(II)* ***(a)*** *Blank ,* ***(b)*** *10 ng mL^{-1},* ***(c)*** *100 ng mL^{-1},* ***(d)*** *1000 ng mL^{-1} and* ***(e)*** *5000 ng m L^{-1}*

The fluorescence characteristics of the developed optode were also studied by carrying out the measurements at $\lambda_{exc/em}$ = 535/564 nm corresponding to maxima excitation and emission wavelengths (Fig. 5.21).

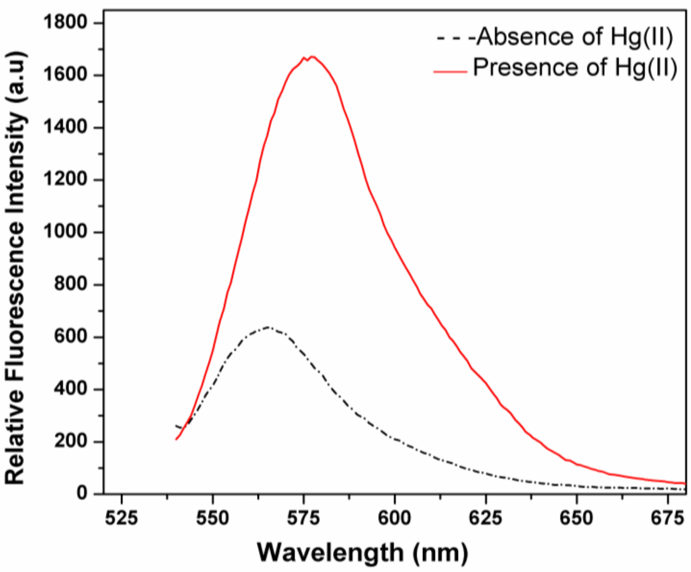

Fig. 5.21 *Comparison of change in the fluorescence spectrum of the optode sample equilibrated with solution having 10 ng mL^{-1} Hg(II) concentration (solid line) with respect to spectrum of a blank optode (broken line)*

It can be seen from Fig. 5.21 that there was a significant enhancement in relative fluorescence intensity of an optode film in the presence of 10 ng mL^{-1} of Hg(II) with respect to a blank. However, we have preferred absorbance method over fluorescence in our studies because of its simplicity in the measurement and amenability to use as an on-site sensor.

Selectivity of the optode

The aim of the present work is to develop an optode that is simple and useful for quick on-site determination of mercury ions in aqueous samples, especially ground water samples. Hence, the selectivity of the optode towards Hg(II) ions in the presence of a wide range of ions commonly found in such samples e.g. alkali or alkaline earth metal (Na^{+}, Ca^{2+}, $K^{+}$and Mg^{2+}) and other heavy metal ions (Cd^{2+}, Zn^{2+}, Cr^{3+}, Cu^{2+}, Fe^{2+}, Fe^{3+}, Pb^{2+} and Ni^{2+}) was investigated (Fig 5.22).

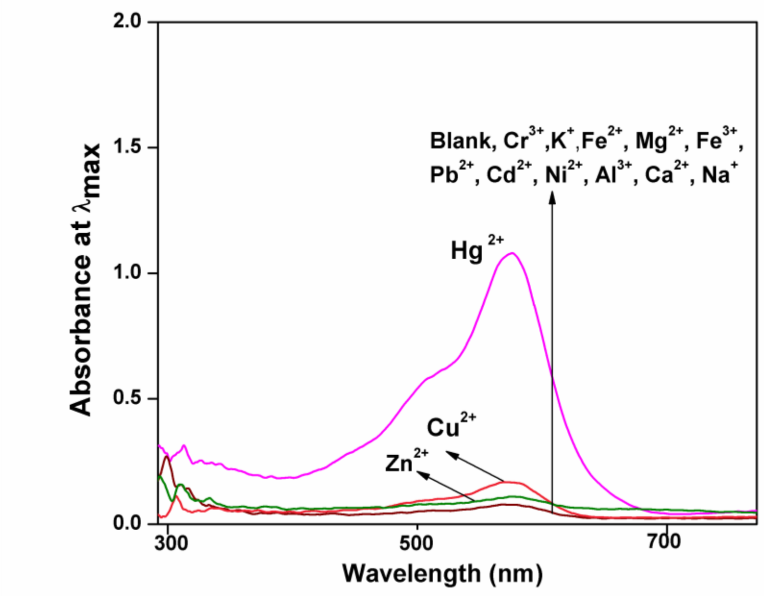

Fig 5.22 *Individual UV-Vis spectra of the optode sample in the presence of different metal ions (500,000 ng mL*$^{-1}$ *of each* Na^{+}, Ca^{2+}, K^{+}, Mg^{2+}, *1000 ng mL*$^{-1}$ *of each* Cd^{2+}, Cr^{3+}, Fe^{2+} , Fe^{3+}, Cu^{2+} , Pb^{2+} , Zn^{2+}, Al^{3+}, Ni^{2+}*) and Hg(II) (5000 ng mL*$^{-1}$*)*

The absorbance spectra are shown in Fig. 5.22 and it is clear that none of these ions except Cu^{2+} interferes with the Hg^{2+} absorbance signal. However, Cu^{2+} ions showed a weak absorbance signal. As there are no spectral interferences by the commonly occurring competiting ions except Cu^{2+}, the developed optode is highly selective for mercury detection and determination in the ground water samples.

Reproducibility and stability of optode

The reproducibility in the membrane synthesis was evaluated by comparing the absorbance values of the mercury optodes, synthesized in different batches. The relative standard deviation for the measured absorbance values at λ_{max} = 535 nm was 3.5% indicating a good reproducibility of the optode preparation. The stability of the synthesized optode was investigated by measuring the absorbance of the membrane as well as the equilibrating solution. No peak was observed for the solution which confirmed that the immobilized Rh6G-P derivative is quite stable in the plasticized matrix. The optode has a long shelf life as it can be stored for more than two months under ambient conditions.

5B.3.2 Analytical parameters of optode

The analytical response characteristics of the developed sensor are compared with other rhodamine based optodes reported in literature (Table 5.6). It can be clearly seen from the Table that the detection limit achieved using the optode synthesized in the present work is lower than that obtained by most of the solid state sensors based on rhodamine derivatives.

Table 5.6 *Comparison of the detection limits obtained in different molecular probes.*

Material	**Detection Limit**	**Reference**
Rh6G-P immobilized CTA optode	1.3 ng mL^{-1}	Present work
Rh 6G derivative incorporated P 30 polymeric membrane	60 ng mL^{-1}	476
Multifunctional mesoporous microspheres	10 ng mL^{-1}	477
Quantum dot SiO_2–rhodamine nanoparticles	0.52 ng mL^{-1}	478
Poly(ethyleneoxide)-b-poly(N-isopropylacrylamide-co-RhBHA) chemosensor	1.6 ng mL^{-1}	479

5B.4 Sensing mechanism of optode

The sensing element incorporated in the optode for selective Hg(II) determination is a phenyl-thiosemicarbazide rhodamine 6G derivative (Fig 5.14(c)). It exists in the spirocyclic form predominantly. Addition of mercuric ion leads to the spirolactam ring opening forming oxadiazole derivative followed by cyclization [476]. This results in the highly conjugated rhodamine system that causes development of pink color (Fig. 5.23(a)). Fig. 5.23 also shows the blank synthesized optode membrane (b) and the one equilibrated with Hg(II) solution having dark pink color (c).

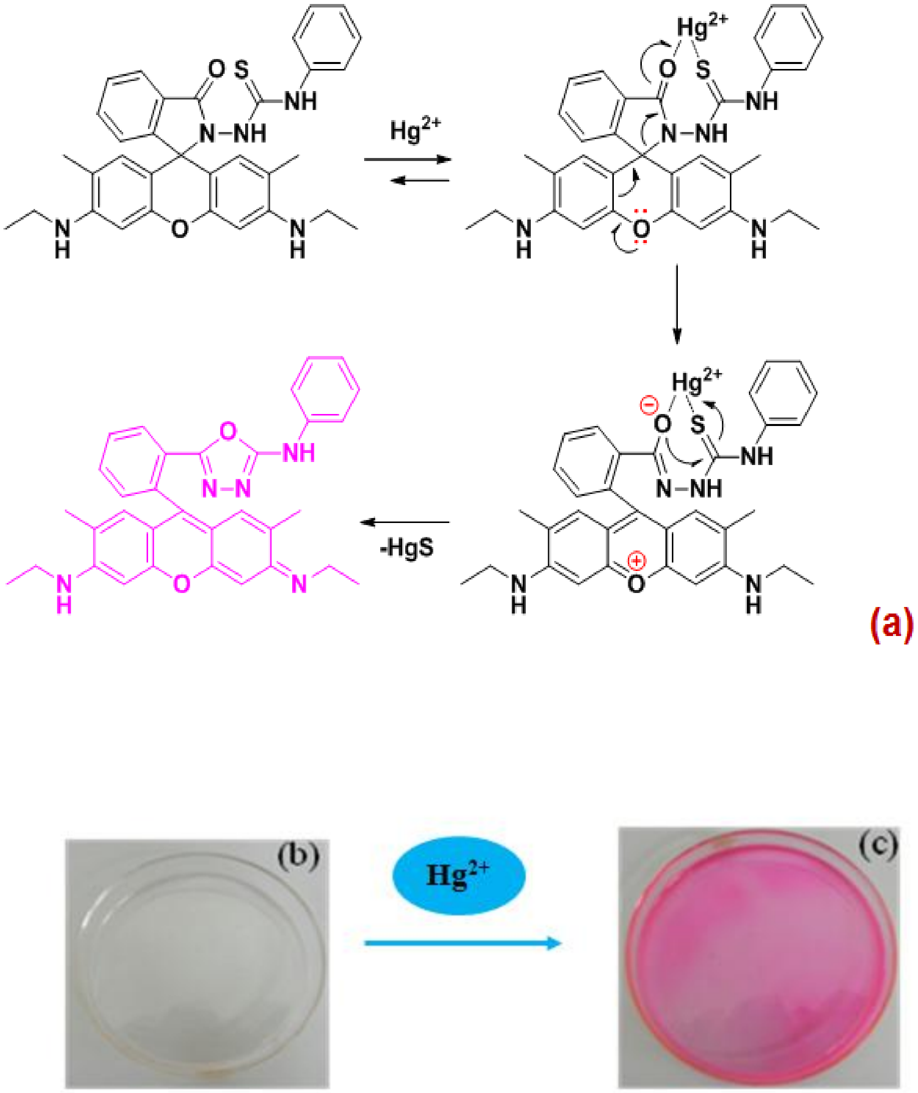

Fig. 5.23 ***(a)*** *Hg^{2+} recognition mechanism by the incorporated Rh6G-P derivative in the optode* ***(b)*** *Blank synthesized film and* ***(c)*** *Optode membrane equilibrated with Hg(II) solution*

5B.5 Application to real sample

The applicability of the developed optode was tested in groundwater samples collected from Thirumanglam area, Madurai, Tamilnadu. The samples were filtered through 0.45

μm filter paper prior to their analysis. Samples were spiked with three different concentrations of Hg(II) ions and were equilibrated with 2x1 cm^2 size membrane. The resultant absorbance of the optode was measured. The pH range of these samples was between 6.1-7.2 and hence they were used as such without pH adjustment. The results of the recovery studies in the solutions spiked with different concentrations of mercury are presented in Table 5.7.

Table 5.7 *Analysis of Hg(II) in groundwater samples collected from Madurai*

Sample	**Spiked Hg(II) Concentration (ng mL^{-1})**	**Hg(II) detected (ng mL^{-1})**	**Percentage recovery (%)**
GW-1	50	48.00 ± 0.68	96.0
GW-2	500	491.00± 0.21	98.2
GW-3	1000	996.00 ± 0.34	99.6

Values are presented as (mean ± 1s), n=5.

The recoveries were in the range of 96–100%. The relative standard deviations were within ± 2 % as shown in Table 5.7. Therefore, the developed optode can be used for the determination of Hg(II) ions in groundwater samples owing to its high selectivity and sensitivity.

5B.6 Conclusions

A highly selective and sensitive color changeable and fluorescent turn-on optode for Hg(II) detection in aqueous solution has been developed. The optode has been synthesized by the immobilizing a phneylthiosemicarbazide rhodamine 6G derivative in a cellulose triacetate plasticized support using room temperature solution casting method.

The developed optode changes its color from colorless to dark pink when equilibrated with Hg(II) solution. The intensity of the color increases linearly with Hg(II) concentration. The optode has good response characteristics with respect to its signal stability, reproducibility, selectivity. The detection limits of Hg(II) were found to be 10 ng mL^{-1} and 1.3 ng mL^{-1} from the naked-eye color change and absorption spectral change respectively.

Moreover, the developed optode could serve as a practical colorimetric sensor for on-site measurement of Hg(II) and does not require any additional equipment. The optode was selective for Hg(II) ions in presence of high concentration of commonly occurring cation. Therefore, the present optode can act as a highly efficient Hg^{2+} test kit in natural water samples. The efficacy of the developed optode has been demonstrated by analyzing groundwater samples.

Chapter -6

SUMMARY AND FUTURE SCOPE

6.1. Outcome of present work

Monitoring the quality of water and decontamination of water containing toxic elements, above permissible limits has been a subject of topical interest. Various analytical methods and methodologies for the monitoring and removal of ultra-trace concentration of toxic metal ions have been developed. The major limitation associated with highly sensitive analytical methods is because of the fact that they are lab based methods which are not amenable for on-site quantification. Similarly the sorbents developed so far have problem of desirable selectivity and applicability for environmental conditions. It is not desirable to alter the chemical conditions of natural waters. Most of the work till date is limited to synthesizing sorbents in form of polymeric beads and resins which can be easily applied for column applications in laboratory.

In the present thesis, the scope was limited to developing functionalized polymer sorbents for removal of fluoride, mercuric and boron from various aqueous streams. Different routes of functionalization of the sorbents were studied for tailoring the properties of existing polymers. For analytical applications, special emphasis was given for synthesizing the sorbents in form of polymer sheets having fixed binding sites and reproducible geometry. The microporous sheets used for anchoring the desired polymers via different polymerization routes were commercially available poly(propylene) membranes and in-house synthesized polymer inclusion membranes.

In-situ UV irradiation is one of the methods which has been used for in situ polymerizing the desired monomers in the pores of the selected host poly(propylene) substrate. This method of polymerization is amenable to synthesize matrix supported tailored polymer sheets for solid phase extraction of fluoride and mercuric ions from various aqueous streams. A new inorganic-organic hybrid polymer sorbents consisting of poly (bis[2-(methacryloyloxy)-ethyl]phosphate) crosslinked in the pores of two different types of substrates viz. fibrous and microporous (sheet) with varying morphology were prepared. These substrates were further conditioned for selective fluoride sorption by forming thorium complex with phosphate groups on bis[2-methacryloyloxy)-ethyl] phosphate (MEP). In order to test stability of the Th-complex in the sorbent, thorium leaching from the sorbents was studied in ground water and aqueous solutions with varying pH. ICP-MS analyses confirmed that there was no leaching of thorium from the sorbent in the treated aqueous samples. After confirming the non leachability of thorium in the sample solutions, these tailored sorbents were further studied for their selectivity towards fluoride in aqueous media having different chemical conditions. The fibrous sorbent was found to take up fluoride with a faster rate (15 min for ≈76% sorption) than the sheet sorbent. This clearly shows that the fluoride sorption characteristics varied with the physical architecture of poly(propylene) host substrates used for anchoring Th-poly(MEP). Comparison of the fluoride loading capacity with the reported sorbents showed that the loading capacity of sheet sorbent (4320 mg kg^{-1}) developed in this work was higher than many other sorbents reported in the literature.

The integrated process which couples magnetic separation together with surface complexation, adsorption, ion-exchange and solvent extraction is called as "Magnetically

Assisted Chemical Separation” (MACS). MACS has high potential for treating large volume of samples with faster rates. Therefore a fluoride ion selective magnetic sorbent has been synthesized by the encapsulation of Fe_3O_4 nanoparticles in a network of Zr(IV) complexed poly(acrylamide) (Zr–PAM).

This magnetic sorbent has been found to be efficient for the selective preconcentration of fluoride ions from natural waters. The Zr-PAM/ Fe_3O_4 composite developed in the present work retains the super paramagnetic properties of Fe_3O_4 nanoparticles, and the results reveal that the sorption is rapid. The composite has a considerably higher fluoride sorption capacity (124.5 mg g^{-1}) compared to other super-paramagnetic fluoride sorbents reported in the literature. ICP-MS analysis showed that there was no leaching of Zr(IV) ions from the sorbent in the treated aqueous samples indicating a strong chemical binding between the Zr(IV) ions and the functional groups of PAM. Since PAM is a neutral polymer, the positive charge on ZrO^{2+} ions provide binding sites for anions, particularly fluoride ions, which have a strong affinity towards Zr(IV). The water content of the synthesized composite was found to be 98 wt% suggesting that the composite has reasonably good hydrophilicity and free volume which are the properties required for sorption as the SEM images showed that the composite does not have a microporous structure. The saturation magnetization of 4.5 emu g^{-1} of the magnetic composite with 10 wt% Fe_3O_4, was high enough for magnetic separation to be carried out using external magnet.

Both the polymer sorbents developed in the present work for fluoride extraction were found to be reusable after desorption of fluoride using NaOH solution. The applicability of the sorbents was tested for selective removal of fluoride from water samples collected from Channu region of Punjab, India. The fluoride concentration left in the treated samples was found to be well below the permissible limit of WHO.

Using in-situ crosslinking of a preformed polymer, a sorbent selective for boron under seawater conditions was developed. The pores of a commercially available poly(propylene) membrane were functionalized by room temperature in situ crosslinking of poly(vinylbenzyl chloride) with a cyclic diamine piperazine. The precursor membranes were chemically modified with N-methyl D-glucamine (NMDG) which is selective for boron. The specific affinity between the vicinal diols of NMDG and the boric acid leads to formation of highly stable tetradentate complex. In addition to that the presence of an amine functional group helps in efficient chelating of boric acid by neutralizing the protons released in the formation of tetradentate complex during complexation thus leading to increase in boron uptake The maximum boron sorption capacity in form of boric acid determined experimentally was 28 mg g^{-1} outperforming most of the sorbents reported in literature in terms of the sorption capacity. The studies also showed that trace concentrations of boron were quantitatively removed from water at neutral pH. Therefore, it can be applied easily to seawater samples having pH 6-7 without varying its chemical parameters. Due to matrix elimination in the sorption process, the sorbent based preconcentration method was extended for its applicability in the determination of boron by widely used curcumin method of boron determination. The selective preconcentration of boron in the NMDG-sorbent followed by its desorption makes quantification feasible in the presence of nitrate. The results obtained using the developed method was also validated using ICPMS, and the results were found to be in a reasonably good agreement.

Two type of sheet sorbents has been synthesised for the preconcentration and determination of mercuric ions in aqueous solution. These are silver nanoparticles (AgNPs) embedded poly(acrylamide) grafted poly(propylene) sheet (Ag-PAM-PP) and 1,8-octanedithiol functionalized gold coated poly(propylene) sheet (HS-octyl-S-Au-PP). The functional groups acrylamide and thiol provided the binding sites for mercury ions; whereas the in-situ formed silver nanoparticles further enhanced the mercury sorption by reducing the mercuric ions to Hg^0 through the galvanic reaction. The reduced mercury was held on the sheet sorbent by amalgam formation. Various factors that influence the preconcentration of mercuric ions from aqueous solution have been investigated. Based on the comparison of the experimental results, it has been observed that, Ag-PAM-PP has showed 96% uptake compared to 64% by HS-Octyl-S-Au-PP sorbent. Therefore Ag-PAM-PP substrate was used as a template to preconcentrate and measure mercury in aqueous solution. Ag-PAM-PP had shown superior performance for Hg^{2+} uptake from the natural water samples in terms of other parameters such as sorption capacity, sorption kinetics and working pH range. The preconcentration of mercury ions from a large volume of aqueous solution was used to extend the lower limit of concentration range that can be quantified by the EDXRF and CVAAS. The sorbed Hg(II) from aqueous samples was quantitatively detected within 1 min using EDXRF. The LOD (3σ) for CV-AAS (RSD = 2%) and EDXRF (RSD = 5%) are 6 and 30 μg L^{-1}.

Preconcentration methods not only help in enhancing the detection limits of the method but also eliminate the spectral interference caused by undesirable components in the matrix. In this method the preconcentration of Hg^{2+} on polymeric sheets lowered the existing detection limits of EDXRF 100 fold as the poly(propylene) matrix of the base substrate being of low Z elements does not interfere with the determination of mercury which is a high Z element. The extremely low detection limits achieved by the developed methodology were further used for the determination of Hg^{2+} in the ground water and seawater samples in the presence of a high concentration of interfering ions. The results demonstrate the validity of these sorbents for the preconcentration of Hg^{2+} from the real sample solutions. It was observed that the preconcentration factor of 12 can be achieved in the 1x1 cm^2 Ag-PAM-PP sample which can further be enhanced by increasing the initial sample volume. The mechanism of mercury sorption is clearly expalined by taking into account its complexation with the amide groups of poly(acrylamide) grafted on poly(propylene) substrate and the galvanic reaction of Ag Nps (formed in situ by sodium borohydride reduction) with the sorbed Hg^{2+}.

A highly selective and sensitive color changeable optode for Hg(II) detection in aqueous solution has been developed by immobilizing a phneylthiosemicarbazide rhodamine 6G derivative in a cellulose triacetate plasticized support using room temperature solution casting method. The developed transparent film changes its color on interaction with mercuric ions which inturns facilitates the quantitative detection of mercury from aqueous matrices spectrophotometrically with a detection limit of 1.3 ng mL^{-1}. The high selectivity of the developed optode towards mercuric ions in presence of high concentration of commonly occurring cations in ground water samples can be further explored for its use as a colorimetric strip sensor for the on-site detection and determination of mercury.

6.2. Future scope

The tailored polymer sorbents developed for fluoride, boron and mercuric ions have high potential for the remediation as well as analytical applications. However, the remediation of the targeted ions from large volume samples has not been explored. This requires development of appropriate process scheme using suitable physical form of sorbent developed in the present work. It should be noted that the chemical architecture of the sorbent is responsible for the selective sorption of targeted ion. Therefore the functionalized sorbents developed in the present work with higher sorption capacities would lead to lower inventory of the sorbents. The better mechanical integrity and the ease of handling of the sheet sorbents can make the decontamination process more user-friendly and cost-effective technique and it does not suffer from the problems associated with other conventional methods. Using bulk polymerization, the same sorbents can also be made in the bead forms for using them in the ion-exchange columns. The functionalized sheet sorbents developed can be utilized for modifying the transport properties of the membranes and as a base material for developing the membrane based chemical sensors. The understanding of mechanism of incorporation of nanoparticles in a sheet would be useful for controlling the shape, size and spatial distribution of several metal nanoparticles in the polymer matrix. This study would also be useful for designing nanocomposite membranes for a desired application. The optode developed in the present work can be used for the on-site mercury detection by just a visual colour change. Similarly other sheet sorbents can be synthesised and further be explored as a base material for developing the membrane based analytical methods for other toxic ions.

REFERENCES

References

1. The Millennium Development Goals Report, United Nations, **2008.**
2. S. N. Kulshreshtha, *Water Resources Management.*, 1998, **12**, 167.
3. F.R. Rijsberman, *Agricultural Water Management.*, 2006, **80**, 5.
4. R. A. Lavoie, T. D. Jardine, M. M. Chumchal, K. A. Kidd and L. M. Campbell, *Environ. Sci.Technol.*, 2013, **47**, 13385.
5. V. Mudga, N. Madaan, A. Mudgal, R.B. Singh and S. Mishra, *The Open Nutraceuticals Journal.*, 2010, **3**, 94.
6. K. R. Fox, *Journal of Contemporary Water Research and Education.*, 2004, **129**, 18.
7. M.N. Murty and S. Kumar, India Infrastructure Report (2011).
8. R.L. Droste, Theory And Practice Of Water And Wastewater Treatment., John Wiley &Sons, New York (1997).
9. H.B. Bradl, Heavy Metals in the Environment: Origin, Interaction and Remediation., Elsevier: Amsterdam, The Netherlands, (2005).
10. K. Kadirvelu and C. Namasivayam, *Adv. Environ. Res.*, 2003, **7**, 471.
11. M. Kobya, E. Demirbas, E. Senturk and M. Ince, *Bioresource Technology.*, 2005, **96**, 1518.
12. J.E. Fergusson, The Heavy Elements: Chemistry, Environmental Impact and Health Effects., Pergamon Press: Exeter, UK (1990).
13. V. K. Garg, R. Kumar and R. Gupta, *Dyes and Pigments*, 2004, **62**, 1.
14. L. Wang, X.L. Wu, W. H. Xu, X.J. Huang, J.H. Liu and A.W. Xu, *Appl. Mater. Interfaces.*, 2012, **4**, 2686.

15. B. Gao, Y. Gao and Y. Li, *J. Chem. Eng.*, 2010, **158**, 542.
16. N. Zaitseva, V. Zaitsev and A. Walcarius, *J. Hazard. Mater.*, 2013, **250-251**, 454.
17. E.B Simsek, D. Duranoglu and U. Beker, *Sep. Sci. Technol.*, 2012, **47**, 1334.
18. P.S Suchithra, L. Vazhayal, A.P. Mohamed and S. Ananthakumar, *J. Chem. Eng.* 2012., **200**, 589.
19. E. Repo, J.K. Warchoł, A. Bhatnagar and M Sillanpaa, *J. Colloid Interface Sci.*, 2011, **358**, 261.
20. P Ge, F. Li, and B. Zhang, *Pol. J. Environ. Stud.*, 2010, **19**, 301.
21. Y. Pang, G. Zeng, L. Tang, Y. Zhang, Y. Liu, X. Lei, Z. Li, J. Zhang and G. Xie, *Desalination.*, 2011, ***281***, 278.
22. L. Wang, J. Zhang, and A. Wang, *Desalination.*, 2011, **266,** 33.
23. L. Mercier and T.J. Pinnavaia, *Environ. Sci. Technol.*, 1998, **32,** 2749.
24. A. Walcarius, *Chem. Mater.*, 2001, **13**, 3351.
25. D. G. Kim, H. Kang, S. Han, and J.C. Lee, *Appl. Mater. Interfaces.*, 2012, **4,** 5898.
26. G. Paun, E. Neagu, A. Tache, G.L. Radu and V. Parvulescu, *Chem. Biochem. Eng. Quart.*, 2011, **25,** 453.
27. X.F. Wen, K. Wang, P.H. Pi, J.X.Yang, Z.Q. Cai, L.J. Zhang, Y. Qian, Z.R. Yang, D.F. Zheng, and J. Cheng, *Appl. Surf. Sci.*, 2011, **258,** 991.
28. B.J. Sparks, E.F. Hoff, L. Xiong, J.T. Goetz and D.L. Patton , *Appl. Mater. Interfaces.*, 2013, **5**, 1811
29. Y.Y. Yu, and E.C. Chen, *Mater. Chem. Phys.*, 2003, **82**, 388.

30. S. Nagappan, M.C. Choi, G. Sung, S.S. Park, M.S, Moorthy, S.W. Chu, W.K. Lee and C.S. Ha, *Macromol. Res.*, 2013, **21**, 669.
31. C. Rottman, G. Grader, Y. de Hazan, S. Melchior, and D. Avnir, *J. Am. Chem. Soc.* 1999., **121**, 8533.
32. J.D. Date, L. Moet, J.A. Koster, B. de Boer and P.W.M. Blom, *Chem. Mater.*, 2007, **19**, 5856.
33. M. He, F. Qiu, and Z. Lin, *J. Phys. Chem. Lett.*, 2013, **4**, 1788.
34. F.L. Souza, P.R. Bueno, E. Longo and E.R. Leite, *Solid State Ion.*, 2004, **66**, 83.
35. C.F. Lee, D.A. Leigh, R.G. Pritchard, D. Schultz, S.J. Teat, G.A. Timco, and R.E.P. Winpenny, *Nature.*, 2009, **458**, 314.
36. A. Singh, N.P. Singh, R.A. Singh, *Bull. Mater. Sci.*, 2011, **34**, 1017.
37. D.J Collins and H.C. Zhou, *J. Mater. Chem.*, 2007, **17**, 3154.
38. J.L.C Rowsell, A.R Millward, K.S Park and O.M. Yaghi, *J. Am. Chem. Soc.*, 2004, **126**, 5666.
39. G. Raj, C. Swalus, A. Guillet, M. Devillers, B. Nysten and E.M. Gaigneaux, *Langmuir.*, 2013, **29**, 4388.
40. G. Fu, X.Yue, and Z. Dai, *Biosens. Bioelectron.*, 2011, ***26***, 3973.
41. G.H. Gwak, S.M. Paek and J.M.Oh, *Eur. J. Inorg. Chem.*, 2012, **56**, 5269.
42. T.P. Chou, C. Chandrasekaran and G.Z. Cao, *Journal of Sol-Gel Science and Technology.*, 2003, **26,** 321.
43. Y. A. Zolotov, G.I. Malofeeva, O.M. Petrukhin and A.R. Timerbaev, *Pure & Appl. Chem.*, 1987, **59(4)**, 497.

44. L. Yurloval, A. Kryvoruchko and B. Kornilovich, *Desalination*, 2002, **144**, 255.

45. L.F. Greenlee, D.F. Lawler, B.D. Freeman, B. Marrot and P. Moulin, *Water Res.*, 2009, **43,** 2317.

46. Y. Benit and M.L. Ruiz*, Desalination.,* 2002, **142,** 229.

47. M.G. Sujana, R.S. Thakur and S.B. Rao, *J. Colloid Interface Sci*., 1998, **206,** 94.

48. S. Ayoob, A.K. Gupta and V.T. Bhat, *Crit. Rev. Environ. Sci. Technol*., 2008, **38**, 401.

49. S. Meenakshi and R.C. Maheshwari, *J. Hazard*. *Mater*., 2006, **137**, 456.

50. B.V.Apparao, S. Meenakshi and G. Karthikayan, *Indian J. Environ. Prot.*, 1998, **10**, 292.

51. S M Rao and P Mamatha, *Current Science.*, 2004, **87**, 942.

52. S Vignehwaran and C Visavanathan, Water Treatement processes: Simple options (CRC, Press, New York) (1995).

53. M F Yang and J. C. Liu, *J. Environ Eng*., 2007, **133**, 419.

54. J Y Park, H J Byun, W H Choi and W H Kang, *Chemosphere.*, 2008, **70**, 1429.

55. T Majima and H Takaskuti, *Water Purif Liq Wastes Treatment.*, 1987, **28**, 433.

56. L.S. McNeill and M. Edwards, *J. American Water Works Assoc.*, 1997, **89**, 75.

57. A. Yilmaz, R. Erdem, M. Boncukcuoglu, and M. Kocakerim, *J. Hazard. Mater.*, 2007, 149, 475.

58. P. Remy, H. Muhr, and I. Ouerdiane. *Environmental Progress.*, 2005, **24**, 105

59. Turek, Marian, D. Piotr, J. Trojanowska, and A. Campen, *Desalination* ., 2006,

205, 192.

60. Garcia-Soto, M. D. M. de la Fuente, and E. M. Camacho, *Sep. Pur. Technol* , 2006, **48**, 36
61. Kitano, Yasushi, M. Okumura, and M. Idogaki, *Geochemical Journal*, 1978., **12**, 183
62. A. Shafeeq, A. Muhammad, W. Sarfraz, A. Toqeer, S. Rashid, and M. K. Rafiq, *Engineering and Technology*., 2012, **6**, 1259.
63. S. J. Lee, Y.C Seo, J. Jurng and T. G. Lee, *Atmospheric Environment*, 2004, **38**, 4887.
64. Yu. A. Zolotov and N. M. Kuzmin, “Preconcentration of trace elements”, Elsevier, Amsterdam (1990)
65. W. Franklin Smyth, “Analytical Chemistry of Complex Matrices”, Wiley Tubner, New York, (1999).
66. E. Jackwerth, A. Mizuike, Y. A. Zolotov, H. Berndt, R. Hohn and N. M. Kuzmin, *Pure & Appl. Chem*., 1979, **51**, 1195.
67. M. Yumono and S. Ebd, *Arch. Pharm. Med. Chem*., 1997, **330**, 348.
68. C. Pham Huy, F. Nadji, MI. Postura and M. Norman, *Annales pharmaceutiques francaises.*, 1991, **49(3),** 139.
69. B. Tural, S Tural and H Hosgoren, *Turk J Chem* ., 2007, **31**, 163.
70. I Tsuboi, E Kunugita and I Komasawa, *J Chem Eng Japan.*, 1990, **23**, 480.
71. A Poslu Kena and L W Dudeney, *Hydrometallurgy.*, 1983, **10**, 47.
72. T Kwon, M Hirata, T Hano and T Yamagishi, *Sep. Sci. and Tech.*, 2005,**40**, 1415.

73. T Kwon, M Hirata, T Hano and T Yamagishi, *Solvent Extraction and Ion Exch.*, 2005, **40**, 391.
74. M Karakaplan, S Tural, B Tural, Y Turgut and H Hogoren, *Solvent Extraction and Ion Exch.*, 2004, **22**, 897 .
75. Advanced Organic Chemistry, Reactions & Mechanisms and Structures, 4th edition, John Wiley & Sons, N.Y. (1992).
76. Y. Baba, Y. Umezaki and K. Inoue, *Solvent Extraction and Ion Exch* 1986,**19**, 27.
77. R. Singh and S. N. Tandon, *Talanta, 1997,* **44**, 843.
78. M. L. P. Reddy, A. D. Damodaran and M. C. S. Reddy, *Radiochim. Acta,* 1997, **76**, 109.
79. R. Sahu, S. M. Sondhi and B. Gupta, *J Radioanal. Nucl. Chem.,1995,* **200(6),** 509.
80. M. L. P. Reddy, S. Sujatha, T. R. Ramamohan, T. Prasada Rao, C. S. P. Iyer and A. D. Damodaran, *Radiochim. Acta.,1995,* **69**, 201.
81. K. Inoue, R. Yasukawa, N. Miura, Y. Baba and K. Yoshizuka, *Solvent Extraction and Ion Exch.*, 1992, **10(5),** 769.
82. T. F. Baumann, 1. G. Reynolds and G. A. Fox, *React. Funct. Polym.*,2000, **44(2),** 111.
83. T.F. Baumann, J. G. Reynolds and G. A. Fox, *Chem. Eng. News.,* 1998, **76(3),** 37.
84. T. F. Baumann, J. G. Reynolds and G. A. Fox, *Chem. Commun.,* 1998, **16**, 1637.
85. T. Sato, J. Ishikawa and K Sato, *Process Metallurgy.,* 1992, **7A**, 913.
86. T. Sato, S. Ikoma and T. Nakamura, *Hydrometallurgy.*, 1980, **6**, 13.

87. K N. Brewer, R. S. Herbst, 1. Y. Glagolenko and T. A. Todd, *Solvent Extraction and Ion Exch.*, 1998, **16(2)**, 487.
88. A. T. Yordanov, 1. T. Mague and D. M. Roundhill, *Inorg. Chem.*, 1995, **34**, 5084.
89. A. T. Yordanov, O. M. Falana, H. F. Koch and D. M. Roundhill, *Inorg. Chem., 1997,* **36**, 6468.
90. G. G. Talanova, H. S. Hwang, V. S. Talanov and R. A. Bartsch, *Chem. Commun., 1998,***8,**1329.
91. P. Rao, O. Enger., E. Graf, M. W. Hosseini, A. D. Cian and l.Fischer, *European J lnorg. Chem., 2000,* **7**, 1503.
92. M. K. Rao and M. Metre , *International Journal of Science and Research.*, 2014, **3**, 2319.
93. R.H. McKee and W.S. Jhonston, *Industrial Engineering Chemistry*., 1934, **26 (8),** 849.
94. H.S. Parmar, J.B. Patel, P. Sudhakar and V.J. Koshy, *J. Environ. Sci. Eng.*, 2006, **48**,135.
95. D. Mohan, K.P. Singh and V.K. Singh, *J. Hazard. Mater*. 2008, **152**, 1045.
96. R. Sivabalan, S. Rengaraj, B. Arabindoo and V. Murugesan, *Indian J. Chem. Technol*. 2003, **10**, 217.
97. R.S. Sathish, N.S.R. Raju, G.S. Raju, G.N. Rao, K.A. Kumar and C. Janardhana, *Sep. Sci. Technol*. 2007, **42**, 769.
98. R.S. Sathish, S. Sairam, V.G. Raja, G.N. Rao and C. Janardhana, *Sep. Sci. Technol.*, 2008, **43**, 3676.

99. G. Alagumuthu and M. Rajan, *J. Chem. Eng.* 2010, **158**, 451.

100. A.K. Chaturvedi, K.P. Yadava, K.C. Pathak and V.N. Singh, *Water Air Soil Pollut*. 1990, **49**, 51.

101. W. Nigussie, F. Zewge and B.S. Chandravanshi, *J. Hazard. Mater.,* 2007,**147**, 954.

102. Y. C. Engeloglu, E. Kir and M. Ersoz, *Sep. Purif. Technol*., 2002, **28**, 81.

103. A. Tor, N. Danaoglu, G. Arslan and Y. Cengeloglu, *J. Hazard. Mater,* 2009, **164**, 271.

104. V.K. Gupta, I. Ali and V.K. Saini, *Water Res.,* 2007, **41**, 3307.

105. A. C. Iinarli, O. Bic. Er and M. Mahramanlio glu, *Fresenius Environ. Bull*., 2005, **14**, 520.

106. B. Kemer, D. Ozdes, A. Gundogdu, V.N. Bulut, C. Duran and M. Soylak, *J. Hazard. Mater.*, 2009, **168**, 888.

107. C. Venkobachar , L. Iyengar L and A. Mudgal, *Proceedings of the 2nd international workshop on fluorosis and defluoridation of water*, International Society for Fluoride Research (1997).

108. R. Mckee and W.S. Johnston, *Ind. J. Environ. Health.*, 1999, **41**, 53.

109. R.E. Benson, D. L. Porth, and O.R. Seency, *Chemical Abstracts.*, 1940, **30**, 179.

110. R.J. Myers, and D.S. Herr, *Chemical Abstracts.*, 1945, **39**, 4417.

111. K. Venkataramanan, N. Krishnaswamy and Ramakrishna, *Indian Journal of Medical Research.*, 951, **39**, 57.

112. S. Meenakshi and N. Viswanathan, *J. Colloid Interface Sci.,* 2007, **308**, 438.

113. M. Safarikova and I. Safarik, *J Magn Mater,* 1999., **194**, 108.

114. P. Xu, G. M. Zeng and D. L. Huang, *Science of the Total Environment*, 2012, **424**, 1.

115. C. L. Warner, W. Chouyyok and K. E. Mackie, *Langmuir.,*2012, **28**, 3931.

116. A. E. Karatapanis, D. E. Petrakis, and C. D. Stalikas, *Anal. Chim. Acta* 2012, **726**, 22.

117. H. Yang, Z. Tian, J. Wang, and S. Yang, *Sensors and Actuators B.*, 2012, **161**, 429.

118. A. S. Teja and P. Y. Koh, *Progress in Crystal Growth and Characterization of Materials.*, 2009, **5**, 22.

119. Z. Liu, H. Wang and C. Liu, *Chem. Commun.*, 2012, **48**, 7350.

120. J. K. Oh and J. M. Park, *Progress in Polymer Science.*, 2011, **36**, 1168.

121. S. Laurent, D. Forge and M. Port, *Chemical Reviews*, 2008, **108**, 2064.

122. Y. Li, Y. Hu, G. Huang, and C. Li, *Particuology.*, 2013, **11**, 460.

123. R. W. Saunders and J. M. C. Plane, *Journal of Aerosol Science.*, 2010, **41**, 475.

124. C. F. Chang, C. Y. Chang and T. L. Hsu, *Desalination.*, 2011, **279**, 375.

125. B.Z. Can, Z. Ceylan and M.M. Kocakerim, *Desalin. Water Treat*. 2012., **40**, 69.

126. Y. Inukai, Y. Tanaka, T. Matsuda, N. Mihara, K. Yamada, N. Nambu, O. Itoh, T. Doi, Y. Kaida and S.Yasuda, *Anal. Chim. Acta.,* 2004, **511**, 261.

127. A. Sabarudin, K. Oshita, M. Oshima and S. Motomizu, *Talanta.,* 2005, **66,** 136.

128. M. Bryjak, A. Koltuniewicz and A. Trochimczuk, Report for NATO science programme, Development of an Innovative Treatment Process for Geothermal Wastewater, (2004).
129. K. Sasaki, H. Takamori, S. Mariyama, H. Yoshizaka and T. Hirajima, *J. Hazard. Mater.*, 2011,**185**, 1140.
130. M.M. de la Fuente García-Soto and E. Munoz Camacho, *Desalination*, 2009, **249**, 626.
131. I. Kipcak and M. Ozdemir, *Chem. Eng. J.*, 2012, **190**, 68.
132. Ch. Irawan, J.C. Liu and Ch. Wu, *Desalination*, 2011, **276**, 322.
133. Y.T. Wei, Y.M. Zheng and J.P. Chen, *Water Res.*, 2011, **45 ,** 2297.
134. N. Bicak, N. Bulutcu, B.F. Senkal and M. Gazi, *React. Funct. Polym.*, 2001,**47**, 175.
135. A. Dresche, R. Kucharowski, W. Kluge and T. Schwarz, *Anal. Chim. Acta.*, 1989, **219** , 273.
136. N. Geffen, R. Semiat, M. Eisen, Y. Balasz, I. Katz and C. Dosorets, *J. Membrane Sci.*, 2006, **286**, 45.
137. M. Bryjak, J. Wolska and N. Kabay, *Desalination.*, 2008, **223**, 57.
138. N. Hilal, G.J. Kim and C. Somerfield, *Desalination.*, 2011**, 273**, 23.
139. H. Yavuz Ersan and S. Piranbasi, *J. Appl. Polym. Sci.*, 2011, **121**, 1610.
140. B.F. Senkal and N. Bicak, *React. Funct. Polym*. 2003, **55**, 27.
141. R.M. Roberts, *Ind. Eng. Chem. Prod. Res. Dev.*, 1971, **10**, 356.

142. S.V. Krishnan, B.K. Gullett, and W. Jozewicz, *Environ. Sci. Technol.*, 1994, **28(8),** 1506.

143. M. Steijns, A. Peppelenbos and P. Mars, *J. Colloid Interface Sci.*, 1976, **57(1)**, 181.

144. J.A. Korpiel, and R. D.Vidic, *Environ. Sci. Technol.*, 1997, **31(8),** 2319.

145. W. Liu, R.D. Vidic, R. D., and T.D. Brown, *Environ. Sci. Technol.*, 1998, **32(4),** 531.

146. W. Shaban, Al Rmalli, A. A. Dahmani, Abuein M Mohammed and A. A. Galiza, *J. Hazard. Mater.*, 2008, **152**, 955.

147. J.Z. Chen, X.C. Tao, J. Xu, T. Zhang and Z.L. Lin, *Process Biochem*. 2005, **40**, 3675.

148. V. Dushenkov, P.B.A.N. Kumar, H. Motto and I. Raskin, *Environ. Sci. Technol*. 1995, **29**, 1239.

149. D. Karunasagar, M.V. Balatama, S.V. Rao and J. Arunachalam, *J. Hazard. Mater.*, 2005, **118**,133.

150. M.J. Ahmed and Md.S. Alam, *Spectroscopy*, 2003, **17**, 45.

151. C. Green-Ruiz, *Bioresour. Technol*., 2005, **97**, 1907.

152. J. M. Randall, R. L. Bermann , V. Garrett and A.C. Waiss Jr., *Forest Prod*., 1974, **24(9),** 80.

153. G. Vaazquez., G. Antorrena., J. Gonzaa lez and M.D. Doval, *Bioresource Technol*., 1994, **48**,251.

154. C. M. Jr. Flynn., T.G. Carnahan and R. E. Lindstrom , Report of Investigations # 8427. United States Bureau of Mines (1980).

155. M. Grover and M. S. Narayanaswamy, *J. Inst. Eng. (India) Environ.*, 1982, **63**, 36.

156. R. A. Gri., R. R. Frost., A.K. Au, G.D. Robinson G. D. and N. F Shrimp, *Environ. Geol. Note.*, 1977, **79**, 1.

157. E.J. Roberts and S.P. Rowland , *Envir. Sci. Technol*. 1973, 7,552.

158. M.S. Masri , F.W. Reuter and M. Friedman , *J. Appl. Polymer Sci*., 1974, **18**, 675.

159. P. Mire Izky, A.F. Cirelli, *J. hazard. Mater.*, 2009, **167**, 10.

160. S. Loeb and S. Sourirajan, *Advances in Chemistry.*, 1963, **28,** 117.

161. J.M.S. Henis and M.K. Tripodi, *Sep. Sci. Techol.*, 1980, **15**, 1059.

162. P.I. Ndiaye, P. Moulin, L. Dominguez, J.C. Millet and F. Charbit, *Desalination.,* 2005, **173**, 25.

163. L. Paugam, C.K. Diawara, J.P. Schlumpf, P. Jaouen and F. Quemeneur, *Sep. Purif. Technol*., 2004, **40**, 237.

164. M. Hichour, F. Persin,, J. Molenat, J. Sandeaux and C. Gavach, *Desalination.*, 1999, **122**, 53.

165. K. Hu and J.M. Dickson, *J. Membr. Sci.*, 2006, **279**, 529.

166. M. Hichour, F. Persin, J. Sandeaux and C. Gavach, *Sep. Purif. Technol.*, 2000, **18**, 1.

167. S. Bason, A. Ben-David, Y. Oren and V. Freger, *Desalination*, 2006, **199**, 31.

168. A. Szymczyk and P. Fievet, *J. Membr. Sci.*, 2005, **252**, 77.

169. X. Lefebvre and J. Palmeri, *J. Phys. Chem. B.,* 2005, **109**, 5525.

170. X. Lefebvre, J. Palmeri, and P. David, *J. Phys. Chem. B.,* 2004, **108**, 16811.

171. J. Palmeri, P. Blanc, A. Larbot and P. David, *J. Membr. Sci.,* 1999, **160,** 141.

172. J. Cervera, V. Garcia-Morales and J. Pellicer, *J. Phys.Chem. B.,* 2003, **107,** 8300.

173. F. Durmaz, H. Kara, Y. Cengeloglu and M. Ersoz, *Desalination*, 2005, **177**, 51.

174. N. Kabay, O. Ara, S. Samatya, Yu. U. Yuksel and M. Yuksel, *J. Hazard. Mater.,* 2008, **153,** 107.

175. S. Annouar, M. Mountadar, A. Soufiane, A. Elmidaoui, M. A. Sahli, M.A. and A. Menkouchi, *Desalination,* 2004, **165**, 437.

176. M. A. Sahli, A. Annouar, S. Tahaikt, M. Mountadar, A. Soufiane, and A. Elmidaoui, *Desalination*, 2007, **212**, 37.

177. P. Glueckstern and M. Priel, *Desalination*, 2007, **205**, 178.

178. C. Jacob, *Desalination.* , 2007, **205** , 47.

179. B.L. Rivas, E.D. Pereira, M. Palencia and J. Sanchez, *Prog. Polym. Sci*., 2011, **36,**294.

180. B.L. Rivas, E.D. Pereira and I. Moreno-Villoslada, *Prog. Polym. Sci.,* 2003, **28,** 173.

181. B.F. Smith, T.W. Robison, B.J. Carlson, A. Labouriau, G.R.K. Khalsa, N.C. Schroeder, G.D. Jarvinen, C.R. Lubeck, S.L. Folkert and D.I. Aguino, *J. Appl. Polym. Sci.*, 2005, **97**, 1590.

182. C. Dilek, H.O. Ozbelge, N. Bicak and L. Yilmaz, *Sep. Sci. Technol.*, 2002, **37**, 1257.

183. B.M. Smith, P. Todd and C.N. Bowman, *Sep. Sci. Technol*., 1999, **34**, 1925.

184. C.O. Doganay, H.O. Ozbelge, L. Yilmaz and N. Bicak, *Desalination*, 2006, **200**, 286.

185. C.O. Doganay, H.O. Ozbelge, N. Bicak, N. Aydogan and L. Yilmaz, *Sep. Sci. Technol*., 2011, **46**, 581.

186. A. A. Burbano, S. S. Adham and W. R. Pearce, *J. Am. Water Works Assoc.*, 2007, **99,** 116.

187. H. W. Liang, X. Cao, W. J. Zhang, H. T. Lin, F. Zhou, L. F. Chen and S. H. Yu, *Adv. Funct. Mater*, 2011, **21**, 3851.

188. J. Yuan, X. Liu, O. Akbulut, J. Hu, S. L. Suib, J. Kong and F. Stellacci, *Nat. Nanotechnol.*, 2008**, 3,** 332.

189. X. Zhang, T. Zhang, J. Ng and D. D. Sun, *Adv. Funct. Mater*., 2009, **19,** 3731.

190. M. Sugiura, M. Kikkawa and S. Urita, *Sep. Sci. Technol.*, 1987, **22** , 2263.

191. J.S. Kim, S.K. Kim, J.W. Ko, E.T. Kim, S.H. Yu, M.H. Cho, S.G. Kwon, and E.H. Lee, *Talanta.*, 2000, **52,** 1143.

192. J.S. Kim, S.K. Kim, M.H. Cho, S.H. Lee, J.Y. Kim, S. G. Kwon, and E. H. Lee, *Bull. Korean Chem. Soc*., 2001, **22,** 10760.

193. A.M. Sastre, A. Kumar, J.P. Shukla and R.K. Singh, *Sep. Purif. Methods*, 1998, **27**, 213.

194. A.J. Schow, R.T. Peterson and J.D. Lamb, *J. Membr. Sci.*, 1996, **111**, 291.

195. R. T. Peterson, J.D. Lamb, Bartsch, J D.Way (Eds.), ACS Symposium Series 642, American Chemical Society, Washington (1996)

196. J C Aguilar, M Sanchez-Castellanos, S.M.E. Rodriguez and J De Gyves, *J. Membr. Sci.*, 2001, **190**, 107.

197. D.T. Newcombe, T. J. Cardwell, R. W. Cattrall and Spas D. Kolev, *Laboratory Robotics and Automation.*, 2000, **12**, 200.

198. M. Lerchi, E. Bakker, B. Rusterholz, and W. Simon, *Anal.Chem.*, 1992, **64**, 1534.

199. K. Wang, K. Seiler, B. Rusterholz, and W. Simon, *The Analyst*, 1992, **117**, 57.

200. G. R. Amiet, J. R. Farrell, P. J. Iles, and T. J. Sands, *Australian Journal of Chemistry.*, 2001, **54**, 27.

201. C. Sanchez-Pedreno, M. S. Garcia, J. A. Ortuno, M. I. Albero and E. Ballester, *J. Anal. Chem.*, 2001, **369**, 680.

202. A. Safavi and M. Sadeghi, *Anal. Chim. Acta.*, 2006, **567**, 184.

203. M. Shamsipur, T. Poursaberi, A. Avanes, and H. Sharghi, *Spectrochimica Acta. Part A,*, 2006, **63**, 43.

204. A.M. Stervin and T. Prasad Rao, *Talanta*, 2004, **63**, 225.

205. J. Remacle and B. Volesky, CRC Press, Boca Raton, FL, 1990, 83.

206. K.H.J. Buschow and F.R. de Boer. Physics of Magnetism and Magnetic Materials. Kluwer Academic/Plenum Publishers, (2003).

207. L. Michalowsky, Magnettechnik, Fachbuchverlag Leipzig, (1993).

208. P.R. Haddad, P.E. Jackson , *Journal of Chromatography Library*, 1990, **46,** 1.

209. P.M. Cummins, O. Dowling, B.F. O'Connor, Ion-Exchange Chromatography: Basic Principles and Application to the Partial Purification of Soluble Mammalian Prolyl Oligopeptides. In: Walls D Loughran ST. (ed.) Protein Chromatography Methods and Protocols. New York: Springer., (2011).

210. GE Healthcare, Ion Exchange Chromatography & Chromatofocusing: Principles and Methods Handbook.

211. K.E.Jarvis, A.L. Gray, R.S. Houk, " Handbook of Inductively couples Mass Spectrometry", Blabkie., Chapman and Hall: Glasgow., New York, (1992).

212. Monstar, Inductively couples Mass Spectrometry", Wiley-VCH, New York, (1997).

213. F. C. Wu, R. L. Tseng and R. S. Juang, *J. Chem. Eng.*, 2009, **150**, 366.

214. J. Febrianto, A. N. Kosasih, J. Sunarso, Y. H. Ju, N. Indraswati and S. Ismadji, *J. Hazard. Mater.*, 2009, **162**, 616.

215. G. McKay, Y. S. Ho and J. C. Y. Ng, *Separation and Purification Methods*, 1999,**28**, 87.

216. W. Plazinski, W. Rudzinski and A. Plazinska, *Advances in Colloid and Interface Science*, 2009, **152**, 2.

217. Y. S. Ho, *Water Research.*, 2006, **40**, 119.

218. Y. S. Ho and G. McKay, *Water Research.*, 2000, **34**, 735.

219. S. Sen Gupta and K. G. Bhattacharyya, *Advances in Colloid and Interface Science*, 2011, **162**, 39.

220. V. K. Tyagi and S. L. Lo, *Renew. Sust. Energy. Reviews.*, 2013, 25, 708.

221. M. Tiemann, *Congressional Research Service*, www.crs.gov, 1.

222. F. Shen, X. Chen, P. Gao and G. Chen, *Chem. Eng. Sci.*, 2003, **58**, 987.

223. G. de la Puente, J.J. Pis, J.A. Menéndez and P. Grange, *J. Anal. Appl. Pyrolysis.*, 1997, 43,125.

224. A. Bhatnagar, E. Kumar and M. Sillanpaa, *Chem. Eng. J.*, 2011, **171**, 811.

225. W.H.O., Guidelines for Drinking Water Quality, Geneva, (2004).

226. C.B. Dissanayake, *Int. J. Environ. Stud,*. 1991, **19**, 195.

227. M. Islam and R.K. Patel, *Chem. Eng. J.*, 2011, **169**, 68.

228. http://www.fluoridealert.org/health/.

229. N.J. Chinoy, *Indian J. Environ. Toxicol.*, 1991, **1**, 17.

230. P.T.C. Harrison, *J. Fluorine Chem.*, 2005, **126,** 1448.

231. W.B. Apambire, D.R. Boyle and F.A. Michel, *Environ. Geochem.*, 1997, **33**, 13.

232. N.B. Reddy and K.S.S. Prasad, *Indian J. Environ. Health* 2003., **45**, 285.

233. F. Diaz-Barriga, A. Navarro-Quezada, M. Grijalva, M. Grimaldo, J.P. Loyola-Rodriguez and M.D. Ortiz, *Fluoride.*, 1997, **30,** 233.

234. E. Kruse and J. Ainchil, *Argentina Environ. Geol,*. 2003, **44**, 86.

235. WRC, Distribution of fluoride-rich groundwater in Eastern and Mogwas region of Northern and North-west province, WRC Report No. 526/1/01 Pretoria,

(2001).

236. N. Azbar and A. Turkman, *Water Sci. Technol.*, 2000, **42,** 403.
237. M. Agarwal, K. Rai, R. Shrivastav and S. Dass, *J. Cleaner Prod.*, 2003, **11,** 439.
238. L.F.M. Wang and J.Z. Huang, *Social Sci. Med.*, 1995, **41**, 1191.
239. H. Mjengera and G. Mkongo, *Phys. Chem. Earth.*, 2003, **28,** 1097.
240. P.L. Bishop and G. Sansoucy, *J. Am. Water Works Assoc.*, 1978, **70**, 554.
241. R. Malaisamy, A. Talla-Nwafo and K.L. Jones, *Sep. Purif. Technol.*, 2011,**77**, 367,
242. M. Tahaikt, R. El Habbani, A. Ait Haddou, I. Achary, Z. Amor, M. Taky, A. Alami, A. Boughriba, M. Hafsi andA. Elmidaoui, *Desalination*, 2007, **21,** 246.
243. S.U. Hong, R. Malaisamy and M.L. Bruening, *Langmuir*, 2007, **23**, 1716.
244. N. Kabay, O. Arar, S. Samatya, U. Yuksel and M. Yuksel, *J. Hazard. Mater.*, 2008, **153**, 107.
245. N. Das, P. Pattanaik and R. Das, *J. Colloid Interface Sci.*, 2005, **292**, 1.
246. X. Fan, D.J. Parker and M.D. Smith, *Water Res.*, 2003, **37,** 4929.
247. I.B. Solangi, S. Memon and M.I. Bhanger, , *J. Hazard. Mater.*, 2009, **171**, 815.
248. I.B. Solangi, S. Memon and M.I. Bhanger, *J. Hazard. Mater.*, 2010, **176**, 186.
249. I.B. Solangi, A.A. Bhatti, M.A. Kamboh, S. Memon and M.I. Bhanger, *Desalination*, 2011, **272**, 98.
250. I.B. Solangi, A.A. Bhatti, M.A. Kamboh, S. Memon and M.I. Bhanger, *Sep. Sci. Technol.*, 2011, **46**,1113.
251. M. Islam, P.C. Mishra and R. Patel, *Chem. Eng. J.*, 2010, **166**, 978.

252. E.K. Unnikrishnan, S.D. Kumar and B. Maiti, *J. Membr. Sci.*, 1997, **137**, 133.

253. P. Ding, K.L. Huang, G.Y. Li and W.W. Zeng, *J. Hazard Mater.*, 2007, **146**, 58.

254. N. Viswanathan and S. Meenakshi, *J. Hazard. Mater.*, 2010, **178**, 226.

255. C. Sairam Sundaram, N. Viswanathan and S. Meenakshi *J. Hazard. Mater.* , 2009, **172**, 147.

256. C. Sairam Sundaram and S. Meenakshi, *J. Colloid Interface Sci*., 2009, **333,** 58.

257. G. Karthikeyan, A. Shanmuga Sundarraj, S. Meenakshi and K.P. Elango, *J. Indian Chem. Soc.*, 2004, **81**, 461.

258. N. Viswanathan and S. Meenakshi, *J. Hazard. Mater.*, 2010, **176**, 459.

259. C. Sairam Sundaram, N. Viswanathan and S. Meenakshi, *Bioresour. Technol*., 2008, **99**, 8226.

260. C. Sairam Sundaram, N. Viswanathan and S. Meenakshi, *J Hazard. Mater*., 2008, **155**, 206.

261. N. Viswanathan, C. Sairam Sundara and S. Meenakshi, *J. Hazard. Mater*., 2009, **161**, 423.

262. N. Viswanathan, C. Sairam Sundaram and S. Meenakshi, *Colloid Surf. B.*, 2009, **68**, 48.

263. M. Malakootian, M. Moosazadeh, N. Yousefi and A. Fatehizadeh, *Afr. J. Environ. Sci. Technol.* 2011**,5**, 299.

264. S. Meenakshi, C. Sairam Sundaram and R. Sukumar, *J. Hazard. Mater*, 2008, **153,** 164.

265. M. L. Chen, L. L. Suo, Q. Gao and Y. Q. Feng, *Electrophoresis*, 2011, **32**, 2099.

266. Q. Zhao, Q. Lu and Y. Q. Feng, *Anal. Bioanal. Chem.*, 2013, **405**, 4765.

267. J. Tong and L. G. Chen, *Anal. Lett.*, 2013**, 46,** 1183.

268. Z. C. Xiong, L. Y. Zhang, R. S. Zhang, Y. R. Zhang, J. H. Chen and W. B. Zhang, *J. Sep. Sci.*, 2012, **35,** 2430.

269. Y. Liu, H. F. Li and J. M. Lin, *Talanta*, 2009, **77**, 1037.

270. W. N. Wang, Y. P. Li, Q. H. Wu, C. Wang, X. H. Zang and Z. Wang, *Anal. Methods*, 2012, **4,** 766.

271. Y. P. Wang, Y. Sun, Y. Wang, C. Z. Jiang, X. Yu, Y. Gao, H. Q. Zhang and D. Q. Song, *Anal. Methods*, 2013, **5**, 1399.

272. Z. Y. He, D. H. Liu, R. H. Li, Z. Q. Zhou and P. Wang, *Anal. Chim. Acta*, 2012, **747**, 29.

273. F. Yang, R. Shen, Y. M. Long, X. Y. Sun, F. Tang, Q. Y. Cai and S. Z. Yao, *J. Environ. Monit.*, 2011, **13**, 440.

274. Z. Y. He, D. H. Liu, Z. Q. Zhou and P. Wang, *J. Sep. Sci*., 2013, **36**, 3226.

275. Y. B. Luo, Q. W. Yu, B. F. Yuan and Y. Q. Feng, *Talanta.*, 2012, **90,** 123.

276. A. A. Karamani, A. P. Douvalis and C. D. Stalikas, *J. Chromatogr*. A, 2013, **1271**, 1.

277. Q. H. Wu, M. Liu, X. X. Ma, W. N. Wang, C. Wang, X. H. Zang and Z. Wang, *Microchim. Acta*, 2012, **177**, 23.

278. Q. Han, Z. H. Wang, J. F. Xia, S. Chen, X. Q. Zhang and M. Y. Ding, *Talanta*, 2012, **101**, 388.

279. J. Ding, Q. Gao, D. Luo, Z. G. Shi and Y. Q. Feng, *J. Chromatogr. A*, 2010, **1217**, 7351.

280. M. Y. Hou, X. H. Zang, C. Wang and Z. Wang, *J. Sep. Sci.*, 2013, 36, 3242.

281. Y. N. Jiao, S. L. Fu, L. Ding, Q. Gong, S. H. Zhu, L. B. Wang and H. Li, *Anal. Methods*, 2012, 4, 2729.

282. J. Hristov, L. Fachikov, *China Particuology*, 2007, **5**, 11.

283. R.D. Ambashta, M. Sillanpaa, *J. Hazard. Mater.*, 2010, **180**, 38.

284. H. Heidari and H. Razmi, *Talanta*, 2012, **99**, 13.

285. W. N. Wang, R. Y. Ma, Q. H. Wu, C. Wang and Z. Wang, *Talanta,* 2013, **109**, 133.

286. J. Xie, T. S. Liu, G. X. Song, Y. M. Hu and C. H. Deng, *Chromatographia*, 2013, **76**, 535.

287. N. Li, L. Qi, Y. Shen, Y. P. Li and Y. Chen, *J. Chromatogr. A*, 2013, **1316**, 1.

288. W. Ma, F. Q. Ya, M. Han and R. Wang, *J. Hazard. Mater.*, 2007, **143**, 296.

289. J. Wang, F. Fang, H. Yue, Q. Guo and Z. Xu, *Adv. Mater. Res.*, 2013, 634, 367.

290. L. Chai, Y. Wang, N. Zhao, W. Yang and X. You, *Water Res.*, 2013, **47**, 4040.

291. P. K. Raul, R. R. Devi, I. M. Umlong, S. Banerjee, L. Singh and M. Purkait, *J. Nanosci. Nanotechnol.*, 2012, **12**, 3922.

292. C. F. Chang, P. H. Lin and W. Holl, *Colloids Surf. A*, 2006, **280**, 194.

293. X. Zhao, J.Wang, F. Wu, T.Wang, Y. Cai, Y. Shi and G. Jiang, *J. Hazard. Mater.*, 2010, **173**, 102.

294. M. Bhaumik, T. Y. Leswi, A. Maity, V. V. Srinivasu and M. S. Onyango, *J. Hazard. Mater.*, 2011, **186,** 150.

295. S. M. Maliyekkal, Anshup, K. R. Antony and T. Pradeep, *Sci. Total Environ.*, 2010, **408**, 2273.

296. L. Liang, J. He, M. Wei and X. Duan, *Ind. Eng. Chem. Res.*, 2006, **45**, 8623.

297. L. Liang, J. He, M. Wei, D. G. Evans and Z. Zhou, *Water Research*, 2007, **41**, 1534.

298. X. S. Li, L. D. Xu, Y. B. Shan, B. F. Yuan and Y. Q. Feng, *J. Chromatogr. A*, 2012, **1265**, 24.

299. Z. M. Zhang, W. Tan, Y. L. Hu and G. K. Li, *J. Chromatogr. A*, 2011, **1218**, 4275.

300. C. Y. Li and L. G. Chen, *Chromatographia*, 2013, **76**, 409.

301. J. R. Meng, C. Y. Shi, B. W. Wei, W. J. Yu, C. H. Deng and X. M. Zhang, *J. Chromatogr. A*, 2011, **1218**, 2841.

302. N. Thakur, S. A. Kumar, D. N. Wagh, S. Das, A. K. Pandey, S. D. Kumar and A. V. R. Reddy, *J. Hazard. Mater.*, 2012, **201–202**, 193.

303. C. Venkobacher and L. Iyengar, Defluoridation of water using activated alumina – a report, UNICEF Project No. CE/UNICEF/ 9132, (1998).

304. Y. H. Li, S. Wang, X. Zang, J. Wei, C. Xu, Z. Luan and D. Wu, *Mater. Res. Bull.*, 2003, **38**, 469.

305. S. Jain and R. V. Jayaram, *Sep. Sci.Technol.*, 2009, **44**, 1436.

306. P.P. Power and W.G. Woods, *Plant Soil*, 1997, **193**, 1.

307. F. Jay Murray, *Regul. Toxicol. Pharmacol*., 1995, **22**, 221.

308. S. Sahin, *Desalination*, 2002, **143**, 35.

309. A.J. Wyness, R.H. Parkaman and C. Neal, *Sci. Total Environ.*, 2003, **314**, 255.

310. J.L.Parks and M. Edwards, *Crit. Rev. Env. Sci. Technol*., 2005, **35**, 81.

311. Earl L Muetterties, "The Chemistry of Boron and its Compounds", New York : John Wiley & Sons, Inc. , (1967).

312. S. Sarp, M.S. Thesis, Ege University, Izmir, (Turkey, 2006).

313. C. Neal, K.K. Fox, M.L. Harrow and M. Neal, *Sci. Total Environ*., 1998, **210**,41.

314. D.S. Kostick, , Boron. Mineral Commodity Summaries, U.S. Geological Survey, (2008).

315. J.Takano, K. Miwa and T. Fujiwara, *Trends Plant Sci*., 2008, **13(8)** , 451.

316. P.H. Brown and H. Hu, *Plant Soil*, 1997, 196 , 211–215.

317. R.O. Nable, G.S. Banuelos and J.G. Paull, *Plant Soil*, 1997, **193**,181.

318. K.W. McLeod and T.G. Ciravolo, *Wetlands*, 1998, **18(3),** 431.

319. K.L. Tu, L.D. Ngheim and A.R. Chivas, *Sep. Purif. Technol*., 2010, **75**, 87.

320. C.M. Su and D.L. Suarez, *Environ. Sci. Technol*., 1995, **29**,302.

321. R.E. Zeebe, A. Sanyal, J.D. Ortiz and D.A. Wolf-Gladrow, *Mar. Chem*., 2001, **73**, 113.

322. C. Marston, M. Busch and S. Prabhakaren, Proceedings of European Desalination Society Conference on Desalination and the Environment, Santa Margerita Ligure, Italy, 2005.

323. A. Sagiv and R. Semiat, J. *Membr. Sci*., 2004, **243**, 79.

324. D. Prats, M.F. Chillon-Arias and M. Rodriguez-Pastor, *Desalination*, 2000, **128**, 269.

325. M. Kawasaki, M. Hirose, T. Ohara and S. Kimura, *Membrane*, 1999, **24(5)**, 296.

326. K. Fukunaga, M. Matsutaka, K. Ueyama and S. Kimura, *Membrane,* 1997, 22(4), 211.

327. P. Dydo, M. Turek, J. Ciba, J. Trojanowska and J. Kluczka, *Desalination,* 2005, **185,** 131.

328. R. Kunin and A.F. Preuss, *Ind. Eng. Chem. Res. Prod. Dev*., 1964, **3(4),** 304.

329. M. Badruk, N. Kabay, M. Demircioglu, H. Mordogan and U. Ipekoglu, *Sep, Sci. Technol*., 1999, **34**, 2553.

330. M.O. Simonnot, C. Castel, M. Nicolai, C. Rosin, M. Sardin and H. Jauffret, *Water Research*, 2000, **34**, 109.

331. A.E. Yilmaz, R. Boncukoglu, M.T. Yilmaz and M.M. Kocakerim, *J. Hazard. Mater.*, 2005, **117** , 221.

332. Y. Cengeloglu, A. Tor, G. Arslan, M. Ersoz and S. Gezgin, *J. Hazard. Mater*., 2007, **142**, 412.

333. N. Ozturk and D. Kavak, *J. Hazard. Mater*., 2005, **127**, 81.

334. D. Kavak, *J. Hazard. Mater.*, 2009, **163**, 308.

335. N. Ozturk and D. Kavak, *Adsorption* , 2004, **10**, 245.

336. S. Karahan, M. Yurdakoc, Y. Seki and K. Yurdakoc, *J. Colloid Interface Sci*., 2006, **293**,36.

337. L. Melnik, O. Vysotskaja and B. Kornilovich, *Desalination,* 1999, **124**, 125.

338. N. Nadav, M. Priel and P. Glueckstem, *Desalination*, 2005, **185**, 121.

339. N. Kabay, I. Yilmaz, S. Yamac, S. Samatya, M. Yuksel, U. Yuksel, M. Arda, A. Saglam, T. Iwanaga and K. Hirowatari, *React. Funct. Polym*., 2004, **60**, 163.

340. N. Bicak and B.F. Senkal, *J. Appl. Polym. S*ci., 1998, **68**, 2113.

341. X. Li, R. Liu, S. Wu, J. Liu, S. Cai and D. Chen, *J. Colloid Interface Sci.*, 2011, **361**, 232.

342. N. Bicak, O. Ozbelge, L. Yilmaz and B.F. Senkal, *Macromol. Chem. Phy*s., 2000, **201**, 577.

343. M.F. Chillon Arias, L. Valero i Bru, D. Prats Rico and Pedro V. Galvan, *Desalination*, 2011, **278**, 244.

344. M. Gazi and N. Bicak, *React. Funct. Polym*., 2007, **67**, 936.

345. N. Bicak, M. Gazi and B.F. Senkal, *React. Funct. Polym*., 2005, **65**, 143.

346. N. Geffen, R. Semiat, M.S. Eisen, Y. Balazc, I. Katz and C.G. Dosoretz, *J. Membr. Sci*., 2006, **286**, 45.

347. T. Vasudevan, S. Das, A.K. Debnath and A.K. Pandey, *J. Membr. Sci.*, 2009, **342**, 113.

348. M. Gazi, B. Senakal and N. Bicak, *Macromol. Symp*., 2004, **217**, 215.

349. O. Kaftan, M. Acikel, A. Eroglu, T. Shahwan, L. Artok and C.Y. Ni, *Anal Chim. Acta* , 2005, **547**, 31.

350. L. Wang, T. Qi and Y. Zhang, *Colloids Surf: A Physicochem. Eng. Aspects*, 2006, **275**, 73.

351. M.R. Hayes and J. Metcalef, *Analyst*, 1962, **87**, 956.

352. W.J. Ross and J.C. White, *Talanta*, 1960, **3**, 311.

353. IPCS Elemental mercury and inorganic mercury compounds: human health aspects. Geneva, World Health Organization, International Programme on Chemical Safety (Concise International Chemical Assessment Document 50) (2003).

354. G. F. Nordberg, B. A. Fowler, M. Nordberg, and L. T. Friberg, "Mercury," in Handbook on the Toxicology of Metals, Eds., chapter 33, Elsevier, New York, NY, USA, 3rd edition, (2007).

355. World Health Organization, "Inorganic mercury: environmental health criteria 118," in International Programme on Chemical Safety, World Health Organization, Geneva, Switzerland, (1991).

356. U. S. Environmental Protection Agency. Mercury Study for Congress: Health Effects of Mercury and Mercury Compounds., EPA-452/R-97-007.,Environmental Protection Agency: Washington, DC, (5) (1997).

357. M. Richardson, The Safety of Dental Amalgam, ISBN 0-662-24873-2, Minister of Health, Canada, (1996).

358. J.Burger, C. Jeitner and M.Gochfeld, *Journal of Toxicology and Environmental Health.*, 2011, **74**, 863.

359. Environmental Health Department, Ministry of the Environment, Minimata Disease: The History and Measures, Ministry of the Environment, Government of Japan, Tokyo, Japan, (2002).

360. F. Bakir, S. F. Damluji, and I. Amin Zaki, *Science*, 1973, **181**, 230.

361. S. B. Skerfving and J. F. Copplestone, *Bulletin of the World Health Organization*, 1976, **54,** 101.
362. T. W. Clarkson, L. Magos, and C. Cox, *Journal of Pharmacology and Experimental Therapeutics*, 1981, **218**, 74.
363. P. Zeitz, M. F. Orr, and W. E. Kaye, *Environmental Health Perspectives*, 2002, **110**, 129.
364. J. G. Schwartz, T. E. Snider, and M. M. Montiel, *American Journal of Emergency Medicine*, 1992, **10**, 258.
365. F. N. Kudsk, *Acta Pharmacologica et Toxicologica*, 1965, **23**, 263.
366. J. B. Hursh, T. W. Clarkson, and M. G. Cherian, *Archives of Environmental Health*, 1976, **30**, 302.
367. D. W. Eggleston and M. Nylander, *The Journal of Prosthetic Dentistry*, 1987, **58**, 704.
368. G. F. Nordberg and F. Serenius, *Acta Pharmacologica et Toxicologica*, 1969, **27**, 269.
369. T. W. Clarkson, L. Magos, and M. R. Greenwood, *Biology of the Neonate*, 1972, **21**, 239.
370. G. Guzzi, M. Grandi and C. Cattaneo et al., *American Journal of Forensic Medicine and Pathology*, 2006, **27**, 42.
371. J. W. Reinhardt, *Advances in Dental Research*, 1992, **6**, 110.
372. L. Bjorkman, B. F. Lundekvam and T. Laegreid, *Environmental Health*, 2007,**6**,30.

373. M. E. Crespo-Lopez, G. L. Macedo and S. I. D. Pereira, *Pharmacological Research*, 2009, 6**0**, 212.

374. C. J. Lin and S. O. Pehkonen, *Atmos. Environ.*, 1999, **33**, 2067.

375. P. Grandjean, H. Satoh, K. Murata and K. Eto, *Environ. Health Perspect*., 2010, **118**, 1137.

376. P. Grandjean and P. Weihe, *Environ. Res*., 1993, 61, 176.

377. D. C. Rice, *Environmental Res.*, 2004, **95**, 406.

378. Mercury in Drinking-water, WHO *Guidelines for Drinking-water Quality*, WHO/SDE/WSH/05.08/10

379. G. Kazantzis, *Medicina del Lavoro*, 2002, **93**, 139.

380. D. Cossa, J. Sanjuan, J. Cloud, P. B. Stockwell and W. T. Corns, *J. Anal. At. Spectrom*., 1995, **10**, 287.

381. G. Xin, Z. Chuguang, J. Zexiang and T. Zhiyong, *Microchim. Acta*, 2004, **148**, 221.

382. N. Bicak, S. Sungur, M. Gazi and N. Tan, *Sep. Sci. Technol*., 2003, 3**8**, 201.

383. I. Karadjova, S. Arpadjan, J. Cvetkovic and T. Stanlov, *Microchim. Acta*, 2004, **147**, 39.

384. D. Leyva, J. Estevez, A. Montero and I. Pupo, *X-Ray Spectrom*., 2007, **36**, 355.

385. M. Vircavs, A. Pelne, V. Rone and D. Vircava, *Analyst*, 1992, **117,** 1013.

386. M. V. Balarama Krishna, D. Karunasagar, S. V. Rao and J. Arunachalam, *Talanta*, 2005, **68**, 329.

387. E. M. Soliman, M. B. Saleh and S. A. Ahmed, *Talanta*, 2006, **69**, 55.

388. Y. Zhai, X. Chang, Y. Cui, N. Lian, S. Lai, H. Zhen and Q. He, *Microchim. Acta*, 2006, **154**, 253.

389. J. C. A. de Wuilloud, R. G. Wuilloud, R. A. Olsina and L. D. Martinez, *J. Anal. At. Spectrom.*, 2002, **17**, 389

390. T. Duan, X. Song, J. Xu, P. Guo, H. Chen and H. Li, *Spectrochim. Acta, Part B*, 2006, **61**, 1069.

391. B. C. Mondal and A. K. Das, *Anal. Chim. Acta*, 2003, **477**, 73.

392. J. Chwastowska, A. Rogowska, E. Sterlinska and J. Dudek, *Talanta*, 1999, **49**, 837.

393. S. R. Segade and J. F. Tyson, *Talanta*, 2007, **71**, 1696.

394. A. Krata, K. Pyrzynska and E. Bulska, *Anal. Bioanal. Chem.*, 2003, **377**, 735.

395. S. Diez, J.M. Bayona, *Talanta* , 2008, **77,** 21.

396. K. Leopold, M. Foulkes, P.J. Worsfold, Trends *Anal. Chem*, 2009, **28(4)** ,426.

397. M. Behbahani, A. Bagheri, M. Taghizadeh, M. Salarian, O. Sadeghi, L. Adlnasab and K. Jalali, *Food Chemistry*, 2013, **138**, 2050.

398. L.S.G. Teixeira, A.C.S. Costa, J.C.R. Assis, S.L.C. Ferreira and M. Korn, *Microchimica Acta*, 2001, **137** , 29.

399. M.E. Mahmoud, in: Proceeding of the 25th FACSS Conference, Austin, TX, USA, (1998).

400. Mohamed E. Mahmoud, *Anal. Chim. Acta*, 1999, **398**, 297.

401. A. Apilux, W. Siangproh, N. Praphairaksit, O. Chailapakul, *Talanta* 2012, **97**, 388.

402. K. Farhadi, M. Forough, R. Molaei, S. Hajizadeh, A. Rafipour, *Sensors and Actuators B.*, 2012, **161**, 880.

403. Ali Moghimi and Ali Mazloumifar, *Afr. J. Pure Appl. Chem* , 2013, **7(3),** 122.

404. E. Sumesh, M.S. Bootharaju and T. Pradeep, *J. Hazard. Mater*., 2011, **189**, 450.

405. K.P. Lisha, Anshup and T. Pradeep, *Gold Bull.*, 2009, **42**, 144.

406. Y. Kim , R.C. Johnson and J.T. Hupp, *Nano Let*ters, 2001, **1**,165.

407. P. Prakash, P. Gnanaprakasam, R. Emmanuel, S. Arokiyaraj and M.Saravan, *Colloids Surf B Biointerfaces*, 2013,1**08**, 255.

408. N. Ahmad, S. Sharma, M.K. Alam, V.N. Singh, S.F. Shamsi, B.R. Mehta and A. Fatma, *Colloids Surf B Biointerfaces*, 2010, **81(1),** 81.

409. R.S. Patil, M. R. Kokate, S. M. Pawar, S. H. Han and S.S. Kolekar, *Adv.Nat. Sci. Nanosci. Nanotechnol.*, 2012, **3**, 2043.

410. M. A. Majeed khan, S. Kumar, M. Ahamed, S.A. Alrokayan and M.S. Alsalhi, *Nanoscale Res Lett.*, 2011,**6**, 434.

411. H. B. Sonmez, B. F. Senkal and N. bicak, *Journal of Polymer Science: Part A: Polymer Chemistry*, 2002, **40,** 3068.

412. A. Henglein, *J. Phys. Chem*., 1993, **97**, 5457.

413. A.Hengleinand and C. Brancewicz, *Chem. Mater*, 1997, **9**, 2164.

414. R. Kunkel and S. E. Manahan, *Anal. Chem.*, 1973, 45, 1465.

415. M. Lopez-Artiguez, A. Camean, and M. Repetto, *Journal of Analytical Toxicology*, 1993, **17**, 18.

416. N. H. Bings, A. Bogaerts, and J. A. C. Broekaert, *Anal. Chem.*, 2006, **78,** 3917.

417. P. Pohl, *Trends in Analytical Chemistry*, 2009, **28**, 117.

418. T. Mayr, S. M. Borisov and T. Abel, *Analy. Chem.*, 2009, **81**, 6541.

419. J. Gasparik, D. Vladarova and M. Capcarova, *J. of Environ. Sci. and Health A*, 2010, **45**, 818.

420. K. E. Lorber, *Waste Management and Research*, 1986, 4, 3.

421. K. Camman, G. Guibault, E. Hall, R. Kellner, H. L. Schmidt, O. S. Wolfbeis, The Cambridge Definition of Chemical Sensors (1996).

422. R. W. Cattrall, Chemical Sensors, Oxford University Press Inc., New York (1997).

423. A. Lobnik, “Absorption-based sensors,” in Optical Chemical Sensors, F. Baldini, A. N. Chester, J. omola, and S. Martellucci, Eds., , Springer, Amsterdam, The Netherlands, (2006).

424. S. Nagl and O. S. Wolfbeis, “Classifiction of optical chemical sensors and biosensors based on fluorescence and phosphorescence,” in Standardization and

Quality Assurance in Fluorescence Measurements I, vol. 5 of Springer Series on Fluorescence, (2008)

425. C. McDonagh, C. S. Burke, and B. D. MacCraith, *Chemical Reviews*, 2008, **108**, 400.
426. J. F. Fernandez-Sanchez, R. Cannas, S. Spichiger, R. Steiger and U. E. Spichiger-Keller, *Sensors and. Actuators*, *B: Chemical*, 2007, **128**, 145.
427. R. N. Dansby-Sparks, J. Jin, S. J. Mechery, U. Sampathkumaran, T. W. Owen, B. D. Yu, K. Goswami, K. Hong, J. Grant and Z. L. Xue, *Anal. Chem*., 2010, **82**, 593.
428. S. Sumiya, T. Sugii, Y. Shiraishi and T. Hirai, *J. Photochem.Photobiol. A: Chemistry*, 2011, **219**, 154.
429. X. Cheng, S. Li, A. Zhong, J. Qin and Z. Li, *Sensors & Actuators B: Chemical*, 2011, **157**, 57.
430. A. Coskun, M.D. Yilmaz and E.U. Akkaya, *Org. Lett*., 2007, **9**, 607.
431. B. Liu and H. Tian, *Chem. Commun.*, 2005, **25**, 3156.
432. K.C. Song, J.S. Kim, S.M. Park, K.C. Chung, S. Ahn and S.K. Chang, *Org. Lett*., 2006, **8**, 3413.
433. E.M. Nolan and S.J. Lippard, *Chem. Rev*., 2008, **108**, 3443.
434. X. Guo, X. Qian and L. Jia, *J. Am. Chem. Soc*, 2004,**126**, 2272.
435. Y. K. Yang, K. J. Yook and J. Tae, *J. Am. Chem. Soc*, 2005, **127**, 16760.
436. M. H. Ha-Thi, M. Penhoat, V. Michelet and I. Leray, *Org. Lett*, 2007, **9**, 1133.
437. E. M. Nolan and S. J. Lippard, *J. Am. Chem. Soc*, 2007, **129**, 5910.

438. Z. X. Han, H. Y. Luo, X. B. Zhang, R. M. Kong, G. L. Shen and R. Q. Yua, *Spectrochimica Acta Part A*, 2009, 7**2**, 1084.

439. Y. M. Li, X. L. Zhang, B. C. Zhu, J. Xue and L. L. Yan, *The Journal of Fluorescence*, 2011, **21**, 1343.

440. X. J. Zhu, S. T. Fu, W. K. Wong, J. P. Guo and W. Y. Wong, *Angewandte Chemie International Edition*, 2006, **118**. 3222.

441. J. Wang and X. Qian, *Organic Letters*, 2007, **8**, 3721.

442. L. Praveen, V. B. Ganga, R. Hirumalai, T. T. Sreeja, M. L. P. Reddy and R. L. Varma, *Inorganic Chemistry,* 2007, **46,** 6277.

443. M. H. Lee, S. Lee, S. H. Kim, C. Kang and J. S. Kim, *Org. Lett*, 2009, **11**, 2101.

444. S. V. Wegner, A. Okesli, P. Chen and C. He, *J. Am. Chem. Soc*, 2007, **129**, 3474.

445. K. C. Chiang, C. Huang, C. W. Liu and H. T. Chang, *Anal. Chem.*, 2008, **80**, 3716.

446. C. X. Tang, Y. Zhao, X. W. He and X. B. Yin, *Chem. Commun.*, 2010, **46**, 9022.

447. M. Virta, J. Lampinen and M. Karp, *Anal. Chem.*, 1995, **67**, 667.

448. X. Liu, Y. Tang, L. Wang, J. Zhang, S. Song, C. Fan and S. Wang, *Adv. Mater.*, 2007, **19**, 1471.

449. G. K. Darbha, A. Ray and P. C. Ray, *ACS Nano*, 2007,**1**, 208.

450. D. Li, A. Wieckowska and I. Willner, *Angewandte Chemie International Edition*, 2008, **47**, 3927.

451. X. Xue, F. Wang and X. Liu, *J. Am. Chem. Soc*, 2008, **130**, 3244.

452. L. Wang, J. Zhang, X. Wang, Q. Huang, D. Pan, S. Song and C. Fan, *Gold Bull*, 2008, **41**, 37.

453. X.J. Zhu, S.T. Fu, W.K. Wong, J.P. Guo and W.Y. Wong, *Angew. Chem. Int. Ed*., 2006, **45,** 3150.

454. H. Zheng, Z.H. Qian, L. Xu, F.F. Yuan, L.D. Lan and J.G. Xu, *Org. Lett*., 2006, **8**, 859.

455. W R Seitz, *Anal. Chem*., 1984, **56**, 16A.

456. B. Kuswandi and R. Narayanaswamy, *Sensors and Actuators B*, 2001, **74**, 131.

457. H. Tavallali and M. Yazdandoust, *Eurasian J. Anal. Chem.*2008, **3**, 284.

458. B. Kuswandi, Nuriman, H.H. Dam, D.N. Reinhoudt and W. Verboom, *Anal. Chim. Acta*, 2007,**591**,208.

459. Y. Kalyan, A. K. Pandey, P. R. Bhagat, R. Acharya, V. Natrajan, G. R. Naidu and A.V.R.Reddy, *J. Hazar. Mater*, 2009,**166**, 377.

460. L. K. Chau and M. D. Porter *Anal. Chem*, 1990, **62**, 1964.

461. R.W. Ramette and E.B. Sandell, *J. Am. Chem. Soc*., 1956, **78**, 4872.

462. H.N. Kim, M.H. Lee, H.J. Kim, J.S. Kim and J. Yoon, *Chem. Soc. Rev*., 2008, **37**, 1465.

463. X. Chen, T. Pradhan, F.Wang, J.S. Kim and J. Yoon, *Chem. Rev*., 2012, **112**, 1910.

464. T. H. Maren, *Anal. Chem*, 1947, **19**, 487.

465. T. Prasada Rao and T. V. Ramakrishna, *Analyst*, 1980, **105**, 674.

466. M. Balcerzak, *Analyst*, 1988, **113**, 129.

467. M. H. Lee, J.S.Wu, J. W. Lee, J. H. Jung and J. S. Kim, *Org. Lett.*, 2007, **9,** 2501.

468. D. Wu, W. Huang, C. Duan, Z. Lin and Q. Meng, *Inorganic Chemistr*y, 2007, **46**, 1538.

469. H. Yang, Z.G. Zhou, K.W. Huang, M.X. Yu, F.Y. Li, T. Yi and C.H. Huang, *Org. Lett*., 2007, **9**, 4729.

470. W. Shi and H. Ma, *Chem. Commun*, 2008, 1856.

471. X. Q. Zhan, Z. H. Qian, H. Zheng, B.Y. Su, Z. Lan and J. G. Xu, *Chem. Commun*, 2008, 1859.

472. G.D. Bohoyo, M. I. Rodriquez-Caceres, M. C. Hurtado-Sanchez and A. Munoz de la Pena, *Applied Spectroscopy*, 2010, **64**, 520.

473. F. J. Orriach-Fernandez, A. Medina-Castillo, J. F. Fernandez-Sanchez, A. Munoz de la Pena and A.Fernandez-Gutierrez, *Anal. Methods*, 2013, 5, 6642.

474. J.S. Wu, I.C. Hwang, K.S. Kim and J.S. Kim, *Org. Lett*, 2007, **9**, 907.

475. S. K. Ko, Y. K. Yang, J. Tae and I. Shin, *J. Am. Chem. Soc*, 2006, **128**, 14150.

476. M.H. Lee, S.J. Lee, J.H. Jung, H. Lim and J.S. Kim, *Tetrahedron*, 2007, **63**, 12087.

477. C. Wang, S. Tao, W. Wei, C. Meng, F. Liu and M. Han, *J. Mater. Chem*., 2010, **20**, 4635.

478. H. Liu, P. Yu, D. Du, C. He, B. Qiu, X. Chen and G. Chen, *Talanta*, 2010, **81**, 433.

479. J. Hu, C. Li and S. Liu, *Langmuir*, 2009, **26**, 724.